Die Expeditionen ANTARKTIS X/6-8 des Forschungsschiffes „POLARSTERN" 1992/93

The Expeditions ANTARKTIS X/6-8 of the Research Vessel "POLARSTERN" in 1992/93

Herausgegeben von / Edited by
Ulrich Bathmann, Victor Smetacek, Hein de Baar,
Eberhard Fahrbach, Gunter Krause,
unter Mitarbeit der Fahrtteilnehmer/
with contributions of the participants

Ber. Polarforsch. 135 (1994)
ISSN 0176 - 5027

ANTARKTIS X/6-8

29 September 1992 - 24 February 1993

KOORDINATOR/COORDINATOR

Victor Smetacek

ANT X/6:	Punta Arenas - Cape Town FAHRTLEITER/CHIEF SCIENTIST Victor Smetacek
ANT X/7	Cape Town - Ushuaia FAHRTLEITER/CHIEF SCIENTIST Eberhard Fahrbach
ANT X/8	Ushuaia - Bremerhaven FAHRTLEITER/CHIEF SCIENTIST Gunter Krause

Aufmachung und Zusammenstellung dieses Berichtes erfolgten durch Ingrid Lukait.
The layout and technical editing of this Report was carried out by Ingrid Lukait.

INHALT / CONTENTS

EINLEITUNG

Die zehnte Antarktisexpedition des FS "POLARSTERN" begann am 14. November 1991 und endete am 24. Februar 1993. In diesem Berichtsheft werden die drei letzten Fahrtabschnitte ANT X/6, 7 und 8 dokumentiert.

Zum Fahrtabschnitt ANT X/6 lief FS "POLARSTERN" von Südamerika (Punta Arenas) am 29.9.92 in Richtung zentrales, nördliches Weddellmeer aus. Im Rahmen des Internationalen Geosphären/Biosphären Programms (IGBP) wurden hiermit Untersuchungen zur Joint Global Ocean Flux Study (JGOFS) im Südpolarmeer begonnen. Alle 51 eingeschifften Wissenschaftler/innen aus Deutschland, den Niederlanden, Frankreich, Belgien, Dänemark und Schweden untersuchten Aspekte des biologischen Kohlenstoffkreislaufs im offenen Wasser und im eisbedeckten Ozean. Hierfür wurden 11 Transekte auf 6°W zwischen dem eisbedeckten Weddellmeer im Süden bis nach Norden in den Bereich der Polarfrontzone bearbeitet. Ziel der Untersuchungen war die Erfassung von biologischen, chemischen und physikalischen Bedingungen, die die Planktonentwicklung und somit die Kohlenstoffdynamik im Ozean während der Meereisschmelze bestimmen. Dabei wurden besonders die Systeme des Meereises, der Ozeandeckschicht und der Grenzfläche Wasser-Meeresboden untersucht. Eine Vielzahl von Experimenten in den Kühlcontainern und Laboratorien von POLARSTERN halfen bei der Aufklärung wichtiger biologischer Prozesse einzelner Organismengruppen (Phyto-, Bakterio- und Zooplankter) und Lebensgemeinschaften (Mikrobielles Netzwerk, Meereisgemeinschaft). Pünktlich am Morgen des 30. November 1992 lief das Schiff in Kapstadt ein.

Am 3. Dezember 1992 verließ FS "POLARSTERN" Kapstadt zum folgenden Abschnitt ANT X/7, der quer durch das zentrale Weddellmeer zurück nach Südamerika (Ushuaia) verlief, wo das Schiff am 22. Januar 1993 eintraf. Dieser Fahrtabschnitt war vorwiegend physikalisch-ozeanographischen Arbeiten gewidmet, die unmittelbar nach Verlassen südafrikanischer Hoheitsgewässer Richtung Süden mit dem Bestimmen der Vertikalstruktur von Temperatur und Strömung in der Wassersäule begann. Im weiteren Verlauf der Fahrt wurden Verankerungen von Strömungsmessern und Sinkstoffallen ausgewechselt und im Meereis meteorologisch/ ozeanographische Bojen ausgesetzt. Nach erfolgreichem Abschluß der notwendigen Lösch- und Ladearbeiten für die Neumayerstation in der Atkabucht begann das ozeanographische Kernprogramm dieser Fahrt zwischen Kapp Norvegia und der Joinville-Insel mit Messungen von Vertikalprofilen der Temperatur, des Salzgehaltes und von Spurenstoffen im Meerwasser. Zusätzlich wurden 18 Verankerungen geborgen und 9 neu ausgelegt. Ziel dieser Untersuchungen ist die Aufnahme und Bilanzierung der Zirkulation und der Wassermassenverteilung im zyklonalen Weddellwirbel sowie seine Stellung und sein Einfluß zur Klimawirksamkeit der Ozeane. Diese Arbeiten werden im Rahmen des World Ocean Circulation Experiment (WOCE) durchgeführt. Untersuchungen zur Biologie des Phyto- und Zooplanktons, am Benthos, zur Nährsalzchemie, zur Ermittlung bakterieller Aktivität und zur Wirkung der erhöhten UV-B-Strahlung aufgrund der Ausdünnung der Ozonschicht vervollständigten das wissenschaftliche Programm dieses Fahrtabschnittes. Aufgrund der zügig durchgeführten Arbeiten und der günstigen Eis- und Wetterverhältnisse konnte das Schiff 50 Meilen weiter entlang des Larsen Schelfeises nach Süden vordringen, als es 1893 Kapitän Larsen möglich gewesen war. Zum Abschluß der Fahrt lieferte das Schiff Material an die argentinisch-deutsche Station Jubany auf King George Island

und verlieh an das spanische Forschungsschiff "HESPERIDESA" die ozeanographische CTD-Sonde, dessen eigene Sonde ausgefallen war.

Auf der Rückreise nach Deutschland, die am 24. 1. 1993 begann, wurden die langfristigen Beobachtungsprogramme für großskalige Prozesse im Atlantik fortgeführt. Neben den routinemäßig durchgeführten Erfassungen chemischer Spurenstoffe, der globalen Verteilung von CO_2 in Luft und Oberflächenwasser, des Ozongehaltes, der Temperaturverteilung in Oberflächenwasser und Atmosphäre kam erstmals ein neu entwickeltes Schiff-LIDAR Gerät zum Einsatz. Dieses Gerät liefert für die Fernerkundung wichtige Daten zu optischen Eigenschaften und zum Planktongehalt im Oberflächenwasser. Die Fahrt verlief überaus erfolgreich; der Äquator wurde am 7. Februar auf 26°W überschritten. Nördlich der Nordseeinsel Texel - 110 Meilen von Bremerhaven entfernt - geriet das Schiff allerdings vom 20. zum 21.2.93 in einen heftigen NW-Sturm mit gewaltiger Grundsee, die zu beträchtlichen Schäden im Wohnbereich und an Deck führte. Daher lief "POLARSTERN" am 24. Februar 1993 mit 14 Stunden Verspätung in Bremerhaven ein.

Auf allen Fahrtabschnitten sorgte die schon gewohnte gute Kooperation zwischen Kapitänen, Offizieren, Besatzung und den Wissenschaftlern an Bord für den reibungslosen und sehr effektiven Einsatz der Geräte und des Schiffes. Mit Hilfe der direkt an Bord empfangenen Satellitenkarten gelang mehrmals eine gezielte, einsatzorientierte und optimale Navigation des Schiffes. Nicht zuletzt gebührt der Logistik und den Sekretärinnen der Fahrtleitungen im AWI Dank für ihre umfangreiche und effektive Unterstützung.

FOREWORD

The tenth Antarctic expedition of RV "POLARSTERN" began on 14. Nov. 1991 and ended on 24 Feb. 1993. This report deals with the last three legs ANT X/6, 7 and 8.

The cruise leg ANT X/6 started 29 Sept. 1992 in Punta Arenas commencing the Joint Global Ocean Flux Study (JGOFS) in the Southern Ocean which is a core project within the International Geosphere/Biosphere Programme (IGBP). All 51 scientists from Germany, The Netherlands, France, Belgium, Denmark and Sweden investigated the major aspects of global carbon flux in the open ocean and in ice-covered areas. The main goals of this cruise were the assessment of biological, chemical and physical processes on plankton development and carbon dynamics in the ice free areas and in the marginal ice zone. The systems of the sea-ice, the upper mixed water column and the sea-sediment interface received special attention. Various experiments were conducted on board POLARSTERN to investigate specific biological processes of phyto-, zooplankton and bacteria and the microbial network.
On 3 December 1992 POLARSTERN left Cape Town for its ANT X/7 leg. Physical oceanography dominated the scientific activities which started on the way south to the Neumayer station which was supplied during this leg. In addition to investigations *on route* of the vertical structure of the water column in terms of temperature and currents, moorings with current meters and sediment traps were exchanged in the northern Weddell Sea. The main aim of the cruise, however, was the repetition of a hydrological transect between Kapp Norvegia and Joinville within a long-term program of the World Ocean Circulation Experiment (WOCE). Accordingly 18 mooring were recovered and 8 new ones deployed together with a closely spaced

CTD-transect. The ultimate scientific aim of these investigations is the documentation and a budget of the water circulation in the Weddell Gyre as part of the global ocean circulation and its impact on global climate. In addition, investigations on plankton and benthos, on nutrients, on bacterial activities and on the effect of UV-B radiation on marine organisms completed the scientific programme. As everything went smooth and conditions of the sea-ice and the weather were perfect, POLARSTERN could penetrate along the Larsen Shelf Ice 50 nautical miles further to the south than Capt. Larsen was able to travel in 1893. After supply of the Argentine-German station on Jubany, King George Is., POLARSTERN arrived at Ushuaia on 22 January 1993.

The return to Germany across the Atlantic Ocean began on 24 January 1993. Measurements of chemical trace elements, CO_2 in ocean surface and atmosphere, ozone concentrations and temperature distributions, were carried out as part of a long-term programme for large scale processes in the Atlantic. In addition, a newly developed ship's LIDAR was successfully employed to measure ocean surface temperature and chlorophyll content which both are essential ground truth parameters for remote sensing by satellites. The successful trip was interrupted shortly by a storm in the night of 20/21 January close to the island of Texel in the North Sea. Heavy waves damaged the ship's deck and some cabins. Therefore, POLARSTERN arrived 14 hrs late on 24 February at Bremerhaven.

We wish to thank captains, officers and crew for the excellent co-operation on all legs, one of the most important factors for successful work at sea. Satellite maps provided useful information on sea-ice distribution and thickness and helped to navigate the ship in complicated situations. Last but not least thanks are due to AWI logistics and the secretaries of the chief scientists who effectively supported our research.

ANT X/6 "FRÜHLING AM EISRAND"
PUNTA ARENAS - CAPE TOWN - 29.09.92 - 30.11.92

1. Fahrtverlauf

FS "Polarstern" begann ihre ANT X/6 - Fahrt mit der Bezeichnung "Frühling am Eisrand" in Punta Arenas am 29. 9. 92 (Fig. 6.1.1). Das zentrale Thema dieser international besetzten Fahrt war der biologische Kohlenstoffkreislauf im offenen Wasser und im eisbedeckten Ozean und wurde im Rahmen der Southern Ocean - Joint Global Ocean Flux Study (SO - JGOFS) untersucht. Alle 51 Eingeschifften der wissenschaftlichen Gruppen an Bord bearbeiteten Fragen im Rahmen dieses Programms, das sich als Teil des Internationalen Geosphären/Biosphären Programms (IGBP) formiert hat. Ziel der Untersuchungen ist die Erfassung saisonaler und regionaler Veränderungen des Kohlenstoffkreislaufs im Weddellmeer zur Zeit der Eisschmelze als Funktion von hydrographischen, chemischen und biologischen Parametern. Da der südliche Ozean durch hohe Nährstoffkonzentrationen charakterisiert ist, war ein wichtiger Punkt unserer Untersuchungen die Frage nach den limitierenden Prozessen für die Phytoplanktonentwicklung.

Die erste vollständige Station (Sta. 857) wurde am 2. Oktober, nach erfolgreich verlaufener Teststation (Sta. 856), mit dem wichtigsten Gerät der Reise - eine CTD-Rosette bedient von unseren holländischen Kollegen - an einer Position durchgeführt 57°S 49°W, die schon mehrfach 1988/89 während der EPOS-Reise (European Polarstern Study) beprobt worden war.

Von dieser Station ostwärts bis zum Untersuchungsgebiet wurde entlang des 57°S Breitengrades (einmal am Tag) eine Reihe von hydrographisch-chemischen und biologischen Messungen an Stationen durchgeführt, um zu überprüfen, ob westlich der South Sandwich Inseln die Produktivität im Plankton höher ist, als auf der bisher wenig untersuchten östlichen Seite und in wieweit hydrographische Bedingungen bzw. das Meereis hierfür verantwortlich sind. Zusätzlich wurden Chlorophyll Fluoreszenz in 8 m Wassertiefe zusammen mit Temperatur und Salinität während der gesamten Fahrt fortlaufend aufgezeichnet. Die Oberflächenregistrierungen wurden in Transekte eingeteilt (Fig. 6.1.2).

Die Eisbedeckung im Osten wurde schnell sehr dicht, so daß zwischen 10° und 15°W der Transekt nach Norden bis 56°S verschoben wurde. Am 11. Oktober wurde eine günstige Gelegenheit für einen allgemeinen Ausflug auf eine sehr große Eisscholle genutzt.

Als Hauptuntersuchungsgebiet legten wir aufgrund der aktuellen Eislage (Bordbeobachtungen; Eiskarten des NOAA-Satelliten, USA; Wetterkarten der Bordwetterwarte) für die nächsten Wochen den 6°W Meridian fest, auf dem wir auf 10 Nord-Süd-Schnitten einen Monat lang die räumlich/zeitliche Entwicklung der Bakterio-, Phyto- und Zooplankter in ihrem physikochemischen Umfeld messend beobachteten.

Fig. 6.1.1 Die Fahrtroute von "Polarstern" während ANT X/6
Cruise track of "Polarstern" during ANT X/6

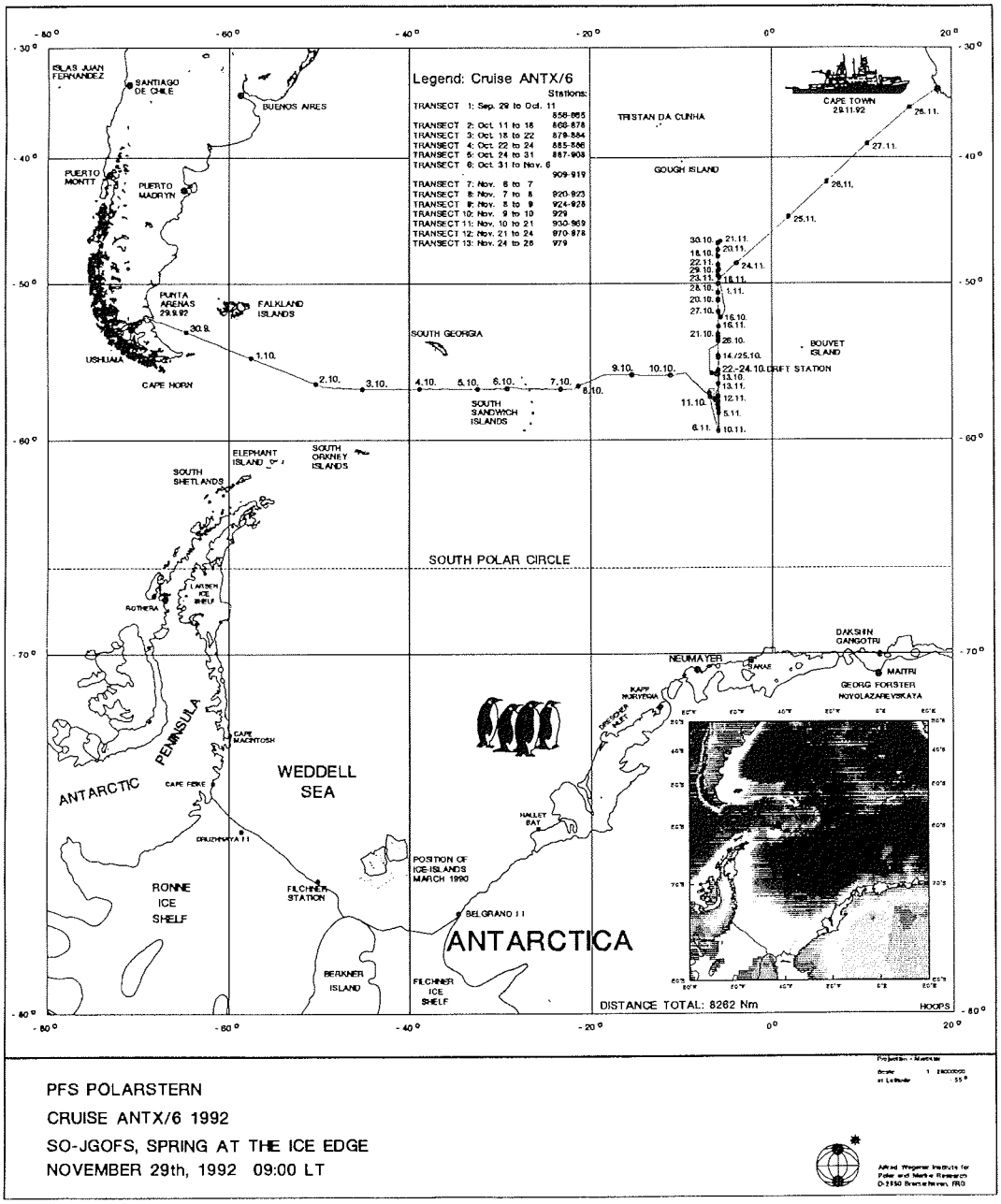

PFS POLARSTERN
CRUISE ANTX/6 1992
SO-JGOFS, SPRING AT THE ICE EDGE
NOVEMBER 29th, 1992 09:00 LT

Fig. 6.1.2 Transekte entlang 6°W
Transects along 6°W

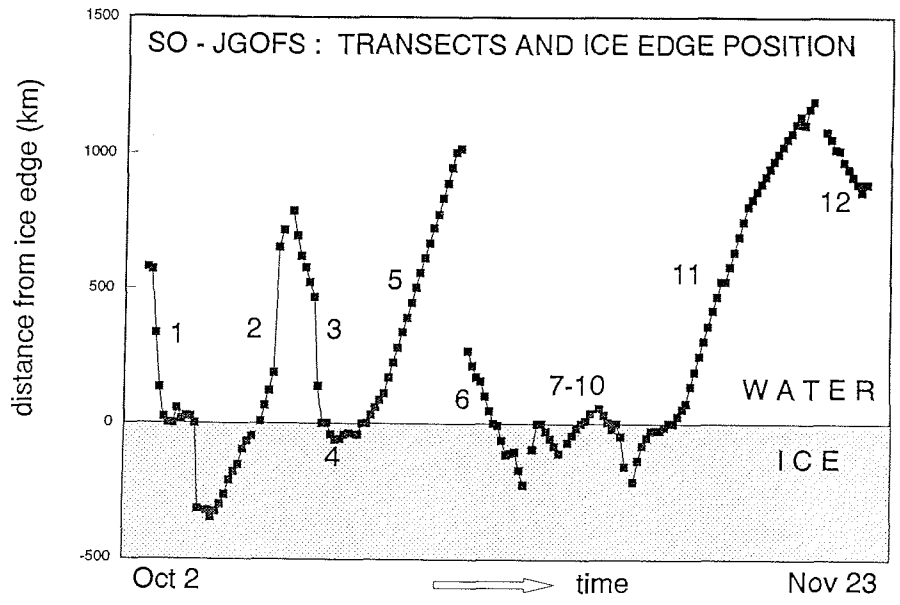

Die erste Schnittfahrt (Trans. 2), die am 13 Oktober mit der Station 868 tief im vollständig mit Meereis bedeckten Weddellmeer bei 60°S mit Stationen im Abstand von 30 sm begann, führte bis nördlich zur Polarfront bei 47°S. Dieser Schnitt wurde am 15.10. bei 53°00´ S (Sta. 876) durch einen Sturm unterbrochen. Die Arbeiten wurden am 17 10. an der Polarfront bei 49°S (Sta. 877) wieder aufgenommen und am 18.10. durch Sta. 879 bei 48°S beendet. Unmittelbar anschließend begann Transekt 3 in Richtung Süden mit Stationen bei 49°30´, 50°00´ und 50°30´S; wieder mußte dann die Arbeit aufgrund stürmischer Witterungsverhältnisse abgebrochen werden. Die kombinierten Daten der Transekte 2 und 3, die demzufolge zwischen 51° und 53°S eine Lücke aufweisen, zeigen, daß wir Ende Oktober überall die Spätwintersituation im Plankton angetroffen hatten: Geringe Biomassen und niedrige Produktionswerte zeichnete das Phytoplankton aus bei hohen Nährsalzkonzentrationen; die Kohlendioxidkozentrationen im Oberflächenwasser standen mit der Atmosphäre im Gleichgewicht. Allein die Zooplankter (vorwiegend Krill und große calanoide Copepoden) waren schon sehr zahlreich und aktiv aber nur unter und zwischen dem Eis im Weddellmeer.

Die Packeisgrenze im Süden hatte sich seit unserem letzten Besuch erheblich verändert, denn ein 100 km breites, lockeres Eisfeld ragte wie eine Halbinsel nach Norden in unser Untersuchungsgebiet hinein. Wir vermuteten hier flache Schmelzwasserlinsen, in denen günstige Lichtbedingungen für Algenwachstum herrschten.

Daher wurden am 22. 10. um 07:45 Uhr bei 56°S, 7°W Driftstudien begonnen (Sta. 886 und Transekt 4), wobei Sinkstoffallen an Oberflächenbojen in einer ausgedehnten Wake offenen Wassers zwischen den aufgebrochenen Eisschollen ausgesetzt wurden. 48 Stunden später, aufgrund der sehr schwierigen Eis- und Windverhältnisse, wurde diese Studie am Morgen des 10.10. nach zwei 24-stündigen Inkubationsexperimenten und einer Reihe von Wassersäulenmessungen beendet. Geringe Biomassen, hohe vertikale Heterogenität in allen Parametern, die zermalmende Wirkung der Eisreibung auf unsere Geräte und die ständig zunehmende Windgeschwindigkeit zwangen uns zu diesem Schritt.

Der nächste Süd-Nord-Transekt 5 begann am 24.10. bei 56°S; 6°W (Sta. 887) und endete erfolgreich und ohne Unterbrechung am 30.10. bei 47°S (Sta. 907) in der Polarfrontzone. Hier waren die Chlorophyllkonzentrationen spürbar angewachsen, im Gegensatz zum Eisrand und im ACC. Nach einer Tiefenstation bei 46° 52´S und 5° 43´W kehrten wir auf Transekt 6 zur Eiskante zurück mit der Absicht, durch eine bessere räumliche Auflösung mittels 30 sm kurzem Stationsabstand am Eisrand (vom 2.11. bei 55°00´S (Sta. 909) bis zum 6.11. bei 59°30´S (Sta. 919)) vermutete Schmelzvorgänge erfassen zu können. Diese detaillierten Untersuchungen ergaben keine Indizien für Biomasseakkumulation in der Schmelzwasserzone, die eine allerdings geringe stabile Wasserschichtung aufwies. Vermutlich waren die Schmelzwasserlinsen zu kurzlebig für einen Wachstumserfolg.

Die Registrierung der Oberflächenwassertemperatur bewies die dauernde Existenz eines Streifens wärmeren Wassers an der ACC/Weddell Front bei ca. 58°S. Da diese Tatsache den ständigen Auftrieb wärmeren zirkumpolaren Tiefenwassers, einen Abtrieb schwereren Weddellmeer-Oberflächenwassers und entsprechende Biomasseakkumulation an der Oberfläche vermuten ließ, wurde dieses Phänomen genauer untersucht. Dementsprechend wurden die Transekte 7 bis 10 und die CTD-Stationen 920 - 928 kleinräumig über der Front plaziert. Unsere Arbeiten wurden wiederum von einem kurzen aber heftigen Sturm unterbrochen.

Das letzte, große Süd-Nord-Transekt (11) begann am 10.11. bei 59°30´S in einem dichten Feld großer Eisschollen, die ebenfalls beprobt werden konnten (Sta. 930). Das Transekt wurde mit einem Stationsabstand von 30 sm erfolgreich am 21.11. bei 47°00´S beendet. Zuvor waren am 20.11. vom Schlauchboot aus genaue Untersuchungen des Oberflächenwassers um einen großen Eisberg durchgeführt und dabei Spurenmetalle beprobt worden, die im Verhältnis zur Schmelzwasserschichtung am Eisberg untersucht werden sollen.

Der Stationsabstand zwischen 48°00´S und 50°00´S wurde während Transekt 12 (Sta. 970 bis 977) auf 15 nm verringert, mit noch feinerer Auflösung an den "hot spots" (Sta. 972 und 978). In der Nacht vom 23./24. 11. wurde dieses Transekt abgeschlossen und "Polarstern" dampfte sofort Richtung Kapstadt.

Die Situation hatte sich Ende November vollständig gewandelt. Aus den Meßdaten der vertikalen Profile der Wassersäule und von den kontinuierlichen Registrierungen von Temperatur, Salzgehalt, Kohlendioxid und Chlorophyll im Oberflächenwasser konnten wir für den untersuchten Monat ein dreidimensionales Bild der Entwicklung im Plankton und den Folgen für den Kohlenstoffffluß zeichnen: Nicht an der schmelzenden Eiskante - wie im Westen des Weddellmeeres (EPOS-Gebiet) -, sondern an der Polarfront hatten sich mindestens zwei starke Algenblüten gebildet, die sich bis

in einhundert Meter Wassertiefe erstreckten. Die Gesamtbiomassen (>280 mg Chl.*a* m^{-2}) entsprachen jeweils denen, die sonst nur von flachen Schelfmeeren bekannt sind; die gemessene Produktion von 3 g Kohlenstoff m^{-2} Tag^{-1} wird im Weltmeer kaum überschritten. Ein Teil der Algen aus der einen Blüte (*Corethron* spp.) befand sich in sexueller Phase und hinterließ ihre verlassenen Silikatschalen, ein Vorgang der in solchem Ausmaß nie beobachtet worden war. Intakte, mit Plasma gefüllte Zellen der anderen Blüte (dominiert von *Fragilariopsis kerguelensis*) fanden sich bis in über 300 m Wassertiefe. In beiden Fällen wurde also biologisches Material (biogenes Silikat bzw. organischer Kohlenstoff) aus der Ozeandeckschicht in die Tiefen des Ozeans "gepumpt". Die Effektivität dieser "Biologischen Pumpe" drückte sich in einer Abreicherung von Kohlendioxid im Karbonatsystem des Oberflächenwassers aus; auch durch die Abreicherung von ^{234}Thorium wurde der Export von partikulärem Material dokumentiert.

Bakterielle Biomasse und Produktion entwickelten sich parallel zum Phytoplankton und zeigten Höchstwerte gegen Ende November in der Polarfront. Durch diese enge Kopplung zwischen Primärproduktion und heterotrophem Abbau in der Wassersäule wird ca. ein Drittel des organischen Materials schon im Oberflächenwasser wieder abgebaut. Am Meeresboden nahm die geochemische Arbeitsgruppe die Auswirkung absinkenden organischen Materials auf den Chemismus des interstitiellen Wassers auf, anhand von Profilen mit 0,1 mm Meßabstand von pH und Sauerstoff. Das hierfür verwendete Freifallgerät wurde mehrfach erfolgreich in über 3500 m Wassertiefe eingesetzt.

Diese Algenblüten wurden in der Polarfrontzone durch eine mehrfache "blätterteigartige" Überlagerung verschiedener Wassermassen hydrographisch begünstigt. Diese besondere hydrographische Situation konnten wir mittels zahlreicher, in kontinuierlicher Folge durchgeführter Vertikalprofile mit der CTD vermessen. Günstige biologische Voraussetzungen waren durch das anfängliche Fehlen ausreichend großer Populationen von Algenkonsumenten (Zooplanktern) gegeben, deren Bestände durch Fänge mit fünf verschiedenen Netztypen unterschiedlichster Maschenweite erfaßt wurden.

In diesen beiden Bedingungen (Hydrographie und Zooplanktonbestand) unterschied sich die Situation an der Eisrandzone im nördlichen Weddellmeer: Die bereits erwähnten Zooplankter übten hier einen hohen Fraßdruck auf die geringen Phytoplanktonbestände aus, wie wir in den Experimentcontainern unter verschiedenen biologischen und physikalischen Bedingungen nachvollziehen konnten. Die Eisschmelze führte darüber hinaus nicht zu einer ausreichenden Stabilität des oberen Wasserkörpers. Tiefe vertikale Durchmischung mit relativ ungünstigem Lichtklima für die Phytoplankter (d.h. ungünstige Wachstumsbedingungen) war die Folge. Die Phytoplanktonproduktion und der vertikale Partikelfluß waren gering.

Der gewonnene, umfangreiche und für das Weddellmeer bisher einmalig kohärente Datensatz wurde bereits an Bord in einer Datenmatrix erfaßt und allen Beteiligten zur Verfügung, Ergänzung und weiteren Verarbeitung in ihre Heimatinstitute mitgegeben. Einige wichtige Parameter wie zum Beispiel die vorgefundenen natürlichen Konzentrationen von Eisen im Meerwasser - einem für die Primärproduktion im offenen antarktischen Ozean offenbar raren aber dennoch essentiellen Element - oder die Ergebnisse zahlreicher Experimente mit natürlichen Bakterien, Phyto- und Zooplanktonpopulationen werden im Laufe des Frühjahres 1993 ausgewertet. Im

Herbst werden während eines gemeinsamen Workshops die entsprechenden Veröffentlichungen vorbereitet, deren Präsentation während des ASLO-Symposiums im Frühjahr 1994 geplant ist.

Nach einer allerletzten CTD-Wasserprobennahme am 25.11. bei 45°30´S, 01°08´E liefen wir pünktlich am 30. 11. 1992 morgens in Kapstadt ein, nicht ohne einige Tage zuvor Kapitän Suhrmeyer, der seit dem Bau und der Jungfernreise vor 10 Jahren auf 'Polarstern' war, im Rahmen einer kleinen Feier von der Polarforschung verabschiedet zu haben. Es war eine großartige Reise, an der Kapitän, Offiziere und Besatzung entscheidend beteiligt waren.

1. Introduction and cruise itinerary

The aim of the cruise ANT X/6, termed "Spring at the ice edge", was to follow and compare spring development of the pelagic system in ice-covered and open water masses. The eastern part of the Atlantic sector of the Southern Ocean was chosen as the study site and transects extending from the ice edge of the eastern Weddell Sea, across the Antarctic Circumpolar Current (ACC) and into the Polar Front were to be conducted.

RV "Polarstern" left Punta Arenas at noon of 29 Sept 1992 with 51 scientists representing 5 European countries on board and eventually worked on the transects shown in Fig. 6.1.1. On 2 Oct the CTD rosette was successfully tested (Sta. 856) and the first "real" station (857) conducted at 57° South 49° West. The position had been sampled 4 times by the EPOS (European Polarstern Study) Leg 2 cruise carried out from November to early January of 1988/89. Chlorophyll fluorescence together with salinity and temperature was registered continuously throughout the cruise. The surface registrations have been given transect numbers indicated in Fig. 6.1.2. Trans. 1 was carried out along the 57th parallel with one station every day in order to record the productivity gradient shown to exist along the rim of the Weddell Sea by satellite imagery. Simultaneously, this latitudinal section provided two extended transects from open ACC water into loose ice cover of the Weddell Sea, one to the west of the South Sandwich islands and the other to the east. Ice cover in the East was very heavy so the transect was shifted to 56°S between 20° and 15°W. On 11 Oct we enjoyed an excursion on a large ice floe.

On the basis of topography and ice cover the 6°W meridian was chosen as the study site and on 13 Oct the first station (868) of Trans. 2 was carried out deep in closed pack ice. From there stations were conducted at 30 nm intervals northward till Sta. 876 at 53° 00´ on 15 Oct; the transect had to be interrupted after this station because of a storm and the next station was carried out when calmer waters were reached at the Polar Front at 49°S (877) on 17 Oct Trans. 2 was continued till Sta. 879 at 48°S on 18 Oct From there we commenced transect 3 on our way south, sampling stations at 49°30´, 50°00´and 50°30´S; the last station had to be interrupted after the first CTD again because of a storm. A station gap between 51° and 53° was enforced on these first south-north-south transects (2 & 3).

The pack-ice edge had changed significantly since our last visit and a 100 km broad loose ice field now extended northward like a peninsula in the study area. We intended carrying out a drift station in this marginal ice zone next by attaching the

sediment trap to a reasonably large ice floe. The location chosen was within the ice peninsula at about 56°S and 7°W; the rationale for site selection was the assumed presence of a shallow melt-water layer subjected to an adequate light supply within this dispersed ice field. Time stations following drifting sediment traps were to be occupied in appropriate localities. Research projects included many individual specialities in addition to covering all 20 core parameters of the JGOFS protocol as the cruise was part of the Joint Global Ocean Flux Study. The drifter had to be deployed in a broad band of open water between fields of crushed ice because we were unable to locate an adequate floe. The drift station (886 and transect 4) was commenced on 22 Oct at 7:15 and the drifter recovered 48 hrs later on the morning of 24 Oct Two 24 hrs in situ incubations and a series of water column measurements were obtained in this period. We found it very difficult to keep track of the drifter as it was engulfed frequently in ice fields that, because they were wind-driven, moved faster than the underlying water mass. Besides, biomass was very low and horizontal heterogeneity in water column structure marked during the drift. Wind speeds increased considerably at the end of the drift station.

South-north transect 5 was commenced on 24 Oct at 56°S; 6°W (Sta. 887) and ended successfully without interruption on 30 Oct at 47°S (Sta. 907) in the Polar Front. Chlorophyll concentrations had increased significantly at the Polar Front but were at much the same low levels at the ice edge as they were in the open ACC. After carrying out a deep station at 46° 52´S and 5° 43´W we returned south to the ice edge (Trans. 6); the plan was to carry out a detailed transect (7) at 30 nm station intervals from open water deep into closed pack ice. The rationale for this short detailed transect was to obtain better spatial coverage of the situation at the melting ice edge than achieved with the drifter. The first station of this short section (still transect 6) was commenced on 2 Nov at 55°00´S (Sta. 909) and the last (Sta. 919) at 59°30´S on 6 Nov in pack ice cover that was breaking up and melting. This detailed evaluation of the broad, melting ice edge indicated that accumulation of phytoplankton biomass was not occurring in the region although melt-water layers - albeit not strongly stratified - were indeed present. Possibly, the residence time of these shallower layers was not long enough to enable significant build-up of biomass.

Surface temperature registrations indicated the persistent presence of a band of warmer water at the ACC/Weddell front at ca. 58°S. As this could only be explained by upwelling of warm Circumpolar Deep Water and a corresponding downwelling of denser Weddell surface water, a closer examination of the phenomenon was called for as it affected surface layer dynamics and hence biomass accumulation. Accordingly, we carried out a grid of CTD stations (920 - 928 and Trans. 7 - 10) across the front which was unfortunately interrupted by a brief but intense storm.

The final major south to north transect (11) was commenced on 10 Nov at 59°30´S after reaching the first extensive ice field and a floe sufficiently large to sample (Sta. 930). The transect was completed successfully with stations at 30 nm intervals on 21 Nov at 47°00 S. A detailed study of the surface water around a large ice berg was conducted from an inflatable boat on 20 Nov to record trace metal concentrations in its vicinity and to relate these to melt-water plumes emanating from it.

Phytoplankton biomass had increased significantly at the front and 2 distinct blooms each dominated by very different diatom species (*Fragilariopsis kerguelensis* and

Corethron criophilum) were present. It was decided to use the remaining time to sample these blooms in detail. Stations were conducted at 15 nm intervals from 48°00´ - to 50°00´S (Trans. 12 and sta. 970 to 977) with more detailed stations at the "hot spots" (sta. 972 and 978). The transect was completed on the night of 23/24 Nov after which "Polarstern" steamed to Cape Town.

A final CTD deep cast was carried out on 25 Nov at 45°30´S and 01°08´E. RV "Polarstern" reached Cape Town punctually on 30 Nov 1992.

2. Wetter

Die Wetterlage bei Auslaufen Punta Arenas am 29. Sept. war durch ein Hoch über dem zentralen Weddellmeer und ein Tief westlich der Drake Passage gekennzeichnet. Dementsprechend wurden vor dem ostwärts ziehenden Tief nördliche Winde angetroffen, die allmählich bis 8 Bft zunahmen, später auf Nordwest drehten und langsam wieder auf Bft 6 abnahmen.

In der ersten Oktoberwoche arbeitete sich "Polarstern" mit einigen Stationen, die erste Untersuchungen ermöglichten und vor allem der Erprobung des wissenschaftlichen Gerätes diente, langsam nach Osten vor. Dabei etablierte sich ein Hoch über der Antarktischen Halbinsel. Zwischen ihm und dem kräftigen Subtropenhoch nördlich von 45°S entstand eine Tiefdruckrinne, die sich von Feuerland über die Falklands bis in die Gegend von Kap Norwegia erstreckte. In ihrem Bereich wurden vorwiegend schwache westliche, später umlaufende Winde angetroffen.

Am 7./8. Okt. erfolgte dann ein Kaltluftvorstoß mit rascher Entwicklung eines kleinen Randtiefs, auf dessen Rückseite kurzzeitig Südost 8 - 9 auftrat. Die anschließende Stabilisierung ging einher mit mäßigem Südwest bis Westwind.

Am Abend des 10. Oktober wurde erstmals während der Reise die Eiskante erreicht und bei herrlichem Hochdruckwetter wurde die Eisfahrt mit Ziel 56°S/6°W fortgesetzt, um dort (wegen der aktuellen Eislage) den ursprünglich für 0° geplanten Meridianschnitt zu beginnen.

Bis 14. Oktober wurden bei andauernder Hochdrucklage Untersuchungen im Eis durchgeführt. Am 15. Oktober ging es dann mit Nordkurs wieder ins offene Wasser. Inzwischen hatte sich ein umfangreiches Tiefdrucksystems im Raum Süd-Georgien / Orkadas entwickelt, auf dessen Vorderseite Nordwest bis Nord 8 angetroffen wurde. Der südliche Kern dieses Systems intensivierte sich noch und erreichte am 16. Oktober in der östlichen Weddellmeer, durch Bojenmeldungen belegt, einen Kerndruck von 948.1 HPA.

Auf ca. 50°S/15°W entwickelte sich an der Kaltfront dieses Tiefs eine Welle zu einem kräftigen Randtief, das südsüdostwärts über den Schiffsort zog und uns für einige Stunden Nordost Bft 10 brachte. Auf der Rückseite brach der Wind in kurzer Zeit zusammen, um in der Folge mit einem von Westen heranschwenkenden Hochkeil allmählich aus Südwest wieder aufzufrischen.

Ab 17. Oktober wurde wieder Südkurs gesteuert. Zwischen einem vom Weddellmeer nordnordostwärts ziehenden Tief und einem relativ kräftigen Hochkeil nahm am 19.

und 20. Oktober der Süd bis Südwestwind auf 9 bis 10 Bft zu, wobei beginnende Schiffsvereisung zu beobachten war. Wegen dieser ungünstigen Bedingungen mußten einzelne Stationen auf diesem Transekt ausgelassen und auf einen späteren Termin verlegt werden.

Das Eis wurde wieder am 21. Oktober erreicht. Bei ruhigem Hochdruckwetter konnten Stationen im Eis durchgeführt werden, wobei auch Drifter ausgesetzt und wieder aufgenommen wurden.

Ab 25. Oktober, auf dem nächsten Transekt nach Norden, war eine kräftige Sturmtiefentwicklung südlich von 60°S zu beobachten. Unser Reisewetter wurde durch diese weit südlich stattfindende Entwicklung mit mäßigen westlichen Winden günstig beeinflußt. Das Tief erreichte am 28./29. Oktober mit belegten 945 HPA wiederum einen recht tiefen Kerndruck. Im Fahrtgebiet herrschte weiterhin recht ruhiges, allerdings nebliges Wetter. Bis zur Breite von 47°S wurden zahlreiche Eisberge angetroffen.

Während der nächsten Tage lag die schwach ausgebildete Frontalzone zwischen 50° und 60°S, im Fahrtgebiet herrschte dabei bis zum 5. November überwiegend ruhiges Wetter. Dann entwickelte sich im Weddellmeer eine sehr kräftige Zyklone, die im Anhang etwas ausführlicher beschrieben ist. Der an ihrer Nordflanke in den nächsten beiden Tagen herrschende Weststurm behinderte die Arbeit erheblich und machte sie zeitweise unmöglich, so daß am Abend des 9. November wiederum ins Eis gesteuert wurde.

Die Forschungsarbeiten wurden bei überwiegend gutem Rückseitenwetter mit einzelnen Schneeschauern im Eis bis zum 12. November fortgesetzt. Anschließend wurde wiederum der Weg nach Norden eingeschlagen, wobei noch ein relativ kleines, aber kräftiges Tief mit kurzzeitig Sturmstärke erreichendem Nordwest zu überwinden war.

Ab 13. November setzte sich nach Abzug dieser Störung zunehmende Stabilisierung von Westen her durch. Der kräftige Druckanstieg ließ den Südwestwind nochmals kurz auf 8 Bft zunehmen. In den nächsten Tagen blieb die ruhige Hochdrucklage erhalten. Am 15. November wurde eine weitere interessante Tiefdruckentwicklung eingeleitet. An diesem Tag war erstmals auf ca. 30°S 30°W eine Wellenstörung im Satellitenbild erkennbar, die sich in der Folge rasch intensivierte und dann südostwärts zog. Im Gegensatz zu dem im Anhang beschriebenen kalten Tief, das entlang der Küste des Antarktischen Kontinents zieht, war dies ein Beispiel für eine Zyklone, die sich in den subtropischen Breiten an den Ostküsten der Kontinente entwickelt und unter Verstärkung nach etwa 50°S zieht. Auf seiner Vorderseite trat kurzzeitig Nordost 8 Bft auf. Der maximale Druckfall betrug ca. 50 HPA/3h. Das Tief wurde zwischen 45° und 50°S, etwa auf dem Greenwich Meridian nahezu stationär und füllte sich rasch auf. Die letzten zwei Wochen der Reise waren wiederum durch eine sich ständig regenerierende Hochdrucklage geprägt. Der Zustand des Ozeans ließ dabei zeitweise vergessen, daß sich das Schiff in den "Roaring Forties", einer der sturmreichsten Breiten der Erde bewegte. Dieser Eindruck wurde nur unwesentlich durch ein Tief gestört, das sich am 23. November erstmals auf etwa 40°S 35°W zeigte, bis zum 25. November unter Teiltiefbildung nach 55°S 20°W zog und unseren Aufbruch in Richtung Kapstadt am 24. mit nordöstlichen, später nordwestlichen Winden 8 Bft begleitete. In "The Antarctic Pilot, 1974" ist die nördliche

Grenze für Eisberge mit einem mittleren Abstand von 45 sm auf der Länge von 06°W bei etwa 52°S angegeben. Weit nördlich dieser Grenze, noch auf 46°S wurden jedoch während dieser Reise sehr viele Eisberge in wesentlich größerer räumlicher Dichte beobachtet.

2. Weather

When Polarstern left Punta Arenas, areas of high and low pressure were located over the central Weddell Sea and west of Drake Passage respectively. Therefore, northerly winds with Bft 8 occurred which changed to Northwest and decreased to Bft 6. During the following weeks a high pressure area established itself at the Antarctic Peninsula. Between this and the subtropical high pressure centre north of 45°S a trough of low pressure stretched from Tierra del Fuego along the Falkland Is. to the area of Kapp Norvegia with moderate westerly winds.

Investigations of the sea ice were conducted until 14 Oct. under a stable high pressure system. We left the ice heading north on 15 Oct. and entered a low pressure regime in the open Weddell Sea which originated in the area off South-Georgia/ Orcadas. Winds increased to Bft 8 coming from North and Northwest. The centre of this system was registered in the eastern Weddell Sea by sea-surface meteorological buoys and had 948.1 HPA.

At 50°S 15°W a second low pressure system developed beside the first one and headed south-south-east towards the ship's position. We measured Bft 10 during this time. Behind this front wind calmed down changed to Southwest and increased slightly after some hours.

On 17 Oct. we steamed south again. At the front between a low pressure system passing from the Weddell Sea towards north-north-east and a stable high pressure system, wind increased to Bft 9 and 10 on 19 and 20 Oct., coming from south to southwest. Ice formed on deck of the ship and stations had to be cancelled because of the bad weather conditions.

When we reached the sea ice on 21 Oct. low winds dominated the high pressure system in the area. After 25 Oct., while steaming north again, a strong and stormy low pressure system was observed south of 60°S. Consequently, we had favourable light westerly winds. This low pressure system had its minimum on 28/29 Oct. with 945 HPA. Fog and calm winds accompanied our route north until 5 Nov. Thereafter, a strong Cyclone developed in the Weddell Sea which is described later in more detail. A result of this cyclone were westerly storms and the ship had to stop scientific work for the coming days until we reached areas of sea ice again on 9 Nov.

Under reasonable weather conditions work started again till 12 Nov., interrupted only briefly by some snow showers. We decided to steam north again and consequently were hit by a storm coming from the Northwest. Fortunately, this storm moved on after 13 Nov. leaving winds of Bft 8 behind. Weather stabilised thereafter but not for long. On 15 Nov. another low pressure system developed. On satellite pictures irregularities were observed at 30°S 30°W, which increased and shifted to Southeast. In contrast to the low pressure system which is described later, this cyclone was one of those which originate in the subtropics at the east coasts of continents and migrate to

50°S. At its fronts winds had Bft 8, pressure reduction was 50 HPA/3 hrs. The low pressure system of 15 Nov. remained and filled at 45° and 50°S at the Greenwich meridian.

The last two weeks of the cruise were characterised by various steadily regenerating highs. Although in the area of the roaring forties the winds were calm. Only on 23 Nov. a low was observed at 40°S 35°W which moved to 55°S 20°W until 25 Nov. Thus, northeasterlies and northwesterlies with Bft 8 accompanied our return to Cape Town.

2.1 Tiefdruckentwicklung im Weddellmeer vom 5. bis 11. November 1992

Nach Schwerdtfeger "Weather and Climate of the Antarctic" (Amsterdam, 1984) wurde der tiefste Luftdruck an einer antarktischen Küstenstation am 3. Sept 1951 in Port Martin (66.8°S 141.4°E) mit 926.9 HPA registriert. Er schreibt weiter, daß aufgrund der Daten von Drifter-Bojen das Auftreten noch tieferer Druckwerte auf dem Ozean als sehr wahrscheinlich anzusehen ist.

Möglicherweise ist zwischenzeitlich ein tieferer Druck tatsächlich gemessen worden, dennoch ist das nachfolgend kurz beschriebene Tief sicherlich in die Kategorie der tiefsten Druckgebilde in dieser Region einzustufen.

Am 5.11.92, 12 UTC lag über dem zentralen Weddellmeer ein Tief mit ca. 955 HPA Kerndruck. Die Position dieses Tiefs war von ECMWF relativ gut erfaßt worden, der vom Modell berechnete Kerndruck betrug 965 HPA.

Bis zum 6.11. 06 UTC hatten sich zwei Kerne gebildet. Der westliche Kern lag dicht vor der Antarktischen Halbinsel, der östliche Teil mit 960 HPA ca. 300 sm westlich von Kap Norwegia, verbunden mit einer markanten Kaltfront, die bei ca. 57°S und 38°W eine beginnende Wellenbildung zeigte. Dieser Kern war vom Modell gut erfaßt. Die Vorhersage für den 8.11. (60 Std.) rechnete das Tief auf 66°S 8°W mit 950 HPA im Kern.

Am 7.11. 06 UTC war die o. g. Welle in den Kern, der nun auf 65°S 20°W lag, einbezogen worden und hatte möglicherweise zu dessen Intensivierung beigetragen. Meldungen der Argos-Bojen signalisierten zu diesem Zeitpunkt einen Kerndruck von unter 930 HPA. Neumayer, ca. 400 sm vom Kern entfernt, meldete zu diesem Termin 955.2 HPA und ENE 11, "Polarstern" auf 58.5°S 06°W, also in ca. 830 sm Entfernung zum Kern, 979.6 HPA und NW 9. Südwestlich vom Hauptkern deutete sich im Satellitenbild ein Sekundärzentrum an. Die Vorhersage des ECMWF rechnete nun für den 8.11. 00 UTC den Kern mit einem Druck von 940 HPA auf 68°S 15°W.

Am 7.11. 12 UTC lag das Tief mit zwei dicht benachbarten Kernen auf 67°S 20°W. Drei Argos-Bojen im Kernbereich meldeten 927.2, 927.5 bzw. 928.7 HPA. Neumayer, Entfernung jetzt ca. 320 sm, meldete 952.7 HPA bei ENE 10 und "Polarstern" auf 58°S 06°W (ca. 660 sm) 974.8 HPA und NW 8 (Fig. 6.2.1). Da die o. g. Argos-Bojen z. T. noch in Zugrichtung des Kerns lagen und dessen Entwicklung noch nicht

abgeschlossen war, ist mit gutem Grund anzunehmen, daß der nächste - leider nicht empfangene Satellitenumlauf - noch niedrigere Druckwerte gezeigt haben würde. Damit hätte der Kerndruck dieses Tiefs unter dem o. g. in Port Martin gemessenen Minimum von 926.9 HPA gelegen.

Am 8.11. 06 UTC wurde der Kern dann mit ca. 930 HPA auf 63°S 13°W analysiert. Die Entfernung zu Neumayer betrug nun ca. 450 sm. Die Station meldete zu diesem Zeitpunkt 946 HPA bei ENE 10. "Polarstern" auf 57.5°S 06°W, in etwa 370 sm Abstand, registrierte 978.6 HPA und NW 8.

Im weiteren Verlauf zog das Tief dann unter allmählicher Abschwächung langsam in östliche Richtung ab, wobei an seiner Nordwestflanke am 9./10.11. auf "Polarstern" nach kurzer Windabnahme erneut NW 8 bis 9 beobachtet wurden.

2.1 The low pressure system in the Weddell Sea between 5 and 11 November 1992

The book "Weather and climate of the Antarctic" by Schwerdtfeger, Amsterdam 1984, described the lowest air pressure at the Antarctic coast (Port Martin, 66.8°S 141.4°E) on 3 Sept. 1951 with 926.9 HPA. The author suggests further that even lower air pressures might very likely occur in the Antarctic Ocean.

Such a low pressure system was seen during our cruise on 5 Nov. 1992, 12:00 at the central Weddell Sea having about 955 HPA. The position of this system was well recorded by ECMWF and we calculated the central pressure with 965 HPA. Until 6 Nov. 06:00 UTC two centres had developed. One was in the west at the Antarctic Peninsula, the east center was 300 nm west of Kapp Norvegia with 960 HPA. The latter was associated by a strong cold front which developed waves at 57°S 38°W. The center of this low could be modelled well and 950 HPA was forecasted for 8 Nov. (60 hrs) for 66°S 8°W.

On 7 Nov. 06:00 UTC the above mentioned wave joined the center at 65°S 20°W and possibly stabilised it. Argos buoys registered 930 HPA. Neumayer station 400 nm south of the center recorded 930 HPA and ENE 11 (POLARSTERN, 58.5°S 06°W) in 830 nm distance of the center 979.6 HPA and NW Bft 9. Southwest of the center a second center was seen on satellite pictures. ECMWF forecast calculated for 8 Nov. 00:00 UTC the center of the low to be 940 HPA at 68°S 15°W.

The situation on 7 Nov. 12:00 UTC was characterised by two lows at 67°S 20°W where three Argos buoys recorded 927.2, 927.5 and 928.7 HPA. Neumayer being 320 nm away recorded 952.7 HPA. ENE 10 and POLARSTERN at 58°S 06°W (680 nm away) registered 974.8 HPA with NW Bft 8 (Fig. 6.2.1). As all station were outside the center of the low, as were the Argos buoys, and as the satellite did not record more informations, the suggested even lower air pressures cannot be verified.

On 8 Nov. 06:00 UTC the low was again registered with 930 HPA at 63°S 13°W. Distance to Neumayer was by then 450 nm. Neumayer records during that time were 946 HPA at ENE 10. Polarstern records in 370 nm distance were 978.6 HPA with NW Bft 8. The next days the low shifted eastwards leaving POLARSTERN with Bft 8 to 9 NW on 9. and 10. Nov.

Fig. 6.2.1 Registrierter Wind und Luftdruck von Bord "Polarstern" bzw. von 2 Wetterbojen zwischen dem 5. und 11. Nov. 1992 im Weddellmeer.
Wind speed and air pressure as measured from board "Polarstern and from 2 meteorological buoys during 5 to 11 Nov. 1992 in the Weddell Sea

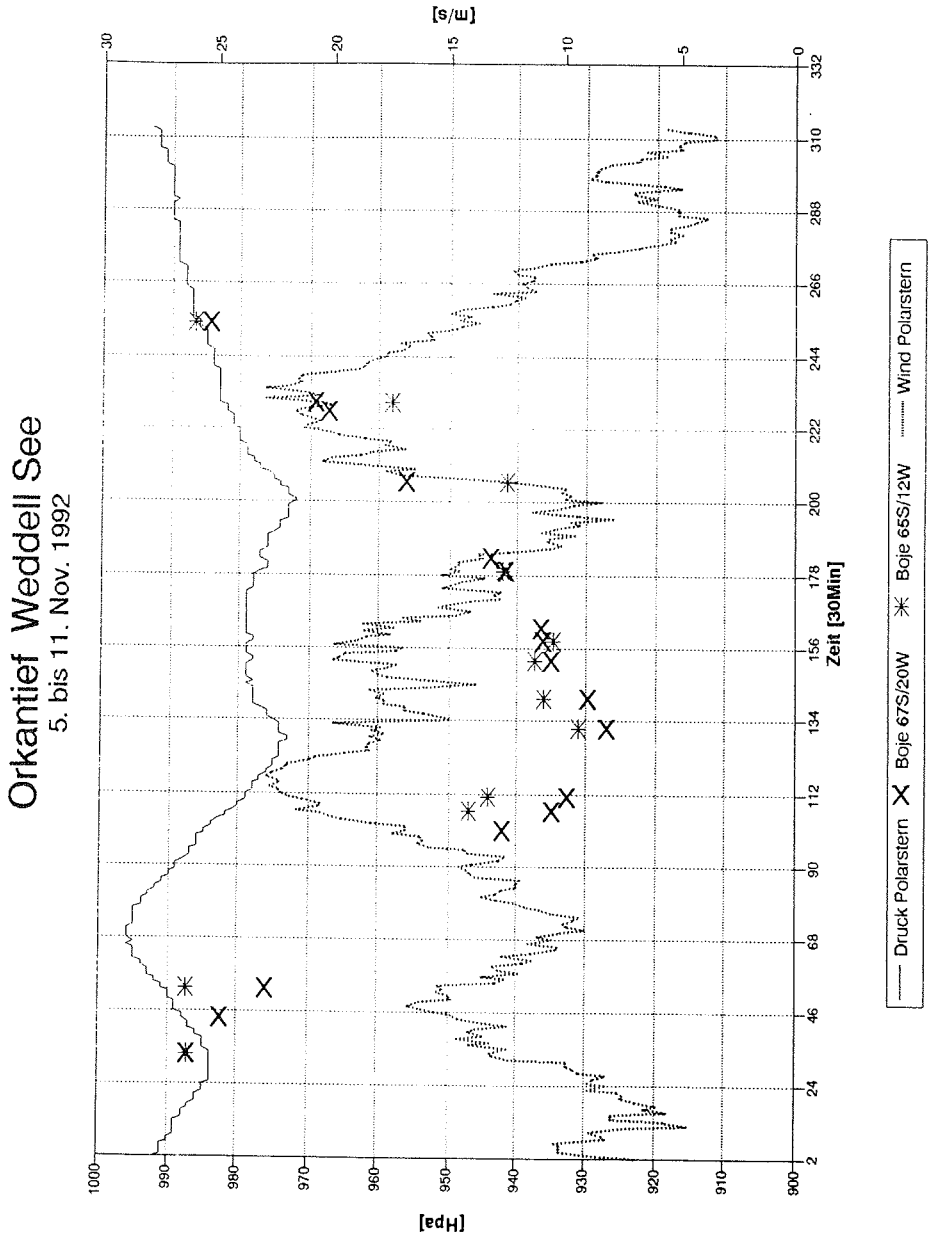

3. Sea-ice cover and icebergs

J.A. van Franeker (IBN-DLO)

Introduction

Ice cover was a parameter in the Southern Ocean JGOFS study because of the important influence of ice on the light regime, stability and salinity of the underlying water, all strongly affecting growth conditions for phytoplankton. Furthermore, the sea ice contains important communities of ice algae, that contribute significantly to the overall biological production of the Antarctic Ocean and that may seed the algal growth off the melting ice edge. Icebergs, apart from being a floating resting place for large numbers of penguins, also influence their environment by fresh meltwater and possibly the release of (micro-)nutrients into the surrounding water.

Methods

Methods for ice observations have been described in the "Protocol for ship- and airborne observations on the structure, physical properties and coverage of sea ice in the framework of Southern Ocean (SO) JGOFS activities" (Ackley et al. 1992). At three hour intervals and/or at regular station positions records are made of the percentages of the sea surface covered by different types of ice, with additional data on the characteristics of the ice (thickness, snow cover, ridging, and occurrence of ice algae). Nomenclature of ice is largely following WMO standards (World Meteorological Organisation 1985). As far as possible, these observations are made in such a way that resulting figures are representative averages for a rather wide area around the ship (5 to 10 km range). Following the SO-JGOFS methods, ice observations were conducted at every station position, and also between stations when these were more widely spaced. Results have been summarised in a SO-JGOFS ice database (ICESUM-ANT X/6 available in MAC Excel3, and MS-DOS Lotus3 or ASCII file) made available to participants. The database specifies the total ice cover into three major types: snow-covered floes (first-year or older ice), new ice (grease, nilas, grey ice etc.), and brash ice (small fragments of the wreckaged forms of other types of ice). The relative contribution of each of these ice types is relevant for light conditions in the underlying water and indicative for melting/freezing conditions. For the same reasons the average diameter of ice floes is listed, as well as temperature and salinity data of surface water and temperature of the air. Finally, the database includes figures for distance to outer ice edge and figures for the number of icebergs in a 12 nautical mile range around the ship at each station (counted by radar observations). In addition to the SO-JGOFS ice observations, records on ice cover were made during each of the more than 1300 ten-minute counts of top-predators (van Franeker, this volume). These data are of a much finer scale than the JGOFS observations, describing ice conditions in the 300 m transect band used for top predator counts, with further differentiation into minima and maxima for ice cover and floe sizes and differentiation into cover by floes, new young ice and brash ice. Part of these data will be included in the database of the surface registration group that lists parameters for each 10 minute period of the cruise.

Results

Sea ice The preliminary results presented here are mainly based on the SO-JGOFS protocol observations. An overall impression of ice distribution was regularly obtained from satellite pictures and ice maps from the Navy-NOAA Joint Ice Center (Suitland) kindly supplied by the meteorological- and radio officers on board "Polarstern". The extent of sea ice and "Polarstern's" cruise track during the initial phase of the cruise (2 to 18 Oct) is shown in Fig.6.3.1 Edge positions have been derived from a combination of actual encounters with the ice, photographs and maps. Towards the east, the ice extended much further north than in the west. During summer melt this pattern changes quickly with a fast southward retreat of ice in the eastern Weddell Sea while in the western sector the ice edge remains in a much more stable position. Fig.6.3.2., derived from NOAA ice maps, clearly reflects the initial phases of this phenomenon during SO-JGOFS. On 1 October the ice edge extended far north, and dense ice of over 90% cover (not shown separately in Fig.6.3.2.) started only a little south of the outer edge. By the end of the cruise, on 26 November the ice edge in between the Antarctic Peninsula and the South Orkney Islands had hardly shifted or even moved a bit north. In the east however, the outer edge had moved south over considerable distance and dense pack ice (> 90% cover) even disappeared at much higher speed. This melting pattern is consistent over different years and is due to the clockwise flow of the Weddell Sea Gyre transporting ice from deep down in the Weddell Sea northwards. As a consequence, there was a noticeable difference in ice characteristics between the EPOS 1988/89 study area along 49°W (van Franeker 1989) with a preponderance of thick and heavily rafted floes, and the area of main investigations in this study along 6°W where always over 90% of floes were flat and relatively thin first-year ice with low frequencies of ridges of pressurised ice. It is impossible to give a detailed account of small scale events in the outer ice edge. From satellite pictures it is evident that there were frequent patterns of eddy shaped ice areas detaching from the denser ice further south. These ice tongues however changed shape and position rapidly, as was experienced during the drift Sta. 866 (21-24 Oct) when the whole ice area in which we were working, moved south-east by at least one degree longitude and the outer ice edge retreated at least 55 km to the south. With such limitations in accuracy in mind, Fig. 6.1.2 illustrates transects and station positions with regard to the outer ice edge. The outer edge is defined as the northernmost extension of belts or fields of ice. In some cases this edge was the same as, or very near to the extension of continuous dense ice cover, but in other cases closed ice was only encountered much further south or not at all. Ice edge positions during the different transects along or near 6°W were:

Transect-No	Date	Edge at Latitude
2	14 Oct.	54°34'S
3/4	22 Oct.	55°31'S(7°00'W)
5	24 Oct.	56°00'S
6	4 Nov.	57°29'S
7/8	7 Nov.	57°00'S
9	8/9 Nov.	57°21'S(6°30'W)
10	9 Nov.	57°56'S(6°46'W)
11	12 Nov.	57°45'S

Fig. 6.3.1 Sea ice extent during Trans. 1 and 2 (Oct 1992)

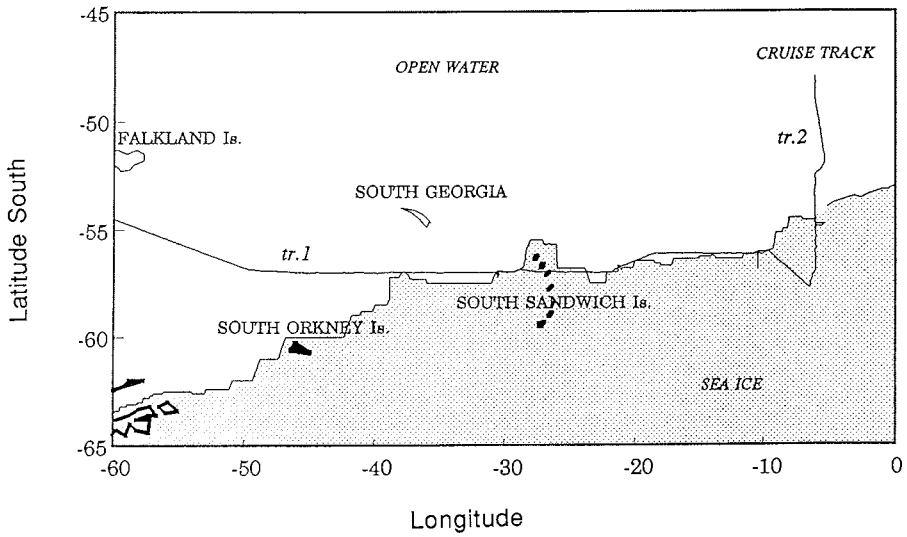

Fig. 6.3.2 Retreat of sea ice 1 Oct - 26 Nov 1992

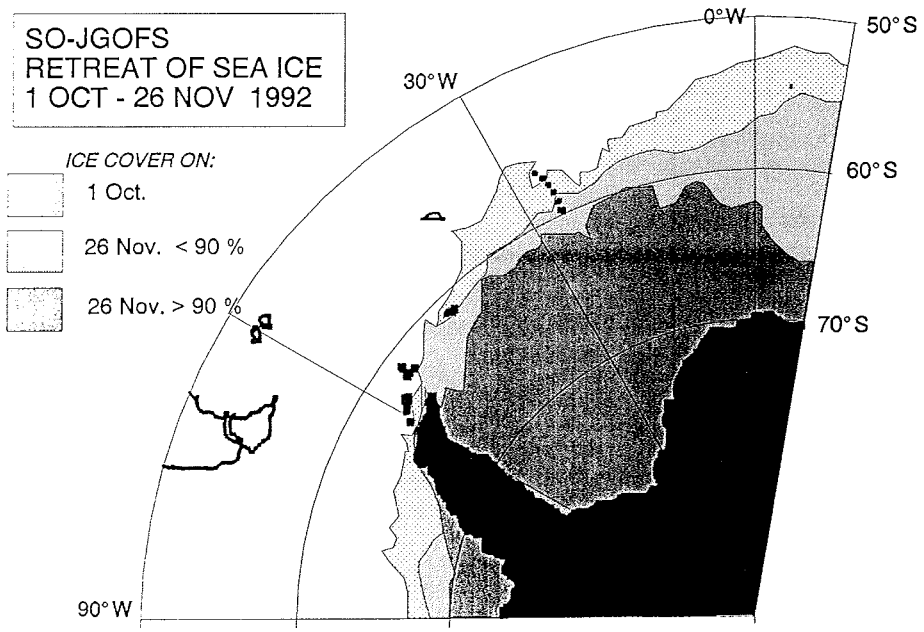

On average, these figures indicate that the ice edge retreated over 12 km per day. However, as indicated already by Fig. 6.3.2, also further south within the ice melting occurred. Fig. 6.3.3 and 6.3.4 illustrate the difference in ice cover during the first and last transect along 6°W (Trans. 2 mid Oct; Trans. 11 mid Nov.). During the latter transect, large new open water areas were encountered within the ice and the large floes (several km diameter) encountered initially had been fragmented into small floes within a month. Brown ice, discoloured from ice algae, occurred in all ice areas in high percentages, although frequency and intensity of discoloration tended to be higher in areas with relatively small floes and near the outer edge. Discoloration was usually strongest at the snow-ice interface and on the bottom of the ice, but intermediate brownish layers at a variety of depths within the ice were extremely common as well. - Icebergs clearly accumulated along the ice edge, numbering sometimes over a 100 in the 12 nm range. Surprisingly, also these iceberg concentrations shifted southward at considerable speed, comparable to that of the sea ice itself (Fig. 6.3.5 and 6.3.6). This southward shift was even noticeable in the short time frame of Trans. 2, 3 and 5 (Fig. 6.3.5) and probably only reflects the southward component of an even faster south-eastern movement of both bergs and sea ice in the study area. Our original explanation that icebergs were concentrated by the meeting of Circumpolar current and Weddell Sea water is weakened by such fast changes in location. Possibly the sea ice also plays a role in the distribution of bergs? Patters of water currents in the study area were extremely complex and variable. The track of an Argos Buoy south of our study area was followed by "Polarstern´s" meteorologists and indicated north-eastern movement in that area (from about 63°S-8°W in early October to 61°S-6°E in late November). It is unclear whether significant melt of the icebergs in the concentration area near the retreating ice edge occurs as a contribution to the drop in salinity of the surface water. A smaller, but consistent accumulation of icebergs also occurred in the north at the Polar front. At least on a local scale these heavily melting bergs must contribute to lowered salinity levels, and possibly elevated (micro-)nutrient levels in the surface waters near the Polar Front. The surroundings of a large melting iceberg were studied in detail on Sta. 967. The size of icebergs near the Polar Front is of evident importance for such studies. A limited amount of information on icebergs sizes is available from observations made by officers of "Polarstern", but has not yet been analysed. As indicated, more detailed information is available in the SO-JGOFS ice- and surface-registration databases.

References

Ackley, S.F., Eicken H., van Franeker J.A. and Wadhams P. 1992. Protocol for ship and airborne observations on the structure, physical properties and coverage of sea ice in the framework of Southern Ocean (SO) JGOFS activities. AWI Bremerhaven.

van Franeker, J.A. 1989. Sea ice conditions. In: Hempel I., Schalk P.H. and Smetacek V. (eds). The Expedition Antarktis VII/3 (EPOS Leg 2) of RV "POLARSTERN" in 1988/89. Ber. Polarforsch. 65:10-13.

van Franeker, J.A. (1994). Top predators: seabirds, seals and whales. (this volume)

World Meteorological Organisation. 1985. WMO sea-ice nomenclature, terminology, codes and illustrated glossary. WMO/DMM/BMO No.259- TP145. Secretariat of the WMO, Genf

Fig. 6.3.3 Ice cover and floe diameter Trans. 2

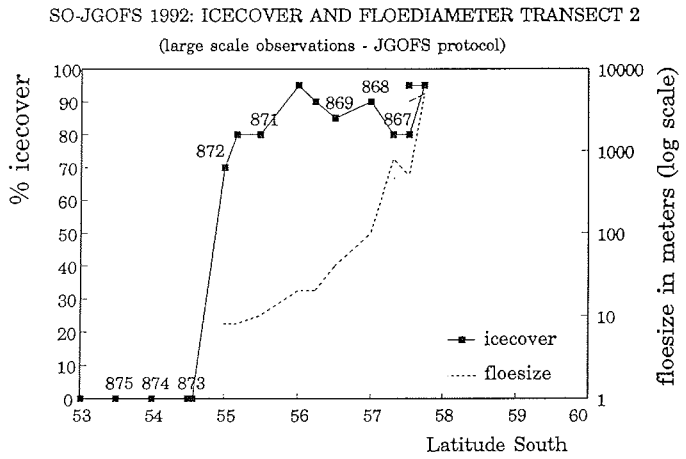

Fig. 6.3.4 Ice cover and floe diameter Trans. 11

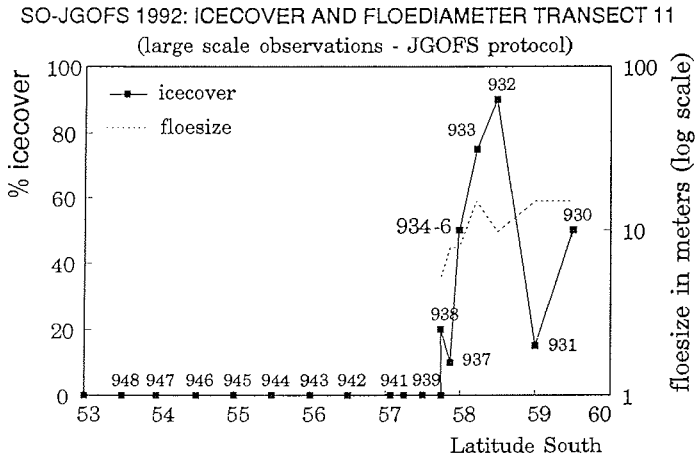

Fig. 6.3.5 Iceberg distribution along 6°W, October (Trans. 2 to 5)

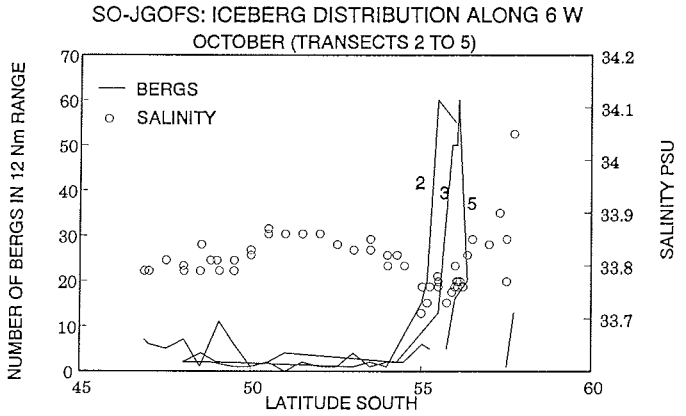

Fig. 6.3.6 Iceberg distribution along 6°W, November (Trans. 10 to 12)

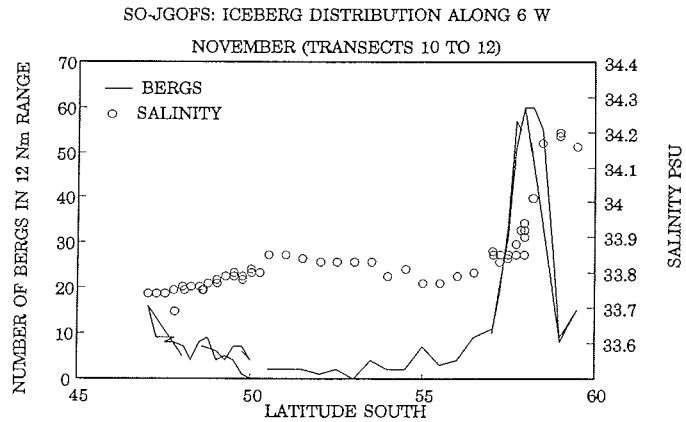

4. Top Predators: Seabirds, seals and whales

J.A. van Franeker (IBN-DLO)

Introduction

Top predators are not listed as core parameter in JGOFS studies as they are generally considered to play a minor role in carbon cycling. In the Antarctic Ocean however, top predator densities can be extremely high, and their occurrence may be of relevance to the export of carbon from the system, either by respiration or by deposition of faecal matter in terrestrial habitat. Huntley et al. (1991) suggested that respiration of Antarctic top predators may transfer back into the atmosphere as much as 20 to 25% of photosynthetically fixed carbon thus significantly affecting the ability of the Southern Ocean to act as a carbon sink. Quantitative information on top predator distribution was therefore important for the purposes of this Southern Ocean study of JGOFS.

Top predator studies and other JGOFS activities are mutually beneficial. The integrated ecosystem approach in JGOFS studies offers an excellent framework for gaining knowledge of the pelagic ecology of marine top predators, as their numbers and distribution can be viewed in the light of detailed physico-chemical and biological data of the environment. The obtained information can assist in the compilation of population estimates for Antarctic species and in the identification of particular environments or geographical areas on which they depend. Such information is needed in issues of management of the Antarctic environment, for example in the framework of the Convention on the Conservation of Antarctic Marine Living Resources.

Methods

Observations of seabirds, seals and whales were made from an outdoor observation post installed on top of the bridge of "Polarstern". The unobstructed clear view to all sides is a prerequisite for quantitative observations. For example, only from this position it is reasonably possible to identify which birds are associated with the ship and have to be omitted from quantitative density counts. Methods for bird observations are based on Tasker et al. 1984 and were described in van Franeker 1992. The advantages of this method as compared to the more conventional BIOMASS (1984) method have been evaluated in van Franeker (1990 and submitted). Birds as well as seals are counted in a band transect in time blocks of ten minutes from the moving ship. Ship speed and transect width can be used to convert observed numbers of animals to densities per unit of surface area for each ten-minute period. The width of the transect band usually was 300 m, taken as 150 m to each side of the ship. Depending on viewing conditions such as seastate, light level and glare, the transect band was adapted to allow optimal quantitative observations. For whales, line transect methods (Hiby and Hammond 1989) were prepared. Top predator observations were combined with studies of ice conditions (van Franeker, this volume). Apart from the ice observations according to the SO- JGOFS protocol, details on ice conditions within the transect band were noted for each ten-minute block of top predator observations. Records were also made of seastate and weather (e.g. cloud cover, precipitation). Results of 10 minute observations can be linked with 10 minute averages of all parameters stored in "Polarstern's" computer system (INDAS). Additional to the quantitative top predator counts, qualitative information

was collected on the occurrence of species outside transect band counts or observations at oceanographic stations.

Results

About 1300 ten-minute observations were conducted during the cruise. Systematic observations were started when approaching the northern end of the EPOS Leg 2 (1988-1989) study area at 57°S-49°W. Observations were conducted whenever daylight and weather conditions permitted, during Trans. 1 (eastward travel to JGOFS study area; 2 to 12 Oct) and Trans. 2 to 12 (north-south transects on or near 6°W; 12 Oct to 24 Nov.). Only a few systematic observations were conducted on the homeward voyage to Cape Town (Trans. 13; 24 to 29 Nov.). Polarstern's cruise track and the initial extent of sea ice are shown in Fig. 6.4.1. All quantitative data on top predators, as well as associated ice observations, have been summarised in the SO-JGOFS Surface Registration Database which is available to participants. Top predator data inserted into this database are total bird density plus separate densities for penguins, albatrosses and petrels, total seal densities, and finally whale numbers. Densities are given as number of animals per square kilometre for each ten-minute period when quantitative counts were made. It has to be emphasised that these figures are raw data on observed numbers of animals within the 300 m transect band. During further analysis, calculations will be made to assess the effects of obvious sources of bias. Some such sources of bias may be mentioned here since they also are indicative of interesting phenomena:

Cruising parallel along strong gradients:
During most of Trans. 1 "Polarstern" sailed to the east along the northern rim of the ice edge. During the observations it became evident that very often strong gradients existed of decreasing animal densities with increasing distance from the outer edge. At or very close to the ice edge, concentrations of for example Fur Seals and Chinstrap Penguins occurred, that were much less frequent at only a few hundred meters away from the ice. Analysis of this material requires a completely different scale as compared to analysis of data of the north-south transects perpendicular to such gradients. This paper will restrict itself to the larger scale phenomena that emerge from the north-south transects.

Concentrations of animals on icebergs.
The band-transect method used for counts will only produce representative results when the ship follows a more or less straight transect line, or at least does not systematically circumnavigate particular phenomena in the environment. Fortunately, "Polarstern´s" cruise track in the ice areas encountered during JGOFS largely conformed to this condition, or methods could be adapted to avoid bias in counting results. Icebergs however, have to be avoided and bergs in the intended cruise track were often circumnavigated at large distances of many hundreds to over a thousand meters, so way out of the transect band. Such icebergs, especially along the ice edge and further north in open water, often carried large concentrations of (Chinstrap) Penguins and sometimes petrels (Antarctic Petrel, Snow Petrel, Antarctic Prions). Avoidance of such bergs by the ship will inevitably result in an underestimate of densities by counts in the 300 m transect band. During the cruise, records were kept of approximate numbers of animals on bergs within 2 km distance and perpendicular distances of bergs to the ships track were noted. Analysis of these data will have to show whether such data are best included by line- or by band-transect methods.

Fig. 6.4.1 Study area cruise track and initial extent of sea ice (early Oct 1992)

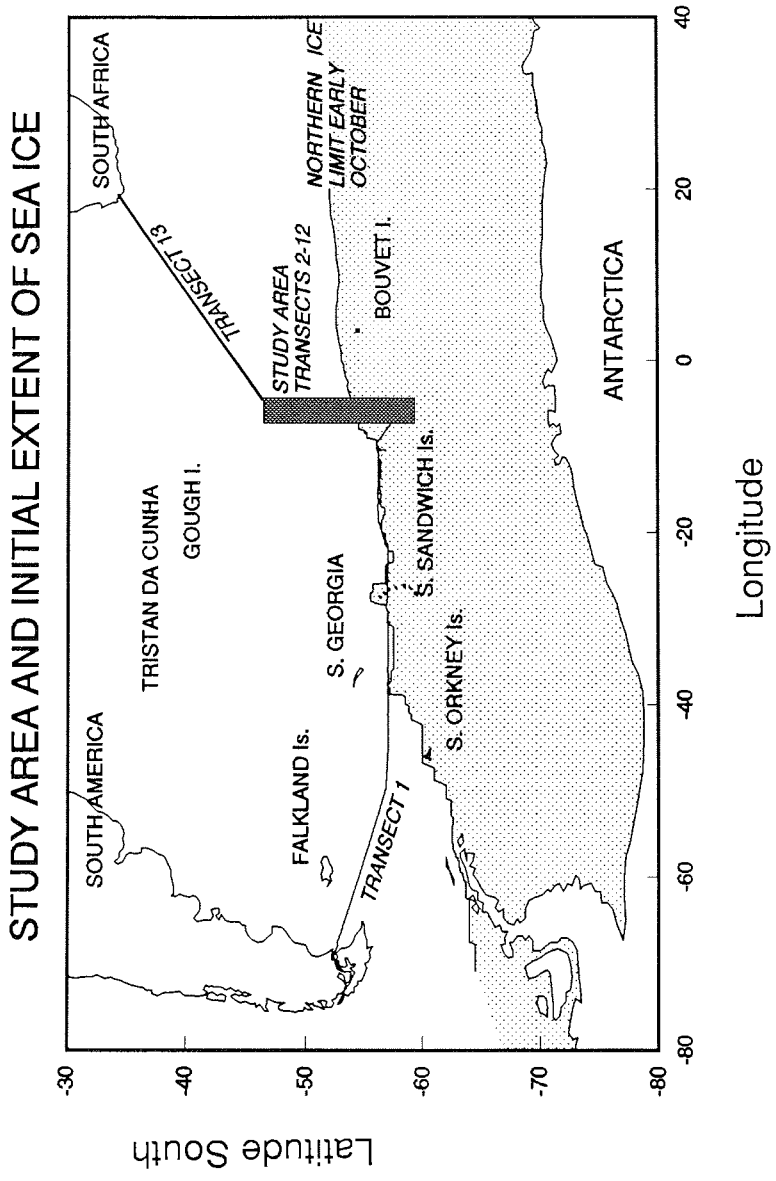

Data presented in this paper do not yet take animal concentrations on icebergs into account and thus underestimate densities.

Diurnal patterns.
Some species show diurnal patterns in activity that may bias results of observations. This problem is especially pronounced in Crabeater Seals which haul out onto the ice during day but enter the water for feeding later in the afternoon and during night time. From published data (Erickson et al. 1989) and personal observations during EPOS Leg 2 (van Franeker 1992) and SO-JGOFS, correction factors have to be calculated to correct data of observed numbers of animals for the time of observation. No such corrections have been applied here. The resulting underestimate for seal figures may be considerable and could be in excess of 50%.

Having acknowledged such possible sources of bias, a preliminary assessment of densities of top predators during SO-JGOFS can be made. Fig. 6.4.2 gives an overall impression of top predator densities during the north-south transects along 6°W (combined data for Trans. 2 to 12; 959 ten minute observations between 12 Oct and 23 Nov. 1992). Since sea ice cover, and in particular the ice edge were apparent major determinants of top predator distribution, data have been grouped according to distance from the ice edge at the time of observation. Information on birds has been displayed as separate densities for the major groups: penguins, albatrosses and petrels. Distances from the ice edge shown at the x-axis refer to outer limits of zones (for example, -25 km indicates the zone from 0 to 25 km north of the ice; -75 the zone of 25 to 75 km north of the ice, etc.). The importance of the ice edge in top predator distribution is evident in Fig. 6.4.2. Seals occurred almost exclusively in the ice zones. Close along the edge some Fur Seals were present, but generally the large majority of seals were Crabeaters, with a small admixture of Leopards and very occasionally Ross Seals. Chinstrap Penguins dominated the penguin group: almost all penguins around the ice edge and in open water up to considerable distances to the north were Chinstraps. Only around the Polar Front area far to the north they were replaced by Rockhopper and/or Macaroni Penguins and an occasional King Penguin. Deeper in the ice the Chinstraps were replaced by relatively low densities of Adelie Penguins and the odd Emperor Penguin. In a wide zone around the ice edge, and all the way into the ice, the petrel community was dominated by Antarctic Petrels, with also good numbers of Snow Petrels. In open water further north, the petrel group gradually became more diverse with many Antarctic Prions and local abundance of Southern Fulmars. Closer to the Convergence more species appeared with relatively high numbers of Soft-plumaged Petrels and regular appearance of Albatrosses (Light- mantled Sooty-, Grey-headed-, Black-browed-, and Wandering Albatross). The occurrence of small numbers of species from other bird groups, such as Arctic Terns, Dominican Gulls and Antarctic Skua's has not been shown in Fig. 6.4.2. Figures for whale observations are not given as no whales were observed during systematic counts. A very few Mink Whales were observed at stations along the ice edge or in the ice and a group of two or three unidentified whales was seen somewhat further north. Most whales were seen on the way back to South Africa (Trans. 13), among them a large group of Killer Whales and a spectacular Southern Right Whale. A list of bird- and mammal species observed is given as an appendix to this paper. The observed pattern of top predator distribution is rather different from the one observed in the western Weddell Sea during EPOS Leg 2 (van Franeker 1992). During EPOS, a rise in animal densities when entering the sea ice was observed similar to the one now, but densities remained high when travelling deeper

into the ice. For JGOFS, low densities of Adelie Penguins in the ice of the eastern Weddell Sea are mainly responsible for the decline in animal densities deeper into the ice. Distance from breeding areas might be an explanation for this lack of Adelie Penguins, which is supported by a high proportion of one year old animals among them. However, Chinstrap numbers seem much less affected by distance from colonies. Possibly the melting pattern of sea ice in the eastern Weddell Sea makes the area unattractive to Adelie Penguins.

Another interesting phenomenon emerging from Fig. 6.4.2 is that enhanced primary production in the Polar Front area was not reflected in a generally enhanced occurrence of top predators. In local areas high numbers of birds were observed, but without a straightforward pattern. Whether this means that primary production in this area is not converted to trophic levels available to top predators, or that there are other reasons for low top predator densities, is uncertain at this moment. It is evident however, that the carbon flux through the top predator component is relatively much lower in the Polar Front area than in the sea ice area where primary production seemed low and top predator densities high.

Overall densities of top predators were considerably lower in the SO-JGOFS area as compared to the EPOS area. Densities of both birds and seals in the eastern Weddell Sea as shown in Fig. 6.4.2. are only half to one-third of the densities observed in the western Weddell Sea in December 1988. Differences in distances from breeding colonies, but also characteristics of the structure, melting and flow patterns of sea ice, and related differences in productivity levels in water- or ice-biota may be explanatory factors that will have to be considered in further analysis. Seasonal phenomena may be partly responsible for the almost complete lack of whales in the SO-JGOFS study area. A preliminary assessment of estimated carbon requirements of top predators during SO-JGOFS is given in Fig. 6.4.3. Calculations were made by assuming an average daily fresh-food requirement of 850 grams for penguins, 800g for Albatrosses, 200g for Petrels and 16700g for Seals and an average 10% carbon contents of food. For details on methods to calculate fresh-food requirements see van Franeker (1992). Consumption rates vary from about 0.1 to 0.3 mgC/m^2/day in open water to about 0.5 to 1 mgC/m^2/day in ice covered areas. Higher carbon requirements in the ice as compared to top predator densities in that area are caused by the high energy demands of Crabeater Seals.

In further analysis, species specific consumption rates will be calculated. It has to be remembered that figures for density and carbon requirements are based on raw data not corrected for biases mentioned earlier, and are therefore preliminary minimum estimates that will be improved during later analysis. Comparisons of carbon fluxes to top predators with production in lower trophic levels should be made on a year round basis. Most of the species contributing significantly to top predator densities in Fig. 6.4.2 are present in the area and require similar levels of nourishment throughout the year. In an initial assessment of annual budgets, the above daily consumption rates may indicate that in ice areas a minimum of about 20 grams of photosynthetically fixed carbon per m^2 per year is required to support the top predator component (assuming a 1 mg per m^2 daily carbon requirement of top predators throughout the year; a top predator diet of half zooplankton and half fish; and a simple food chain of phytoplankton-zooplankton-(fish)-top predator with 10% efficiency in each level). Much lower requirements seem to exist in the open water areas, including the Polar Front.

Fig. 6.4.2 Average densities of top predators along transects 2 to 12 at 6°W

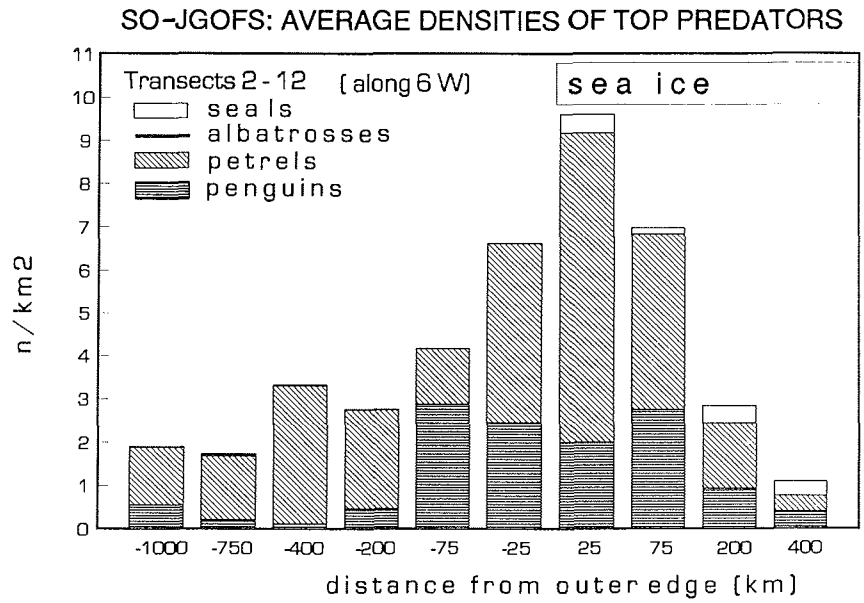

Fig. 6.4.3 Calculated carbon intake by top predators along Trans. 2 to 12 at 6°W

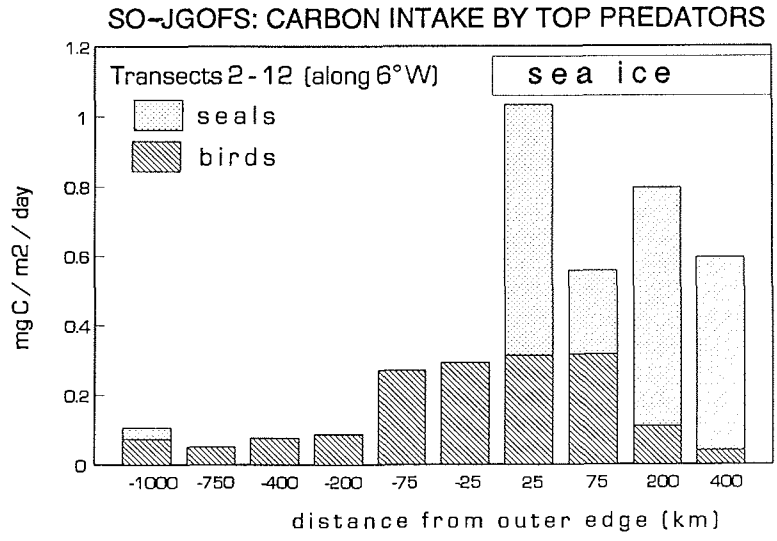

References

BIOMASS Working Party on Bird Ecology. 1984. Recording observations of birds at sea (revised edition). BIOMASS Handb. 18:1-20.

Erickson, A.W., Bledsoe L.J. and Hanson M.B. 1989. Bootstrap correction for diurnal activity cycle in census data for Antarctic seals. Mar. Mammal Sci. 5:29-56.

Hiby A.R. and Hammond P.S. 1989. Survey techniques for estimating cetaceans. In: Donovan G.P.(ed). The comprehensive assessment of whale stocks: the early years. Rep.Int.Whal.Comn (Special Issue II). Cambridge. pp 47-80.

Huntley M.E., Lopez, M.D.G. and Karl D.M. 1991. Top predators in the Southern Ocean: a major leak in the biological carbon pump. Science 253:64-66.

Tasker M.L., Hope Jones P, Dixon T and Blake B.F. 1984. Counting seabirds at sea from ships: a review of methods employed and a suggestion from a standardized approach. Auk 101:567-577.

van Franeker, J.A. 1990. Methodes voor het tellen van zeevogels op zee: een pleidooi voor vergelijkend onderzoek. SULA 4:85-89.

van Franeker, J.A. 1992. Top predators as indicators for ecosystem events in the confluence zone and marginal ice zone of the Weddell and Scotia seas, Antarctica, November 1988 to January 1989 (EPOS Leg 2). Polar Biol. 12:93-102.

van Franeker, J.A. (1994). Sea ice cover and icebergs. (this volume)

van Franeker, J.A. (submitted). A comparison of different methods for counting seabirds at sea in the Southern Ocean.

LIST OF SPECIES OBSERVED

Species observed only near the continental areas of South America and South Africa have been omitted.

PENGUINS		
Aptenodytes patagonicus	King Penguin	Polar front, rare (4)
Aptenodytes forsteri	Emperor Penguin	Pack ice, occasional (12)
Pygoscelis adeliae	Adelie Penguin	Pack ice, common
Pygoscelis antarctica	Chinstrap Penguin	Ice edge, abundant
Eudyptes chrysocome	Rockhopper Penguin	Polar front, regular
Eudyptes chrysolophus	Macaroni Penguin	Polar front, regular
ALBATROSSES		
Diomedea exulans	Wandering Albatross	open water/Polar Front, regular
Diomedea melanophris	Black-browed Albatross	open water/Polar Front, regular
Diomedea cauta	Shy Albatross	north of study area only, incidental
Diomedea chrysostoma	Grey-headed Albatross	open water/Polar Front, regular
Diomedea chlororhynchos	Yellow-nosed Albatross	north of study area only, incidental
Phoebetria fusca	Sooty Albatross	open water/Polar Front, rare
Phoebetria palpebrata	Light-mantled Sooty Albatross	open water/Polar Front, regular
PETRELS AND SHEARWATERS		
Macronectes giganteus	Southern Giant Petrel	ice + open water, regular
Macronectes halli	Northern Giant Petrel	open water north, regular?
Fulmarus glacialoides	Southern Fulmar	open water, common
Thalassoica antarctica	Antarctic Petrel	pack-ice and (off) ice edge, abundant
Daption capense	Cape Petrel	open water, regular
Pagodroma nivea	Snow Petrel	pack-ice and ice edge, abundant
Pterodroma macroptera	Great-winged Petrel	north of study area only, occasional
Pterodroma lessoni	White-headed Petrel	Polar Front, incidental
Pterodroma brevirostris	Kerguelen Petrel	off ice edge up to Polar Front, regular
Pterodroma mollis	Soft-plumaged Petrel	Polar Front, common
Pterodroma incerta	Atlantic Petrel	Polar Front, occasional
Halobaena caerulea	Blue Petrel	open water, common (locally abundant)
Pachyptila desolata	Antarctic Prion	open water, abundant
Procellaria aequinoctialis	White-chinned Petrel	open water, incidental
Calonectris diomedea	Cory's Shearwater	north of study area only, incidental
Puffinus gravis	Great Shearwater	Polar Front, occasional
STORM- AND DIVING PETRELS		
Oceanites oceanicus	Wilson's Storm-petrel	rare (1)
Fregretta tropica	Black-bellied Storm-petrel	open water, common
Fregetta grallaria	White-bellied Storm-petrel	Polar Front, occasional
Pelecanoides sp.	Diving petrel spec.	Polar Front, common
OTHER BIRDS		
Larus dominicanus	Dominican Gull	ice edge, incidental
Catharacta skua lonnbergii	Antarctic Skua	open water, incidental
Sterna sp. (paradisea)	Tern spec. (Arctic)	pack ice and ice edge (common Nov.)
SEALS		
Lobodon carcinophagus	Crabeater Seal	pack ice and ice edge, common
Hydrurga leptonyx	Leopard Seal	pack ice, regular
Ommatophoca rossii	Ross Seal	pack ice, incidental (4)
Arctocephalus gazella	Antarctic Fur Seal	ice edge, regular
WHALES		
Balaenoptera acutorostrata	Mink Whale	pack ice and ice edge, rare (4)
whale sp??	medium to large whale	open water, rare (2) (plus some north)
Eubalaena australis	Southern Right Whale	north of Polar Front, rare (1)
Orcinus orca	Killer Whale	north of study area only (group of >15)

5. Hydrography and dissolved inorganic chemistry

5.1. Hydrography

C. Veth, R. de Koster, S. Ober. (NIOZ)

The southern Atlantic Ocean is characterised by zonally structured series of watermasses separated by frontal regions. In the area of investigation between 47-60°S near the 6°W meridian the following watermasses are found. At the far southern end the northernmost part of the Weddell Gyre is separated from the Antarctic Circumpolar current by the ACC-Weddell front and at the northern end of the section the Polar Front is the boundary between the southern Antarctic Circumpolar Current and the northern equivalent. Sections through the ACC including the frontal zones have been measured before at different longitudes, in particular in the Drake Passage (Sievers and Nowlin, 1984) and near the Greenwich meridian (Whitworth and Nowlin, 1987), the latter being close to the area under investigation. In the present study more attention is paid to smaller details in the section between 47-60°S and the evolution of parameters over a period of seven weeks during spring. Near the ACC-Weddell front the melting of ice is an important parameter determining the structure of the water column. The interaction of the meandering frontal zone with the outer parts of the sea-ice field is clearly visible from satellite pictures at places where the ice-edge is near to the frontal zone. The eddy activity, which is also known from studies in the Weddell-Scotia area of the Southern Ocean is a feature related to frontal zones. In this region it is known that the fronts extend down to the bottom, which means that one can expect instabilities to find place at different depths, but not necessarily synchronised. As a consequence of that one may expect complicatedly structured profiles of temperature and salinity near the frontal zones. This may even cause strong interleaving of watermasses of different origin which penetrate through isopycnal surfaces. This interleaving may play an important role in the export of carbon-dioxide through the sinking of algae which have been transported through interleaving to levels where primary production is prevented because of lack of sufficient light.

Objectives.

The main goal of the physical research in this region is the establishment of the physical framework in which the evolution of the local ecosystem takes place. In practise that means that the structure of the water column is measured at different places and times in such a way that the spatial structure of the water column in this sea area and the evolution with time of that structure is known. In particular quantities as the depth of the wind-mixed layer, the sea surface temperature etc. are forcing functions for the primary production of phytoplankton. To reach this goal, a number of transects had to be measured several times. The repetition is necessary to investigate the influence of the forcing parameters of the physical system as the wind speed, amount of global radiation, ice-cover, etc. These data will be used for validation of a one-dimensional wind-mixed layer model which was developed with data from the EPOS-project (leg 2). The model predictions will be used in a coupled physical-ecophysiological model. For this study measurements of the structure of the water column down to 200 m are enough. To study the influence of frontal effects on the structure it is necessary to look deeper and a combination of shallow and deeper casts are necessary, down to 1500 m. The required data must be obtained in a series

of transects over the ice-edge during the period of ice retreat and over the frontal zones under investigation.

Work at sea.

During this project a CTD/Rosette-system of The Netherlands Institute for Sea Research was used consisting mainly of:

In situ:
-CTD-type: Seabird SBE9 plus with temperature, conductivity and depth sensor, the sample frequency is 24 Hz.
-Dissolved oxygen sensor
-Fluorometer (Chelsea Instruments Aquatracka)
-Transmissometer (Sea Tech, 25 cm)

Water sampling:
-Rosette: General Oceanics 24 positions steppermotor
-For normal work NOEX and NISKIN bottles
-For ultra-clean sampling GoFlo bottles
The rosette frame is teflon coated stainless steel for ultra clean sampling.

Deck unit: SBE11 plus
Seabird software was used.

For the CTD-sensors pre-and post calibration is done by Seabird Electronics Inc. During the cruise in situ calibration is done with electronic reversing thermometers and pressure meters (SIS) and bottle analysis of salinity with a Guildline Autosal model 8400A using standard sea water ampules.

A total of 248 CTD-casts were carried out. Almost 60.000 liter seawater was brought on deck to meet the demand of 50 craving scientists. CTD-data were processed directly after the cast and the profiles of different parameters were available together with the data measured simultaneously with the closing of a sample bottle. The data were transferred into the data-base.

CTD-casts down to a depth of 1500 dbar took place in general at latitude intervals of half a degree, with extra casts for incubation work at each whole degree. A number of deep stations to the bottom have been done and casts for special water requirements.

Preliminary results.

Comparison of the hydrographical data from the CTD-system shows that the general features found near the Greenwich-meridian (Whitworth and Nowlin,1987) are also found at the 6°W meridian. The whole pattern is shifted about 2 degrees to the north, but even small details are similar. Clearly visible is the Winter Water layer which reaches the surface in the ice-covered part and places where recently ice has melted (Fig. 6.5.1) and is found under a warmer layer (Fig. 6.5.2) more north. The North Atlantic Deep Water is found in the deeper layers. Because the section is worked with a denser spacing, more structure is visible, in particular near the frontal zones, where intervals of $^1/_4$ degree were applied. The details show that the fine-structure near the

fronts may be related to eddy activity, as well as at the Polar Front as the ACC-Weddell front. In the profiles near the frontal zones traces of interleaving are clearly visible and often distinct layers of water from possibly different origin lay on top of each other (Fig. 6.5.3). Transmissiometer readings and fluorometer readings show often discontinuous jumps over the boundaries of these layers, indicating that the phytoplankton is from different watermasses. Higher turbidity was regularly found in the subsurface layer.
The plots of isopleths of salinity (Fig. 6.5.1) and temperature (Fig. 6.5.2) show the melting of the sea-ice and the subsequent growth in sea-water temperature after the melting. In contrast to the situation during EPOS leg-2 on which the wind-mixed layer modelling was based, the ice-edge did not retreat in a simple way but melting took place in a large area and ice was blown by the wind in all directions, which has consequences for the determination of the contribution of the fresh water input to the stability (Fig. 6.5.3) of the water column.
The area between the fronts is an area with strong wind forcing which shows up in the depth of the wind-mixed layer.

References

Sievers, H.A. and W.D. Nowlin, Jr. (1984) The stratification and water masses at Drake Passage. J. Geoph. Res. 89(11): 489-514.
Whitworth III, Th. and W.D. Nowlin, (1987) Water Masses and Currents of the Southern Ocean at the Greenwich Meridian.

Fig. 6.5.1 Section of salinity along Trans. 11.

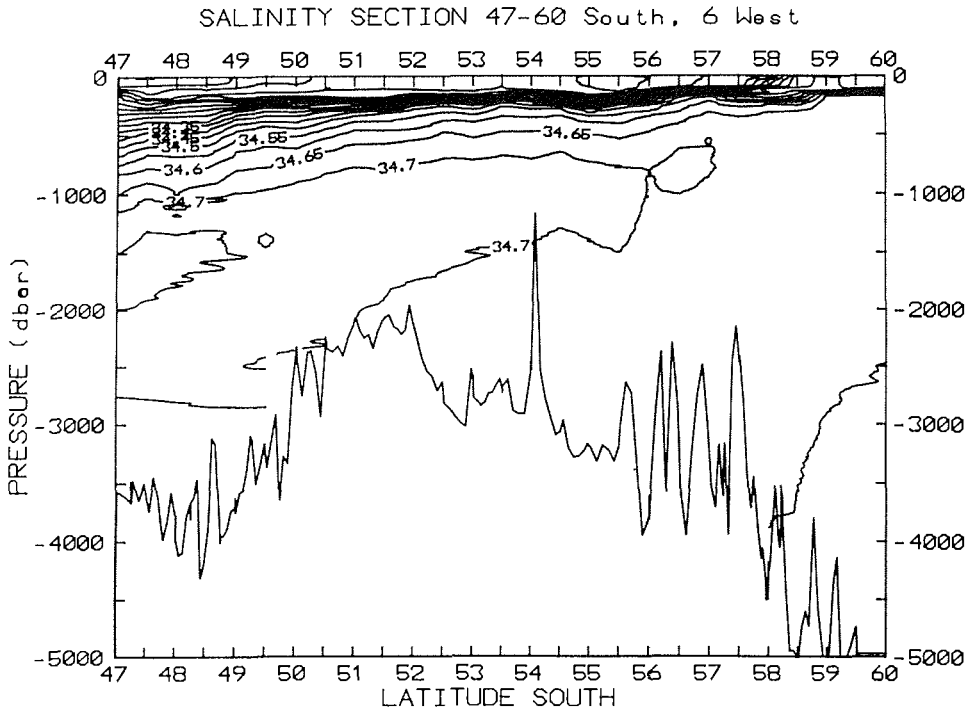

Fig. 6.5.2 Section of temperature along Trans. 11.

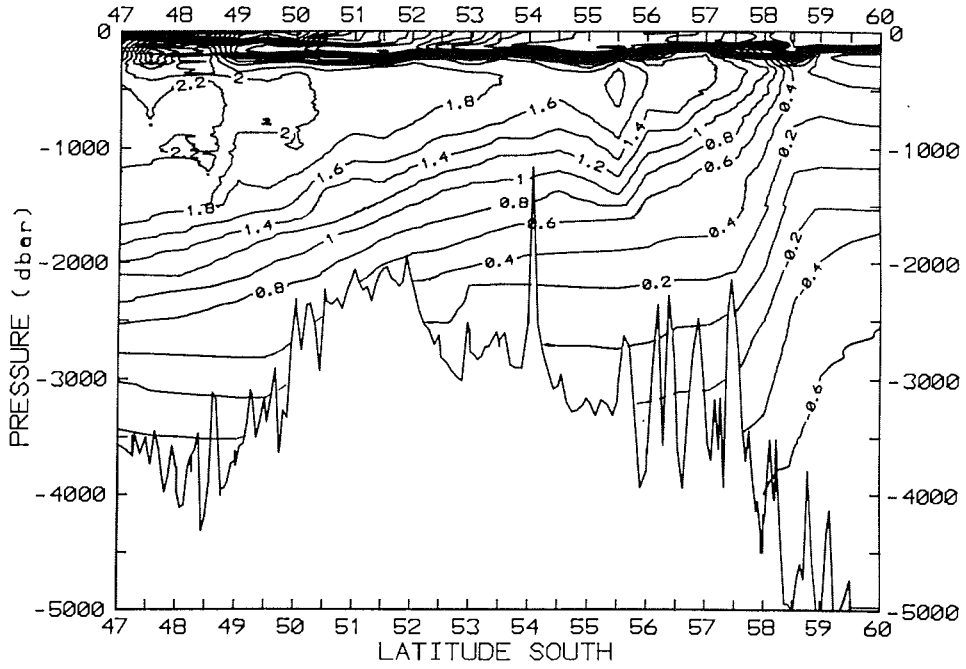

Fig. 6.5.3 Section of potential density along Trans. 11.

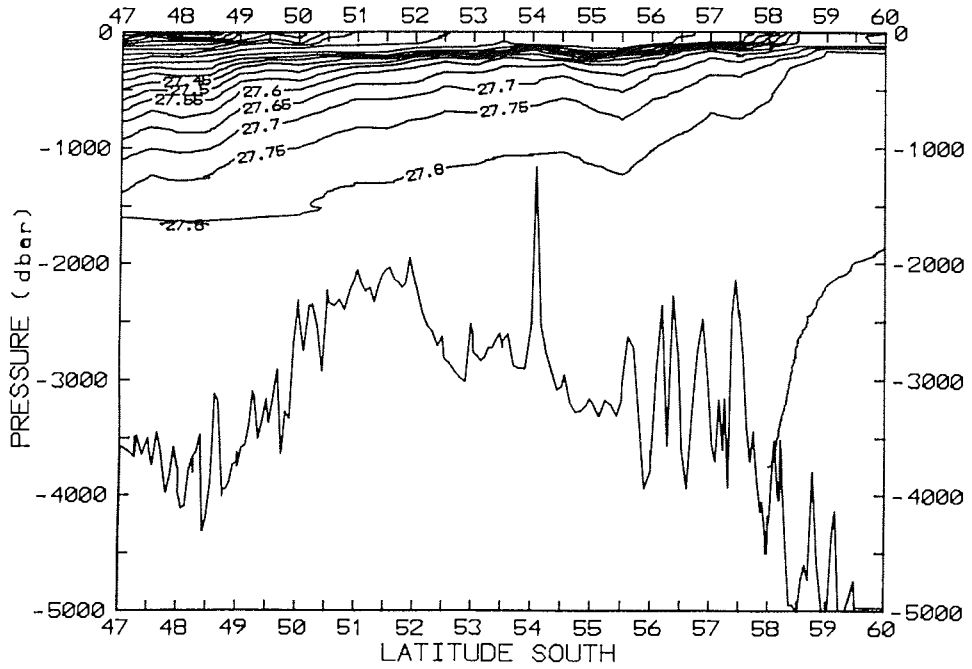

5.2. Dissolved oxygen

R. Manuels (NIOZ)

Method

Oxygen samples have been taken and analysed as duplicates according to the Winkler method, following the recommendations described in WOCE Hydrographic Program "Operations and Methods (July '91), with the exception of a calibration method described below, and using a photometric High Precision Oxygen Titrator. Titrations have taken place in, with great precision calibrated, whole flasks. Firstly preservation of the chemicals and sodiumthiosulphate calibration standard during storage for several months under extreme circumstances asked for adequate precautions. Secondly, during the cruise, because of the very cold ocean water in the Antarctic region, a gas bubble problem had to be solved. Both issues will be discussed in this report.

Standardisation of the Winkler High Precision titration.
Consulting the WOCE Hydrographic Program "Operations and Methods", chapter "Dissolved Oxygen", we notice major deviations between the proposed calibration procedures and that of Tijssen (1981). Previously Van Bennekom and Manuels have tried to convince the author, Dr. C.H. Culberson, that weighing all the chemicals, including the calibration solutions, gives the best results. In this manner many volumetric correction formulas do not have to be used. It allows the use of a calibration method during the cruise by weighing small amounts of a stock solution of KIO_3 in oxygen flasks that have been closed by PVC stoppers and transported very carefully. These solutions have proven to be stable several months after preparing them. During preparation all the solutions are being filtered over Whatman GF/F-filters. Preservation of the $Na_2S_2O_3$-solution takes place in thoroughly cleaned 1-liter brown flasks, in which 0.5 ml chloroform has been added and that are to be stored by 4°C.

Bubbles.
Gas bubbles emanated from in the samples after preparing them under normal laboratory temperature circumstances. Because of the coldness of Antarctic ocean water, in this period of the year even below -2°C, the samples contain much dissolved gases. The last step during a titration, following the Winkler method, is to add 20N H_2SO_4-solution until a pH of about 2 has been reached. The precipitate dissolves by stirring but at the same time, in samples at about 20°C, many gas bubbles start to come out of the iodine coloured solution and disturb the titration completely. Therefore the titration procedure has to be standardised at low temperatures. During titration the temperature of a sample should not increase above 10°C. As the light beam through the iodine solution causes a quick increase of the temperature due to absorption of the light, samples have been stored under water in a water bath at 4-5°C and the titration program modified as to allow the quick pre-addition of about 90% of the titration solution. The oxygen flasks should have completely flat bottoms so that stirring at high speed can take place without causing extra bubbles. Only stirring at high speed yields good titration curves on an in-line recorder. To avoid condensation of water vapour from the humid laboratory air on the wall of an oxygen flask dry compressed air was blown through the cuvet house.

Calibration.
The Sodium Thiosulfate solution was calibrated on shipboard. Because of the already known oxygen values in the Antarctic region the titre of the $Na_2S_2O_3$-solution has been chosen to be about 0.2000. On board every week this value has been calibrated as the mean value out of three oxygen flasks as described above. The titre of the first flask has been calibrated three times, they were 0.1953, 0.1952 and 0.1953. The titre of the second flask has been calibrated also three times, they were 0.1948, 0.1949 and 0.1949. Before using this standard a few drops of chloroform have been added. The titre of the third flask has been calibrated two times, they were 0.1950 and 0.1950. Before using this standard a few drops of chloroform have been added as well.

Seawater blanco.
From the first station after leaving Punta Arenas (Sta. 857) and at each so called "meso-station" during the two main transects from 11 until 31 October 1992 at two or more depths out of each 1500 m cast and each deep water cast two or more sea water blanco's have been sampled. Values were very reproducible and virtually perfect replicates of the mean value of 0.8 mmol/l O_2. Together with the described method of titre calibration subtraction of this mean value from each oxygen value measured during ANTX/6 should lead to accurate final values. Because of correction of the dissolved oxygen values the temperature of the samples during addition of $MnCl_2$- and NaOH/KI-reagents and the temperature of the $Na_2S_2O_3$-solution during titration have been measured. The concentration of dissolved oxygen, determined from whole flask titrations has been calculated from the following equation

$$O_2 = \frac{Ml_{thio} * Titre_{thio} * [1-0.00025(T_{thio}-20)] * 10^6}{4 * [V_{20}(1+0.00001 * (T_{sample}-20))-3]} - 1.05\ \mu mol/l$$

where, 0.00025 and 0.00001 are cubic coefficients of thermal expansion of water and borosilicate glass,
T_{thio}= Temperature of the titrant during titration,
V_{20}= Volume of an oxygen flask at 20°C,
T_{sample}= Temperature of a sample during addition of the reagents, that cause the precipitation, immediately after sampling, 3 ml have to be subtracted from the corrected V_{20}, because of the addition of the reagents that cause the precipitation,
1.05 = empirical constant derived from the amount of oxygen found in the reagents that cause the precipitation. This amount increases the end concentration and should therefore be subtracted. Ml_{thio} and $Titre_{thio}$ are corrected according to WOCE Hydrographic Program "Operations and Methods".

Throughout the cruise we always used clean and "dry" oxygen flasks. The flasks were rinsed occasionally with a detergent solution to keep them free of grease. Dispensers were of top quality, without air bubbles and with clean tips. The samples were always shaken twice, the second time at least 15 minutes after the addition of the $MnCl_2$- and the H_2SO_4-solution.

Results.

After having solved the start-up problems about 1600 oxygen samples have been taken at all meso-stations and analysed as duplicates. Routinely the duplicates differ

~0.1% of the highest values of 370 µmol/l that have been measured in the northern part of the four main transects, from deep in the ice at 60°S until 47°S, along the 6°W meridian. As an example dissolved Oxygen concentrations for Trans 11 are shownSmall titration problems leading to less then optimal duplicates have been caused by the occasionally instability of the fine main electrical power circuit on board RV POLARSTERN. The cause of these instabilities remained a mystery which could not be found and solved, despite the intensive searching of the electricians of the ship.
In collaboration with Peter Bjornsen, Frank Jochem, Paul Kähler and Anke Weber three incubation experiment programs have taken place. Objectives of these programs and the first results are published elsewhere in this report. All dissolved oxygen data have been stored in the NIOZ-data base SHIPMAN and will be available as soon as possible after the cruise as appointed between the members of ANT X/6. Plankton blooms cause changes in the content of dissolved oxygen. These changes can be easily calculated, as percentage of the 100% value, with the help of this data base.

Culberson, C.H. (1991) Dissolved Oxygen, chapter in: WHP Operations and methods - July 1991.

Fig. 6.5.4 Section of dissolved oxygen [µM] along Trans. 11.

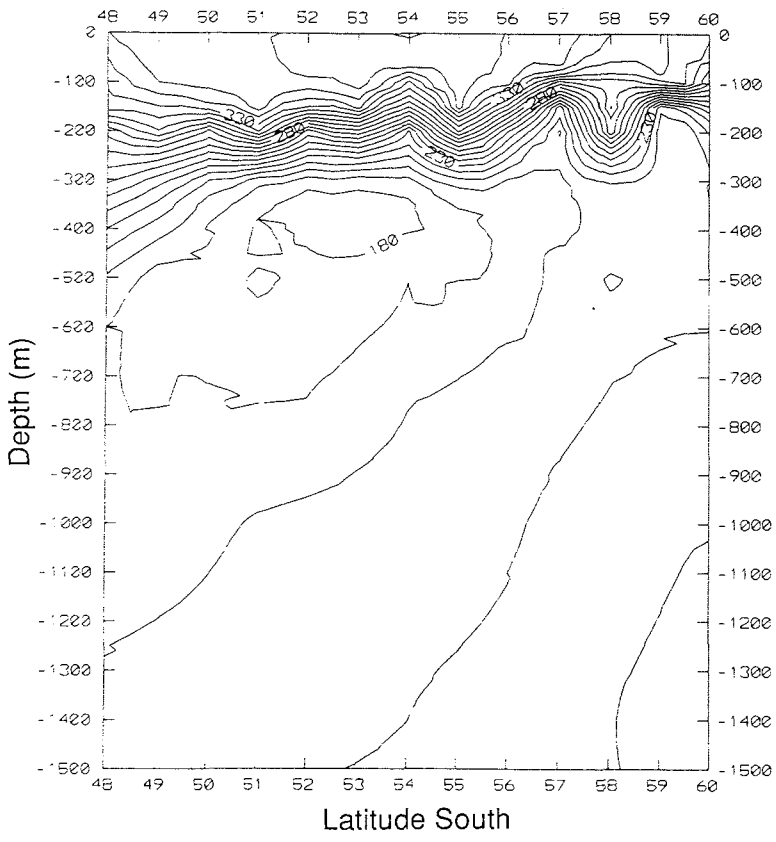

5.3. Nutrients

K. Bakker (NIOZ), P. Fritsche (IFM), J. Poncin (IEM)

Samples collected by the CTD rosette sampler as well as many samples of shipboard incubation experiments were analysed for nutrients. Measurements of ammonia were done by the hand method (Poncin, see below). Silicate, nitrate, nitrite and phosphate were analysed by Bakker and Fritsche with a Technicon AAII auto analyser kindly provided on loan from the nutrient group of Dr. G.Kattner AWI. We are very grateful to this group also for their preparations of the instrument and accompanying standards which we used as an additional reference.

Procedure

The samples were analysed using daily prepared standards diluted from stocks into artificial "seawater" (ASW) of the same total salt content as the samples (using NaCl as the salt and demineralized water with resistivity 18MOhm as the diluent). ASW was also used as wash water between the samples as to avoid matrix problems on the auto analyser. Blank measurements of ASW obtained values below the detection limits for phosphate, nitrate, nitrite and silicate.

Samples were as soon as possible taken in polyethylene bottles and measured within 12 hours after collection; in the meantime they were kept cool and dark in a refrigerator at 2°C. Volumetric flasks for dilution were pre-calibrated giving linearity with correlation coefficients of at least 0.999 for 4 calibration points.

For the CTD/Rosette profiles the maximum sample value was compared with the full scale standard value to obtain optimum resolution of the system. Along with every run of CTD/Rosette samples were put in a standard mixture containing a stable nutrient-cocktail representing all the parameters in order arrive at an independent control of overall accuracy. This cocktail is also used routinely in other Dutch JGOFS cruises as to arrive at a uniform quality global data set. In the near future it will be very useful to have such a standard as an international reference in order to harmonise the results between all JGOFS cruises. The independent cocktail of nutrients ran daily as a standard has proven very useful also within the context of the own cruise. For some phytoplankton growth experiments with low nitrate uptake the initial values showed a noisy trend between 28.6 µM and 28.2 µM but after statistic adjustment to the running mean of the cocktail we found much more significant trends in time for this experiment. Obviously this alleviated the problem that the in-run precision at any given day is much better than the accuracy between runs/days. For stronger nitrate uptakes this is off course off less important, the signal being much greater than the offset between runs.

The samples were measured with a sample rate of $30hr^{-1}$ using 80 seconds sample- and 40 seconds wash-time to reach a steady state level, while an online computer was attached to the system doing the calculations such as a correction for baseline- and gain drift. The gain drift correction sometimes was necessary, because even during short runs of no more than 50 measurements the last standard would be a bit higher than the one at the beginning (in front of the samples). This difference was caused by evaporating of water from the cups due to the low relative air humidity in the lab. Air humidity was very low; about 48% rel. humidity at 47°S, likely lower again towards the south. We measured the evaporation of a standard in a sample cup

under those conditions during 5 hours. Not surprisingly we found ~7% higher values for all the nutrients in this standard cup directly followed by a fresh standard cup with the same standard. Hence we were forced to run the samples as quickly as possible after putting them in cups, maximum 50 cups in a run.

The methods used for the various nutrients were:
- Silicate: Measured as the reduced molybdenum blue complex at 660 nm, with ascorbic acid as reductant; using oxalic acid to eliminate the phosphate interference.

- Ortho-phosphate: Formation of the reduced molybdo-phosphate complex at pH 0.9-1.1 whereby potassium-antimonyl tartrate was used as a catalyst and ascorbic acid as reductant. The developed colour was measured at 880 nm. The method has been described by Murphy and Riley.

- Nitrate and nitrite: Nitrate was reduced to nitrite using a copperized cadmium coil (reduction>95%) with imidazole as buffer agent. Used were two channels, one for nitrate plus nitrite with a cadmium coil in the first stage sample line, and the other for nitrite alone, using the same colour reagent for both. The pink colour was formed after diazotation with sulphanilamide and naphtylethylenediamine measured at 550 nm for both channels; nitrate was obtained by subtracting the nitrite values from the first channel.

Using these methods our overall statistics for this cruise were:

Detection limits:	precision:		accuracy:	
silicate	0.4µM	0.4µM	100.0µM +/-	1.5µM
o-phosph	0.01µM	0.02µM	2.0µM +/-	0.05µM
nitrite	0.005µM	0.01µM	0.5µM +/-	0.01µM
nitrate	0.15µM	0.30µM	30.0µM +/-	0.5µM

Results:

In total about 5500 samples measurements were made for phosphate, silicate, nitrate and nitrite with standard methods run on a Technicon AAII auto analyser. About 65% of the samples were collected by a CTD rosette sampler. Shown as an example are sections of silicate, nitrate and nitrite drawn by hand for Trans. 11 (Fig. 6.5.5). The silicate data in the deeper water column were used as a check for leaking samplers. Similar checks were done for nitrite data for the upper layer above 150 m with mean NO_2 values of 0.3 µM NO_2, the same check was done for checking the Gerard samplers of the geochemistry group.

About 35% of the measurements were done in samples taken from miscellaneous experiments such as assessments of primary production, biogenic silicate production, phytoplankton growth versus grazing and others. Because of the wide variety of sample types we adhered to a strict rule of putting a simple code on the sample bottles (one letter followed by a number from 1 to 1000) as to avoid mix-up of samples.

Fig. 6.5.5 The distributions of phytoplankton nutrients a) silicate, b) nitrate c) nitrite, and (next page) d) phosphate along the Trans. 11 (Sta. 930 - 969)

a)

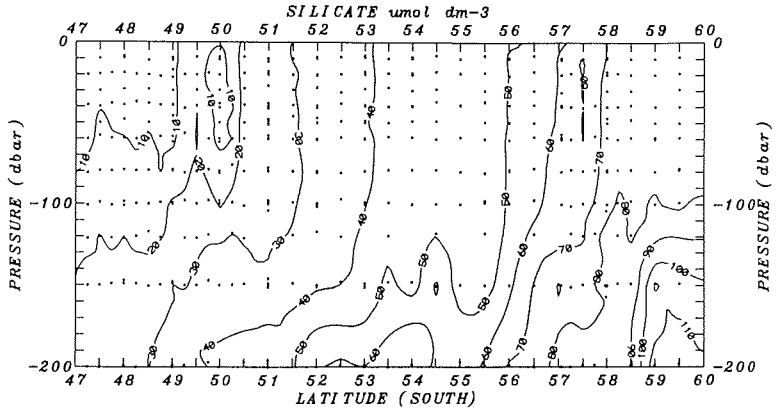

b)

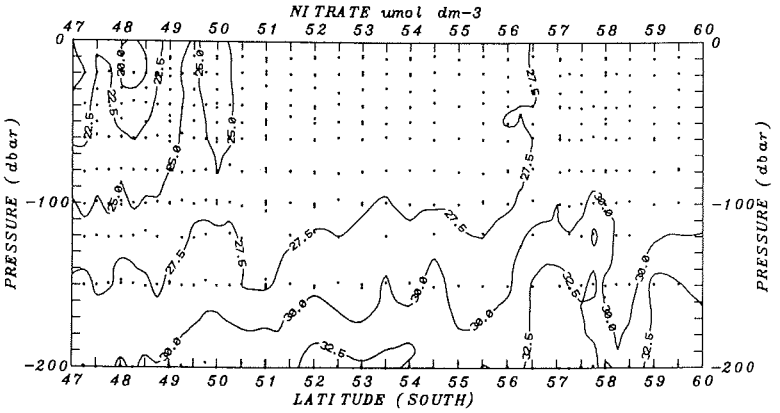

c)

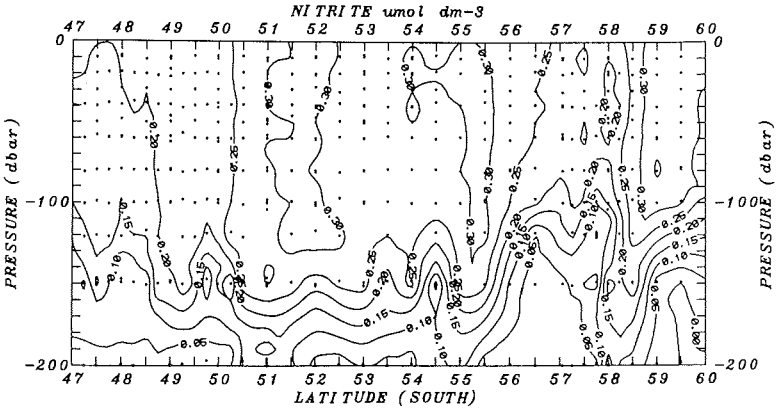

Fig. 6.5.5d)

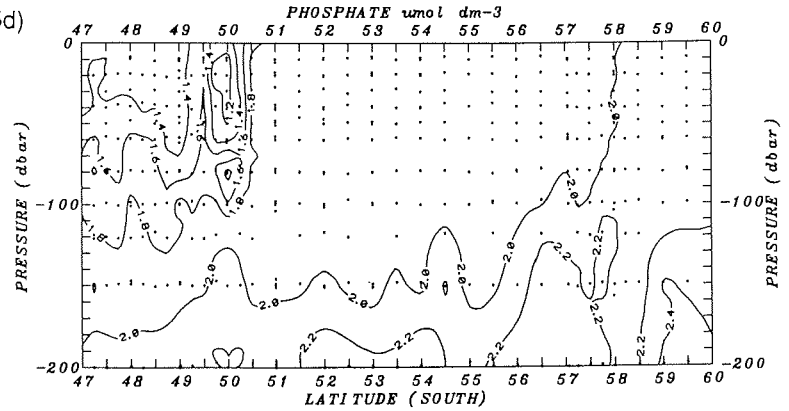

5.4. Ammonium

J. Poncin (IEM)

Sampling was carried out at each station, between 10 and 300 m (10-20-30-40-60-80-100-150-200-300 m). Additional sampling, without ammonia, was carried out at 1000 and 1500 m for reasons indicated below.

Method

Ammonium concentrations were determined manually as described by Koroleff (1976). In order to prevent contamination and/or evolution of this substance over time, samples were immediately mixed with reagents, then stored in the dark. At room temperature, it was necessary to wait for 14h before dosage. This time could be decreased to 8h when maintained at 27°C (when sampling was more frequent). Ammonium concentrations in samples were determined with reference to standards (0.1 to 1 µM), prepared two-fold in freshly prepared deionized water. Water sampled from 1000-1500 m was used for reference (zero concentration in ammonium). Detection limit of the method and precision are of the order of 0.02 µM.

Results

Ammonium concentrations in the study area were not high (0.86 µM maximum) and values were often between 0.05 and 0.15 µM, which is low compared to other Antarctic areas. Ammonium concentrations of 1 µM or more have indeed often been recorded in the Ross sea (Biggs et al. 1985), the Scotia Weddell area (Rönner et al. 1983), and in the Indian Ocean sector (Verlencar et al. 1990).

The highest values (NH_4 max=0.86 µM) were measured between 47°S and 51°S (Trans. 11- Fig. 6.5.6) and at 59°S (Trans. 6 and 11 NH_4 max=0.59 µM). In this last area which corresponds to Weddell Gyre water special bacteria or heterotrophic activity have not been noticed (in first preliminary). Perhaps these ammonium concentrations are due to different characteristics of the water masses.

Other lower but significant peaks were noticed:

(i) To the east of the Sandwich Island (57°S, 30°W -NH_4 =0.25 µM between 20 and 80 m).
(ii) Between 57° and 58°S (NH_4 max=0.23 µM at 80-100 m) during Trans. 2 in the closed pack- ice zone.
(iii) Between 51°30 and 52°S (0.3 to 0.39 µM from 10 to 150 m) during Trans. 5 in the permanent open ocean zone.
(iv) At 58°S (0.2 to 0.3 µM between 150 and 200 m) during Trans. 6 and 11 in the marginal ice zone.

Fig. 6.5.6 The distribution of ammonia along Trans. 11.

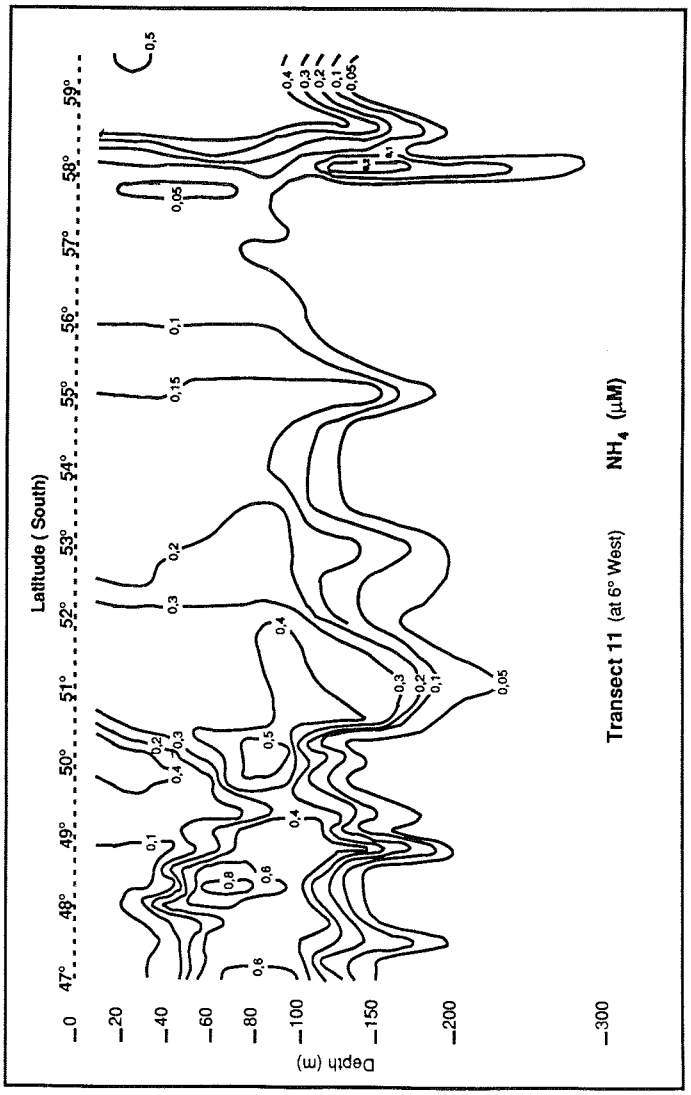

Of special interest is the increase of ammonium during three weeks in the same zone (Trans. 5 and 11) as concentrations between 47°S and 52°S increased by about 50% (on average).

Reference

Koroleff, F. (1976) Determination of ammonia. In: Grasshoff, K.(ed.) Methods of seawater analysis. Verlag Chemie, Weinheim, p. 126-133.
Biggs, D; Anos, A. F.; Holm-Hansen, O. (1985) Oceanic studies of epipelagic ammonium distributions: the Ross Sea ammonium flux experiment. In: Siegfried, W.R., Condy, P.R., Laws, R.M.(eds): Antarctic nutrient cycles and food Webs. Springer-Verlag, Berlin, pp. 93-103.
Rönner, U.; Sörensson, F.; Holm-Hansen, O. (1983) Nitrogen assimilation by phytoplankton in the Scotia Sea. Polar.Biol. 2: 137-147.
Verlencar, X. N.; Somasunder, K.; Qasim, S. Z. (1990) Regeneration of nutrients and biological productivity in Antarctic waters. Mar. Ecol. Prog. Ser. 61: 41-59.

6. Carbon dioxide system

6.1. Total Carbon dioxide

M. Stoll (NIOZ)

Total carbon dioxide in discrete samples was determined by the Coulometric method (Johnson et al., 1987). Samples were poisoned with 0.05 - 0.1 ml of saturated mercury(II) chloride solution to prevent changes due to biological activity. They were than analysed with an automated extraction line. A subsample is acidified with 8.5% phosphoric acid and bubbled through with CO_2-free nitrogen gas. The released CO_2 gas is captured in ethanol-amine solution with an indicator which is photometrically backtitrated. Standards reference seawater as supplied by Dickson were determined regularly as a quality control check. Precision amounts to ≈ 1.5 µmol/kg. Overall 1454 samples were analysed and the results entered into the ANT X/6 database.

6.2. Alkalinity

J. Rommets (NIOZ)

For the determination of the alkalinity 125 ml sea water samples were titrated at 20°C with 0.1 M hydrochloric acid in a closed cell modified after Bradshaw and Brewer (1988). A Gran plot was made of the data points after the second equivalent point. For the calculation the constants of Goyet and Poisson (1989) were used. About five samples could be analysed in one hour with an accuracy of 1 micro-equivalent per kg seawater. Most of the samples were taken at the full degree mesostations at 20, 40, 60, 80, 100, 150, 200, 300, 500, 1000 and 1500 m, occasionally until the bottom. Overall more than 800 samples had been analysed.

References

Bradshaw, A.L. and P.G. Brewer (1988) Mar. Chem. 34: 155-162.
Goyet, C. and A. Poisson (1989) Deep-Sea Research 36(11): 1635-1654.

Objectives

The research on the partial pressure of CO_2 consisted of two parts:

A: Underway measurements of the partial pressure of CO_2 (pCO_2) in surface water and marine air throughout the cruise from 57°S30°W (5 Oct 92) to 43°S3°W (26 Nov. 92). Once combined with data on salinity, temperature, chlorophyll and nutrients, the results will provide information on the effect of different watermasses, ice melting and biological activity on the CO_2 system of surface waters. The CO_2 flux between the atmosphere and the ocean will be calculated by using the Liss-Merlivat relationship, which multiplies the partial pressure difference between both media by a temperature and wind speed dependent coefficient. The temperature of the upper surface layer of the ocean was registered by an infrared pyrometer as to allow the flux calculations.

B: Discrete samples were taken from the CTD together with O_2, total CO_2 and alkalinity. Combination of pCO_2 with total CO_2 and alkalinity will show the accuracy of the data-set. CTD-profiles of CO_2 components will give information of the watermasses and on biological processes. They will be integrated with the underway measurements. CO_2 chemistry of the brine has been investigated at the two ice stations.

Methods

A: Continuous measurements of pCO_2
Seawater was pumped continuously from 12 m below sea level to an equilibrator. The temperature difference between water at the intake and in the equilibrator was typically less than one degree centigrade. Every 10 minutes the CO_2 content of the head space of the equilibrator was measured by a gaschromatograph. Marine air was pumped from 22 m above sea level. Calibration gases with CO_2 contents of 259, 361 and 473 x 10^{-6} l CO_2 per l artificial dry air by BOC, UK were used. Each GC-run consisted of two calibration gases, an equilibrator sample, followed by marine air and a second equilibrator sample. Overall such takes 19 minutes. CO_2 was converted to methane by a nickel catalyst and detected by an FID-detector. The temperature correction of Copin-Montegut (1988, 1989) will be used.

B: pCO_2 in discrete samples
Discrete samples from 1500, 1000, 500, 300, 200, 150, 100, 80, 60, 40, 20 and 10 m depth from the CTD at all whole degree stations. During the grid and Trans. 12 samples were taken from 200, 150, 100, 60 and 20 m at all whole and half degree stations. All depths in deep casts to the bottom were sampled. 600 ml glass bottles with a screw cap containing a rubber septum were used. Samples were poisoned by adding 0.1 ml of a saturated mercury chloride solution and placed in a water bath of 4.5° to 5°C for minimally one hour. 20 ml of water in each bottle was replaced by calibration gas of 473 x 10^{-6} l CO_2 per l artificial dry air. After at least another hour in the water bath the head space of the sample was injected into the gaschromatograph. A GC-run consisted of one discrete sample and one calibration gas of 473 x 10^{-6} CO_2 by volume. The temperature of the water bath was registered continuously. The temperature correction of Copin-Montegut (1988, 1989) will be applied.

The infrared pyrometer was mounted 22 m above sea level. Continuous registration of skin temperature was performed. The pyrometer was calibrated before and after

use with a black radiator mounted in a thermostat water bath calibrated with a sensitive Pt-100 thermometer.

Preliminary results

Data on pCO_2 given below are preliminary, as so far only a rough temperature correction has been applied and as calibration gases will be further calibrated. The volume fraction of CO_2 in marine air has been rather constant throughout the cruise at about 353 x 10^{-6} l CO_2 per l by dry air.

Below a broad overview of the online pCO_2 data in surface water during the Trans. 6 to 11 is given. (Fig. 6.6.1) The partial pressure of CO_2 in surface water at 6°W decreased from south to north. Highest pCO_2 values of 390 dPa CO_2, equivalent to 37 dPa supersaturation of the water, were registered well in the closed pack ice zone at 58°30'S, Sta. 919. Further north in the ice pCO_2 values were 373 dPa at 58°S and 365 dPa at 57°30'S. This drop in pCO_2 seemed to coincide with the front between the Antarctic Circumpolar Current and the Weddell Gyre. The effect of the melting ice zone and the ice edge, which occurred at this latitude during Trans. 6,7,8 and 9, needs further study.

In the open water pCO_2 levels gradually decreased from 365 dPa at 57°30'S to 360 dPa at 54°30'S and 51°20'S with a maximum at 54°S of 368 dPa during Trans. 6. pCO_2 decreased from 360 dPa at 51°20'S to 345 dPa at 49°S during Trans. 6. Three weeks later during Trans. 11 the sharp decrease in pCO_2 started further north at 50°20'S, from where values dropped from 365 to 340 dPa at 49°50'S. This drop was connected to high biological activity. Minima of pCO_2 related to high biological activity occurred during in Trans. 6 ,11 and 12 at 49°S and 47°S. The pCO_2 values of these minima dropped from 345 to 320 dPa at 49°S and from 345 to 305 dPa at 47°S between Trans. 6 and 11. As a whole pCO_2-values north of 50°S were lowered by 10 to 40 dPa between Trans. 6 and 11.

The skin temperature of the water was 0.7 to 3°C colder than its bulk temperature at 8 m depth and 1.6°C colder to 1.6°C warmer than the air temperature. These deviations of the skin temperature from the bulk water and air temperature are significant for calculation of the CO_2 fluxes between the ocean and the atmosphere.

Reference

Copin-Montegut, C. (1988) A new formula for the effect of temperature on the partial pressure of CO_2 in seawater. Mar. Chem. 25: 29-37.
Copin-Montegut, C. (1989) Corrigendum. Mar. Chem. 27: 143-144.

Fig. 6.6.1a+b

Preliminary values of pCO_2 in surface waters calculated by hand from raw data of a) Trans. 6 and b) Trans. 11. Note strong decrease of pCO_2 in Polar Front (~48°S) over time interval from about 06/11 to 21/11 of 1992, related to evolution of spring bloom.

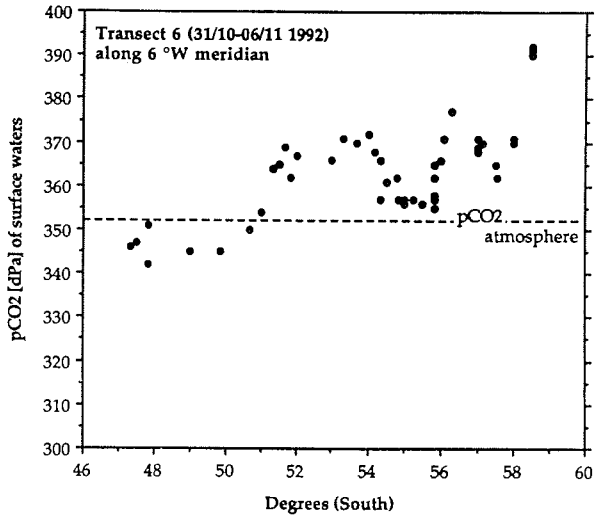

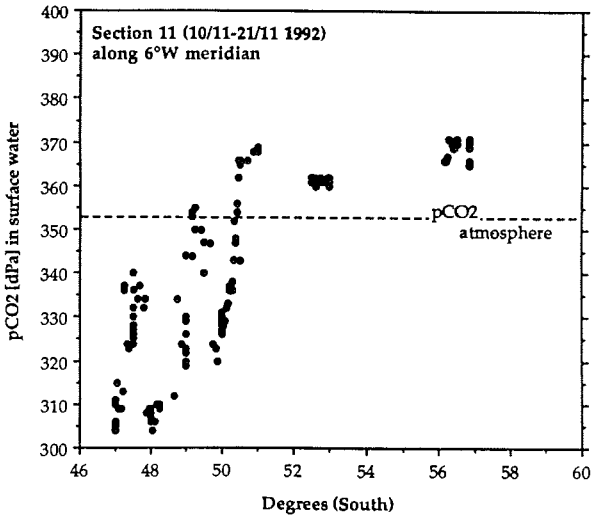

6.4. DOC/DON

A. Antia, P. Kähler (SFB)

Dissolved organic carbon and nitrogen (DOC and DON) were measured by a high-temperature catalytic oxidation technique, modified after Suzuki et al. (1988). This involves the combustion of a 100 µl seawater sample at 900°C in an oxygen stream in the presence of a platinum catalyst. The combustion gases CO_2 and NO are measured by infra-red and chemoluminescence detectors respectively. The instrumental set-up and analytical procedure are described in the Methods section of this report. We have achieved significant improvements in the reproducibility and a long-term stability in calibration of the machine, both major problems in the measurement of DOC/N, by the use of precombusted catalyst and alternate injection of distilled water to clear the catalyst of salt deposits.

Samples were taken from all transects for the measurement of DOC and, at selected stations DON, of which odd numbered stations were measured on board, and even numbered stations will be measured in the laboratory. We directly measure total organic carbon (TOC) and total dissolved nitrogen (TDN), calculating DOC and DON values by subtraction of POC and inorganic nitrogen compounds respectively. In most of the profiles, there were relatively constant TOC values between 60 and 70 µM, with a surface or near-surface increase to about 100 µM at some stations (Fig. 6.6.2). We have not been able to correlate this to differences in the water masses sampled or proximity to the frontal zones encountered, where differences in other biological parameters (Chl.*a*, primary production, bacterial production and biomass) are evident (Fig. 6.6.3). Elevated TOC concentrations were found only at some stations close to the ice edge (Fig. 6.6.2).

Fig. 6.6.2 Depth profiles of DOC at two stations in the southern Atlantic. Sta. 917 in open water; Sta. 931 in the marginal sea-ice zone

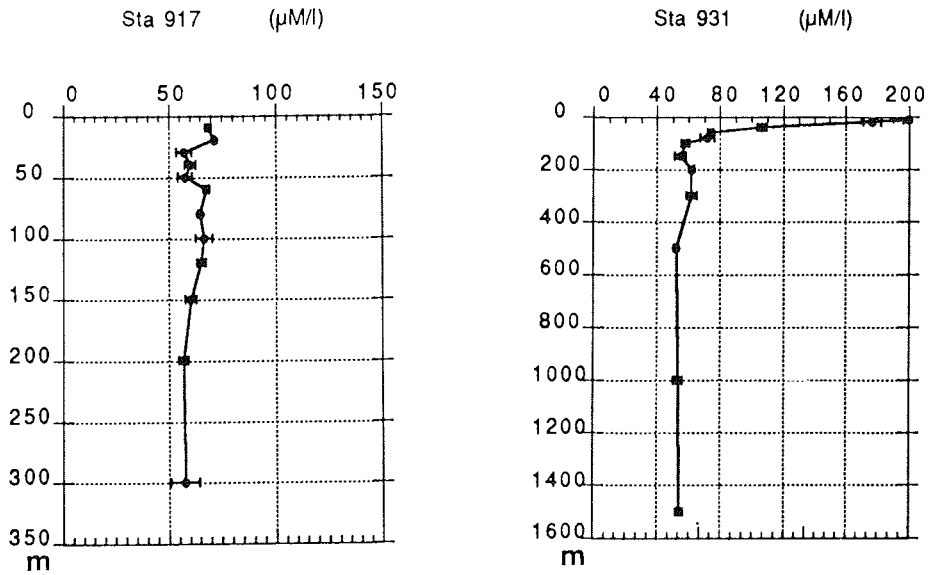

Fig. 6.6.3 Depth profiles of dissolved organic nitrogen (DON) and of nitrate (DIN). Upper pannel station in the North Atlantic at 47°N20°W on 15.04.1992.
Lower pannels: 3 stations in the polar South Atlantic at 6°W on 24.10.1992 prior to spring bloom deveopment: Sta. 879 at 48°S, Sta. 881 at 49°S, Sta. 895 at 50°S.

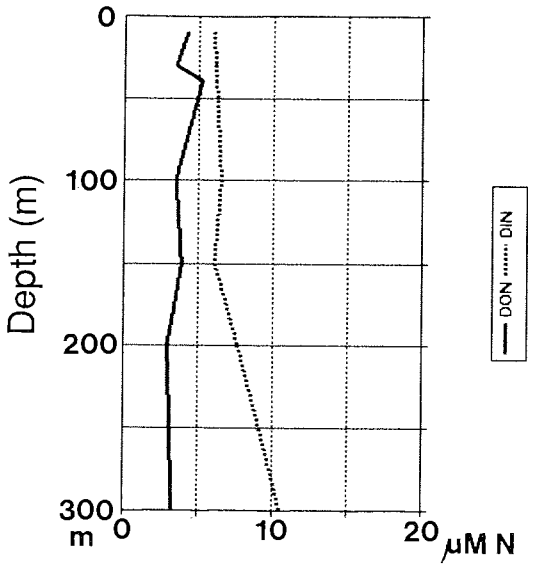

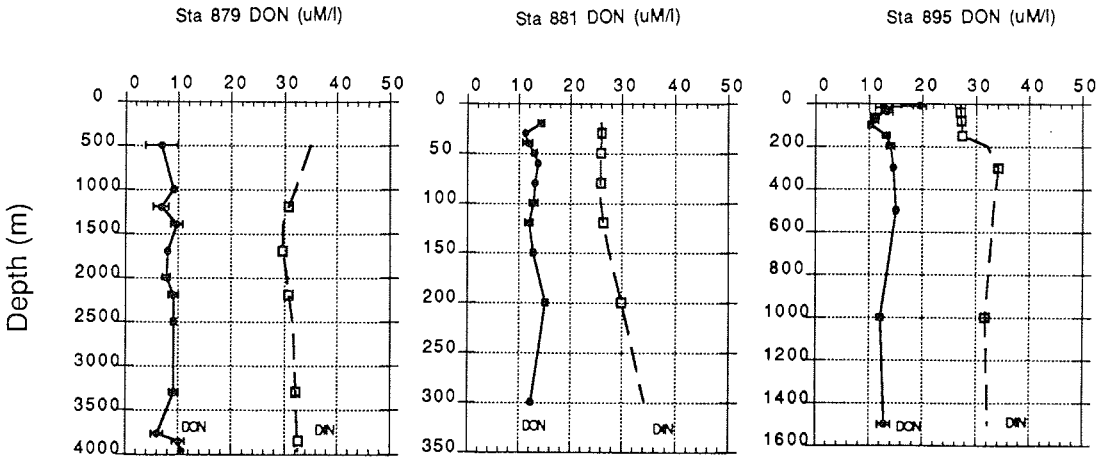

Previous measurements by our group in the North Atlantic have shown values of ca. 80 µM in deep waters for DOC and 4 µM for DON (Fig. 6.6.3); whether there is indeed a difference in the deep water values of the North Atlantic and the Antarctic Oceans, or whether this is due to differences in the machine blanks will be resolved by concurrent measurements of conserved samples from the respective cruises.

Incubation experiments were performed to measure the consumption of DOC in deep water (1000 m), surface water (20 m) and surface water inoculated with sea ice (Fig. 6.6.4). Parallel to the measurement of TOC in these incubations oxygen consumption was also determined. Initial results indicate that the high TOC levels in sea ice decrease with time, consisting primarily of biologically degradable material. TOC concentrations and its decrease with incubation time were lower in surface water without ice and deep water respectively. (see Bjørnsen, Kähler & Manuels).

DOC was also measured at selected stations in pore water from the multicorer samples (see Section: Benthic boundary processes; R.v.d.Loeff & Antia)

Reference

Sugimura, Y. and Y.Suzuki (1988) A high temperature catalytic oxidation method for the determination of non-volatile dissolved organic carbon in seawater by direct injection of a liquid sample. Mar. Chem. 24, 105-130

Fig. 6.6.4 Oxygen utilization as result of DOC-consumption in filtered sea water from the polar southern Atlantic:
Water from 1000 m depth, from sea surface (20 m) sea ice and water from decks incubation experiments (tank) was added to the treatments

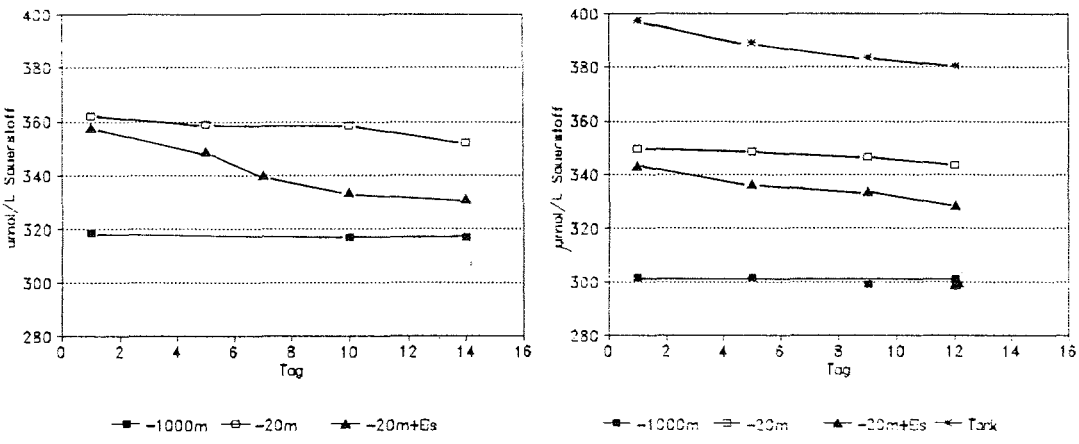

7. Trace metals

H. de Baar, J. de Jong, M.A. van Leeuwe, B. Löscher (NIOZ), R. Scharek (AWI)

Introduction.

During Ant X/6 samples were collected for a study of horizontal and vertical distribution of trace elements in the Southern Atlantic Ocean. The study focuses on Fe, Co, Cu, Ni, Zn, Pb, Cd, Ag, Mn and the Rare Earth Elements (REE). Both the dissolved and the particulate phase will be analysed. Additionally, the effect of trace metals on phytoplankton was studied by means of enrichment experiments performed on several stations.

So far, no data exist on trace metal and REE distribution for this part of the Southern Atlantic. These field data are also essential to elucidate the hypothesis of iron limitation on phytoplankton in the Southern Ocean. Production in Antarctic waters seems considerably lower than expected in such nutrient-rich waters. Low iron concentrations may be one of the limiting factors in these area's. As other trace metal concentrations (Mn, Co, Zn) are also very low additional enrichment experiments were performed. The enrichment experiments should give more information about the "Antarctic Paradox."

Methods

- Field sampling program:
To cover the horizontal distribution of trace metals in the upper water layer, samples were taken at each full degree with a set of teflon-coated GoFlo water samplers (10L) attached to a Kevlar hydrowire, to be referred to as Kevlardip (KVD). Standard depths were 40, 60, 100, 150, 200 and 300 m. Exact depths were determined by a SIS pressure meter on the deepest water sampler. Whenever weather conditions allowed a subsurface sample was taken at about 10 m depth using a teflon-coated GoFlo (2L) on a Kevlar hydrowire. This was done contamination free immediately upon arrival at the station from a 10 m long extension on the bow of the ship, while it was slowly steaming against the wind.

To separate the dissolved metals from the particulate metals the upper water layer samples were all pressure filtered in the clean air (class 100) container over precleaned, preweighed polycarbonate filters (0.4 µm poresize, 47 mm diameter). Besides this, additional samples with a volume of 40-50 liter were taken by closing several GoFlo's at three selected depths (usually 40, 80 and 200 m). These samples were filtered over precleaned polycarbonate filters (0.2 µm pore-size, 142 mm diameter).

For the vertical distribution deep water samples were taken at 18 depths using the GoFlo's mounted on a teflon-coated CTD rosette frame (12 depths below 500 m), combined with a KVD (6 depths) for the upper layer. In this way deep casts were executed on an East-West transect from Punta Arenas till the research area at 6° W, as well as on the several North-South transects along the same meridian. On the way back to Cape Town a final deep cast was taken, during which also four water samplers of a new type (NOEX) were used for trace metal and REE sampling.

At two stations (51°00'S, 6°00'W and 48°30', 6°00'W) in situ pumps were deployed to collect particulate matter from large volumes up to 1000 L at depths throughout the water column. Considering possible contamination by the metal parts of these pumps only REE will be determined. Fortunately, there exist living in situ pumps in the ocean: salps. They filter several tens of litres of sea water per day, the particulate matter of which is collected in the 'guts'. Whenever possible salps were collected freshly from net catches and their stomachs frozen and stored for later trace metal analysis.

The content of trace elements in ice floes and the input by melting icebergs will be measured in ice samples and surface snow as well as in surface water samples taken from a zodiac in the melt water wake of an iceberg.

Pretreatment and analysis of the samples will be done in the home laboratory using Graphite Furnace Atomic Absorption Spectrophotometry for the trace metals and Isotope Dilution Mass Spectrometry or ICP/MS for the REE.

- Experiments.
Water was taken with GoFlo samplers mounted on a teflon-coated rosette frame. As soon as the frame was recovered, the GoFlo's were removed and mounted to the wall of a specially designed clean air (class 100) cool container. Teflon tubes leading trough the wall of the container were then connected to the GoFlo's. This system made it possible to sample from the inside without having the water to be exposed to the air.
The seawater was incubated in precleaned, sea water conditioned 20L polycarbonate vessels which were placed on a rolling device, kept at 0 - 1°C receiving light-intensities between 90 - 120 μEs^{-1}. Experiments performed according to Table 6.7.1.

Following the development of the algal community subsamples for species composition, chlorophyll and nutrients (NO_2, NO_3, Si, PO_4, NH_4) were taken regularly, the latter two parameters being measured on board. In order to prevent contamination special caps were placed on the bottles, consisting of two pieces of tubing sticking trough the cap. This enabled sampling without having to take the cap of. Using an air pump provided with a 0.2 µm air filter allowed also clean filtration of particulate matter for Fe analysis at the end of each experiment.

At the start and the end of the experiments larger subsamples were taken from the 20-L bottles. These samples were used to perform the following experiments on board:
- ^{55}Fe-uptake
- ^{14}C-uptake
- ^{15}N-uptake
- microzooplankton grazing (method as described by Landry & Hassett).

Tab. 6.7.1: Overview of enrichment experiments performed during ANT X/6. Temperature and salinity values are taken from shipboard surface registration.

Experiments	Date	Station	Lat.-Long.	depth (m)	Water body	% ice cover	S %	Temp. (C)	20-L bottles	10-L bottles	2-L P.S. bottles	2-L P.E. bottles
Fe-I	04. Okt 92	860	57.00 S 38.10 W	40	ACC	2	33,81	-1,46	3(0), 3(5nM Fe)			
Fe-II	12. Okt 92	867	57.30 S 06.20 W	40	ACC/Weddell mixture	80	33,9	-1,75	3(0), 3(2nM Fe)			
Co	12. Okt 92	867		40							2(0), 2(2nM Co)	
depletion	12. Okt 92	867		40						1(0), 1(2nM Fe)		
Fe-III	19. Okt 92	880	48.80 S 6.00 W	30	ACC from the Polar Front	0	33,81	2,72	3(0), 3(2nM Fe)			
Mn	19. Okt 92	880		30							2(0), 2(2.5 nM Mn)	
Fe-IV	30. Okt 92	907	47.00 S 6.00 W	40	ACC from the Polar Front	0	33,79	2,6	3(0), 3(2nM Fe)			
FeMnCo	30. Okt 92	907		40		0				1(2nM Fe, 0.4 nM Co) 1(2nM Fe, 0.4 nM Co, 2,5nM Fe)		
small	04. Nov 92	915	57.50 S 6.00 W	40	ACC	70	33,82	-1,6			2(0), 2(5nM Fe), 2(10nM Fe)	
Fe-V	10. Nov 92	929	59.00 S 6.30 W	40	Weddell Sea	30	34,2	-1,75	2(0), 2(2nM Fe), 2(5nM Fe)	2(10nM Fe)		
EDTA	10. Nov 92	929		40								2(0), 2(2nM Fe + 10e-5nM EDTA)
FeMn	10. Nov 92	929		40								2(0), 2(2nM Fe), 2(2nM Mn)
Fe-VI	16. Nov 92	949	53.00 S 6.00 W	40	ACC	0	33,83	-0,25	2(0), 2(2nM Fe), 2(5nM Fe)	1(2nM Fe, 0.4 nM Co) 1(2nM Fe, 0.4 nM Co, 2,5nM Mn)		
Zn	16. Nov 92	949		40							2(0), 2(2nM Zn)	
FeCo-FeVI	16. Nov 92	949		40								2(0), 1(2nM Fe, 0.4 nM Co)1(2nM Fe, 0.4 nM Co, 2.5nM Mn)
Combi	28. Okt 92	901	50.00 S - 6.00 W	60	ACC from the Polar Front	0	33,82	1,44	experiment performed in both a 2-L P.E. bottle and a 4-L P.E. bottle, except Zn (4 2-L bottles) additions: 0, 2nM Fe, 2nM Fe + 2nM Mn, 2nM Fe + 0.4nM Co, 2nM Fe+ 2nM Zn, 2nM Fe + 2nM Mn + 0.4nM Co. 2nM Fe + 2nM Mn + 0.4nM Co + 2nM Zn			

Also, subsamples were taken to determine the following parameters, some of which will have to be analysed at home:
- Fe (filtered, unfiltered)
- species composition
- POC/PON
- pigments
- lipids
- bacterial counts and growth rate (thymidine/leucine uptake)
- DOC
- DMSP
- diatom frustules

Preliminary results.

Biomass of the water incubated was generally very low. Therefore, the incubation times were set for a relatively long period, in order to obtain any response. Biomass would increase in all bottles, however an enhancement in the bottles with Fe addition was observed, though not very distinct because of the low chlorophyll levels.

Fig. 6.7.2: Development of Chl.*a* in Experiment 4 in three control bottles without iron addition and three bottles with 2 nM addition of iron.

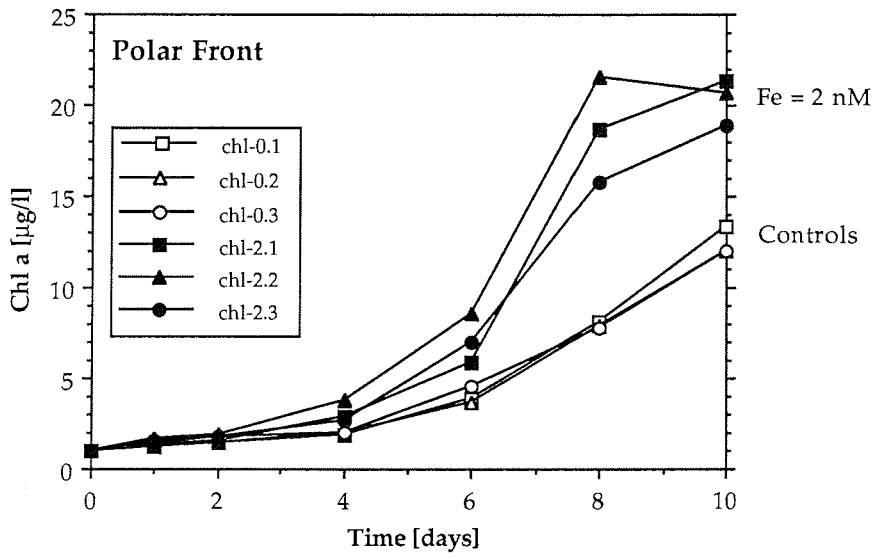

Fig. 6.7.3: Development of nitrate (NO_3) in Experiment 4 in three control bottles without iron addition and three bottles with 2 nM addition of iron.

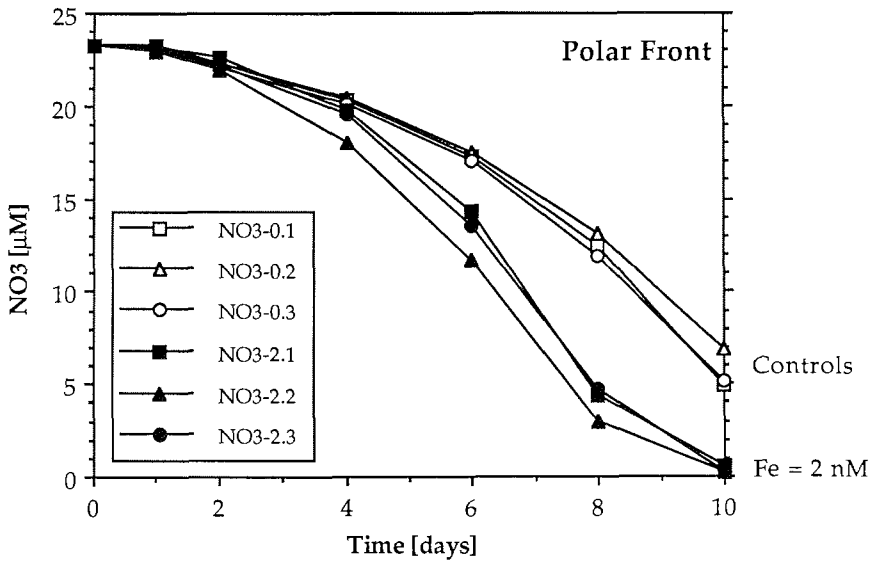

Respective decreases in nutrients (nitrate, phosphate, silicate) could be measured, but were accordingly to the very low biomass accumulation rates in many experiments close to detection limits. However, additional/supplemental data as will be obtained from species composition and the other parameters will give more information necessary to interpret the results of these experiments. A clear response to Fe addition is apparent in one experiment, where water from the polar frontal area was incubated. The higher starting biomass (1 µg Chl.*a*/L), resulted in a sharp increase in chlorophyll in the bottles with addition, comparing to a more moderate growth in the control bottles (Fig. 6.7.2). This also shows in nutrient-uptake; NO_3-assimilation is distinctively higher after addition(Fig. 6.7.3). Grazing experiments support the data. A higher algal growth coefficient together with a higher grazing coefficient indicates a higher biological activity in the microcosms.

According to these results Fe and other trace metals seem to stimulate growth rate and consequently concentrations of biomass in the Atlantic part of the Southern Ocean. However, higher concentrations of these metals would not necessarily overcome the controls set by physical settings and grazing pressure.

8. Phytoplankton biomass distribution

8.1. Quantities and horizontal distribution of chlorophyll *a*

U. Bathmann (AWI)

Surface chlorophyll fluorescence was recorded continuously at 8 m depth throughout the cruise to evaluate the spatial heterogeneity of phytoplankton. Vertical profiles of chlorophyll at stations were done in addition to surface registration and enable calculations of total phytoplankton stocks on a square meter basis.

Along the west-east transect (53°W to 6°W) two distinct areas of chlorophyll distribution at sea surface could be separated (Fig 6.8.1a): west of the South Sandwich Islands the mean phytoplankton biomass was higher (0.5 µg Chl.*a* l^{-1}) and spatial heterogenity greater (max: 1.4 µg Chl.*a* l^{-1}) compared to the eastern part (mean: 0.2 µg Chl.*a* l^{-1}). Maximum surface biomass was associated with the outer region of the MIZ (Sta. 859, about 40°W). The same patterns are reflected in the vertical distribution of phytoplankton biomass with higher standing stocks (>40 mg Chl.*a* m^{-2}) at the west and lower (<25 mg Chl.*a* m^{-2}) at the east (Fig. 6.8.1b).

These data indicate the development of moderate phytoplankton biomass in the ACC between the tip of the Antarctic Peninsula and the South Sandwich Is. Between these Island and 6°W, however, phytoplankton concentrations were still at winter values; ice cover and a 100 m deep layer of winter water (WW) were obviously not conducive for intense algal growth.

Spatial and temporal development of phytoplankton biomass along the 6°W meridian between 46° and 59°S from October to November is summarised in Fig. 6.8.2.a and b. At the marginal ice edge zone (MIZ), a very weak increase of Chl.*a* was measured

Fig. 6.8.1.a: Surface chlorophyll distribution and information on time along 57°S by 10 min averages on continuous sampling

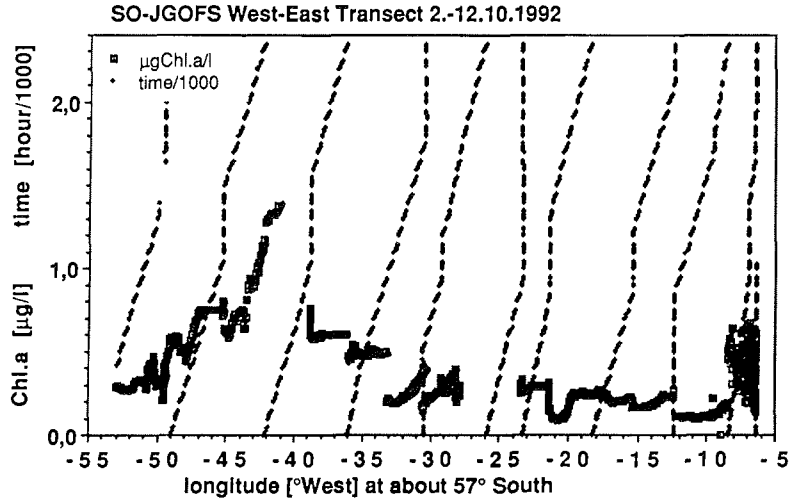

Fig. 6.8.1.b: Distribution of Chl.*a* between 50°W and 0° along the 57° Longitude

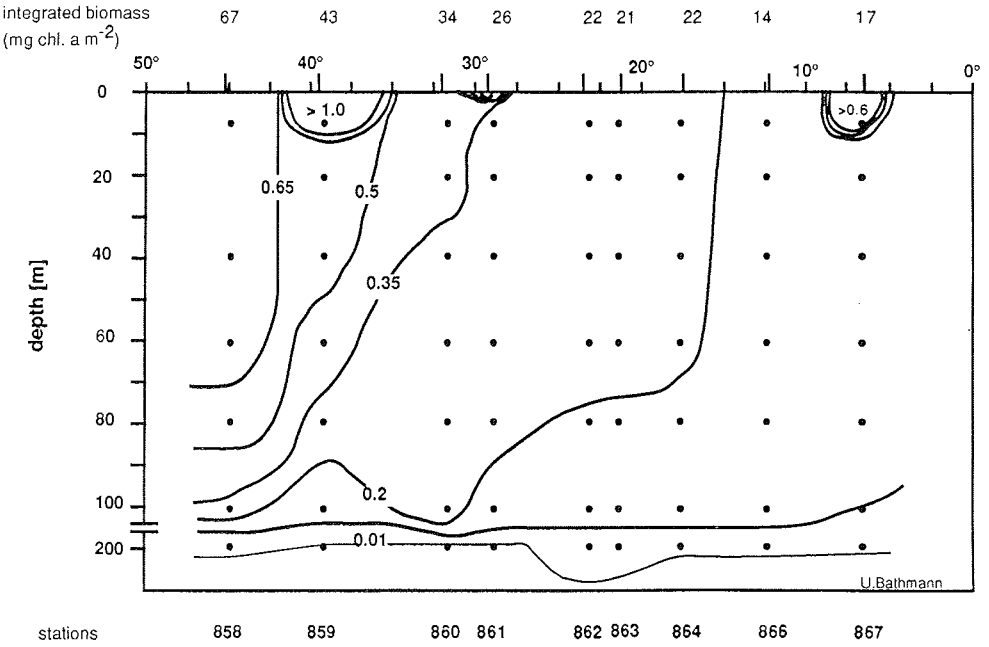

at sea surface down to about 50 m. Between the MIZ and the Polar Frontal Zone (PF), biomass remained constantly below 0.2 µg Chl.*a* l-1. In that area more than 90% of the chlorophyll was found in the plankton fraction < 20 µm. At the PF the most pronounced increase in phytoplankton biomass during the cruise was observed.

Fig. 6.8.2.a: Distribution of Chl.*a* on Trans. 2 & 3 along the 6°W meridian.

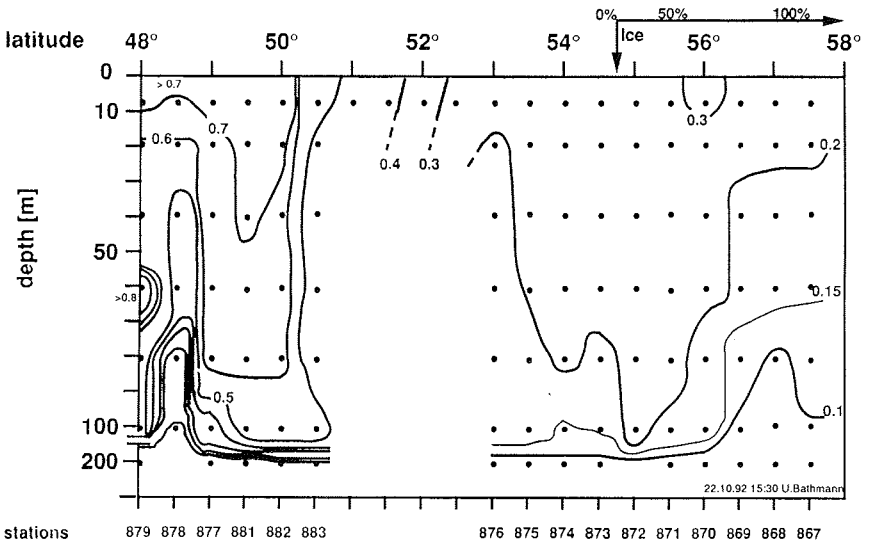

Fig. 6.8.2.b: Distribution of Chl.*a* on Trans. 11 along the 6°W meridian. Areas of dominant zooplankton species are indicated

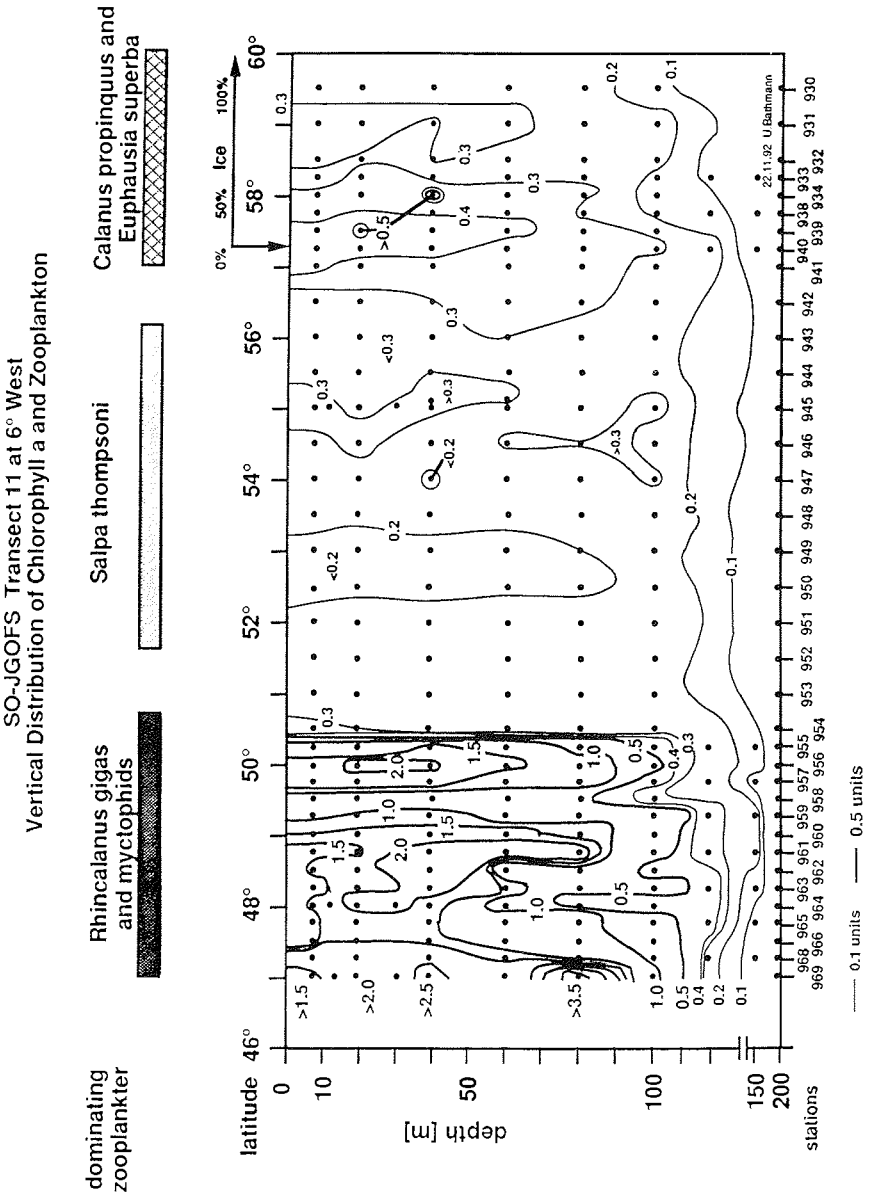

8.2. Standing stocks and distribution of pico- and nanoplankton

S. Becquevort (ULB), A. E. Detmer, F. J. Jochem (IFM)

Introduction

Recent studies show the importance of the microbial loop in the Antarctic food web coexisting in parallel with the classical food chain: diatoms - krill. It is clear that microbial organisms, i.e pico- and nanophytoplankton and pico- and nanoprotozoa must play an important ecological role because of their short generation time and their high growth efficiency. However, there is still little information about their abundance, distribution and activity in the Antarctic marine ecosystem or about their seasonal and regional variations. Therefore, during this cruise, we have taken the opportunity to evaluate the stocks of these microbial organisms at early spring during commencement of seasonal retreat of the ice cover.

Methods

Both autotrophic and heterotrophic pico-and nanoplankton abundances were estimated by epifluorescence microscopy in the upper 200 m layer. For phototrophic organisms, 50-100 ml of glutaraldehyde fixed samples (1%) were filtered onto Irgalanblack pre-stained Nuclepore filters of 0.2 and 0.8 µm pore size, respectively. Samples were stained by either DAPI or Proflavine and counted directly afterwards or kept frozen (-27°C). For heterotrophic organisms stained by Proflavine, Hoechst 33342 stain was additionally applied for checking nucleus presence.

Phototroph abundance in the upper 200 m layer, 1000 m depth respectively was also quantified by flow cytometry (Fluvo II). Fresh and unstained organisms were recognized using blue light excitation (450-490 nm). Chlorophyll (red fluorescence) was measured as >615 nm emission and phycoerythrin (orange fluorescence) as 530-585 nm emission.

Nanoprotozoan grazing on bacteria and phytoplankton was measured by the method proposed by Sherr et al. (1987) based on the uptake of fluorescent labelled particles.

First results

Abundance of autotrophic and heterotrophic flagellates estimated by epifluorescence microscopy

Distribution of autotrophic and heterotrophic flagellate abundance along the meridian 6°W at 20 m depth have been estimated (Fig.6.8.3).

Fig. 6.8.3: Heterotrophic flagellate abundance along the meridian 6°W, for the Trans. a) 2, b) 5 and c) 11.

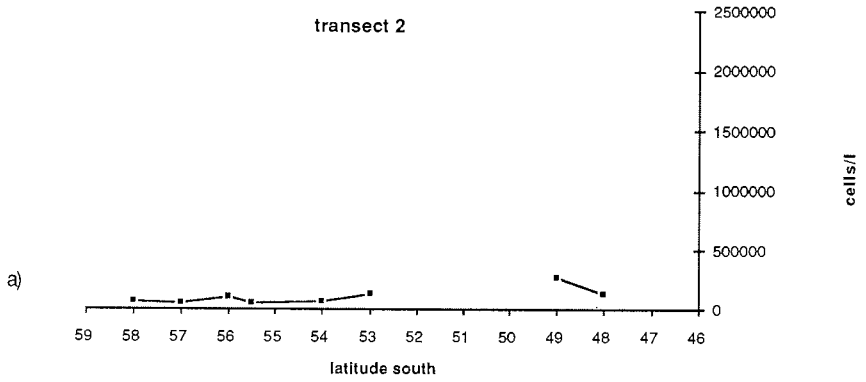

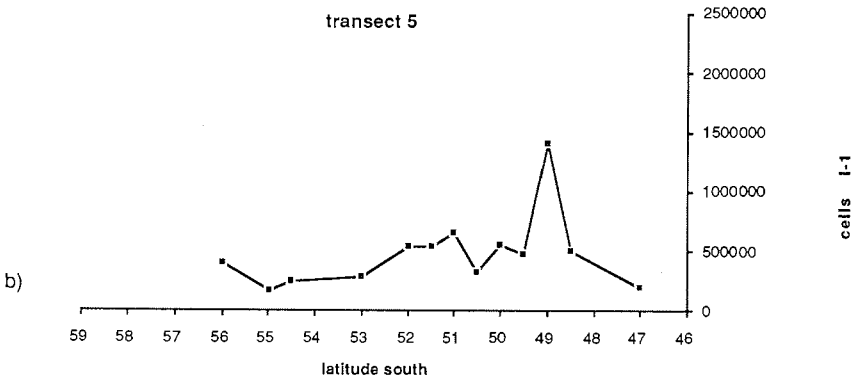

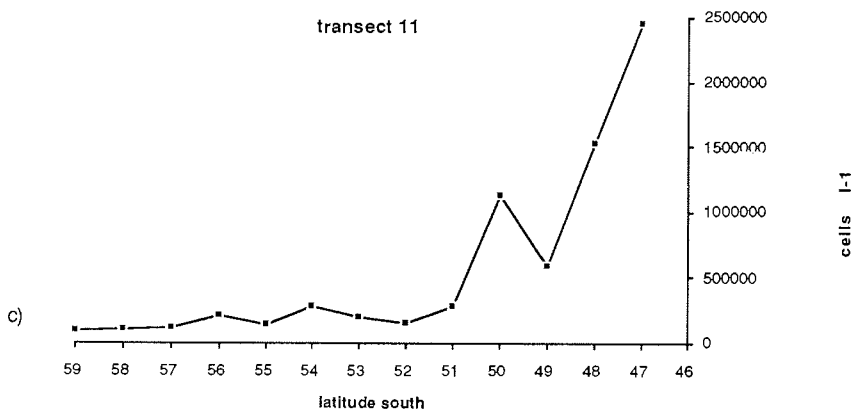

The highest values of heterotrophic flagellate numbers were observed in the Polar Frontal Zone. They were particularly important during Trans. 11, at the north of the Polar Frontal Zone.

Fig. 6.8.4: Distribution (in % of total heterotrophic flagellates) of heterotrophic flagellate taxons along Trans. 11.

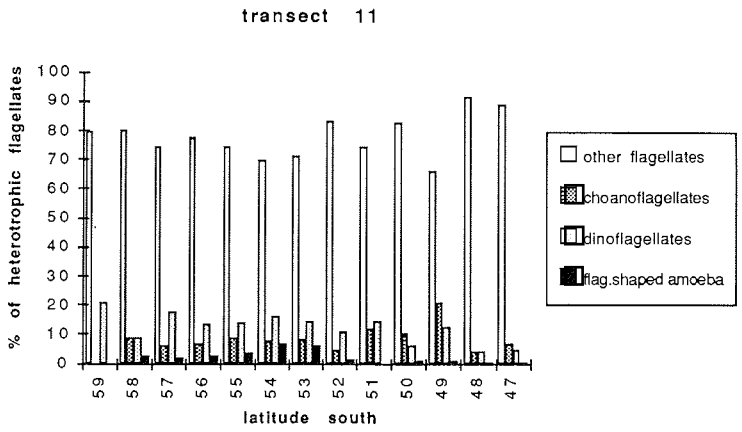

As seen in Fig. 6.8.4, the naked flagellates constituted a large part of the heterotrophic flagellate abundance. Significant numbers of choanoflagellates and heterotrophic dinoflagellates (< 20 µm) were also observed.

The distribution of autotrophic flagellates were less clear (Fig. 6.8.5), and will be analysed with regard to the hydrography and the distribution of the other phytoplankton groups. However, organisms smaller than 5 µm constituted the bulk of autotrophic flagellates such as *Phaeocystis* sp.(Fig. 6.8.6).

Fig. 6.8.5: Distribution of autotrophic flagellate abundances along the Trans. 11.

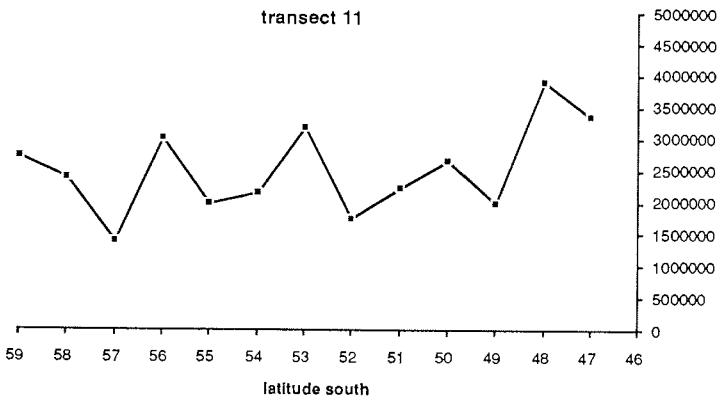

Fig. 6.8.6: Distribution (in % of the total autotrophic flagellates) of autotrophic flagellate taxons along the Trans. 11.

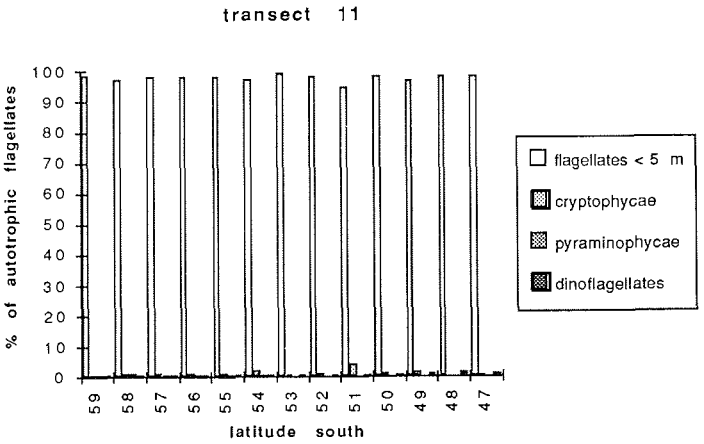

Nanoprotozoan grazing

Kinetics characterising the feeding activity of protozoan compartments will be established from field experiments including biomass and grazing activity measurements. Protozoan ingestion of nanophytoplankton has been measured in the different water masses and protozoa feeding rate control by prey concentration have been studied (Fig. 6.8.7). At this station, consumption rates of 1.82 flagellates and 7.28 bacteria per protozoan and hour have been calculated, respectively.

Fig. 6.8.7: Time course uptake of *Phaeocystis*-FLA (a) and bacteria-FLB (b) for the Sta. 872.

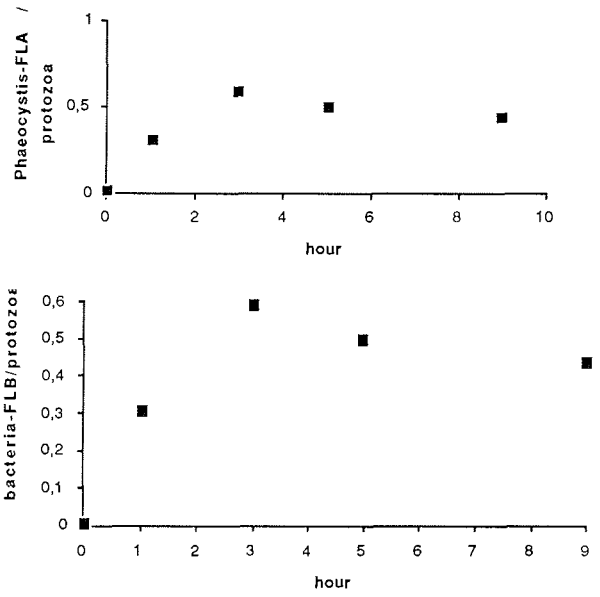

Abundance of autotrophic pico- and nanoplankton measured by flow cytometry

During the cruise leg ANT X/6 two different groups of autotrophic cells or particles smaller than 20 µm could be distinguished by flow cytometry. Chlorophyll containing cells could be easily detected by their red fluorescence. Cells or particles of the second group were characterised by an orange or green autofluorescence and could not be identified further.

Cell concentrations of autotrophic pico- and nanoplankton (unidentified cells/ particles are not included here) ranged between $1x10^6$ and $12x10^6$ ($25x10^6$) cells l^{-1} in the upper 100 m depth. Lowest surface concentrations (10 m/20 m depth, $3x10^6$ to $6x10^6$ cells l^{-1}), occurred on stations 868 (57°S6°W), 919 (59°30'S6°W), 930 (59°50'S6°W) and 931 (59°S6°W), (Trans. 2, 6 and 11), all in watermasses covered by ice. During processing the Trans. 2 and 5, an increase of cell concentrations from $2\text{-}5\cdot10^6$ to $9\cdot10^6$ cells l^{-1} could be observed at the surface while going further north corresponding to the increase of surface chlorophyll content and temperature (U. Bathmann). Comparing data of overlapping positions of the Trans. 2, 5, 6 and 11 showed also an increasing development of surface abundances with time. For example, surface cell concentrations increased from $7x10^6$ to $12x10^6$ cells l^{-1} at 52°S6°W. Similar tendencies could also be observed at other positions.

Different water masses characterised by the variation of abundance or sudden shifts could be distinguished at the Weddell-ACC-Front and the Polar Frontal Zone (Trans. 8/9 and 11/12). At the Weddell-ACC-Front a slight increase of surface cell concentrations from $6x10^6$ to $7x10^6$ cells l^{-1} in the southern direction was observed. This did not clearly represent different water masses. In contrast, a high variability of abundance was observed at the Polar Front. Between 49°S and 48°S, very small-scaled fluctuations (quarter of a degree) could be distinguished. Values ranged between $6x10^6$ to $24x10^6$ cells l^{-1}. The region of the Polar Frontal Zone itself was characterised by lower cell concentrations, whereas values further south or north increased. This did not seem to correlate to surface chlorophyll values.

Cell concentrations of unidentified cells or particles showed some reproducible trends like maximum values between 80 to 100 m depth. Higher abundances were observed in water masses covered by ice. Additionally higher variations in cell number were observed under the ice in contrast to the open water in the upper 100 m depth. Glutaraldehyde fixation of samples was avoided (no artefacts caused by fluorescence of this fixative). Under the epifluorescence microscope very small, bright orange and mostly round shaped particles with a diameter of 0.7 to 1.0 µm were observed at some stations. Enrichment of these cells/particles onto 0.45 µm membranfilters in ASW (artificial seawater medium) was not successful. It is yet not clear, what causes these special signals. One theory considers decomposition products of cryptophytes, which were also observed in the water column. Cryptophytes are the only algae apart of cyanobacteria containing the pigment phycoerthrin which could be responsible for orange autofluorescence. To get further information about this, probably some grazing experiments could be helpful.

Comparison of cytometric cell counts and those by microscope (S. Becquevort) resulted in higher values for flow cytometry. One of the reasons for this difference could be that in the case of microscopy only flagellates were counted whereas total nanoplankton abundance, including also small diatoms, were estimated by flow

cytometry. To test this, more cell counts by epifluorescence microscopy will be done. Also qualitative informations on population structure and composition on the several size classes will be analysed in the institutes.

8.3. Regional distribution of heterotrophic pico- and nanoflagellates

F.J. Jochem (IFM)

The spatial/regional distribution of heterotrophic nano- (HNF) and picoflagellates (HPF) as revealed by 20 m samples showed recurrent features on two south-north transects (5 and 11). Very low abundances were encountered at stations under ice-cover, increasing north of the ice edge. Throughout ice-free ACC water, cell numbers were fairly constant at levels of about 50 ml^{-1} for HNF>10 µm, 500 ml^{-1} for HNF 2-10 µm, and 100-150 ml^{-1} for HPF, respectively. The increase in cell numbers of HNF at the ice edge shifted southwards along with the retreat of the ice in-between the two transects. A pronounced increase of HNF abundance was noted near the frontal zone north of 50°S. This increase was concomitant with higher chlorophyll concentrations and primary production, thus with an overall more productive pelagic system. Higher cell numbers were encountered north of 49°S on Trans. 5 and north of 51°S on Trans. 11 as the productive zone also shifted southwards in-between the transects. Cell numbers were in the range of 100-150 ml^{-1} for HNF>10 µm, 1000-1500 ml^{-1} for HNF 2-10 µm, and 200-400 ml^{-1} for HPF. Generally, cell numbers of the respective organism groups within the three distinguished zones (ice, ACC, frontal zone) were fairly comparable on the two transects and all three size fractions displayed similar trends. Distinct size shifts especially within the two larger size fractions await, however, detailed analysis with respect to the abundance and size distribution of their potential prey. The west/east Trans. 1 (49° to 6°W on 57° S) that more or less followed the ice edge, thereby sometimes cutting into the ice, revealed similar cell numbers as compared to ice edge stations of the two longitudinal transects. However, some pronounced small- and mesoscale variability occurred, which has to be analysed with respect to different water masses encountered (ACC and Weddell Sea water, resp.) as well as to ice cover. Some stations, among them one deep in the ice, showed cell numbers of HNF 2-10 µm of up to 1500 ml^{-1}, thus as high as in the northern frontal zone. The area of 45-40°W and 10-6°W showed highest HNF abundances. These data might suggest pronounced patchiness along the ice edge, high biomasses being encountered not only in ice-free water. Vertical profiles of HNF abundance at 56°S and 48°S 6°W showed fairly constant cell numbers within the euphotic zone and a decrease below.

8.4. Phytoplankton species

R. Crawford, F. Hinz (AWI)

Particulates

64µm mesh Multinet sample at depths down to 300 m in the Polar Frontal Zone showed diatom phytoplankton to be concentrated with a maximum at various positions within the top 100 m. Some species, notably *Fragilariopsis* spp. and *Thalassiosira lentiginosa* were also found in good condition at lower depths. Within the top 100 metres *Corethron cryophilum* showed a maximum that was frequently

higher than that of *Fragilariopsis* and *Asteromphalus roperianus* was more or less restricted to 100-50 m depth. Apstein net samples with mesh of 25µm collected smaller species and the diversity in the top 20 m of the water column appeared to be higher. Spatial distribution data showed some species, notably *Fragilariopsis kerguelensis* and *C. cryophilum* to be ubiquitous though with clear maxima in the region of the Polar Front where both species were in good condition with frequent cell divisions. Other species were restricted in their occurrence to different sections of the research area. Some were only found at the Polar Front, others restricted to near the ice edge-zone where populations were generally low but higher than in the intermediate zone of circum polar current water. Throughout the sampling program faecal pellets and parcels from a number of groups of organisms were found and intact diatom cells could be seen in many of them. At three locations, diatom numbers were low when grazing zooplankton numbers were high.

Diatoms

Unless special conditions required, samples were taken routinely with Apstein Net (25µm mesh) for the surface 20 m and with 64 µm mesh Multinet for depths down to 300 m. A picture of the horizontal and vertical spatial distribution, showed general consistency in all of the South-North transects. It also revealed a picture of change with time. *Fragilariopsis* spp., *C. cryophilum* and to a lesser extent, *Pseudonitzschia* spp. were found at all stations though present in highest numbers towards the Polar Front, north of 51°S especially in Trans. 11, 12. Thus there appeared to be no floristic reason why blooms should not have been developed during the course of the study. *F. kerguelensis* was overwhelmingly abundant at the Polar Front except where *Corethron* was the major species and was again the dominant diatom as far south as 59°30. Minimal populations of diatoms were found at 56°S which, to judge by the high numbers of broken cell walls, were due to grazing by copepods or Krill. Very little was found at 51° and 52° but this was thought to be due to paucity of nutrients in the water column. Other diatoms were also ubiquitous but never achieved the dominance of the above species. Two other groups of species include those found only towards the Polar Front and those restricted to the ice edge (Tab. 6.8.8). Several species, e.g. *Rhizosolenia chunii*, were found in greater abundance on the final transects reflecting temporal changes in the population. *Eucampia*, found more in resting spore form in earlier transects, was later found growing in vegetatively in greater abundance. Diatom minima were found at 56°S on every transect coinciding with low nutrient values at this position. Minima were also found coinciding with high copepod counts at stations 899, 919, 934 and 938 where high numbers of broken frustules indicated heavy grazing.

Diatom populations were concentrated in the top 100 m of the water column although healthy cells of some species, notably *Fragilariopsis* spp. and *Thalassiosira lentiginosa* were often found as deep as 300 m. The position of maximum productivity in the top 100 m varied but where *Corethron* and *Fragilariopsis* were both present in great numbers, the former was found at shallower depths than the latter (but see below). *Asteromphalus roperianus* was remarkable in being rarely found in the upper layers. Diversity was higher in the upper 20 m sampled by Apstein Net but this was thought to be due to the smaller mesh size catching the smaller species. At some stations the population was markedly different at the surface from that at lower depths due to overlayering of water bodies at these positions.

Two dominant species received special attention. *F. kerguelensis* was the most common species of the genus and reached exceptional numbers near the Polar Front on all transects. Here chains were in good condition and 20-30 cells long where elsewhere they were much shorter. However data on cell and chain length will be fully analysed later. At Sta. 978 the water column was sampled down to 1500 m and healthy, intact chains of *F. kerguelensis* and *T. lentiginosa* were found at this depth suggesting rapid sinking through the water column. Examination of deep sediment cores from many stations throughout the cruise revealed that both of these species are much more common than other representatives of the surface populations and both are present largely as intact valves. It is possible that dissolution of other diatoms in the population occurs on the way down through the water column - a fate that *Fragilariopsis* and *Thalassiosira* may escape due to high sinking speeds.

Tab. 6.8.8 Relative abundance of diatoms from Trans. 5 & 11 combined

blank - no records/samples
o - occasional / oo - frequent
x - abundant / xx - dominant/co-dominant / xxx - virtual monoculture

Latitude South	47	48	49	50	51	52	53	54	55	56	57	58	59	59,5
Mainly North														
Chaetoceros convolutus	oo	x	x	oo	oo									
Chaetoceros peruvianus	oo	o	oo	x	oo									
Pleurosigma spec.	o	oo	x	x	o	x	o	o						
Rhizosolenia curvata	oo	x	o	x	o	o								
Thalassionema nitzschioides		o	x	x	oo	oo								
From North to South														
Asteromphalus hookeri	x	xx	x	x	o	o	oo	oo	o	x	oo			
Chaetoceros dichaeta	o	o	oo	oo	oo	oo	o	oo	o	x	oo	oo	o	
Chaetoceros neglecta	x	o	o	oo	oo	xx	x	o	oo	x	oo	o		
Corethron spec.	x	oo	x	xx	x	x	x	xx	x	xx	xx	oo	x	o
Coscinodiscus oculoides	oo	oo	x	oo	o	o	o	oo	x	x	o	o	o	
Fragilariopsis spec.	xx	xx	xxx	xx	xx	xx	xx	xx	xx	xx	xx	oo	xx	xx
Proboscia alata	oo	x	oo	oo	o	x	x	oo	o	o	o	oo	oo	
Pseudonitzschia spec.	xx	oo	x	x	oo	xx	xx	xx	x	oo	x	oo	o	oo
Rhizosolenia styliformis	o	oo	o	oo	o	o	x	oo	oo	oo	x	o	o	
Thalassiosira lentiginosa	x	xx	xx	xx	oo	o	xx	o	o	oo	x	oo	oo	o
Thalassiosira oliverana	o	oo	o	oo	o	o	x	o	o	o	o	o		
Thalassiothrix spec.	x	oo	x	x	oo	o	oo	oo	oo	x	oo	oo		
Mainly South														
Actinocyclus actinochilus	o	oo	x	o	oo	oo								
Banquisia belgicae	o	oo	oo	x	o	o								
Entomoneis spec.	o	x	o	oo	o									
Nitzschia longissima	o	o	o	o	x	o	o							
Stellarima microtrias	oo	oo	x	oo	oo	o								
Asteromphalus roperianus	xx	x	x	x	o	o	x	o	x					
Chaetoceros bulbosum	o	x	x	o	x	x	x	x	o	o				
Chaetoceros cryophilum	o	o	oo	o	x	x	x	x	o	oo	oo			
Eucampia antarctica	oo	x	x	oo	o	o	x	x	o	o				
Navicula transitans	o	x	o	oo	x	o	x	x	x					
Proboscia inermis	x	x	x	oo	x	x	x	x	o	oo	oo			
Thalassiosira tumida	x	x	x	oo	x	o	x	x	x	x	o			
Trichotoxon spec.	x	oo	o	x	xx	x	x	oo	o					

Corethron differs from *Fragilariopsis* in at least two respects. It is unicellular for most of the time and it is lightly silicified where *Fragilariopsis* is very robust. *Corethron* usually forms flocs in the water column with chain-forming and needle-like species such as *Rhizosolenia, Chaetoceros, Thalassiothrix* and *Pseudonitzschia* and it is only occasionally found below 100 m. An exception to this occurred at stations 964 & 969 (48° & 47°S) where *Corethron* was passing through a sexual phase on a massive scale. Gametangia and zygotes were found in the surface 50 m but below 100 m there was an extensive falling out of empty gametangial cell walls. Although they had come apart they had not been broken which suggests that they had not been grazed. We intend to investigate whether this is the only situation in which *Corethron* is likely to be incorporated in the sediments in any significant numbers. Comparison of valve sizes in the sediments may show that most of the valves that reach the bottom are of gametangial size. Further south, at station 960 between the *Corethron* maximum and the *Fragilaripopsis* peaks, the population is dominated by the *inerme* chain-form of *Corethron* in the top 100 m. This is thought to indicate marked changes in the water conditions in this zone - possibly in this case manifesting a slightly higher water temperature.

8.5. Horizontal and vertical distribution of phytoplankton by means of pigment 'finger prints' analysis determined by HPLC

I. Peeken (SFB)

Objectives

To determine the spatial and vertical distribution of algal assemblages, measurements of pigment finger prints with an HPLC (high performance liquid chromatography) were performed. All algae have pigments like chlorophylls and carotinoids. Some of these pigments are distributed over all algal taxa, but a few are characteristic for special groups, like peridinin for dinophyceae, alloxanthin for crytophyceae, 19-hexanoyl-oxyfucoxanthin for prymnesiophytes. The measurements with reversed HPLC allow a rapid determination of different pigments and therefore a rapid qualitative and, with limitations, also a quantitative distribution of phytoplankton biomass and composition. This can be used to identify different water masses.

The retreating ice edge releases phytoplankton cells which contain different pigments compared to open ocean pigment finger prints. With transects passing the ice edge, the influence of seeding or fallout of algal populations should be described.

The detection of chlorophyll degradation products allow to describe the senescence and the pathways through zooplankton communities on the different levels of grazing. With limitations the history of sedimented particles can therefore be evaluated.

Work at sea

To describe the vertical and horizontal distribution of the phytoplankton assemblages, seawater samples were taken during Trans. 1 to 12, normally at standard depths: 20, 40, 60, 80, 100, 200 m, for special purposes also in 10 and 120 m. To follow a possible direct transport of phytoplankton to the seafloor samples from

greater water depths were taken at Sta. 972 (where overlayering of water masses was observed; see Section 5, Hydrography).

From the water depths sampled, seawater (2-8 l) was filtered onto 25 mm GF/F filters (for the deep cast 20 l on 47 mm GF/F) and frozen at -30°C. Ca. 50% of the samples were analysed on board, where a HPLC-system (pump series 400 and fluorescence detector LS1 Perkin & Elmer, UV-Vis detector spectroflow 757 and integration system Waters) was installed. The system was calibrated on board. Pigment concentration was quantified using internal standard (canthaxanthin) and external standards separated from algal cultures or received from D.Repeta (WHOI).

For analytical preparation 50 µl internal standard (canthaxanthin) and 2 ml acetone were added to each sample and thereafter homogenised for 3 minutes in a cell grinder. After centrifugation the supernatant liquid was filled in Eppendorf cups and stored at -30°C until analysis. Just prior to analysis an aliquot (100-200 µl) of the sample premixed with water (HPLC-grade) in the ratio 1:1 (v/v) and injected in the HPLC-system The pigments were analysed by reversed phase C18 HPLC. A spherisorb ODS 3 µm (4.0x125mm) Pharmacia column used and HPLC grade solvents (Biomol). Solvent A was 80% MeOH and 20% of 0.5 molar amoniumacetat solution and solvent B 80% MeOH and 20% acetone. The gradient was run from A to B in 30 minutes and then held for 10 minutes at B.; flowrate 1.5 ml $min.^{-1}$. Eluting pigments are detected by absorbency (436 nm) and fluorescence (Ex: 410 nm, Em: > 600 nm).

Preliminary results:

Although detailed analysis will be performed at home, first results from pigment spectrum analysis indicate that diatoms and prymnesiophytes dominated phytoplankton assemblages. At some stations peridinin as indicator for dinoflagellates were also found. Chl b could be measured in nearly all samples from surface waters, although in small quantities.

Ice treatment:

To study the impact of ice assemblages to the phytoplankton communities, different ice samples from brown ice and ice cores were taken. Ice cores were cut in different horizons, pooled and about 3l filtered seawater was added to every 10 cm^3 of ice. Then the ice was allowed to melt, the amount of ice was determined and subsamples for different analyses were taken.
The same treatment was done with pieces of brown ice.

Preliminary results:

As in samples from the water column, pigments of diatoms and prymnesiophytes dominated. In contrast to the water samples the chl c: Chl.*a* -ratio was much higher.

8.6. Abundance, biomass and growth potential of heterotrophic dinoflagellates smaller than 20 µm

P. K. Bjørnsen, A. C. Nielsen (MBL)

Descriptions of the pelagic carbon flow often discriminates between the so-called classical food chain from phytoplankton to mesozooplankton (>200 µm, mainly copepods) and the microbial loop, via DOC, bacteria, choanoflagellates, microzooplankton to mesozooplankton. This description assumes a fixed (linear) size ratio between predator and prey of about 10. Dinoflagellates, however, show preference of prey of their own size and may effectively graze on prey larger than their own size. This opens new routes in the pelagic food web, and may sustain modes of network control that at present are incompletely understood or even not described.

This contribution focused on the smallest heterotrophic dinoflagellates (smaller than 20 µm) that presumably will feed on nanophytoplankton. Abundance and biomass of heterotrophic dinoflagellates were determined at every half degree latitude at 20, 60 and 100 m depths from Trans. 2-3, 5 and 11.

Ten ml samples were fixed by 150 µl of 25% glutar aldehyde, stained with proflavin hemisulphate (10 ppm final concentration) and filtered onto black polycarbonate filters of 0.2 µm pore size. More than 50 small heterotrophic dinoflagellates (SHD) were counted and sized under an epifluorescence microscope at 600 x magnification and blue excitation. Only dinoflagellates smaller than 20 µm were included in these counts. Biovolume was converted into biomass assuming a carbon density of 0.12 pg C per μm^3.

Growth potential of small heterotrophic dinoflagellates was assessed at every full degree of Trans. 11 by incubating 260 ml samples from 20 m depth on a rotating wheel (0.1 pm) at 0-1°C for 12 days. Subsamples for counts were taken every 4 days.

9. Plankton production rates

General Objectives

In the framework of JGOFS studies, the link between carbon export and control of phytoplankton production (the so-called biological pump) is of special interest. This control can be achieved by three different mechanisms: physical processes (vertical stabilisation of the water column), chemical processes (micro- and/or macro-nutrients depletion) and/or biological factors (life cycles, grazing by nano- and microheterotrophs, by macrozooplankton and/or micronekton, etc...). In Antarctic waters, physical processes are often considered as control factors of phytoplankton, especially in the Permanently Open Ocean Zone (POOZ). For other areas, such as Seasonal Ice Zones (SIZ) or the Polar Front Zone (PFZ) - where stabilisation of the water column is expected to occur either by ice melting processes or frontal overlayering - chemical and biological factors can be more important.

During ANT X/6 cruise, we had the opportunity to visit a region of complex interactions between the factors described above, in an area covering the three main subsystems identified in Southern Ocean waters. Studies have been conducted to

simultaneously investigate the daily production rates of carbon, silicon and nitrogen by natural phytoplankton populations.

9.1. Carbon primary production

S. Mathot (ULB), B. Quéguiner (IEM) , F. Jochem (IFM)

Objectives

Few measurements of primary production are available in the area investigated. The first objective of our study was thus to evaluate the relative importance of the frontal zones (Polar Front and ACC/Weddell Confluence), the ACC and the Weddell Sea in the carbon budget of Antarctic waters, with special regard to seasonality of the physico-chemical environment at the receding ice edge.

Specific experiments were also conducted for the determination of the physiological parameters characterising different phytoplankton communities (i.e. nano-sized phytoplankton and larger diatoms) and their environmental control variables (light adaptation, temperature effect on growth). Whereas the physiological parameters of the first ones were determined during the EPOS expedition (Mathot et al., 1992), those of the second ones have still to be achieved. Short-term ^{14}C incubations at various light intensities (photosynthetic parameters) as well as long-term kinetics of ^{14}C assimilation into four distinct cellular constituents (growth and respiration parameters) were thus conducted on fractionated field samples (>10 µm and <10 µm). These experiments will be integrated in a two-compartment model of phytoplankton growth.

Methods

Incubations were performed according to the protocol recommended by JGOFS except the utilisation of an "in-situ simulated deck-incubator" instead of in-situ incubations. 250 ml samples were collected from depths closer to 100%, 70%, 45%, 22%, 10%, 4.5%, 1.5%, and 0.5% (neutral density screens) of incoming PAR. Samples were incubated for 24 hours in the deck-incubator, in polycarbonate bottles with $NaH^{14}CO_3$ at a rate of 10 µCi per 100 ml sample (Amersham, specific activity = 56 $mCi*mmol^{-1}$). Samples were filtered on Whatman GF/F filters at the end of incubation time, and then treated to release unassimilated $^{14}CO_2$. Scintillation cocktail was added to the filters prior to their radioactivity assaying in a Packard 1900CA Tri-Carb Liquid Scintillation Counter. Occasionally, size-fractionation was also performed onto 10 µm and 0.8 µm or 0.4 µm Poretics filters.

The experimental determination of physiological parameters characteristic of phytoplankton involved two kinds of tracer experiments conducted in parallel under simulated in-situ conditions. For all these incubations, 100 to 250 ml seawater sample, which amount was chosen according to phytoplankton biomass, were incubated in polycarbonate bottles with $NaH^{14}CO_3$ at a rate of 10 µCi per 100 ml sample (Amersham, specific activity = 56 $mCi*mmol^{-1}$). Total and fractionated samples were treated identically.

Experimental determination of photosynthetic parameters involved short-term (4 hours) ^{14}C incubations (based on the Steemann-Nielsen standard method), per-

formed at various fractions of light intensity and at in-situ temperature. Photosynthetic parameters K_{max}, α, and β were calculated by mathematical fitting of the data relative to the photosynthesis-light relationship using the equation of Platt et al. (1980).

Experimental determination of phytoplankton growth (net primary production) and respiration parameters was performed through long-term (24 hours) light-dark kinetics of ^{14}C assimilation into 4 pools of cellular constituents easily separable by biochemical procedure: small metabolites (composed of monomeric precursors for the synthesis of macromolecular compounds), lipids and polysaccharides (constituting together the reserve products of the phytoplankton cell), and proteins. Incubations were conducted at in-situ temperature under saturating illumination (100-170 $\mu E\ m^{-2}s^{-1}$). The light-dark cycle was fixed at 14:10 to simulate environmental conditions. Details on experimental procedure and biochemical fractionation are described in Lancelot and Mathot (1985). Phytoplankton growth and respiration parameters will be further estimated by mathematical fitting of the data relative to the kinetics assimilation of ^{14}C into proteins and storage products, using the equations described in Lancelot et al. (1991).

Results

a. Spatio-temporal evolution:
Four transects of primary production measurements have been conducted on the 6°W meridian in the course of the cruise (Fig. 6.9.1). The results enable to present a temporal evolution of phytoplankton development within the studied area. The following pattern is presented from South (60°S) to North (46°S).

During 2 and 3, conducted between 11 and 22 October 1992 (Sta. 866 to 884), the integrated primary production was very low over most of the transect (range: 27-195 mg C $m^{-2}d^{-1}$), including the Marginal Ice Zone (MIZ) and the Closed Pack Ice Zone (CPIZ). However, stations located near or in the Polar Front (PF) exhibited somewhat higher values (range: 244 - 446 mg C $m^{-2}d^{-1}$).

At Trans. 5 (24 - 31 October 1992) the production was slightly higher (188 to 198 mg C $m^{-2}d^{-1}$) between 56°S and 54°S (MIZ), whereas it rose up slowly, reaching up to 1535 mg C $m^{-2}d^{-1}$ at Sta. 903 (49°S). In between these two extremes, the net primary production dropped to 127 mg C $m^{-2}d^{-1}$.

At Trans. 6 (31 October - 6 November 1992) which was particularly devoted to the study of the SIZ, the production was mainly uniform between 60°S and 55°S, in spite of the retreat of the ice edge to about 58°30'S. Values oscillated between 185 and 325 mg C $m^{-2}d^{-1}$ yet suggesting a slight phytoplankton growth.

At the last transect (Trans. 11: the most famous and tiring one!!!), conducted between 10 and 21 November 1992 (59°S to 47°S), the situation had dramatically evolved on the entire transect: the distinction between the three water masses (Weddell Sea, ACC and PFZ) was obvious, with uniform southern values a little bit higher than in the previous transects (range: 302-357 mg C $m^{-2}d^{-1}$), some extremely low values still characterising ACC waters (range: 80-258 mg C $m^{-2}d^{-1}$) and the emergence of a bloom situation in the PFZ where the integrated production reached very high values (up to 2892 mg C $m^{-2}d^{-1}$).

Fig.6.9.1 Spatio-temporal evolution of primary production along Trans. (2+3), 5, 6 and 11 on the 6°W meridian

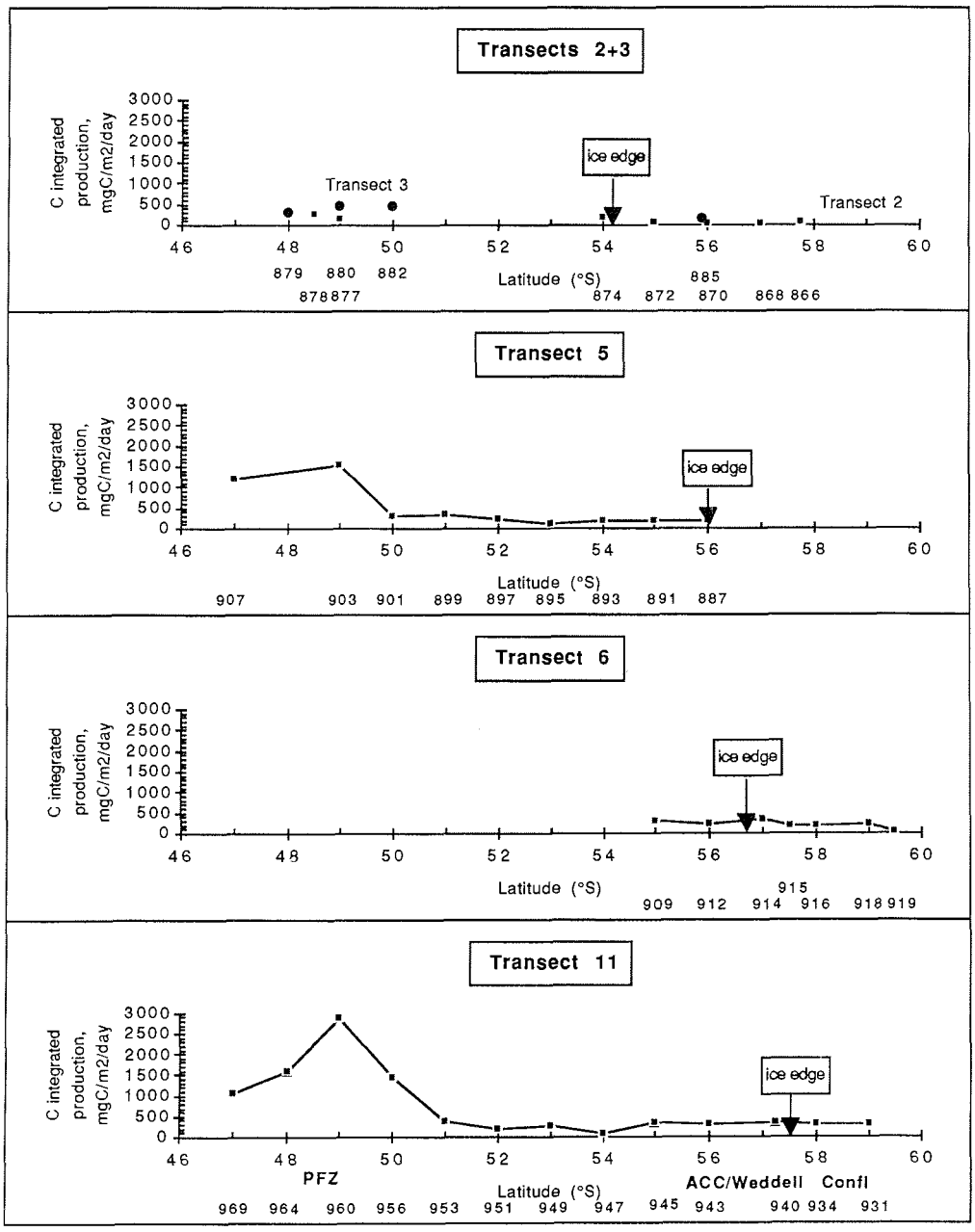

b. Individual primary production rate profiles :

- Production in the SIZ: (Fig. 6.9.2)

The situation observed during transect 6 is characteristic of a typical SIZ with a closed pack ice gradually evolving to MIZ and open water as the ice melts. Under the closed pack ice (Sta. 919, 59°30'S, 85% ice cover), the surface production was relatively low (1.8 mg C $m^{-2}d^{-1}$) and values decreased almost linearly until 100 m. Near the ice edge (Sta. 914, 57°S, 0% ice cover), production values increased near the surface reaching a maximum of 8.4 mg C $m^{-2}d^{-1}$ which can be ascribed to stabilisation of the water column due to a melt water lens. In the outer MIZ (Sta. 912, 56°S) production rates followed the deepening of the wind mixed layer with values still close to 2 mg C $m^{-2}d^{-1}$ up to 60 m depth.

Examining the different transects, it appears that the development of the production in the MIZ is restricted to a narrow horizontal band following the ice edge as previously described in the northwestern Weddell Sea (Lancelot et al., 1991). In the present study area, however, the production extends vertically to depths as high as 150 m which is indicative of a lower stabilization of the surface layer. This can be attributed to the weather conditions which are known to be extremely severe for phytoplankton growth (see C. Veth, this report) and explain the low primary production rates we observed.

- Production in the ACC: (Fig. 6.9.3)

ACC stations usually showed the lowest individual surface production rates in each transect. During each transect, we observed an area of minimal production localised between 52°S and 54°S (i.e., Sta. 947 during Trans. 11, 54°S: 80 mg C $m^{-3}d^{-1}$). The reason of this minimum is still puzzling: is it due to phytoplankton intrinsic (such as low growth rate) or extrinsic (such as heavy grazing pressure) processes? This has to be checked with additionnal data from other working groups. However, the favourable climatic conditions encountered during the last transect (11) have led to the emergence of relatively high production rates in the surface. In such conditions, subsurface maxima can be observed in the vertical profiles. This was observed for example at Sta. 943 (56°S) where a maximum was evidenced between 5-10 m (3.6-3.7 mg C $m^{-3}d^{-1}$) followed by a second maximum at 50 m depth (3.0 mg C $m^{-3}d^{-1}$) which latter could be interpreted as a result of sinking. At this station, production extended vertically to levels as deep as 150 m. As we proceeded northward, the production became more restricted to shallower depths (from 100 m to about 50 m near the Polar Front) with higher production rates encountered in the subsurface. Sta. 953 (51°S) then showed a well-defined maximum of 7.9 mg C $m^{-3}d^{-1}$ at about 30 m depth. Both the vertical extension of production and the appearance of somewhat high subsurface rates under calm weather conditions lead to the conclusion that, in the ACC, wind is the control factor of primary production. However, even in this highly wind-stressed area, small events of localised production can take place near the surface, followed by rapid sinking due to the instability of the water column (deep mixed layer).

Fig. 6.9.2 Typical vertical profiles of the CPIZ (bottom), the ice edge area, and the outer MIZ (up) respectively

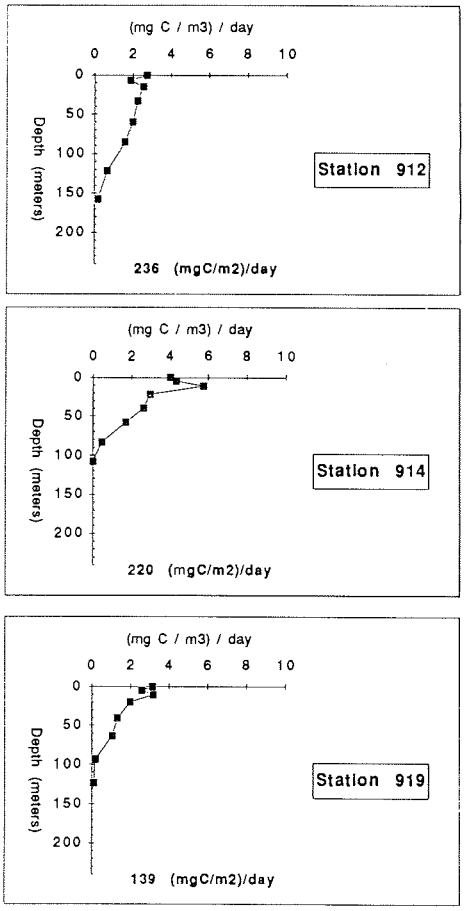

Fig. 6.9.3. Vertical primary production rates in the ACC

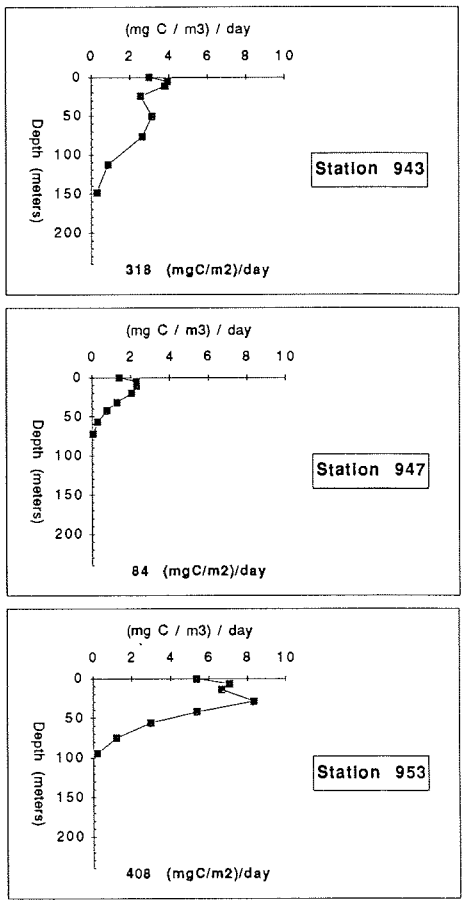

- Production in the PFZ: (Fig. 6.9.4)

From the observations made along all transects it is apparent that a bloom had developed in the PFZ during the study period. This must have been enabled by the shallower mixed layer occurring in the frontal zone. Indeed, for most of the profiles encountered in the PFZ, the production is restricted to waters above 50 m depth. Of peculiar interest is the presence of multiple maximum rates at some of the sampled stations. There are two possible working hypotheses that have emerged from our stimulating team: does this reflect rapid sinking of the populations or is occurrence of overlayering of water masses responsible for the observed pattern? This phenomenon was particularly evidenced at Sta. 903 (49°S, Trans. 5) where three maxima were observed on the profile (60.2 mg C $m^{-3}d^{-1}$ at the surface, 60.3 mg C $m^{-3}d^{-1}$ at about 20 m and 21.4 at about 40 m). Sta. 960 revealed the most relevant integrated value with a subsurface maximum of 76.8 mg C $m^{-3}d^{-1}$ at about 15 m. Preliminary results of the vertical profiles performed in the ACC have thus to be considered further with respect to the complex physical structure of the PFZ.

Fig. 6.9.4 Typical vertical primary production profiles in the PFZ

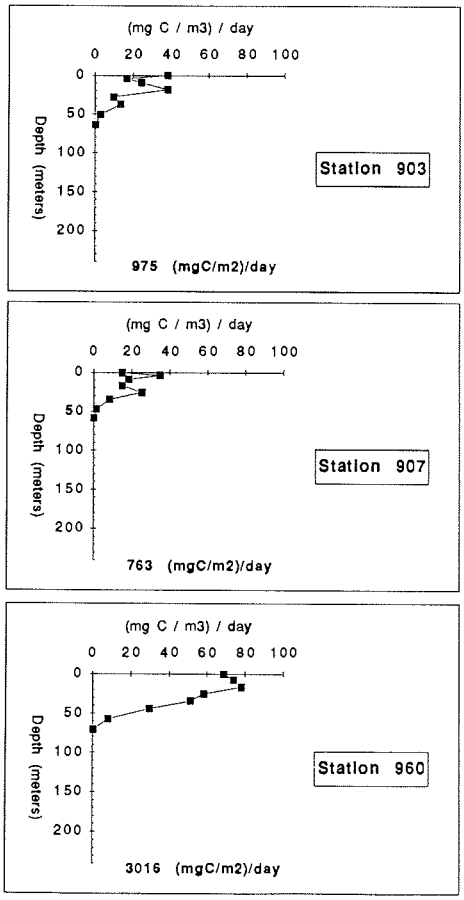

c. Size-fractionated carbon production analysis :

Size-fractionation of primary production has to be treated with caution as methodological problems were evidenced during this cruise: the sum of size fractions was always lower than the total sample. However, taking into account the relative fixation between the two size classes suggests some tendencies. In the CPIZ and the ACC, the bulk of primary production (range: 63-72% in the CPIZ, range: 64-85% in ACC) appeared to pertain to the small (i.e. < 0.4-0.8 µm) phytoplankton. In the MIZ, the repartition was much more variable (range: 50-82%), which could be indicative of ice algae release at some locations where one then would expect higher proportion of primary production in the larger size class. Whereas in the PFZ the reverse situation occurred with 12 to 57% of primary production coming from the smaller size class. It must be pointed out that the importance of the bigger phytoplankton (either as cells or increased chain length) showed an increase as the bloom developed in the PFZ area. This information has to be confirmed by taxonomical identification of phytoplankton.

9.2. Biogenic silica production

B. Quéguiner, L. Teissier (IEM)

Objectives

Despite the importance of the Southern Ocean with regard to the global silicon cycle (75% of the modern global accumulation of siliceous sediments), few direct measurements of biogenic silica production and dissolution rates have been performed hitherto. In order to develop a mathematical model of silicon biogeochemistry for the Southern Ocean, studies have been conducted during Polarstern ANT X/6 cruise to measure those latter parameters and process studies involving kinetics of silicon uptake in different silicate environments as well as light effect on silicate uptake were done. With regard to silicon, the study area appears of special interest for at least two reasons: its location above the sedimentary zone of high biogenic silica deposits, and the existence of a strong silicate gradient in the ACC waters from high values encountered on the Weddell Sea side (> 60 µM Si) to the lowest values of the Polar Front Zone (< 10 µM Si).

Methods

- Biogenic silica production

Biogenic silica production rates (PSi) are determined by the ^{30}Si stable isotope method of Nelson and Goering (1977). The tracer solutions had been passed through Chelex resin before the cruise to limit possible trace metal contamination. 1 l samples are collected from depths closer to 100%, 25%, 10%, 3%, 1% and 0,1% incident PAR. Samples are then drawn in 1 l acid (HCl 0.1 N)-cleaned polycarbonate bottles that had been previously covered with neutral-density nickel screens. Under a laminar flow hood, samples are spiked with 20 µmoles of $Na_2{}^{30}SiO_3$ and placed in a plexiglas incubator maintained at sea surface temperature by constant flow of surface water. After a 24 h incubation the samples are filtered under a laminar flow hood through 47 mm Nuclepore membranes (0.4 µm at each depth and size-fractionation: 0.4-10 µm at 100% and 0.1% depths). Filters are dried for at least 24h at 60°C and

stored in plastic Petri dishes. The determination of the rates of orthosilicic acid uptake (PSi) is performed in the laboratory by mass spectrometry.

- Biogenic silica dissolution
At some stations, biogenic silica dissolution is determined in parallel to PSi by the ^{30}Si stable isotope method of Nelson et al. (1991). 1.6 l samples are collected from depths closer to 100%, 25%, 10%, 3%, 1% and 0,1% incident PAR. Under a laminar flow hood, samples are spiked with 32 µmoles of $Na_2{}^{30}SiO_3$. 1 l of each sample is immediately transferred into acid-cleaned polycarbonate bottles and allowed to incubate during 24 h in a deck incubator maintained at sea surface temperature. 0.6 l remaining are immediately filtered through 0.4 µm Nuclepore filter. The filter is retained for BSi analysis and the filtrate treated to collect the dissolved silicic acid for isotopic analysis. 37.5 ml of Sephadex-cleaned ammonium molybdate/hydrochloric acid reagent are added to the filtrate. The silicomolybdate complex is then extracted on a Sephadex column. After 24 h incubation the 1 l sample is filtered onto 0.4 µm Nuclepore filter. The filter is retained for rSi analysis and the filtrate is treated as described above. $^{28}Si/^{30}Si$ ratios are determined by mass spectrometry. The difference between $^{28}Si/^{30}Si$ ratios in the dissolved phase before and after incubation allows to calculate the rate of dissolution of biogenic silica.

Work at sea

During the different transects conducted on the 6°W meridian, 30 stations have been studied for complete profiles of silicate production within the euphotic zone in the three subsystems: Marginal Ice Zone, Permanently Open Ocean Zone and the Polar Front Zone. Dissolution experiments were done at only two occasions when reasonable biomass was encountered: at Sta. 877 (49°S) and Sta. 879 (48°S), in the Polar Front Zone. Kinetic studies of silicate uptake by natural populations were performed at three stations shared amongst the silicate gradient at 56°S, 51°S and 48°S. One experiment on the effect of light on silicate uptake was done at 56°S.

9.3. Nitrate, nitrite and ammonium based primary production

M. Wunsch (SFB), F. Dehairs (VUA), W. Koeve, L. Goeyens (VUB), J. Poncin (IEM), P. Fritsche (IFM), K. Bakker (NIOZ).

Introduction

Previous investigations in the Southern Ocean have shown that the main type of nitrogen substrate incorporated during primary production changes both regionally and seasonally (Goeyens et al., 1991 a, b; Goeyens, 1992). As concerns the regional variability, it was observed that the marginal ice zone (MIZ) in the Scotia-Weddell Confluence area and the coastal and continental shelf zone (CCSZ) in Prydz Bay, are characterised by predominance of ammonium uptake (f-ratios < 0.5). In contrast, the permanently open ocean (POOZ) of the Scotia Sea, the open ocean zone (OOZ) off Prydz Bay, and the closed pack ice zone (CPIZ) of the Weddell Sea are characterised by predominance of nitrate uptake (f-ratio ≥ 0.5). Production based on ammonium uptake reflects intense recycling of nitrogen in the upper water column, and therefore the fraction of primary production left for export to the deeper ocean and the sediments is reduced. Production based on nitrate uptake should sustain significant export of matter from the upper mixed layer. However, steady state

conditions are probably not attained in the Southern Ocean, where strong seasonal patterns prevail, and nitrate is always abundant. In this environment a significant fraction of nitrate uptake must be fuelling recycled production (Smetacek et al., 1990).

Increasing ammonium uptake rates in MIZ and CCSZ closely follow increased rates of ammonium production, mainly resulting from an increased grazing pressure by micrograzers. These micrograzers have developed closely in pace with the phytoplankton, which showed high productivities in these MIZ and CCSZ environments, as compared to POOZ and OOZ (Mathot et al., 1992). This high phytoplankton productivity in MIZ and CCSZ becomes possible as a result of surface water stabilisation due to meltwater input (Sullivan et al., 1988). However, the very high nitrate depletions (i.e. the water column integrated difference in nitrate content at the time of sampling relative to the winter conditions) indicate that at the very onset of the seasonal bloom, very high nitrate uptake rates must have prevailed, be it for a short period (2 to 3 weeks ?). The build-up of grazing pressure results in significant ammonium accumulation, which then becomes the predominant nitrogen substrate taken up.

It was proposed for the present JGOFS-SO expedition to verify whether the earlier observations pertaining to the Scotia-Weddell Confluence and the Weddell Sea are confirmed for POOZ-OOZ-MIZ-CPIZ systems elsewhere in the open Southern Ocean at great distance from any continental influence. The difference being that in the Scotia-Weddell Confluence area the MIZ, despite a retreat with the receding ice edge, is persistent over the season, while in the Atlantic sector investigated here, the ice edge retreats up to the Antarctic continent leaving essentially an OOZ in its wake. The area investigated here, is also known to be characterised by significant contribution of diatoms in the phytoplankton biomass, as reflected in the high accumulation of biogenic silica in the underlying sediments (DeMaster et al., 1991). The cruise track allowed for studying both regional and seasonal variation. A meridional section (at 6°W) was sampled between the pack ice (the ice-edge moved from 56°S to 59°S between early October to mid-November) and 47°S, covering the whole width of the Antarctic Circumpolar Current (ACC) from south of the ACC-Weddell Front to just north of the Polar Front. The whole sampling period at the 6°W meridian extended between October 11 and November 22 and should have covered the onset of the spring phytoplankton bloom.

Methods

Nitrate, nitrite and ammonium uptake were studied using ^{15}N labelled nitrogen substrates. Nitrate and nitrite spike additions were ≤ 10% of the original concentrations. For ammonium uptake, spike additions (kept constant) resulted in increases of the original concentration from 100 to 20%, depending on the magnitude of the latter. Whenever possible, sample depths were selected from data on photometric depth profiling. They were incubated at corresponding light conditions (using neutral density screens) for 24 hours in an on-deck incubator, kept at surface water temperatures by flow through of surface seawater. For ammonium, incubations during the transect sections were performed only at 100% and 30% of PAR. For nitrite only at 100% PAR and for nitrate at 100%; 66%; 52%; 13%; 6% and 1% of PAR.

Furthermore, in cases where Chl-a concentrations were sufficient (≥ 0.3 µg l^{-1}), post incubation size fractionations were performed. For ammonium and nitrite uptake, size

fractionation was limited to the < 20 µm and the total fractions. For nitrate, size fractions separated were: total; < 20 µm; < 5 µm and < 2 µm.

Diffusion technique to extract the dissolved ammonium from the seawater solution. ^{15}N enrichment in collected substrates (particulate organic matter and ammonium sulphate) will be determined by mass spectrometry (for nitrate) and emission spectrometry (for ammonium and nitrite).

The main sampling effort was concentrated on three north south transects along 6°W, between 59°S and 47°S (Trans. 2, 5 and 11). In addition one shorter ice-edge transect (Trans. 6), between 55°S and 59°30'S; one drift station (Trans. 4), between 55°54'S and 56°22'S, and one short Polar Front section (Trans. 12) were sampled. During transects stations sampled for ^{15}N uptake experiments were spaced at 60 nautical miles. During the drift station samples were incubated at seven different light levels, both, in-situ incubation and in the on-deck incubator.

Enrichments in sampled substrates will be done in the respective land-based laboratories.

References:

Goeyens, L. (1992) New and regenerated production in the Southern Ocean: Regional and seasonal variability, Doctoral Thesis, Vrije Universiteit Brussel, Brussel, 167 pp.

Goeyens, L., F. Sörensson, P. Tréguer, J. Morvan, M. Panouse & F. Dehairs (1991a) Spatiotemporal variability of inorganic nitrogen stocks and assimilatory fluxes in the Scotia-Weddell Confluence area, Marine Ecology Progress Series, 77: 7-19.

Goeyens, L., P. Tréguer, C. Lancelot, S. Mathot, S. Becquevort, J. Morvan, F. Dehairs & W. Baeyens (1991b) Ammonium regeneration in the Scotia-Weddell confluence area during spring 1988. Marine Ecology Progress Series, 78: 241-252.

Mathot, S., J. M. Dandois & C. Lancelot (1992) Gross and net primary production in the Scotia-Weddell sector of the Southern Ocean during spring, Polar Biology, 12: 321-332.

Smetacek, V., R.Scharek & E. M. Nöthig (1990) Seasonal and regional variation in the pelagial and its relationship to the life history cycle of krill, In: Antarctic Ecosystems, Ecological Change and Conservation. K.R. Kerry & G. Hempel (eds.), Springer Verlag, Berlin, 103-114.

Sullivan, C.W., C.R. McClain, J.C. Comiso & W.O.Smith Jr. (1988) Phytoplankton standing crops within an Antarctic ice edge assessed by satellite remote sensing, Journal of Geophysical Research, 93: 12487-12498.

10. Bacteria

10.1. Bacterial biomass and production

S. Becquevort (ULB), P. Bjørnsen, A. Nielsen (MBL), K. Lochte (AWI), A. Weber (IfM)

Introduction

Microbiological field investigations according to the JGOFS core parameter 10 were carried out by several groups during ANT X/6, which are all presented in this chapter under separate headings. The general emphasis of the microbiological investigations was on the quantitative contribution of bacteria to the turnover of organic carbon. Bacterial numbers and biomass were determined separately by Sylvie Becquevort, Thierry De Henau (ULB) and Anke Weber (IFM); bacterial production was determined jointly by Peter Bjørnsen, Alexandra Nielsen (MLB) and Karin Lochte (AWI). In addition to the regular determination of field data on stations, experiments were carried out investigating particular aspects of bacterial growth and mortality under the relevant environmental conditions. These experiments are described in chapter 11, identifying the larger context and indicating cross connections to research described elsewhere in the cruise report.

10.2. Bacterial abundance

S. Becquevort, T. De Henau (ULB)

Objectives

For the estimation of carbon flow in the microbial loop bacterial abundance is an important parameter. Parallel to protozoan grazing experiments, described in section 11, bacterial abundance was determined in natural and experimental samples. These data then serve as input for modelling of the microbial loop. Furthermore, bacterial abundance and biomass are JGOFS core parameters and the field data will enter the JGOFS data base.

Work at Sea

Samples obtained by CTD casts were fixed with formaldehyde (2% final concentration). Bacteria were enumerated on board by epifluorescence microscopy after DAPI staining (Porter & Feig 1980). Biovolumes will be estimated at home, on enlargements of microphotographs. For conversion into bacterial carbon the biovolume dependent C/biovolume ratio proposed by Simon and Azam (1989) will be used.

Bacteria were also enumerated by flow cytometry. Samples were fixed with formaldehyde (2% final concentration) and stained with DAPI (1.25 µg ml^{-1} final concentration). Data acquisition was triggered by the blue fluorescence of DAPI excited by UV light. Fluorescent particles with small forward angle light scatter were scored as bacteria, as seen in Fig. 6.10.1.

The results of flow cytometry will be analysed at home and compared to enumeration of cells and biovolume estimates made by epifluorescence microscopy.

Fig. 6.10.1 Histogram of forward angle light scatter (FALS) intensity related to the size of the particles. The area of interest covering bacteria represented 1.23 10^5 particles ml^{-1} (Sta. 960 at 40 m depth).

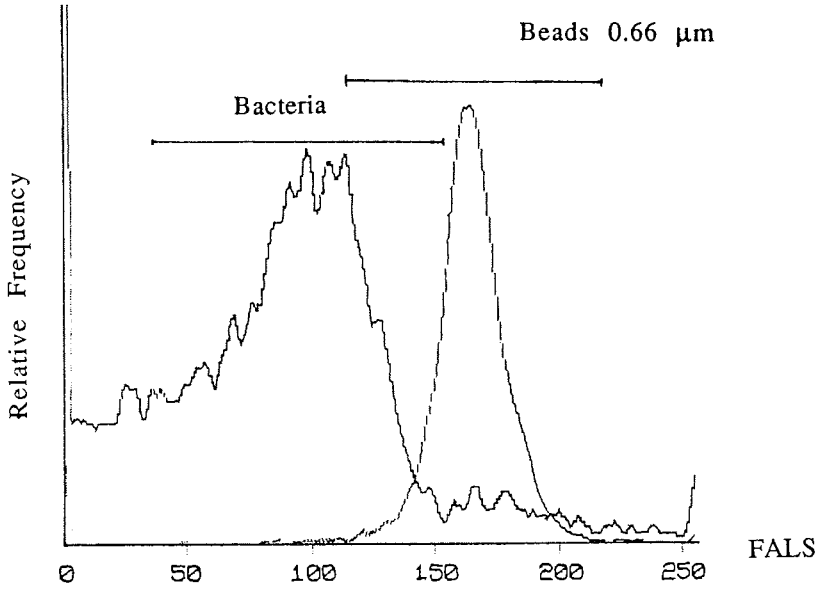

First results.

Distribution of bacteria along the meridian 6°W at different time periods are shown in Fig. 6.10.2.

Fig. 6.10.2 Bacterial abundances along the meridian 6°W for the Trans. a) 2, b) 5 and c) 11.

Fig. 6.10.2a. Trans. 2: 11-22 October

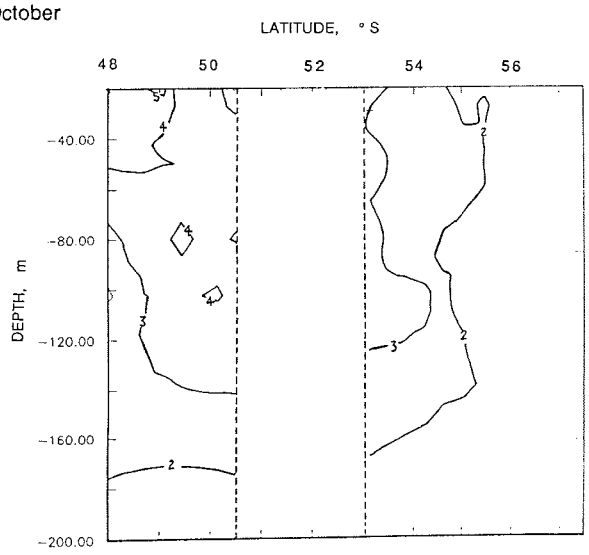

Fig. 6.10.2b. Trans. 5: 24-31 October

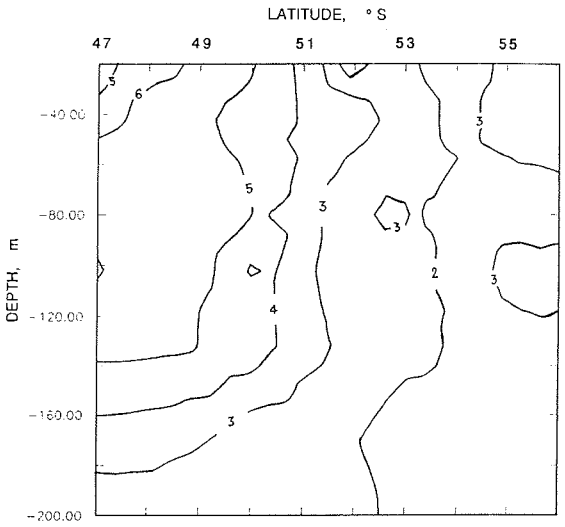

Fig. 6.10.2c. Trans. 11: 10-21 November

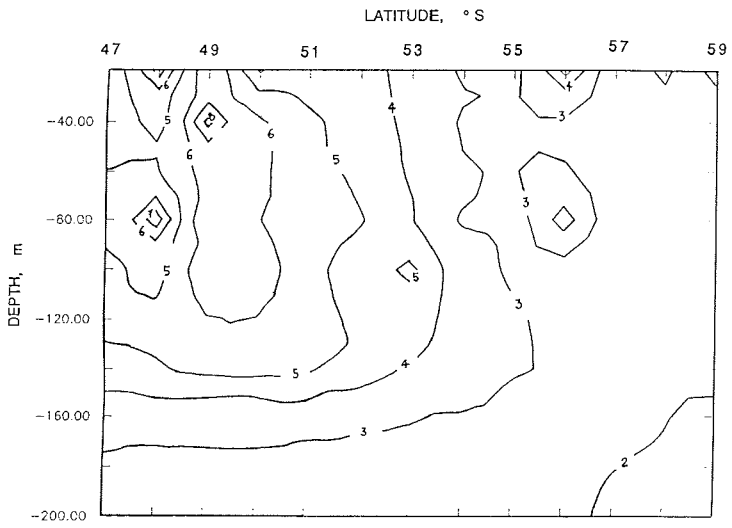

Minimum values of around 2 x 10^5 bacteria ml^{-1} were encountered in the closed Pack Ice Zone. For Trans. 5 and 11, two peaks, one in the surface and the other one in the sub-surface, were observed at about 56°-57°S. It reached 5 x 10^5 bacteria ml^{-1} for the last transect.

Maximum values were observed in the Polar Frontal Zone for all three transects. With time bacterial abundances increased from 5 x 10^5 bacteria ml^{-1} (Trans. 2) to 8 x 10^5 bacteria ml^{-1} (Trans. 11). For the last transect, at 48°S, we observed two peaks, one in the surface and the other one at 60 m depth.

References:

Porter, K.G. and Y.S. Feig (1980) Use of DAPI for identifying and counting aquatic microflora. Limnol. Oceanogr. 25,943-948.
Simon, M. and F. Azam (1989) Protein content and protein synthesis rates of planktonic marine bacteria. Mar. Ecol. Prog. Ser. 51, 201-213.

10.3. Bacterial abundance and biomass

A. Weber (IFM)

Objectives

Bacterial biomass is a large and dynamic component of the planktonic system. Its determination is part of the JGOFS core measurements, and therefore, abundance and biomass were measured according to the JGOFS recommendations on a regular basis in field samples. These data not only give indications about changes in the bacterial standing stock but are also necessary for estimation of the growth rates in connection with bacterial production data.

Work at Sea

The samples for bacterial abundance and biomass were taken on stations at full geographical degrees together with the samples for bacterial production. Five depths between 20 m and 200 m were sampled.

Bacterial abundance was determined in 5-10 ml of formalin fixed samples. They were filtered onto Irgalan pre-stained 0.2 µm Nucleopore filters, a second membrane filter was placed underneath to facilitate even dispersion of the bacteria over the filter. After four minutes of staining by acridine orange, the filters were mounted in immersion oil on microscope slides and counts were made under blue-light excitation using a Zeiss epiflourescence microscope (1000x) with ICS-optics. A total of 245 filters of 41 stations was counted.

Bacterial biomass was estimated by measuring the volumina of 50 randomly selected cells per sample with a New Porton grid which was calibrated by comparison with standard size fluorescent beads. The mean bacterial cellular carbon content within a sample was calculated according to Simon & Azam (1989). Bacterial biomass was calculated by multiplying cell numbers and mean cellular carbon content. No correction was made for possible shrinkage as a result of sample preparation.

The shipboard dataset for bacterial numbers and biomass will be written up in collaboration with H. Giesenhagen (IFM).

Preliminary results

At the present time the dataset of Trans. 2 and 3 is still incomplete. The values of bacterial numbers and biomass obtained so far indicate no significant differences compared to Trans. 5 and 6. Therefore only data of Trans. 5 and 6 (combined) and 11 are presented.

Trans. 5 (24.-30.10.92) & 6 (2.-6.11.92):
The region north of 51°S6°W in the area of the Polar Front was characterised by slightly higher bacterial numbers in 20 m depth (Fig. 6.10.3a). The peak at 50°S coincided with an increase in chlorophyll (see Bathmann this Vol.). Bacterial cells were small and biomass was low. A second increase in bacterial numbers was found between 53°S and 54°S which was not restricted to the surface layer and corresponded to the retreat of the ice cover. The meltwater zone was located at 54°-55°S. Along with the increase in numbers an increase in chlorophyll and biovolume was observed. South of this area, in the ice covered region, all values were relatively uniform and low. This holds true also for bacterial cell sizes.

Trans. 11 (10.-21.11.92):
At this time high bacterial numbers (and biovolumes) were observed in the frontal zone between 47°S to 51°S which were mostly restricted to the surface layer (Fig. 6.10.3b). Another increase was found again in the area of the meltwater lens which had been moving further south to 55°-56°S. Maximum values here tended to be in the depth range of 40-100 m (data not shown). Further south, numbers and biovolumes were as low as two weeks earlier.

Fig. 6.10.3 Bacterial numbers along 6°W at a) Trans. 5 (light symbols) 6 (dark symbols) and b) Trans. 11

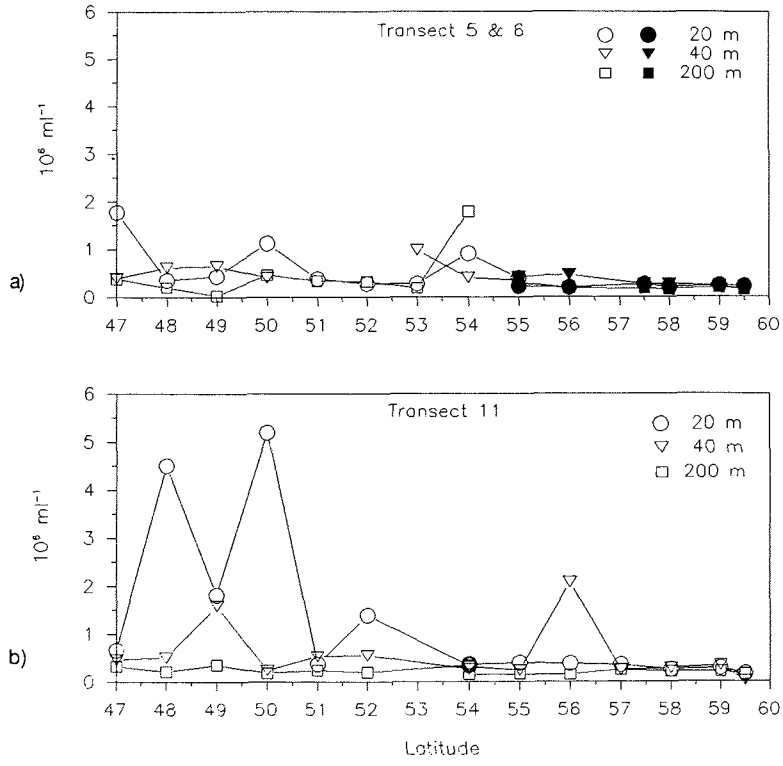

Comparing all results at 6°W, the remarkable changes in the region between 47°S and 51°S clearly confirm the theory of a spring bloom at the Polar Front. The small changes in the area further south indicate that the onset of a spring bloom at the marginal ice zone could not be observed.

As indicated above, not all samples have been analysed onboard Polarstern. The dataset will be completed in Kiel. Furthermore, around 400 samples for the determination of active bacteria by microautoradiography will be processed at the home laboratory in Kiel (H. Giesenhagen).

References

Simon, M and F. Azam (1989) Protein content and protein synthesis rates of planktonic marine bacteria. Mar. Ecol. Prog. Ser. 51, 201-213.

10.4. Bacterial production

P. Bjørnsen, A. Nielsen (MBL), K. Lochte (AWI)

Objectives

Bacterial production is known to consume a large and variable proportion of photosynthetically produced organic carbon. The current view is that approximately 20%-40% of the consumed carbon is converted to bacterial biomass (Bjørnsen & Kuparinen 1991) and the rest is respired or excreted. Thus, heterotrophic carbon conversion by bacteria remineralizes significant amounts of organic carbon already in the upper water column and is largely responsible for the degradation of detrital material below the euphotic zone. Comparison with primary production gives indications about the speed of carbon cycling in the upper mixed layer. Since bacteria are only able to consume dissolved organic carbon (DOC) their impact on the DOC pool, which is also measured on this cruise (see section 6.4), is of interest.

Measurements of bacterial production were carried out routinely as a JGOFS core parameter using two independent measurements: incorporation of ^{3}H-labelled thymidine and leucine. Thymidine is primarily incorporated into nucleic acids giving an indication of DNA replication and cell division; leucine is incorporated into proteins and represents production of biomass. The validity of these assumptions was tested by experiments (section 11.1: Calibration of bacterioplankton production measurements). Further experiments were carried out on board to test the dependency of the production measurements on incubation time, on the concentration of added substrate and on the incubation temperature in the environmentally relevant temperature regime from -2°C to +3°C. The effect of decreasing light regimes on natural populations of algae and bacteria, simulating submergence of water masses, was also tested.

Work at Sea

Water samples were taken from the CTD rosette from 5 depths. The surface sample was taken at a fixed depth of 20 m and the deep sample at 200 m; the three variable depths in-between were selected according to water column structure as indicated by

temperature, transmission and fluorescence profiles from the CTD sensors. In order to best represent the water column, they were selected at the base of the thermocline, the top of the thermocline and one sample in-between 20 m and the top of the thermocline preferably in the peak of fluorescence (if present).

Subsamples of 10 - 20 ml for bacterial numbers and biomass, determined by Anke Weber (see section 10.3), were also taken from these water samples to enable a direct comparison of standing stocks and bacterial production data.

The determination of bacterial production followed largely the method given in Bjørnsen and Kuparinen (1991) with some small alterations. Four 10 ml aliquots of water sample were dispensed into plastic vials; one of these subsamples was fixed by addition of 100 µl 39% formalin amended with cold thymidine and served as a blank. Each sample received methyl-[^{3}H]-thymidine, specific activity 3.11 TBq/mmol (Amersham), to a final concentration of 2nM. The samples were incubated for 2 to 3 hours at 0°C and the incubation was stopped by addition of 100 µl 39% formalin amended with cold thymidine. The samples were filtered through 0.22 µm poresize cellulose acetate filters, pre-soaked in a cold thymidine solution, and rinsed 10 times with 1 ml 5% ice cold TCA. The filters were placed in 5 ml plastic scintillation vials and 4.5 ml scintillation cocktail (Lumagel SB, Baker Chemicals) were added. The radioactivity incorporated in the cold TCA precipitable material on the filter was measured on board by a Packard Liquid Scintillation Counter.

The procedure for measuring leucine incorporation was identical to the thymidine incorporation method described above except for the following differences: The samples received a final concentration of 10 nM L-[4,5-^{3}H]-leucine (Amersham), specific activity 0.522 TBq/mmol. After incubation, the samples were filtered through 0.2 µm poresize polycarbonate filters (Nuclepore).

Preliminary Results

All stations on Trans. 2, 3, 5 and 11 were sampled at 5 depths for both substrates, on Trans. 6 between 55°S and 57°S only full geographical degrees were sampled, and on Trans. 8, 9 and 12 only thymidine incorporation at 4 or 5 depths was determined. This sampling programme resulted in a sum of 86 investigated stations and a total of 771 field samples analysed for thymidine or leucine incorporation.

The conversion factors to convert the incorporation rates of thymidine and leucine to production of bacterial cells or biomass carbon are established in experiments (see chapter 11.1) which are not yet completely analysed. In order to convert the substrate uptake to bacterial production the following provisional conversion factors were used: 1 pmol l^{-1} day^{-1} of tritiated thymidine incorporation (TTI) corresponds to a bacterial net production of 1.1 x 10^6 cells l^{-1} day^{-1}. Cell production was provisionally converted into carbon production assuming a carbon to biomass ratio of 20 fg C per cell (Lee and Fuhrman 1987). For leucine incorporation (LEU) 1 pmol l^{-1} day^{-1} corresponds to a net carbon production of 0.003 µg C l^{-1} day^{-1} or to a gross production (carbon demand) of 0.01 µg C l^{-1} day^{-1} (Bjørnsen and Kuparinen 1991). Final adjustments to the preliminary estimates of bacterial production will be made using the conversion factors determined from the experiments as well as corrections to account for the different environmental temperatures. In order to enable comparison with primary

production data, estimates are given for integrated bacterial production in the upper 300 m water column based on the preliminary conversion factors.

Fig. 6.10.4 Integrated bacterial production over the upper 200 m on Trans. 2 (12.-18.10.92) and 3 (19.-20.10.92) estimated from thymidine and leucine incorporation.

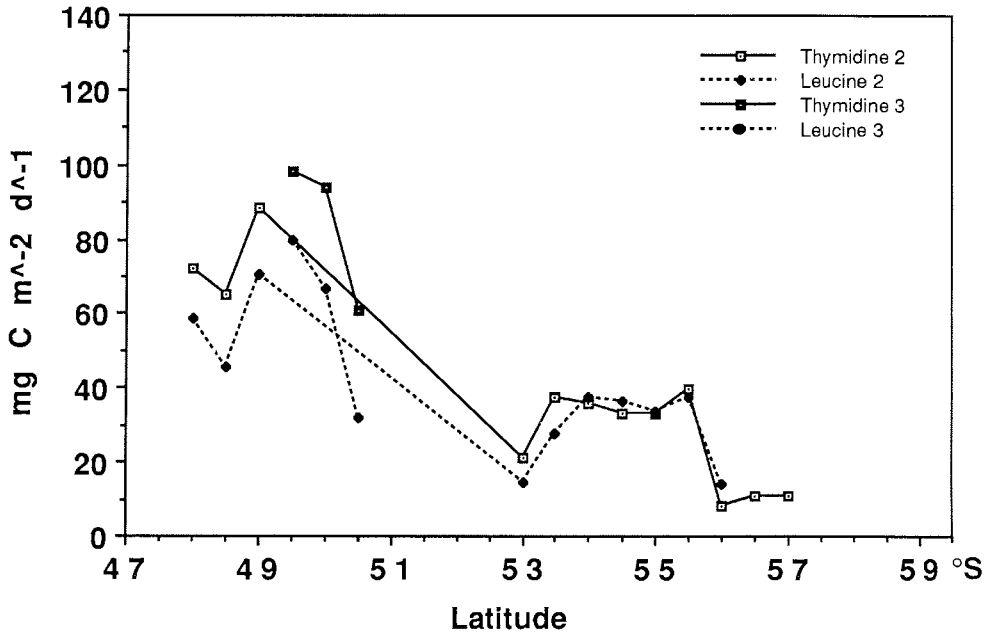

The transects along 6°W between 59°S and 47°S indicated a distinct distribution pattern of bacterial productivity. Integrated bacterial productivity on Trans. 2 showed slightly raised values between 53°30'S - 55°30'S in the approximate area of lower salinities created by meltwater (54°45'S - 55°35'S) (Fig. 6.10.4). Due to storm the region between 53° and 51° could not be sampled, but it appears that north of the meltwater zone productivity was lower. The area of the Polar Front north of 50°S, separating the Antarctic Circumpolar Current and subantarctic water, was sampled by Trans. 2 and 3 and was characterised by bacterial productivity approximately twice as high as in the meltwater zone. A similar pattern of high productivity in the frontal zone gradually decreasing towards the south was observed on Trans. 5 and 6 (Fig. 6.10.5). On Trans. 11 high bacterioplankton productivity was again observed in the frontal zone between 47° to 50°S and low values adjoined south of it (Fig. 6.10.6). Bacterial production was now approximately twice as high as on Trans. 2 and 3 one month earlier. This transect also showed a small increase in the area of the meltwater lens, which was now located at 54°50'S - 56°00'S.

Fig. 6.10.5 Integrated bacterial production over the upper 200 m on Trans. 5 (24.-30.10.92) and 6 (2.-6.11.92) estimated from thymidine and leucine incorporation.

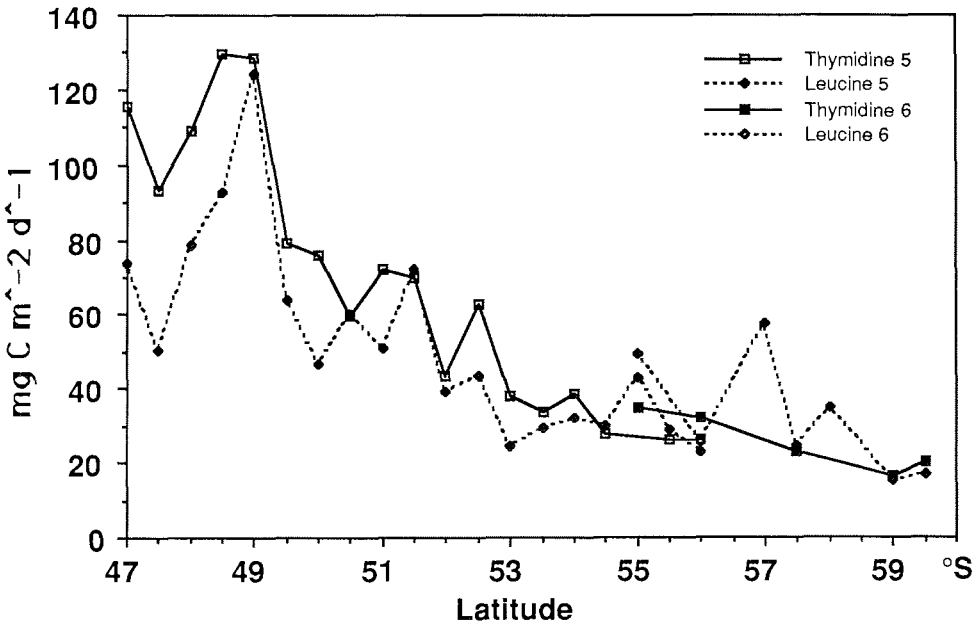

The distribution patterns of bacterial production followed basically the distribution of Chl.*a* (see section 8.1). However the ratio of bacterial production in the upper 300 m water column to the standing stock of Chl.*a* integrated over the same depth was not constant as shown in Fig. 6.10.7 for Trans. 11. In the frontal zone north of 50°S and in the marginal ice zone south of 56°S this ratio was lower than in the 'poor' intermediate zone, which was characterised by low Chl.*a* and low bacterial productivity. Comparison with data on primary production will show whether in this region a larger proportion of the photosynthetically produced organic matter is consumed by bacteria than in phytoplankton rich areas.

Fig. 6.10.6 Integrated bacterial production over the upper 200 m on Trans. 11 (10.-21.11.) estimated from thymidine and leucine incorporation.

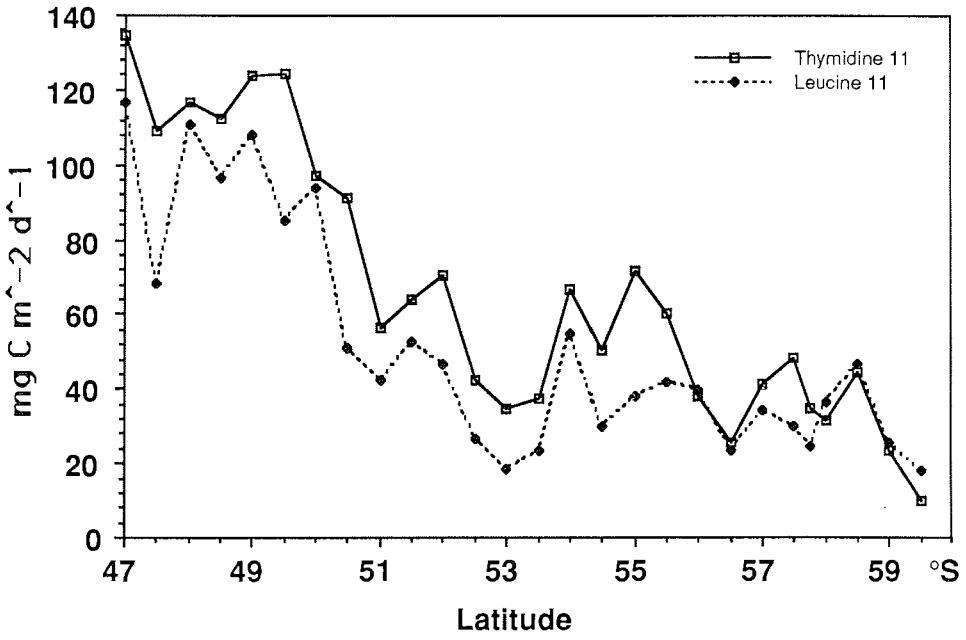

Fig.6.10.7 Ratio of integrated (0-200 m) bacterial production determined by thymidine incorporation (mg C mol^{-1} d^{-1}) to standing stock of Chl.*a* (mg Chl.*a* mol^{-1}) on Trans. 11.

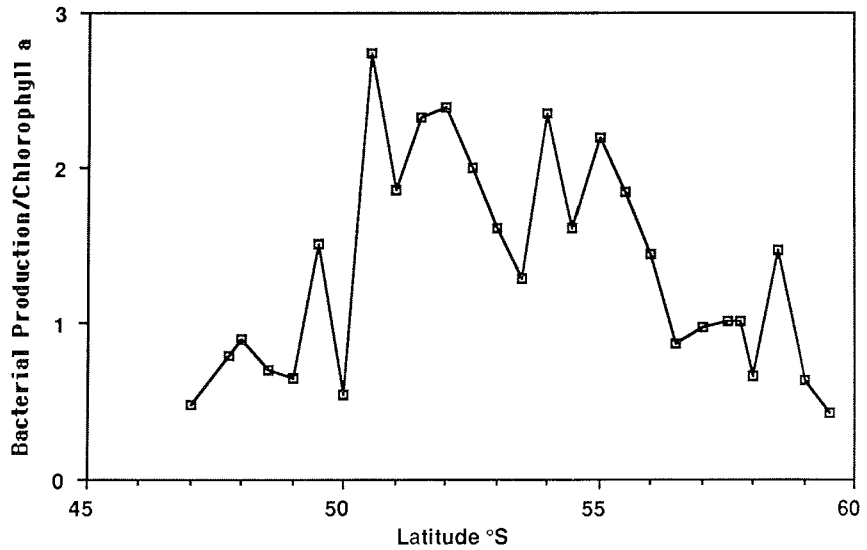

References

Bjørnsen, P.K. and J. Kuparinen (1991) Determination of bacterioplankton biomass, net production and growth efficiency in the Southern Ocean. Mar. Ecol. Prog. Ser. 71: 185-194.

Lee, S.H. and J.A. Fuhrman (1987) Relationship between biovolume and biomass of naturally derived marine bacterioplankton. Appl. Environ. Microbiol. 53: 1298-1303.

11. Experimental work on bacteria, phyto- and microzooplankton

11.1. Experiments on the microbial degradability of DOC and on the calibration of bacterioplankton production measurements

P. Kähler (SFB), P. Bjørnsen (MBL), R. Manuels (NIOZ), K. Lochte (AWI)

Dissolved organic carbon (DOC) constitutes the major organic carbon pool of the ocean, but only a minor fraction of this pool is believed to undergo biological turnover. Due to uncertainties in the methodology of DOC determination in the past, the size of this pool and the rate of bacterial consumption of DOC (c.f. Kirchman et al. 1991) are still uncertain. The experimental set-up of this experiment is designed to investigate bacterial consumption of natural DOC in filtered water samples. It also provides a suitable test system for a calibration of methods, since bacterial production can be determined by the increase in biomass in the absence of mortality from predation.

With this double purpose, experiments were set up twice (at Sta. 886 and 942). Water from 1000 m and 20 m was filtered through 0.8 µm polycarbonate filters letting most of the seawater bacteria pass through. Part of the water from 20 m was enriched with filtered brown ice (approximately 15% vol/vol). Duplicate subsamples of 5L were incubated for 12 days at 0°C and sampled every 2-4 days for measurements of DOC, nutrients, thymidine and leucine incorporation, bacterioplankton abundance and cell volume, and particulate organic carbon concentration. The concurrent consumption of oxygen was measured in separate 100 ml glass bottles harvested in triplicates every 4 days.

Several parameters are to be measured at our home laboratories before conclusive results will emerge. The data presently available suggest that the experimental set-up and the sampling scheme provided an adequate range of activity levels for detection of oxygen consumption (Fig. 6.11.1) and coverage of bacterial production processes (Fig. 6.11.2).

Fig. 6.11.1 Change of dissolved oxygen with time in experiments 1 (Sta. 886) and 2 (Sta. 942) in 0.8 µm filtered sea water from 20 m (circles), from 1000 m (squares) and from 20 m enriched with melted brown ice filtered through 0.8 µm (triangles).

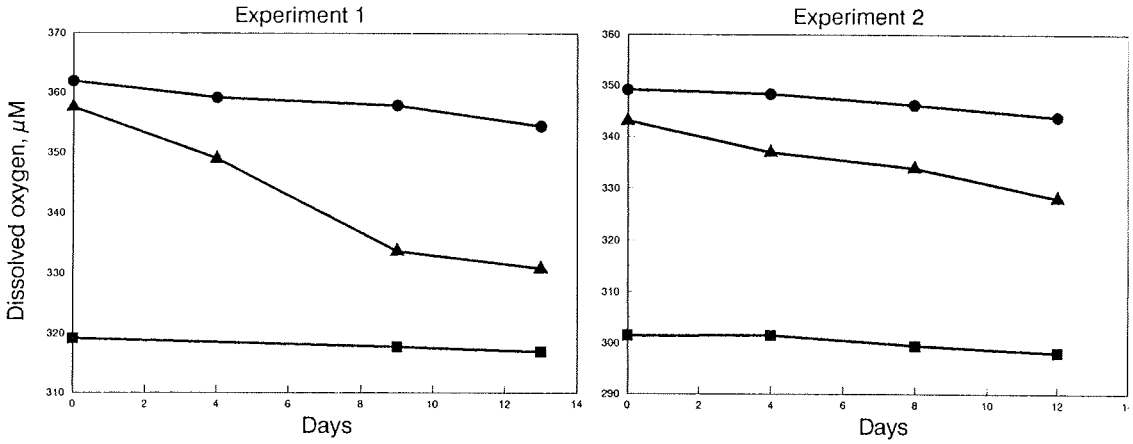

Fig. 6.11.2 Bacterial growth determined by ^{3}H-thymidine and ^{3}H-leucine incorporation and change in bacterial abundance and biovolume in experiment 1 (Sta. 886). Symbols are as in Fig. 6.11.1; solid lines represent incubations in the dark, broken ones incubation in the light.

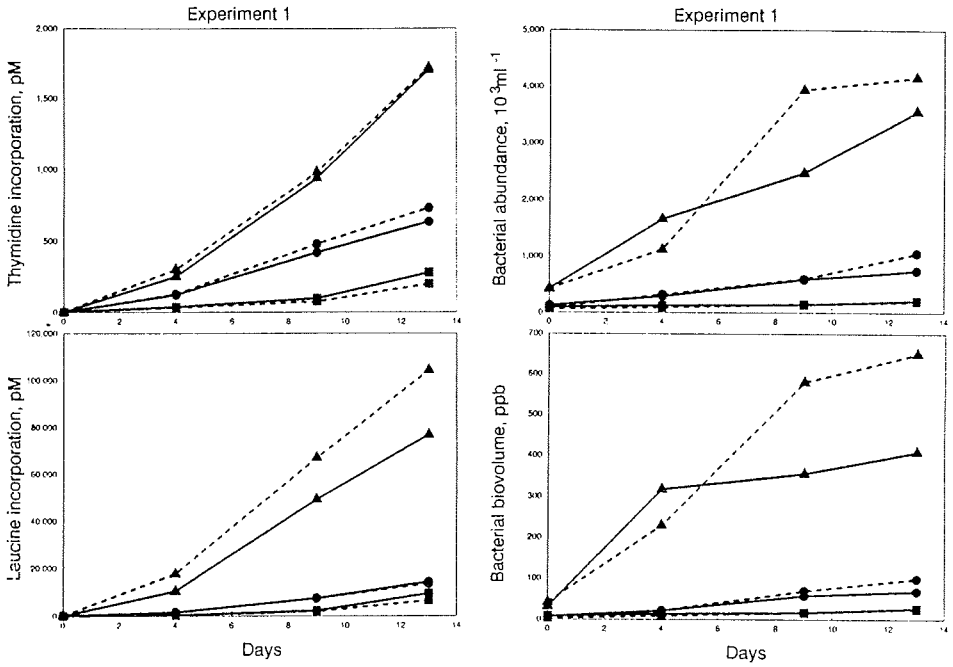

11.2. Experiments on the effect of temperature (-2°C to +3°C) on phytoplankton and bacterioplankton production

K. Lochte (AWI), P. Bjørnsen (MBL), S. Mathot, S. Becquevort (ULB)

The measurement of planktonic processes in the Southern Ocean usually involves long incubation times of water samples during which physical conditions - including temperature - may be different from in situ conditions causing a bias in the results. Often an increase of biological rates of 7% per degree of temperature is assumed (corresponding to a Q_{10} of 2), however, it has been suggested that this effect is stronger at low temperatures, particularly for microheterotrophs (Pomeroy and Deibel 1986).

Fig. 6.11.3 Decrease in incorporation rate (pM h^{-1}) of thymidine (solid line) and leucine (broken line) with decreasing temperature at Sta. 907 (a), 930 (b), 946 (c) and 960 (c). The actual temperatures recorded during the incubation time of 180 min are given below each graph as dotted lines.

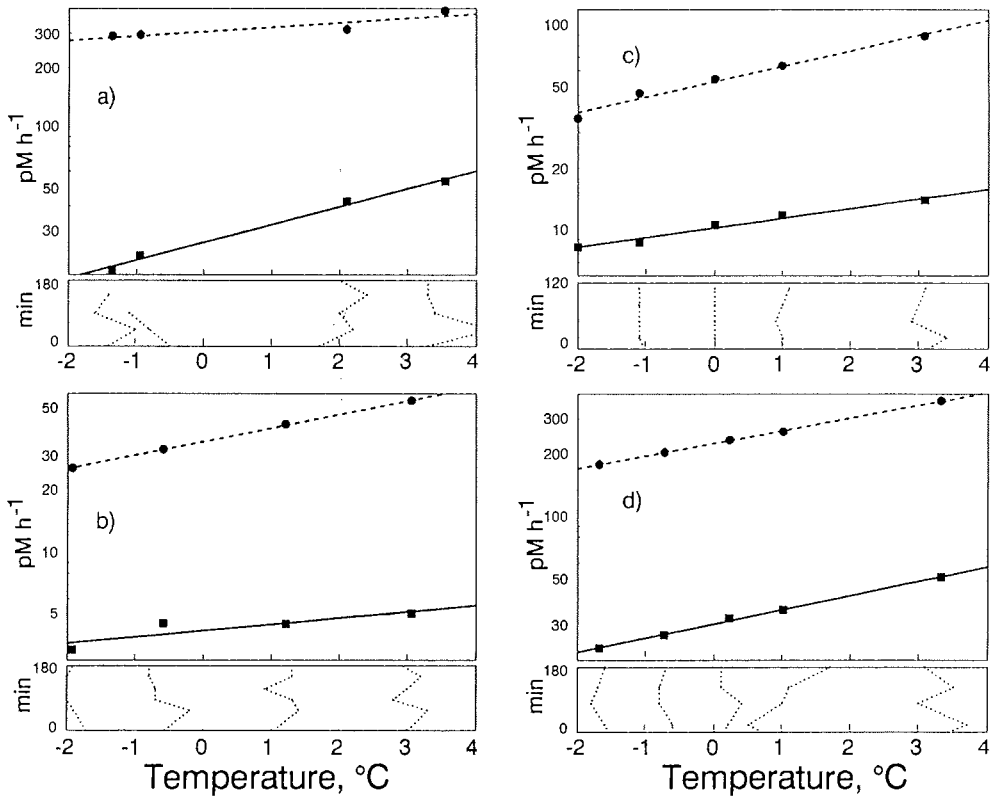

In order to test this hypothesis, surface water from Sta. 886, 895, 907, 930 945 and 960 was allowed to adapt to different temperatures between -2°C and +3°C. Bacterial production was assessed by incorporation of tritiated thymidine and leucine according to the method described in section 10.4, and phytoplankton production was measured (at 4 stations) by incorporation of ^{14}C bicarbonate as described in section 9.1. Bacterioplankton growth rate was followed by microscopic counts in unenriched 1 µm filtrates from 2 stations incubated for 15 days, and in an enriched 0.8 µm filtrate from one station incubated for 5 days.

Preliminary results suggest that bacterioplankton production rate decreases to about half from +3°C to -2°C, suggesting a temperature effect of approximately 15% per degree corresponding to a Q_{10} of 4 (Fig. 6.11.3).

11.3. Effect of diminishing light on natural populations of algae and bacteria

I. Peeken (SFB), K. Lochte, R. Crawford (AWI)

At fronts, overlayering by lighter water over adjacent heavier water would subduct the latter and thereby displace its phytoplankton populations into deeper, less illuminated zones. The floristic and physiological reaction (pigment composition) of phytoplankton to such reduction in light levels and the response of bacteria (growth rates) was investigated in this experiment.

Water samples from the Polar Front containing a mixed population dominated by *Corethron criophilum* and *Fragilariopsis kerguelensis* were amended with enrichment cultures predominantly containing the same species in order to increase the algal biomass for the experiment. The pooled initial sample was dispensed into 8 x 10L glass bottles; two replicate bottles for each treatment. Treatment A: full light; treatment B: completely dark; treatment C: stepwise moderate reduction of light to low light level; treatment D: stepwise strong reduction of light to complete darkness. The light was reduced every 2 days over a period of 1 week. All samples were then brought back again to full light and maintained for a further 9 days before the experiment was terminated. At intervals of 2 to 4 days subsamples were taken for determination of pigment composition by HPLC (see section 8.5), bacterial production by thymidine and leucine incorporation (see section 10.4), bacterial biomass by epifluorescence microscopy. Microscopic investigation of the diatoms was carried out at the beginning, mid-point and end of the experiment.

Preliminary results indicate that during the first days the decrease of pigments in the dark treatments is very low. In the fully illuminated samples phytoplankton biomass increases, as expected. After return to light the algae seem able to recover, independent of the previous treatment. Bacterial production was much higher than in field samples and did not show obvious differences between treatments during the first week. Towards the end of the experiment, samples kept in full light attained highest bacterial production. Microscopic analyses in the home laboratory and corrections for slightly different light levels in the parallel samples are required for evaluation of the experiment.

References

Kirchmann, D.L., Y. Suzuki, C.Garside and H.W.Ducklow (1991) High turnover rates of dissolved organic carbon during a spring phytoplankton bloom. Nature 352: 612-614.

Pomeroy, L.R. and D. Deibel (1986) Temperature regulation of bacterial activity during the spring bloom in Newfoundland coastal waters. Science 233: 359-361.

12. Zooplankton Biomass and Grazing

Objectives

Part of the zooplankton research activities during ANT X/6 concentrated on vertical and horizontal distribution, species, and stage composition of the copepod community in the upper 500 m at the onset of spring. The objectives were to gather informations on life-strategies of organisms in the Southern Ocean HNLC-environment. Other work was done in the framework of a more general checking of the "grazing hypothesis"; i.e. the possibility that herbivory regulates the standing crops of phytoplankton. Such herbivory in general is exerted by a wide size range of heterotrophs, from the smallest flagellates of a few microns to 10 cm long salps. Microcosm-research (Bjørnsen) and other incubation experiments (Klaas and others, Reitmeier, van Leeuwe) dealt with the protozoan consumers of small phytoplankton. Metazoan grazing was covered by
a) quantifying the mesozooplankton (200 µm) carbon biomass in the upper 500 m through the entire Ant X/6 (Gonzalez, Kuipers) and
b) frequently measuring copepod gut content as well as gut evacuation rate in terms of chlorophyll-a (Dubischar, Bathmann) as well as by HPLC (Peeken). A large number of copepod egg-production measurements were made (Gonzalez), the results of which can be used as a measure of grazing as well.

12.1. Mesozooplankton biomass and egg production

B. Kuipers, S. Gonzales (NIOZ)

Sampling.

Mesozooplankton (0.2-20 mm) was sampled by means of two Hydro-Bios multinets in 5 depth strata (0-25-50-100-200-500 m) at all meso- and larger stations of ANT X/6. Mesh sizes of the nets were 200 µm and 64 µm respectively; the finer nets providing also samples for larger sized protozoa (Klaas), complementary information on mesozooplanktonic eggs and developmental stages of copepods smaller than 200 µm.

Each 200 µm net sample was split into two halves (Folsom splitter) and treated differently, one being preserved in 4% buffered formalin for later analysis and the other concentrated in two size fractions (0.2-1 and >1 mm) on pre-weighed GF/C filters and stored at -27°C for later AFDW determination according to the JGOFS protocol. Of the 64 µm net samples one half was preserved in formalin for later analysis in addition to the 200 µm samples.

Directly after the catch, live copepods (in groups of 15-20 adult females of the 6 dominating species) were incubated at ambient temp. (≈ -1°C) in surface water (50 µm sieved bucket sample). Egg numbers were counted after 3 days. In total 159 incubations were made.

After sorting and counting all formalin samples, mesozooplankton carbon biomass can be calculated when size/carbon relationships are known. This will give insight in the degree to which the JGOFS carbon estimates are biased by the presence of occasionally large amounts of phytoplankton on the filters. For this purpose a collection of 556 batches of certain species and stage were picked from the samples and sealed in ampules for later POC determination.

Results:

Table 6.12.1 lists the information on when and where and how the multinet has been deployed. Fig. 6.12.2a, b & c show the latitudinal distribution of members, dry weight and carbon biomass of all mesozooplankton species, respectively. Depth related distribution for biomass of four dominant copepods are shown in Fig. 6.12.3.

The present average egg-productions per female copepod (irrespective of species) given in Fig. 6.12.4 show that production and therefore most probably grazing on phytoplankton started in the meltwater-zone of Trans. 2, followed by the Polar Front region in the open ocean. Fig. 6.12.5 gives details on the production per species, showing that egg-production was rather low through the whole cruise (as compared to some 50-60 eggs per female produced in temperate shelf areas), the bulk being *Calanoides acutus* eggs. The large species *Calanus propinquus*, a striking appearance in our melting zone and ice station catches produced hardly any eggs at all. In the Scotia and Weddell Seas this species is found in densities of over 20 individuals m^{-3} during the Antarctic winter; its reproduction cycle being probably tuned to other factors than phytoplankton growth in the melting zone.

Tab. 6.12.1 List of multinet stations and sample treatment during ANT X/6

date	Stat.nr	≈ Lat miles from 50°S	≈ hr 200	≈ hr 64	MN 200µ formalin	MN 200µ GF/C filters	MN 64µ formalin	MN 64µ form/lugol
3. Okt	858	420,00	10	00	5	10	0	0
4. Okt	859	419,00	09	10	5	10	5	10
5. Okt	860	419,00	18	18	3	6	5	10
7. Okt	862	419,00	09	09	5	10	5	10
8. Okt	863	411,00	10	10	5	10	5	10
9. Okt	864	369,00	09	10	5	10	5	10
11. Okt	866	464,00	21	20	5	10	5	10
12. Okt	867	438,00	17	17	5	10	5	10
12. Okt	868	419,00	23	24	5	10	5	10
13. Okt	869	390,00	07	08	5	10	2	4
13. Okt	870	359,00	18	18	5	0	5	10
14. Okt	871	328,00	02	03	5	10	5	10
14. Okt	872	300,00	11	10	5	10	5	10
14. Okt	873	269,00	20	21	5	0	5	10
15. Okt	874	239,00	06	06	5	0	5	10
15. Okt	875	390,00	12	13	5	10	5	10
15. Okt	876	360,00	20	00	5	0	0	0
17. Okt	877	-60,00	21	21	5	10	5	10
18. Okt	878	-90,00	07	06	5	0	5	10
18. Okt	879	-120,00	10	10	5	10	5	10
19. Okt	881	-30,00	14	15	5	10	5	10
19. Okt	882	-1,00	21	22	5	10	5	10
22. Okt	886-1	364,00	13	16	5	0	5	10
23. Okt	886-2	364,00	03	02	5	0	5	10
23. Okt	886-3	364,00	14	16	5	0	5	10
24. Okt	886-4	364,00	01	00	5	10	0	0
25. Okt	891	300,00	10	00	5	10	0	0
26. Okt	893	240,00	06	09	5	10	5	10
26. Okt	895	360,00	20	21	5	8	5	10
27. Okt	897	120,00	10	11	5	10	5	10
27. Okt	899	59,00	23	24	0	10	5	10
28. Okt	901	0,00	16	17	5	10	5	10
29. Okt	903	-60,00	11	05	5	10	5	10
30. Okt	905	-600,00	01	00	5	10	0	0
30. Okt	907	-361,00	15	17	5	10	5	10
2. Nov	909	300,00	14	16	5	10	5	10
3. Nov	912	361,00	17	19	5	10	5	10
4. Nov	915	449,00	09	11	5	10	5	10
4. Nov	916	479,00	21	22	5	10	5	10
6. Nov	918	540,00	04	05	5	10	5	10
6. Nov	919	569,00	13	15	5	10	5	10
10. Nov	930	570,00	16	16	5	10	5	10
11. Nov	931	540,00	02	00	5	10	0	0
11. Nov	933	495,00	14	16	5	10	5	10
11. Nov	934	480,00	21	22	0	10	5	10
12. Nov	938	465,00	08	09	5	10	5	10
12. Nov	939	450,00	13	14	5	10	5	10
13. Nov	941	420,00	02	03	0	10	0	10
13. Nov	943	360,00	19	22	5	10	5	10
14. Nov	945	300,00	10	15	5	10	5	10
15. Nov	947	240,00	08	07	5	10	5	10
16. Nov	949	180,00	10	11	5	10	5	10
17. Nov	953	60,00	15	16	5	10	4	8
18. Nov	956	0,00	13	14	5	10	5	10
19. Nov	960	-60,00	07	09	5	10	5	10
20. Nov	964	-120,00	03	04	5	10	5	10
21. Nov	969	-180,00	05	07	5	10	5	10
22. Nov	972	-90,00	10	12	5	10	5	10
23. Nov	974	-45,00	09	10	5	10	5	10
23. Nov	978	-15,00	24	01	5	10	5	10
		Totals:			283	514	261	532

Fig. 6.12.2 Latitudinal distribution of all mesozooplankton species:
a) numbers, b) dry weight, c) carbon biomass along Trans. 11

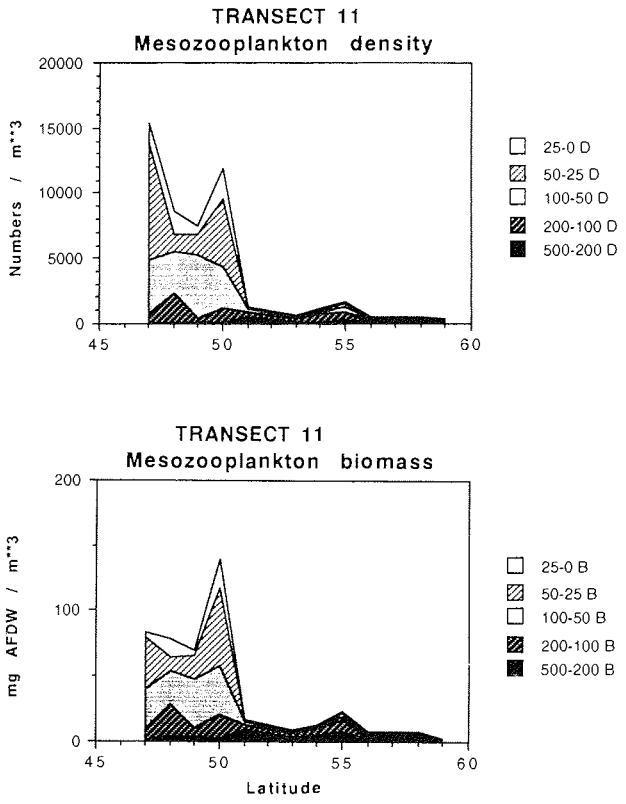

Fig. 6.12.3 Depth related distribution of ash free dry weight (ATDW) of four dominant copepods (development stages C V and C VI)

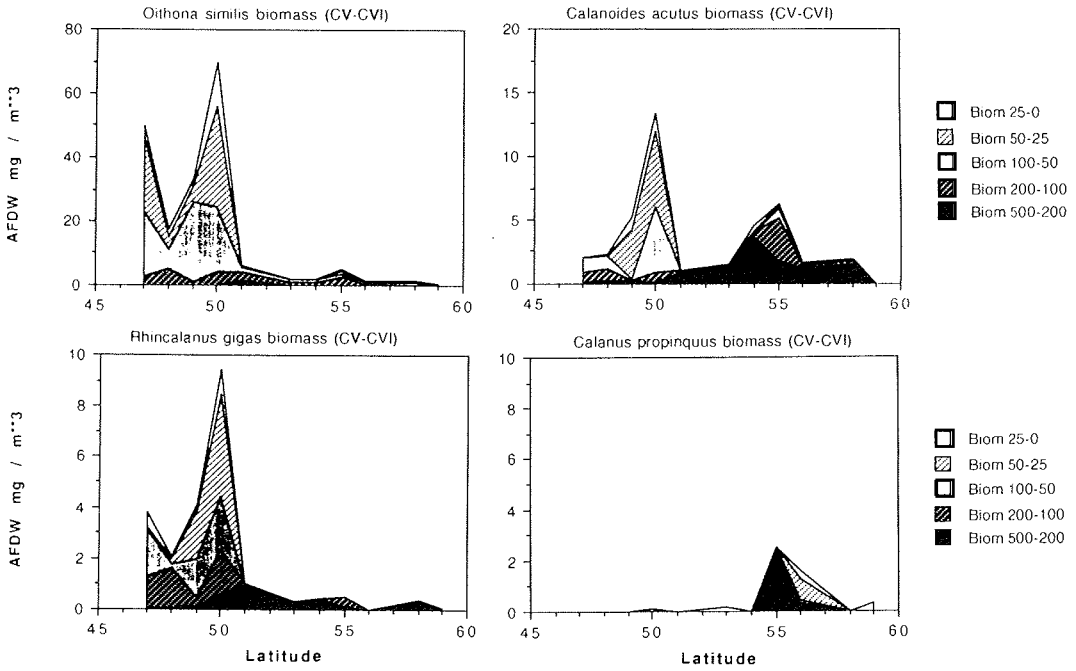

Fig. 6.12.4 Mean daily fecundity of all species of copepods together measured along a transect during 4 different periods (Trans. 2, 5, 6, 11) in spring.

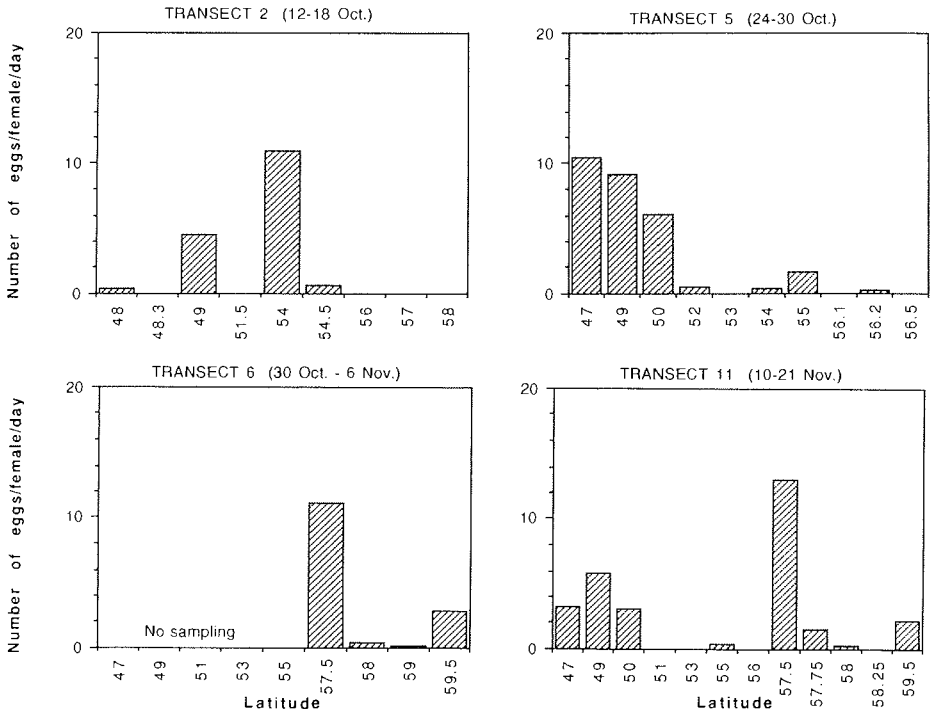

Fig. 6.12.5 Egg production (number of eggs/female/day) of the most abundant calanoid copepods species as determined in experiments carried out along a transect during 4 periods in spring.

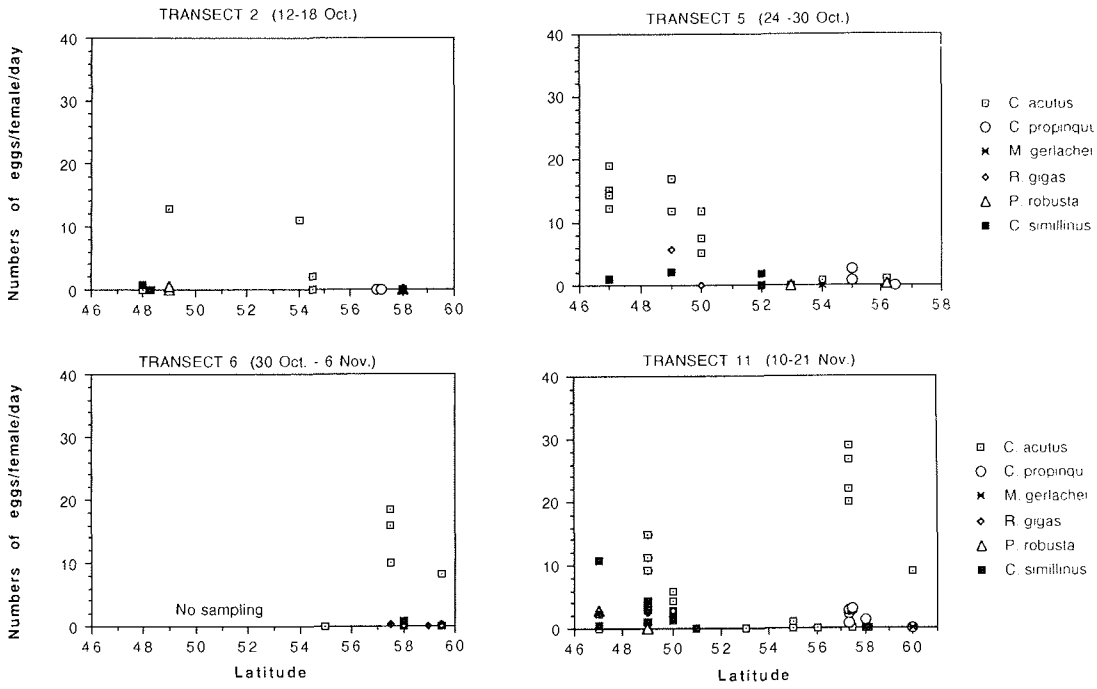

12.2. Mesozooplankton grazing

C. Dubischar (AWI)

In situ-gut fluorescence experiments

Material and Methods

Mesozooplankton grazing experiments with copepods were carried out at several stations in order to assess the *in situ* grazing rates of the dominant large copepod species (>3mm). Following the suggestions of the JGOFS protocol for the core parameters, the gut fluorescence technique was applied. Immediately after capture of the species with a Bongo net (sealed cod end), batches of 10 to 15 individuals, of the dominant species (*Rhincalanus gigas, Calanus propinquus*) were placed into buckets (1 liter) containing filtered sea water. One batch was deep-frozen (-25°C) at once, the others were removed from the buckets and deep-frozen in time intervals of 20, 40, 60, 90, 120, 150 and sometimes 180 min (depending on the amount of the captured animals). Three to five replicates were taken for each time step. After each evacuation series, chlorophyll *a* and the phaeopigment content of the species were

determined by means of a Turner Design Fluorometer. Data are given in chlorophyll *a* -equivalents (Chl.*a* -eq.) as the sum of chlorophyll *a* and phaeopigments. According to theory, the initial slope should represent the gut evacuation rate *in situ*; the reverse representing the gut passage time (in minutes).

Preliminary results:

The study area can be divided into 3 zones:
(1) the marginal ice zone (MIZ) (57°-59°S), where *Calanus propinquus* was found as the dominant mesozooplankton species,
(2) a very copepod-poor area between the MIZ and the Polar Front (51°-56°S), and
(3) the Polar Front (46°-51°S), where copepods were very abundant, dominated by *Rhincalanus gigas.*

The objectives of the study were to assess the grazing impact of *Calanus propinquus* and *Rhincalanus gigas* upon the phytoplankton community at the MIZ and the Polar Front, respectively.

At the beginning of the cruise (Sta. 863, 8.10.1992), *C. propinquus* was found at the MIZ in the surface layer. This situation remained constant until the end of the study. At this station the gut fluorescence was 1.0 ng Chl.*a* -eq Ind^{-1} and the gut passage time (GPT) was 193 min (Fig. 6.12.6). At this time, sea ice coverage was 40-80%. With time, gut fluorescence increased and GPT decreased (Fig. 6.12.6). At Sta. 915 (4.11.1992) the gut fluorescence was much higher (4.43 ng Chl.*a* Ind^{-1}) compared to Sta. 863, and GPT was shorter (102 min.). At Sta. 938 (12.11.1992), when ice melting started, gut fluorescence was even higher (7.89 ng Chl.*a* -eq ind^{-1}) and GPT even shorter (64 min) than at Sta. 915. We developed the hypothesis that grazing pressure of large copepods increased with ongoing melting of the sea-ice.

At the Polar Front, on 18 Oct, *Rhincalanus gigas* was found only in deep layers (< 500 m). These copepods were rich in lipids (microscopical observation). Ten days later at Sta. 903 (29.10.1992) *R. gigas* was very abundant in the surface layer. Its gut fluorescence was very low (0.54 ng Chl.*a* -eq Ind^{-1}) and their GPT was 87 min (Fig. 6.12.7). Twenty days later at Sta. 960 (19.11.1992) the gut fluorescence had increased to 10.77 ng Chl*a*-eq Ind^{-1} and the GPT had decreased to 63 min (Fig. 6.12.7) The results were not always so clear. In the experiments around 14:00 a smaller increase of the grazing activity was observed (Fig. 6.12.8).

Fig. 6.12.6 Gut evacuation series of *Calanus propinquus* at Sta. 863, 915 and 938. The gut content is given in Chl*a*-eq as the sum of chlorophyll *a* and phaeopigments.

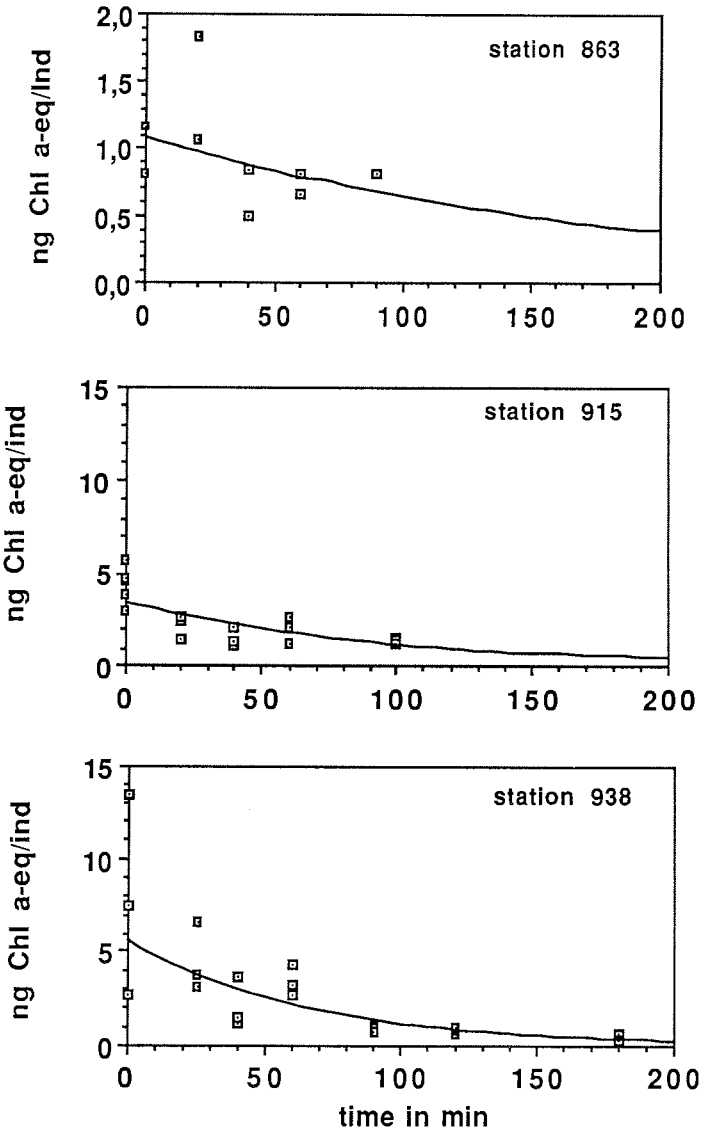

Fig. 6.12.7 Gut evacuation series of *Rhincalanus gigas* at Sta. 903 and 960. The samples were taken in the morning (9:00).

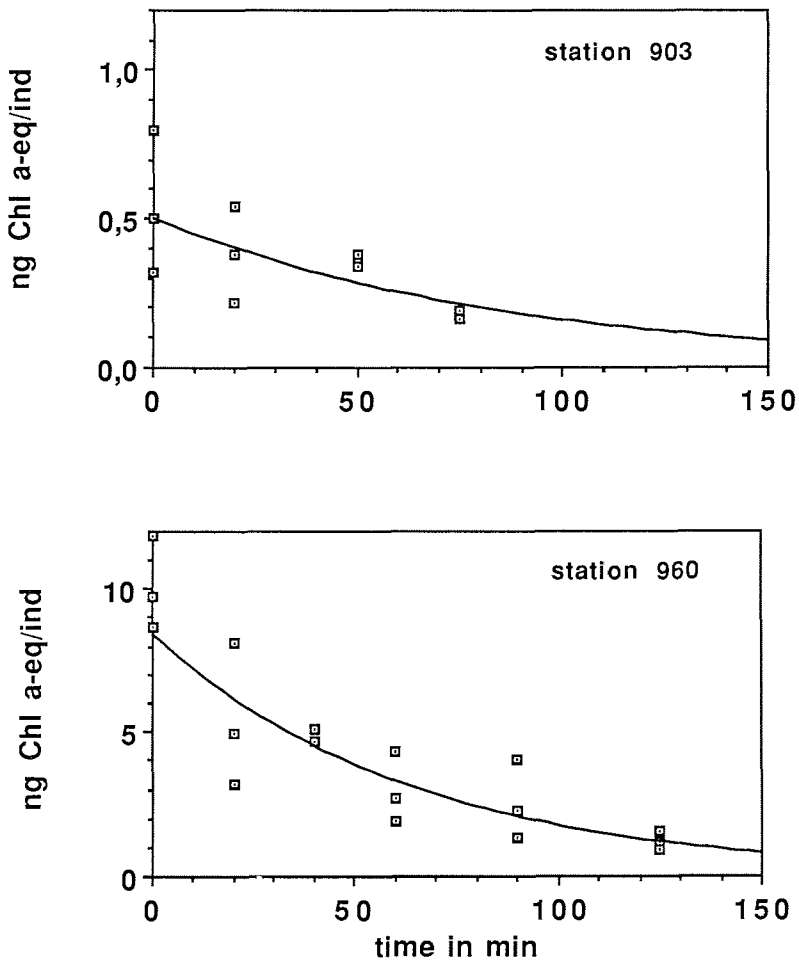

From these results, the following hypothesis was developed: At the beginning of October, *R. gigas* only utilises its lipid reserves remaining in deeper layers. As soon as the species enters surface layers, it also starts to feed on phytoplankton. Later in October the copepods increased their grazing activity and in November, grazing activity upon the phytoplankton bloom at the Polar Front was fully established.

Fig. 6.12.8 Gut evacuation series of *Rhincalanus gigas* at station 901 and 956. The samples were taken in the afternoon (14:00).

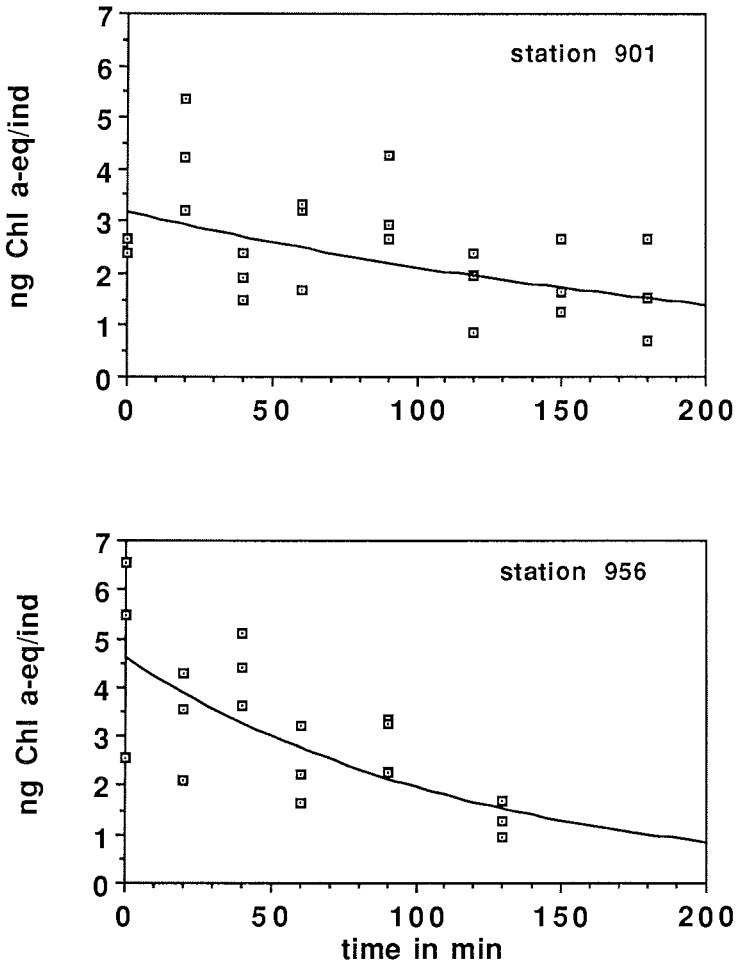

In vitro grazing experiments:

1. Effects of krill (*Euphausia superba*) and copepod (*Calanus propinquus*) grazing on a culture of ice algae

Introduction:

The objectives of this experiment were to assess the effects of Krill (*Euphausia superba*) and copepod (*Calanus propinquus*) grazing on ice algae. This experiment

was part of a joint investigation on the effect of light and grazing on growth and composition of a phyto- and protozooplankton community (see 11.). In the course of this joint experiment the following parameters were measured: chlorophyll (Dubischar), phytoplankton composition (Dubischar, Klaas), bacteria and flagellate cell numbers and biomass (Becquevort), primary production (Mathot), biogenic silica (Quéguiner, Tessier), ammonia concentration (Poncin) and nutrient concentrations (Bakker, Fritsche).

Material and methods

Some pieces of "brown ice" (taken at Sta. 866) were melted in filtered sea-water from the same station and cultured under permanent light conditions for about two weeks. One day prior to the start of the experiment, the culture was placed under light conditions in a day/night rhythm (14/10 hrs.).

3 experimental units were started:
(1) ice algal culture as control (20 l),
(2) ice algal culture with 20 *Calanus propinquus* (20 l)
(3) ice algal culture with 3 Krill (*Euphausia superba*) (10 l)

Samples for chlorophyll measurements were taken every 8 h for the first two days, thereafter every 12 h. Chlorophyll concentration was measured by means of a Turner Design Fluorometer. Samples for phytoplankton (Utermöhl) were taken every 24 h. Ammonia and other nutrients were also measured daily. After 4 days (one day before the end of the experiment) the krill were removed from the experiment.

Preliminary results:

The culture of ice algae(1) was growing exponentially and the chlorophyll concentration increased from ca. 2 µg Chl.*a* l^{-1} to 11.34 µg Chl.*a* l^{-1} in 120 hrs. (Fig. 6.12.9). Krill grazing (3) reduced the chlorophyll concentration within 48 hrs. to 0.73 µg Chl*a* l^{-1} Chlorophyll concentrations remained approximately at this value until the krill was taken out (after 96 hrs.). An increase of the chlorophyll concentration was then observed, but this increase can not be considered as being significant (Fig. 6.12.9). Apparently, krill was grazing to a threshold value which remained nearly constant with time. We expect the Utermöhl-samples to give more detailed information regarding the species composition of the remaining algae.
Grazing of *Calanus propinquus* resulted in a smaller increase of the chlorophyll concentrations compared with the reference (Fig. 6.12.9). After 96 hrs., the chlorophyll concentration reached a plateau (ca. 4.2 µg Chl.*a* l^{-1}).
The grazing of *Euphausia superba* resulted in an considerable increase of the ammonia concentration (Fig. 6.12.9), whereas the concentration in the reference remained at very low levels. The grazing of *Calanus propinquus* led only to a very small increase of the ammonia concentration.

Fig. 6.12.9 Development of chlorophyll and ammonia concentration in Experiment No. 1

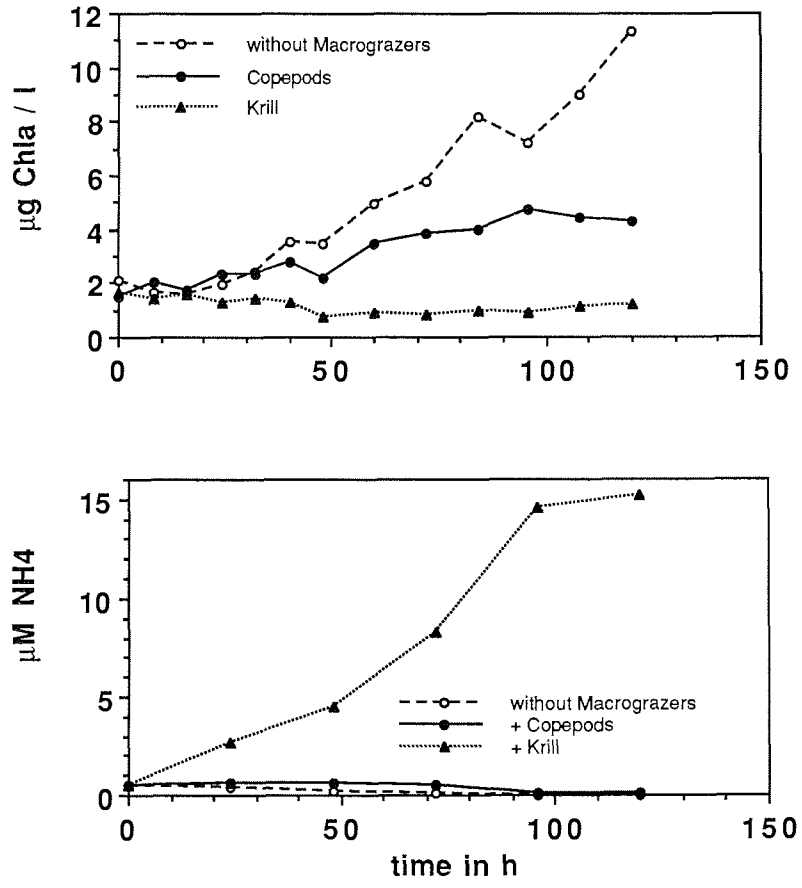

2. Effects of krill (*Euphausia superba*) grazing on the further development of a plankton community

Introduction:

The objectives of this experiment were to assess the impact of krill on a plankton community and to assess the further development of the phytoplankton, the bacteria and the flagellate community after the removal of the krill. This experiment was also part of a joint venture to test the effect of grazing on the silica-dissolution. Parameters were determined as described for the grazing experiment mentioned above. Additionally, diatoms from this experiment were observed with a light microscope and prepared for scanning electron microscopy (Crawford).

Material and methods

Water samples were taken at Sta. 956 by means of a bucket directly from the ocean and filled into 3 Nalgene bottles. One bottle was left untreated as a control and 3 krill each were placed in the other bottles. The bottles were held under day/night (14/10 hrs.) conditions. Samples for chlorophyll measurements, Utermöhl, ammonia and other nutrient measurements were taken as described above. After 2 days the krill were removed from one bottle (K-K), and the experiment was continued for three more days. Three experimental units were started:

(1) water sample as control (10 l)
(2) water sample with 3 Krill (10 l)
(3) water sample with 3 Krill (10 l), but from which the Krill had been removed after 48 h (K-K)

Preliminary results

Within the first 8 h, the krill reduced the chlorophyll concentration of about 1.4 µg Chl.*a* l^{-1} to ca. 0.45-0.6 µg Chl.*a* l^{-1} (Fig. 6.12.10). Both bottles with krill showed similar results even after the krill had been removed from one bottle. After 120 hrs., the chlorophyll concentration in the bottle from which the krill had been removed had increased relative to the concentration in the bottle with krill, but only insignificantly. Ammonia concentration remained at very low levels (0.1 µM) in the control and increased in the containers with krill to about 3 µM during the first two days. In the bottle with the Krill left, the concentration increased further and reached 11.40 µM after 5 days. In the container from which Krill had been removed, the respective concentration decreased after the removal of the Krill, but very slightly.

In addition to the experiments described here, the following experiments were carried out on board. The results of these experiments will be obtained after further work at AWI:

- Impact of the grazing pressure of *Calanus propinquus*, *Calanoides acutus*, *Rhincalanus gigas* and two different krill stages (*Euphausia superba*) upon a plankton community from the MIZ.
- Impact of grazing activity of *Calanus propinquus* and *Rhincalanus gigas* upon a plankton community from the Polar Front with relatively high chlorophyll concentrations.
- Grazing activity and faecal pellet production of *Calanus propinquus*, *Rhincalanus gigas*, *Calanoides acutus* and *Euphausia superba* in relatively low chlorophyll concentration.

Fig. 6.12.10 Development of chlorophyll and ammonia concentration in experiment No. 2. The arrow indicates the time, at which the Krill was removed from one container (K-K).

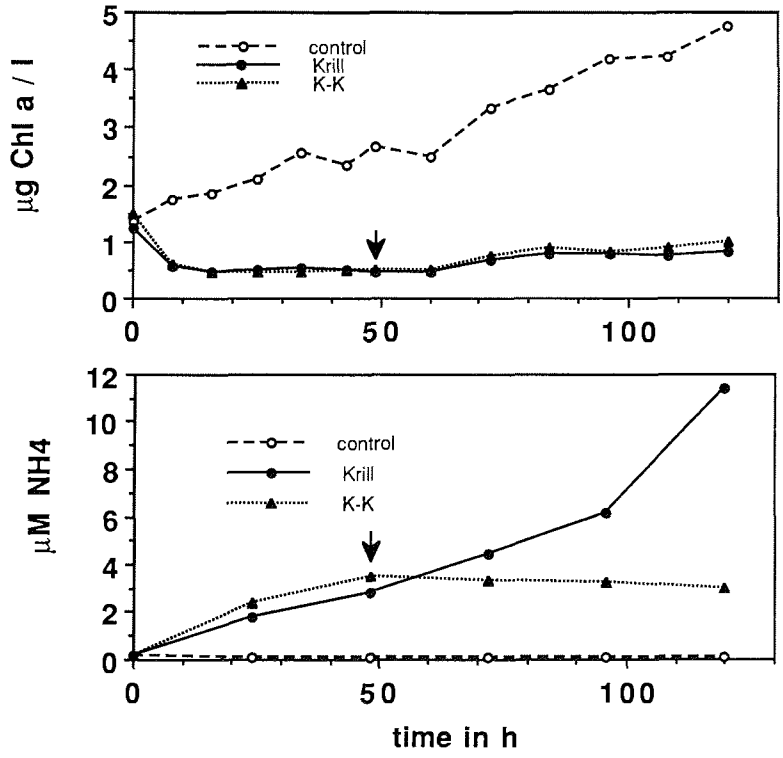

12.3. Grazing of salps

U. Bathmann (AWI)

Feeding experiments with the *Salpa thompsonii* were conducted to measure grazing pressure of single organismns and to calculate salp community grazing in the central ACC. Therefore living, healthy looking animals were carefully extracted from the sealed cod end buckets from the RMT nets. These salps were transferred immediately after capture into 1 or 2 l plexiglass beakers (1 animal per liter) which were filled with prefiltered (GF/F-filtration; 0.4 µm) sea water. After 6 to 12 hours salps were transferred into similar buckets filled with known ambient concentrations of natural phytoplankton. Feeding rates were measured as reduction of chlorophyll from these containers (Fig. 6.12.11) by using the equations given by Frost (1987).

Preliminary results indicate that *Salpa thompsonii* was very abundant in the upper 150 m of the central ACC, forming distinct swarms; the longitudinal extension of salp occurrence was up to 750 km. Species filtration rates determined in ship board

experiments (Fig. 6.12.11) translate to grazing pressure of 10-95 mg C m^{-2} day^{-1} (8-93% of daily PP; see paragraph by Mathot, Jochem et al.).

Frost, B.W. (1987) Grazing control of phytoplankton stock in the Subarctic Pacific Ocean: a model assessing the role of mesozooplankton particularly the large calanoid copepods *Neocalanus* spp. Mar. Ecol. Prog. Ser. 39: 49-68

Fig. 6.12.11 Grazing of salps indicated by reduction of phytoplankton chlorophyll concentrations in 6 experiments and control.

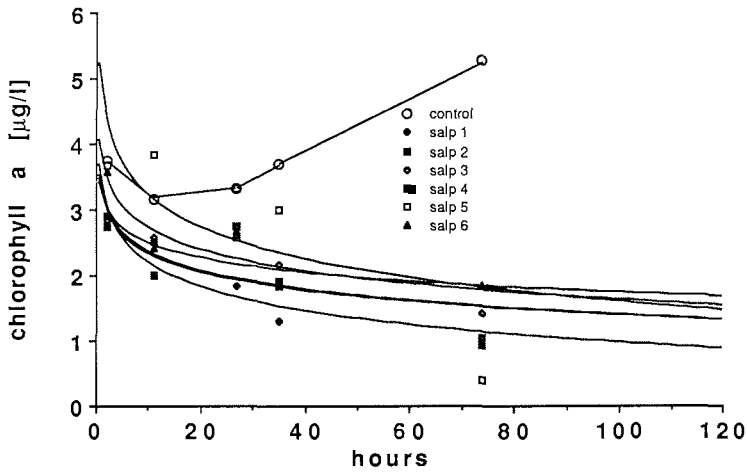

12.4. Microzooplankton grazing

S. Reitmeier (SFB)

Incubation experiments with natural assemblages of microzooplankton (MZP) were carried out to quantify the rates of herbivory and its coupling to apparent phytoplankton growth during ANT X/6. Experiments were conducted at several stations along transects between 47°S and 59°S, encompassing varying hydrographical regimes, across the Polar Front and at stations with overlying ice cover.

During this cruise special focus is on the grazing selectivity of the MZP analysed by flow cytometry, enumeration of autotrophic pico- and nanoplankton and HPLC analysis.

Materials and methods

MZP grazing rates were determined using the seawater dilution method of Landry & Hassett (1982). Water was sampled using 10 l bottles on a CTD rosette or by the use of Gerard bottles. To avoid influence of metazoan grazers natural seawater was prescreened over a 100 µm gauze and diluted with 0.2 µm filtered seawater to concentrations of 20%, 40%, 70% and 100% unfiltered seawater. Water from each dilution was transferred to 2 L polycarbonate bottles, incubated for 24 h on deck at in situ temperature using running seawater. The incubator was shaded with neutral density foil to 30% incident light corresponding to the light level at the sampling depth. Before and after incubation Chl.*a* concentrations were measured fluorometrically after filtration of the seawater onto GF/F filters and extraction with 90% acetone. Nutrient concentrations in the undiluted sample at the start and end were measured to confirm that depletion did not limit phytoplankton growth. 200 ml samples were also taken for light microscopy and fixed with acid Lugols solution.

To get quantitative and qualitative information about grazing selectivity of the MZP, the dilution experiments were also subsampled for enumeration of autotrophic pico- & nanoplankton and measurements by flow cytometer (detailed information about procedure and technical details see Chapter 8).

Results

Microzooplankton grazing rates varied between 0 and 1.8 µg Chl.*a* dm^{-3} d^{-1}, corresponding to 1 to 68% initial Chl.*a* standing stocks at the depths sampled. A significant correlation was found between the coefficients of algal growth and mortality (grazing) (Fig. 6.12.12). Four grazing experiments were conducted between 47 and 49°S in the vicinity of the Polar Front (nos. 1 to 4 in Fig. 6.12.12), where it was apparent that the higher grazing rates accompanied increases in phytoplankton growth rates, indicating a close coupling between the two parameters.

Low values of the algal growth and grazing coefficients were found at the stations in the ACC and within the ice, where Chl.*a* values remained below 0.5 µg dm^{-3}. Light microscopy of fixed samples in the lab will reveal differences in the species composition of the MZP in these areas and results of the flow cytometric measurements show grazing selectivity among the nano- and picoplankton.

The results of the MZP grazing experiments during this cruise will give additional information about the role of the MZP in the pelagic food web in comparison with previous experiments at other locations (Greenland Sea, Central North Atlantic).

Fig. 6.12.12 Correlation of phytoplankton growth vs. grazing

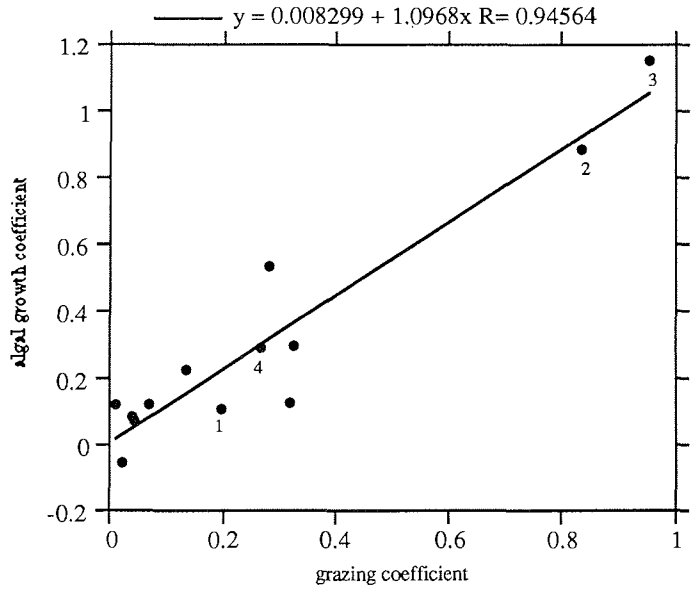

12.5. Pigment degradation due to mesozooplankton grazing

I. Peeken (SFB)

Objectives

Pigments degradation by mesozooplankton was followed in experiments to assess the possible use of pigments as biomarkers in the Antarctic Ocean. In addition, zooplankter were collected and their pigment contents determined.

Experiments:

Pigment degradation during grazing of several zooplankters, mainly *Salpa thompsoni, Euphausia superba* and *C. propinquus* (collected with RMT or Bongo nets and washed in filtered seawater) was followed. The animals were transferred into algae cultures (*Thalassiosira antarctica, Chaetoceros spp., Phaeocystis spp.*) and natural assemblages. After 24 or 48 hours the animals were washed with filtered seawater, frozen and the faecal pellets were collected.

To simulate the process of "melting" ice and the reaction of *C. propinquus* to input of algae, pieces of brown ice were brought into filtered seawater and starving *C. propinquus* were added and 10 individual were collected every 12 hours. Faecal pellets were also sampled frequently. To determine the phytoplankton assemblage subsamples were taken.

Field samples:

The main pigment from the salps collected were phaeophorbides. A highly polar degradation product of Chl.*a* with an absorption maximum at 699 nm (diode array spectrum) was also found.

13. Ecophysiology of ice algae: Dimethylsulfoniumpropionate (DMSP) content during ice melt

D. Meyerdierks, B. Bolt (FBB)

During sea ice formation, a highly concentrated brine remains unfrozen in small channels and pores. These brine-pockets are inhabited by numerous ice algae, mostly diatoms and dinoflagellates which accumulate low molecular weight organic compounds as osmolytes, such as proline or dimethylsulfoniumpropionate (DMSP). DMSP is easily cleaved under alkaline conditions into dimethylsulfide (DMS) and acrylic acid. DMS is volatile and plays an important role in the cloud condensation nuclei (CCN) formation after being oxidised to sulphuric acid and methane sulfonic acid by photochemical processes in the atmosphere.

During ice melt, large amounts of ice algae are released into the water column, perhaps initiating an algal bloom which may result in increasing amounts of DMSP and DMS in the sea and in the atmosphere.

The objectives of our investigations were to estimate the DMSP content of the algae in the vicinity of the retreating ice edge. In parallel, we measured the Chl.*a* concentration as a criterion for phytoplankton biomass.

Sampling and analytical methods

During the various south-north transects of the cruise, water samples from 20 m depth were collected with the CTD every half degree along the 6°W meridian. In addition, 29 vertical profiles with water from 8 different depths were investigated at every second degree. At these profiles, surface water was taken with a bucket. At 48°S 6°W both DMSP and Chl.*a* were measured in size fractions of total, >20 µm, 5-20 µm, 2-5 µm, < 2 µm, respectively. Size fractionated Chl.*a* was done in collaboration with F.J. Jochem (IfM Kiel). Additionally, net samples were analysed for the DMSP content of *Corethron sp.*, the dominant diatom at this station (R. Crawford, AWI). During the drift-station at 56°S and 6°50'W surface water taken with the bucket over 48 hours every second hour was analysed for diurnal variation. During Trans. 1 and 13 samples were taken every 6 hours from the ship's bow membrane pump.

One ice core was collected at each of both ice-stations. One was cut into 20 cm pieces, the other one was cut at the border of different ice types. The cores thawed

enclosed in dialysis tube bathed in running seawater on board of the ship and analysed.

Besides the field measurements the DMSP concentration was also investigated in two iron addition experiments of M. van Leeuwe and R. Scharek (see contribution by them).

For both DMSP- and Chl.*a* measurements phytoplankton was concentrated by filtration of 1-4 L seawater onto glass fibre filters (Whatman GF/F, 4,7 cm diameter).

The intracellular DMSP content was determined as gaseous dimethylsulfide (DMS) using the specific reaction that cleaves DMSP 1:1 into DMS and acrylic acid upon the addition of a strong base. After base (25% NaOH) was added, the filters were incubated in gas-tight vials and head space gas analysis was performed at least 4 hours later using a gas chromatograph (Shimadzu 8 A) with FPD (flame photometric detector). DMSP standards (Research Plus, Bayonne, New Jersey) were treated and analysed in the same fashion.

For Chl.*a* measurements, the filters were homogenized in 90% acetone, centrifuged and the supernatant was determined fluorometrically using a Chlorophyll-Fluorometer (Kleinfeld, Hannover). The fluorometer was calibrated using a Chl.*a* standard solution (Sigma Chemicals).

For each sample taken, 220 ml seawater were fixed by formalin for later taxonomic evaluation and quantification.

Preliminary results

Generally, DMSP concentrations more or less followed Chl.*a* distribution with maximum values near the surface and concentrations near the detection limits below the euphotic zone. One marked exception was encountered at Sta. 964 (48°S, 6°W), with high DMSP values at 150 m depth. Size fractionation studies revealed that the fractions >20 µm and 5-20 µm are mainly responsible for DMSP-production with 60 nM at the surface (20 m) decreasing to 3 nM at 100 m depth. The dominant diatom at this station, *Corethron sp.* (R. Crawford), is probably responsible for the deep maximum of both DMSP and Chl.*a* at 150 m depth (Fig. 6.13.1 & 6.13.2).

The diurnal study during the "drift station" (56°S, 6°50´W) showed low values both for DMSP, ranging between 5 and 8 nM, and Chl.*a* with < 0,3 µg L^{-1} throughout the whole period. After 46 hours, both DMSP and Chl.*a* increased to 16 nM and 0,4 µg L^{-1}, respectively. Distinct changes in environmental conditions, e.g. ice cover, suggest that results of the study cannot be considered diurnal variations only.

As to the regional distribution, lowest DMSP surface concentrations were found at the ice edge (< 10 nM). At ice-covered stations and in open ACC water (51 - 54°S) surface concentrations were slightly higher (10 - 15 nM). South of the Polar Frontal Zone, surface concentrations increased, up to 40 to 60 nM at the biomass rich stations in the frontal zone. DMSP to Chl.*a* ratios displayed a slightly different pattern. Highest ratios of 50 to 60 (90) nmol μg^{-1} were encountered both deep in the ice and

Fig. 6.13.1 Depth distribution of a) fractionated chlorophyll and b) fractionated DMSP at Sta. 964

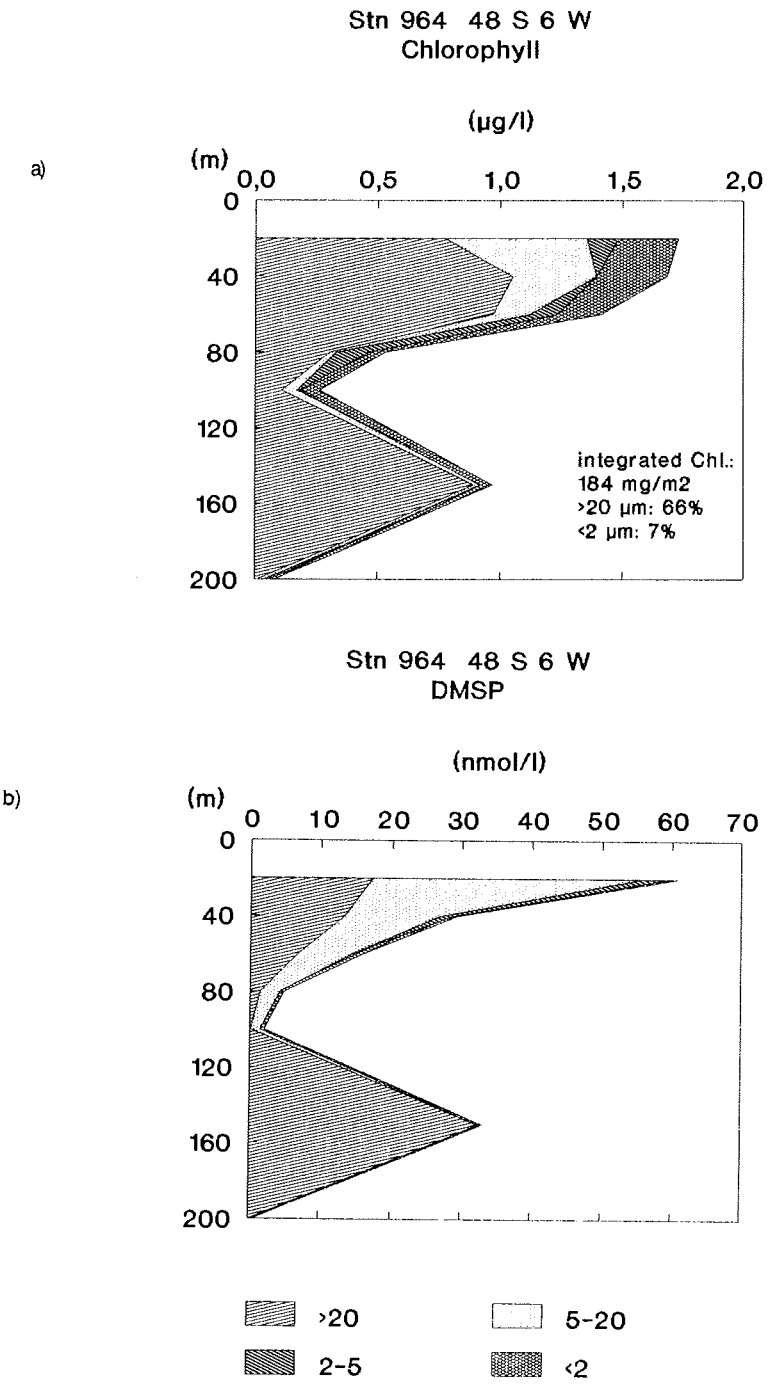

in the Polar Front. The southern edge of the frontal zone as well as the ice edge zone showed lowest ratios of 20 to 30 nmol μg^{-1}, ratios in ACC water in between being 40 to 50 nmol μg^{-1}. Discrepancies in spatial tendencies might reflect different species composition that await further analysis.

The ice cores contained much DMSP in their biomass rich layers. DMSP to Chl.*a* ratios in ice samples from the first ice station were 10 to 50 nmol μg^{-1}. In those of the second ice station, ratios were 1 to 2 nmol μg^{-1}, these samples showing much less *Fragilariopsis sp.* but higher contribution of *Nitzschia sp.* Further taxonomic evaluation and quantification from fixed samples will reveal whether these differences can be systematically related to different species composition in ice floes.

In the first iron experiment with 2 nM Fe addition DMSP concentrations were 149 nM while the control bottles without iron addition contained 131 nM. The second experiment showed lower DMSP concentration of 72 nM with 5 nM Fe and 33 nM without iron addition. For both experiments, DMSP to Chl.*a* ratios were 6 to 11 nmol μg^{-1}. Whereas iron addition seems to accelerate phytoplankton growth, effects on DMSP to Chl.*a* ratio were not clearly discernible.

14. Export Production

We have used four different approaches to estimate the rain rate of particles from the euphotic zone. On two occasions, the particle flux has been measured directly with a sediment trap. A second approach was based on the nitrogen budget in the surface water. In steady state, the nitrate-based new production should balance the loss of nitrogen by sinking particles. Measurements of nitrate uptake with ^{15}N labelled material are described in the section on primary production. The depletion of the natural radioisotopes ^{234}Th and ^{210}Po relative to their parent nuclides provided a third way to estimate the integrated export production over a longer time period. Lastly, the accumulation of barite in sediments and in intermediate water layers appears to be a good tracer for the flux of organic matter.

14.1. Sediment trap deployment

U. Bathmann (AWI)

During ANT X/6 drifting sediment traps were deployed in the Marginal Sea Ice Zone (MIZ) two times to measure vertical particle flux directly 50 m below melting ice flows. Deployments were very difficult due to heavy movements of the ice flow induced by strong winds. These winds forced the surface buoys of the drifters between the ice flows which in term squeezed the Argos drifter and the surface radar reflector.

The drifting experiments were carried out for 24 hours each. Increasing winds and reduced mobility of the ship due to other scientific activities forced us to finish the sediment trap experiment in order not to loose the expensive scientific equipment.

First results from the collected material indicate very little vertical flux of particulate material. The organic matter collected in the traps was dominated by long krill faecal string indicating grazing of these organisms under the sea ice.

14.2. Export production measurements with ^{234}Th and ^{210}Po

M. Ruttgers v d Loeff, J. Friedrich, H. Höltzen (AWI)

Isotopes of the particle-reactive elements Th, Pb and Po are produced in the water column by decay of their relatively soluble U and Ra parents. Adsorbed to particles, these isotopes are removed from the surface water when the particles settle through the water column, thus providing us with a tool to study particle flux rates, production rates in the water column, and sedimentation of particles.

The isotope ^{234}Th (24 days half-life) is a suitable tracer to study the development of a plankton bloom. In the end of the winter, as we found in 1987 in the Bransfield Strait, this isotope is in secular equilibrium with its parent, ^{238}U, the activity of which is accurately known from the salinity. Only some 5% of the activity is bound to particles. With the onset of the plankton bloom, particles become more abundant in the surface water, and the percentage of ^{234}Th activity bound to particles increases. Sinking of particles out of the surface layer shows as a disequilibrium between total ^{234}Th and ^{238}U. This disequilibrium enables us to quantify the export rate of ^{234}Th from the surface water, and if we know the $^{234}Th/C_{org}$ ratio in sinking particles, it becomes also possible to quantify indirectly the export production of organic carbon. This method complements flux rate measurements with sediment traps, and offers the advantage that it measures a time-integrated signal that is moreover independent of the sometimes questionable collecting efficiency of the trap.

Materials and methods

Large-volume water samples were taken with 270-Liter Gerard bottles at 6 depths, usually 20 m, 60 m, 100 m, 200 m, 400 m and 600 m. On two occasions the deepest sample was taken at 1000 m. The water was filtered, and in a 20 kg aliquot of filtrate the dissolved natural radionuclides ^{234}Th, ^{210}Po and ^{210}Pb, together with appropriate yield tracers, were coprecipitated with $Fe(OH)_3$. This precipitate was concentrated, and Th and Po were separated by anion exchange and plated on silver planchets. ^{234}Th was counted on-board with a low-level beta counter The ^{230}Th yield tracer, as well as Po will be counted in the home laboratory with alpha spectrometry. ^{210}Pb will be determined after ingrowth of its daughter ^{210}Po. Some samples for ^{226}Ra, the parent of ^{210}Pb, were collected on MnO_2-coated fiber for later analysis through its daughter ^{222}Rn.
Particulate matter was collected on 142 mm filters and will be analysed by the same techniques at AWI.

As no ^{234}Th activities could be calculated on board, we tried to determine particulate ^{234}Th activity by direct beta counting of 25 mm Nuclepore filters through which 2 to 10 L of water had passed. Count rates were low: only in productive surface waters a count rate of about 1 dpm was observed. After accurate determination of particulate ^{234}Th we will consider whether direct counting is a useful method, and whether self-absorption is reproducible enough to be corrected for.

Automated sampling for particulate and dissolved ^{234}Th was tested with a newly developed "multisampler". As quantitative sampling was not possible due to a malfunction of the apparatus, a real deployment was not considered useful.

14.3. Mesopelagic barite accumulation and export production

F. Dehairs, L. Goeyens (VUB), R. Manuels (NIOZ)

Introduction

There exists increasing evidence that barium sulphate (barite) microcrystals, precipitating in the oceanic environment as a result of biological activity, carry a potential for tracing productivity, both, at geological time scales and seasonal time scales (Turekian and Tausch, 1964; Bishop, 1989; Dymond et al., 1992; Dehairs et al., 1990, 1991, 1992). The process involved in pelagic barite formation appears to be decay of organic matter inside micro-environments, such as mixed biogenic aggregates (Chow and Goldberg, 1960; Bishop, 1988; Stroobants et al., 1991). Dissolution and heterotrophic oxidation may eventually eliminate most of the micro-environment components, except for the barite crystals, which dissolve but slowly (Dehairs et al., 1980) in the undersaturated seawater (Church and Wolgemuth, 1972). As a result of this semi-conservative character, accumulated barite appears as a potential tracer of past productivity. For mesopelagic accumulation of barite the time scales involved are not yet fully understood, but there is evidence, however, that this time scale is of the order of the season's duration to a few years.

During recent studies in the Southern Ocean we have observed interesting correlations between mesopelagic barite accumulations and the type of production prevailing in the investigated area (Dehairs et al., 1992). Briefly, it was observed that environments in which, during the ongoing season, the phytoplankton community switched from essentially a nitrate based productivity (new production) to an ammonium based productivity (recycled production), reflecting increasing importance of organic matter recycling in the upper water column, no significant mesopelagic barite accumulation occurred. The marginal ice zone (MIZ) in the Scotia-Weddell Confluence area and the coastal and continental shelf zone (CCSZ) in Prydz Bay were such environments. On the contrary, in open ocean zones (OOZ), eventually covered by sea ice in winter, and in the closed pack ice zone (CPIZ), new production prevailed all over the season and subsurface accumulation of barite is common. Despite the fact that total productivities in OOZ and CPIZ areas are generally significantly lower than in the MIZ and the CCSZ, the enhanced concentrations of mesopelagic barite suggest significant export of production to occur in these environments.

The present expedition gave the opportunity to study mesopelagic barite accumulation in a Southern Ocean area at great distance from any continental influence. Since at this time of the year sea ice cover reaches still far north (up to 55°S at the beginning of October), we have been able to sample repetitively CPIZ, MIZ and OOZ systems, including the Polar Front, in a relatively restricted area. The difference with the Scotia-Weddell Confluence is that in the present area the ice-edge will retreat till the continent with advancing season, leaving behind an open ocean system. The study of particulate barite distribution was conducted in conjunction with detailed studies of the dissolved oxygen profiles and with other techniques of export production measurement (^{234}Th and sediment trap sampling).

The transects between 59°30'S and 47°S along the 6°W meridian allowed us to cover the entire width of the Antarctic Circumpolar Current (ACC), from south of the ACC-Weddell Front to just north of the Polar Front. Other participants have shown

that at both these fronts, but especially the Polar Front enhanced biomasses and productivity occurred.

Methods

Depending on the suspended matter load, between 5 and 20 l of seawater were filtered on Nuclepore membranes of 0.4 µm porosity. In the home laboratory they will be digested using a $LiBO_2$ fusion method with redissolution in HNO_3. The final solution is analysed for Ba, but also for Sr, Ca, Si and Al content by inductively coupled plasma - optical emission spectrometry (ICP-OES) and ICP-mass spectrometry (ICP-MS).

References

Bishop, J.K.B., (1988) The barite-opal-organic carbon association in oceanic particulate matter. Nature 332: 341 - 343.

Bishop, J.K.B., (1989) Regional extremes in particulate matter composition and flux: Effects on the chemistry of the ocean interior. In: Productivity of the Ocean, Present and Past, Dahlem Workshop Reports, Life Sci. Res. Rep. 44, ed. W.H. Berger, V.S. Smetacek and G. Wefer, J. Wiley, New York, pp117 - 137.

Chow, T.J. and E.D. Goldberg, (1960) On the marine geochemistry of barium. Geochimica et Cosmochimica Acta 20: 192 - 198.

Church, T.M. and K. Wolgemuth, (1972) Marine barite saturation. Earth and Planetary Science Letters 15: 35 - 44.

Dehairs, F., W. Baeyens and L. Goeyens, (1992) Accumulation of suspended barite at mesopelagic depths and export production in the Southern Ocean. Science, November 1992.

Dehairs, F., R. Chesselet and J. Jedwab, (1980) Discrete suspended particles of barite and the barium cycle in the open ocean. Earth and Planetary Science Letters 49: 528 - 550.

Dehairs, F., L. Goeyens, N. Stroobants, P. Bernard, C. Goyet, A, Poisson and R. Chesselet, (1990) On suspended barite and the oxygen minimum in the Southern Ocean. Global Biogeochemical Cycles 4: 85 - 102.

Dehairs, F., N. Stroobants and L. Goeyens, (1991) Suspended barite as a tracer of biological activity in the Southern Ocean. Mar. Chem. 35: 399 - 410.

DeMaster, D.J., T.M. Nelson, S.L. Harden and C.A. Nittrouer, (1991) The cycling and accumulation of biogenic silica and organic carbon in Antarctic deep-sea and continental margin environments. Mar. Chem. 35: 489 - 502.

Dymond, J., E. Suess and M. Lyle, (1992) Barium in deep-sea sediment: A geochemical proxy for paleoproductivity. Paleoceanography 7: 163 - 181.

Stroobants, N., F. Dehairs, L. Goeyens, N. Vanderheijden and R. Van Grieken, (1991) Barite formation in the Southern Ocean water column. Mar. Chem. 35: 411 - 421.

15. Benthic boundary processes

On this cruise we have deployed a multicorer (MUC), a free falling in-situ oxygen and pH profiler (Botty), and in-situ pumps (ISP) according to the list below. Also indicated are the deep-water deployments of Gerard bottles (GWS).

Station	Latitude	Longitude	Depth	Date	Instrument
857/PS2356	56°50	49°34	4390	2/10	MUC
860/PS2357	56°56	30°31	3693	6/10	MUC, GWS
862/PS2358	57°28	23°23	5007	7/10	GWS, ISP
865/PS2359	56°10	12°23	4860	9/10	GWS, ISP
866/PS2360	57°39	06°23	3400	12/10	GWS, ISP
872/PS2361	55°01	05°54	3073	14/10	MUC
876/PS2362	53°02	05°55	2671	15/10	MUC
879/PS2363	48°03	05°59	4159	18/10	MUC
886/PS2364	56°03	06°46	2565	22/10	MUC
891/PS2365	55°01	06°02	3215	25/10	MUC, Botty
899/PS2366	51°00	05°57	2114	28/10	MUC
903/PS2367	49°07	06°00	3525	29/10	MUC
908/PS2368	46°52	05°44	3615	31/10	MUC, GWS, ISP
911/PS2369	55°51	05°56	3995	3/11	MUC, GWS, ISP
917/PS2370	58°23	05°55	5078	5/11	MUC, GWS, ISP
941/PS2371	57°03	05°59	3680	12/11	MUC, Botty
947/PS2372	53°59	06°00	2415	15/11	MUC, Botty
949/PS2373	52°59	05°58	2516	16/11	Botty
956/PS2374	50°00	05°59	2315	18/11	MUC, Botty, GWS
PS2375	49°00	06°00	3400	20/11	Botty
972/PS2376	48°34	06°00	3657	22/11	MUC, Botty, ISP

15.1. Oxygen, nutrients, pH and $CaCO_3$

O. Holby (AWI)

In the cores collected we have measured pH-gradients and oxygen-profiles. Concentration gradients of alkalinity, nitrate, nitrite, ammonia, phosphate and silicate were measured in the interstitial water. Interstitial water was collected by slicing and thereafter squeezing with nitrogen gas in teflon squeezers (filter 0.45 µ). All cores for this purpose were undisturbed, as judged from the overlying water which was perfectly clear, and from nutrient values in overlying water, which agreed with bottom water values. Samples for porosity, organic content, REE, radionuclides and geological work were also collected.

The diffusive flux of oxygen into the sediment can be used to estimate the supply rate of organic material to the sea floor. This is possible because oxygen is the major electron acceptor in the decomposition of organic material at the deep-sea floor. During the decomposition of organic material CO_2 is produced, which favours the dissolution of $CaCO_3$, if it is available. One big problem is that the solubility of calcite is pressure dependent, which makes it impossible to measure undisturbed pH profiles on-board ship in a core from the multicorer. That is why we have tried to make in-situ profiles of oxygen and pH with a free falling bottom lander (Botty).

In the cool lab (3°C) the oxygen profile was measured with a home-built "clark" style oxygen electrode (Revsbech 1988). The oxygen electrodes were calibrated by a two point calibration with the assumption that the signal from the electrodes was linear. Oxygen-free water was made by bubbling with nitrogen gas, and the second point was air-saturated water, in which the oxygen concentration was determined by Winkler titration. The pH-profiles were measured with a commercial pH-electrode (Ingold LOT 406) calibrated with a salt water buffer according to Almgren et al. (1974). Fig. 6.15.1 shows preliminary oxygen results from cores measured in the laboratory. It is to be noticed that the oxygen on Sta. PS2357 is totally depleted already after 2.5 cm penetration into the sediment, which indicates a high flux of easily degradable organic matter to the sediment. This sediment also seems to contain a lot of opal even if it is outside the region Demaster (1981) described as Silica deposit area. The decrease in the NO_3- concentration (Fig. 6.15.2.) suggests that also Sta. PS2356 has a high sedimentation rate of organic matter compared to the stations sampled further east. Another observation from the NO_3-profiles is that oxygen is probably present to more than 20 cm depth in the sediment at all stations sampled on the 6°W meridian.

Fig. 6.15.1 Oxygen profiles measured in the lab. Station numbers indicated by their last 2 digits.

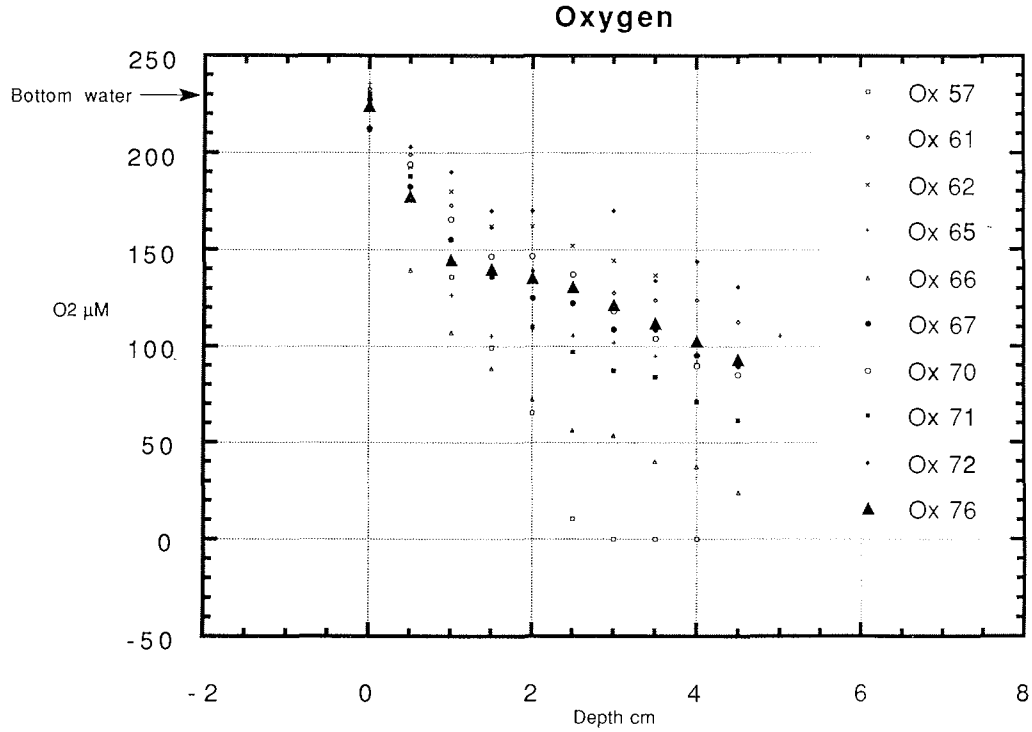

Fig. 6.15.2 NO_3-profiles for stations PS2356 to PS2366

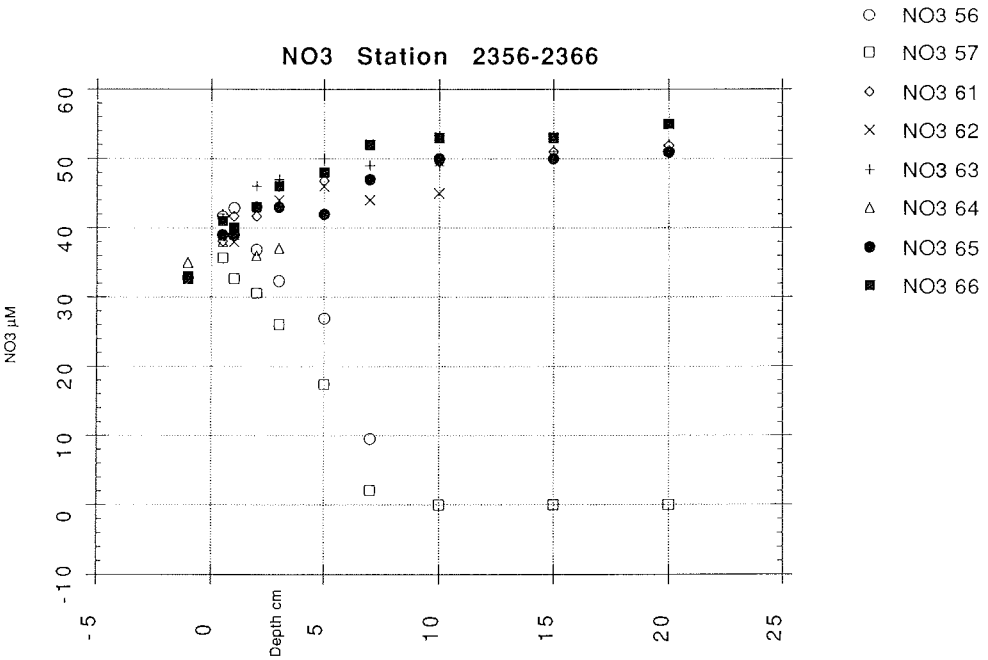

At seven occasions we deployed our new free falling in-situ oxygen and pH-profiler (Botty), a copy of the instrument built at NIOZ/Texel. There were some technical problems, but we succeeded to get 5-cm profiles from three stations: PS2365, PS2374 and PS2376. Apart from this, we also got one-cm long profiles at stations PS2372 and PS2373. Oxygen profiles from Botty are presented in Fig. 6.15.3 and a pH-profile in Fig. 6.15.4. From the oxygen profiles we estimate the thickness of the diffusive sublayer (marked with a line) to be about 0.7 mm at Sta. PS2376 (972). This parameter is required for the calculation of the flux of various substances between the sediment and the water. Fig. 6.15.4 shows a pH profile, measured in-situ with a home-built electrode. As we are not yet able to calibrate these electrodes under the in-situ conditions, the profile is given in raw voltage units rather than pH units. The biggest problems with the lander were that the communication with the acoustic release was unsatisfactory, the power supply was not sufficient, the radio signal was only received occasionally, and the floating in the water was not in an upright position.

Fig. 6.15.3 Oxygen profile from the in-situ profiler at Sta. PS2376. A straight line is fitted to the slope thought to represent the diffusive sublayer.

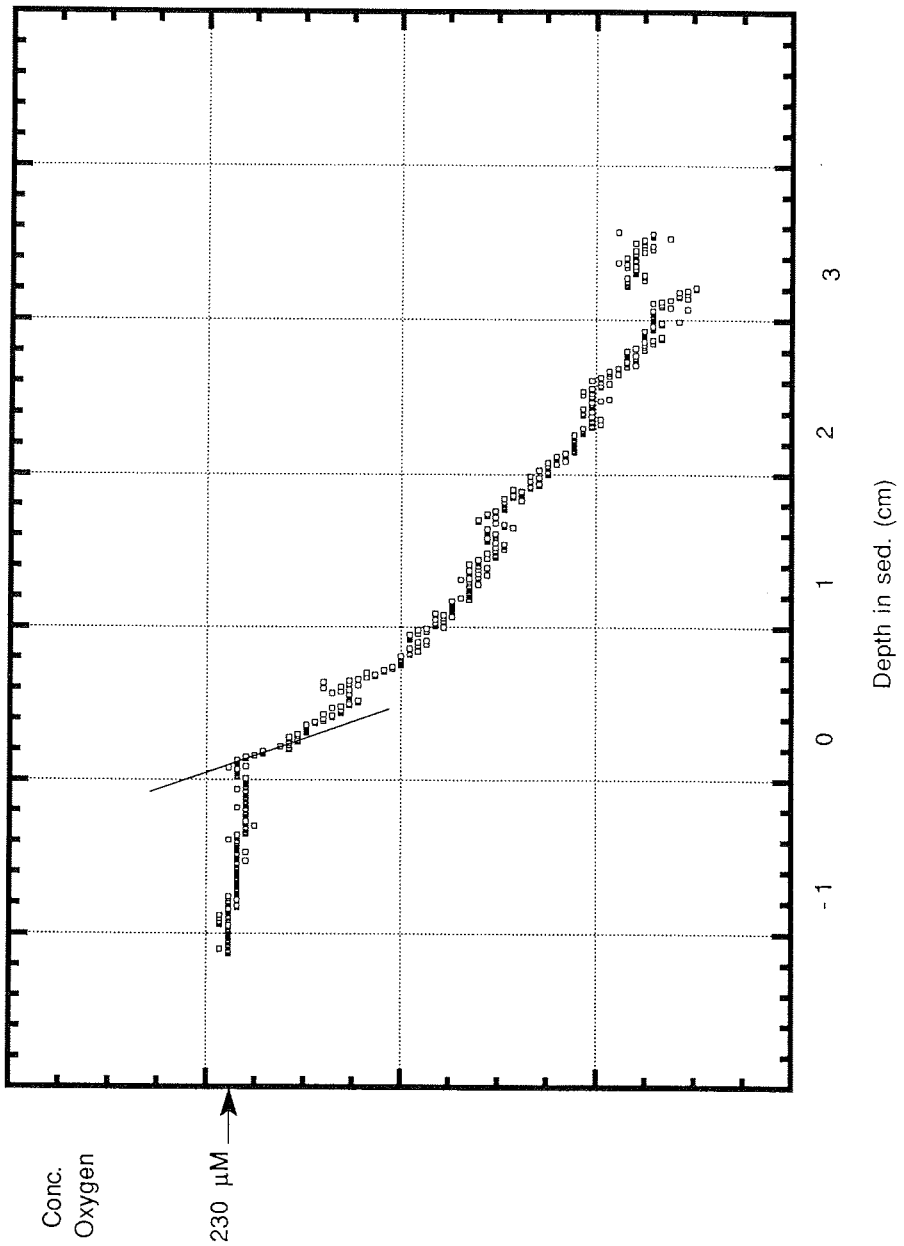

Fig. 6.15.4 pH profile from the in-situ profiler (1000 units is approximately 0.5 pH-unit)

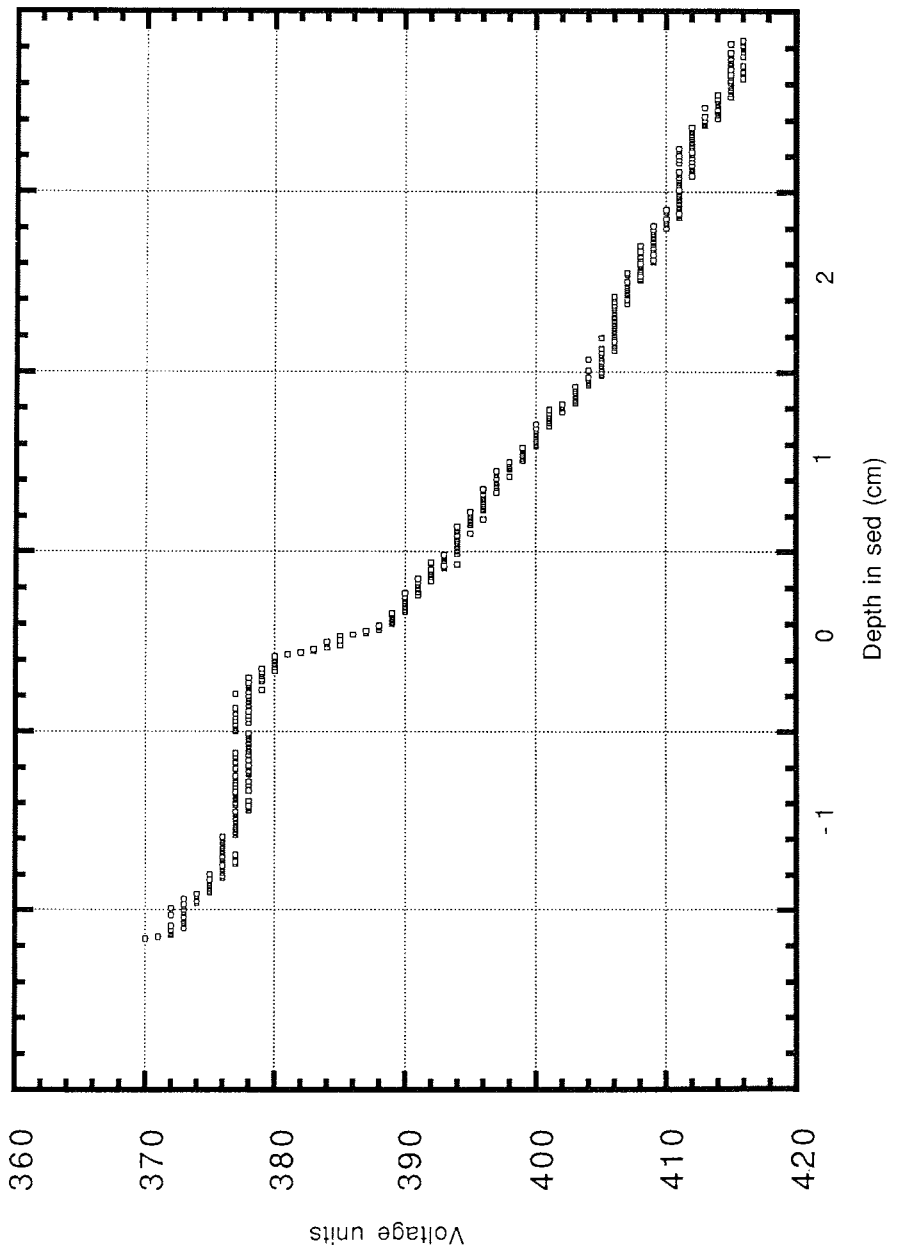

15.2. Microbiological investigations of sediment

K. Lochte (AWI)

Objectives

Sedimenting particulate organic matter primarily consists of macromolecular substances which are degraded at slow rates. Microbial degradation at the deep sea floor requires extracellular enzymatic hydrolysis of the macromolecular organic molecules before the mono- and oligomeric subunits can be taken up by the bacterial cells. In experimental investigations with deep sea sediment supplemented with different amounts of detrital matter stimulation of specific hydrolytic enzymes was found (Boetius & Lochte in press). It is to be expected that the hydrolytic enzyme activity in the sediment reflects the amount of sedimenting organic matter which these sediments receive. This was tested by investigating the enzymatic activity in the upper sediment horizons at one station with high surface water chlorophyll *a* content west of the South Sandwich Islands and along the transect at 6°W between 48°S to 58°30'S covering the productive polar frontal zone and the much less productive regions further south.

Work at Sea

Samples were taken by multiple corer at those stations at which oxygen profiles were also measured (see section 15.1). The top 10 cm of undisturbed sediment cores were sectioned into 0.5 cm layers (in the upper 2 cm horizon), into 1 cm layers (in the 2-6 cm horizon) and into 2 cm layers (in the 6-10 cm horizon). In each section the activity of hydrolytic enzymes was determined with fluorescein diacetate (FDA) according to the method of Meyer-Reil and Köster (1992). This fluorigenic molecule serves as a model substrate for general hydrolytic activity and can be cleaved with varying efficiency by different enzymes. Since FDA was added in saturating concentrations the measured activity is the enzymatic potential within the sample and is directly related to the amount of enzymes present.

Samples for determination of bacterial numbers by microscopy and of benthic biomass by measurement of total phospholipids were also taken and stored until analysis in the home laboratory.

Preliminary Results

By far the highest enzymatic potential activity was found at station 860 on transect 1 at 57°S 30°27'W (Fig. 6.15.5a). The sediment at this station was also characterizied by low oxygen concentrations (see section 15.1). In this region high chl.*a* concentrations were found in the surface waters and both the high enzymatic potential and the low oxygen concentrations indicate high deposition of organic matter at this site.

All other stations investigated along the transect at 6°W between 48°S and 58°30'S showed little variation in enzymatic potential. As examples station 972 in the frontal zone (48°30'S) and station 891 in the less productive region of the Antarctic Cirumpolar Current (55°S) are shown (Fig. 6.15.5b,c).

Fig. 6.15.5a-c Rate of FDA hydrolysis in sediment cores from three different stations: a) west of South Sandwich Islands, b) transect at 6°W at the Polar Frontal Zone and c) transect at 6°W in the less productive region of the Circumpolar Current

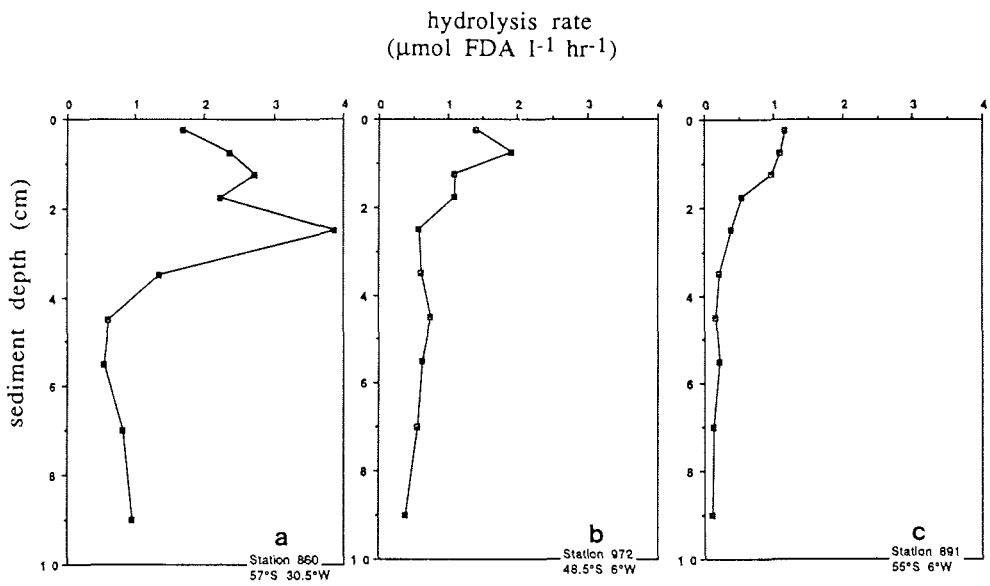

When integrated over the top 10 cm of sediment, the enzymatic potential did not show a consistent trend for the stations along the 6°W transects (Fig. 6.15.6). Although in the surface water phytoplankton development was most vigorous in the Polar Frontal Zone and much less in the adjacent regions further south, this surface productivity was not reflected in sediment enzymatic activity. Bottom topography in this region is highly variable due to ocean ridges formed by the tectonic movements of the South American, African and Antarctic plates. Such bottom topography is likely to influence deposition and erosion strongly and, hence, uncouple export of organic matter from the surface water and the final deposition at the sea floor. Different sediment structure was observed in the cores on board and is an indication of different depositional regimes. This aspect will be investigated further by comparison of the enzymatic potential with the geochemical measurements taken at the same stations (see section 15.1).

Fig. 6.15.6 Rates of FDA hydrolysis integrated over the upper 10 cm of sediment at different stations between 48°S and 58°30'S along the 6°W transect.

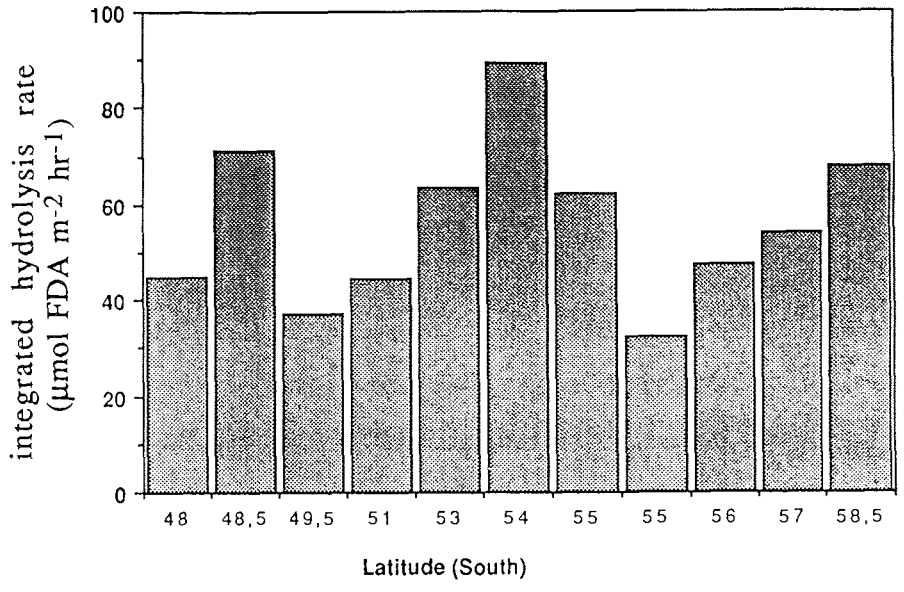

References

Boetius, A. and Lochte, K. (in press) Regulation of microbial enzymatic degradation of organic matter in deep-sea sediments. Mar. Ecol. Prog. Ser.

Meyer-Reil, L.-A. and Köster, M. (1992) Microbial life in pelagic sediments: the impact of environmental parameters on enzymatic degradation of organic material. Mar. Ecol. Prog. Ser. 81, 65-72.

15.3. Pigments

I. Peeken (SFB)

Sediment cores:

From 2-6 sediment cores per station, the first 10 cm were cut in 1 cm slices, pooled and frozen for later pigment determination.

15.4. Nepheloid Layer/Resuspension/Bioturbation

M. Rutgers v d Loeff, O. Holby (AWI)

There is evidence for extensive near-bottom particle transport in the Antarctic Circumpolar Current (ACC). As the fronts in the ACC are known to extend to abyssal depth, high current velocities can be expected even at great depth. Indeed, nephelometer data show a well-developed Benthic Nepheloid Layer (BNL) in the ACC (Biscaye and Eittreim, 1977). Advective transport in the BNL could cause the accumulated sediment to be very different from the particles intercepted with sediment traps. In a trap deployed at 3196 m at the average position of the Polar Front (PF1 at 50°09´S5°46´E, Wefer and Fischer 1991) we observed a sedimentation flux of ^{210}Pb several times smaller than the accumulation rate of this isotope in the underlying sediments, which indeed suggests advective transport. As the radionuclide composition of the sediment is often used for the interpretation of sediment fluxes, it is important to quantify the advective component. For this purpose we have collected particulate matter in the BNL using in-situ pumps. Moreover, disequilibria in the contents of radionuclides in the BNL can give information on resuspension rates. A possible depletion of ^{234}Th in the BNL would allow an estimate of resuspension rates on time scales of months (Bacon and Rutgers van der Loeff, 1989). Longer residence times of particles in the BNL could be estimated from the isotope pairs $^{210}Po/^{210}Pb$ and $^{228}Th/^{228}Ra$. These estimates require a modelling of the adsorption and mixing of the isotopes in the BNL and in the surface sediment.

We selected 6 stations where we could expect significant transport: In deeper canyons like the South Sandwich Trench (eastern slope, Sta. 862) and the Conrad Fracture Zone (Sta. 911), and along mid-ocean ridges (Sta. 865 and 908 W and E of the Mid-Atlantic Ridge; Sta. 866 and 917 on the northern slope of the Weddell Basin).

^{234}Th in surface sediments

Because of the short half-life (24 days) and high reactivity with particles of ^{234}Th, the disequilibrium between ^{234}Th and ^{238}U gives an estimate of the particle mixing rate in the sediment (Aller & DeMaster 1983) on time scales much shorter than with the conventional ^{210}Pb technique (22.4 y halflife). Moreover, it gives the activity of the material potentially resuspended, required for the model describing the ^{234}Th in the BNL.

Sediment samples for determinations of ^{234}Th profiles have been taken on 8 stations. The ^{234}Th measurement was performed by splitting the samples in two aliquots, one of which was spiked with ^{236}U and ^{229}Th yield tracers. Both aliquots were leached on-board in hot 6n HCl. The spiked samples were taken back to Bremerhaven as $Fe(OH)_3$-precipitate. The unspiked samples were separated and measured for ^{234}Th directly onboard. The results have to be corrected for the amount of sediment extracted and for losses during the preparation.

15.5. DOC + ^{228}Ra

A. Antia (SFB) , M.Rutgers v.d. Loeff(AWI)

The distribution of dissolved organic carbon (DOC) measured in some pore water profiles showed high near-surface concentrations implying a diffusive flux of DOC both downward and upward towards the bottom water. Near-bottom profiles of TOC in the water column also showed a bottom source. In order to model the distribution observed in the bottom water, we need to know the vertical mixing rates in the deep waters. We will attempt to use some of the radionuclides measured with the in-situ pumps as tracers for the dispersion of substances with a bottom source. The best candidate is ^{228}Ra (5.8y half-life), produced in the sediment by decay of ^{232}Th.

Fig. 6.15.7 DOC profile in pore water at Sta. 903. The arrow marks the TOC concentration in bottom water 10 cm above the sediment surface.

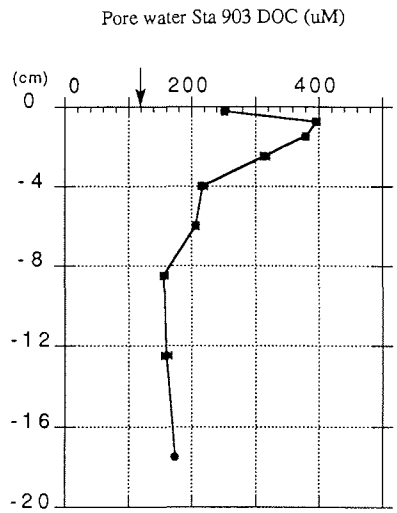

References

Aller, R. C. and DeMaster, D. J. (1983) Estimates of particle flux and reworking at the deep-sea floor using ^{234}Th/^{238}U disequilibrium. Earth Planet. Sci. Lett. 67: 308-318.

Almgren, T., Dyrssen, D. and Strandberg, M. (1974) Determination of pH on the moles per kg seawater scale (Mw) Deep-sea Res. 22: 635-646.

Bacon, M.P. and Rutgers van der Loeff, M.M. (1989) Removal of ^{234}Thorium by scavenging in the bottom nepheloid layer of the ocean. Earth Planet Sci. Lett. 92: 157-164.

Biscaye, P.E. and Eittreim, S.L. (1977) Suspended particulate loads and transports in the nepheloid layer of the abyssal Atlantic Ocean. Mar. Geol. 23: 155-172

DeMaster, D.J. (1981) The supply and accumulation of silica in the marine environment. Geochim. Cosmochim. Acta 45: 1715-1732

Revsbech, N. P. (1988) Microsensor Analysis of Stratified Microbial Communities. Ph. D. thesis Aarhus Univ. Denmark.

Wefer, G. and Fischer, G. (1991) Annual primary production and export flux in the Southern Ocean from sediment trap data. Mar. Chem. 35: 597-613.

ANT X/7

CAPE TOWN - USHUAIA - 03.12.92 - 22.01.92

1. Fahrtverlauf und Zusammenfassung

E. Fahrbach (AWI)

Am 3. Dezember 1992 um 15.00 verließ "Polarstern" Kapstadt. Die ozeanographischen Arbeiten begannen auf unserem Weg nach Süden (Abb. 7.1.1) unmittelbar nach dem Auslaufen mit der Messung von Vertikalprofilen der Temperatur und der Strömung mit XBTs (Expendable Bathythermograph) und dem ADCP (Acoustic Doppler Current Profiler). Zusätzlich wurde die COMED-Anlage zur Aufzeichnung der Temperatur, des Salzgehalts, der Chlorophyll- und Gelbstoffkonzentration sowie der Raman- und der Mie-Streuung in der ozeanischen Deckschicht in Betrieb genommen. Nach der Durchquerung eines sogenannten Agulhas-Ringes, einer Abschnürung des Agulhasstromes, erreichten wir den Antarktischen Zirkumpolarstrom mit seinen Bändern, die der Subtropen-, der Subantarktischen und der Polarfront zugeordnet werden. Am 6. Dezember kam bei 44°45'S, 10°23'E der erste Eisberg in Sicht. Die Polarfront durchquerten wir bei 48°20'S, 7°20'E am 7. Dezember und begannen mit den Verankerungsarbeiten in der Antarktischen Polarfrontzone. Zwei Verankerungen mit Strömungsmessern und Sedimentfallen wurden aufgenommen und neu ausgelegt. An den Verankerungspositionen wurden auch die hydrographischen Messungen mit der CTD-Sonde (Conductivity, Temperature, Depth) aufgenommen.

Den Eisrand erreichten wir am 11. Dezember bei 58°24'S, 2°15'E, nachdem schon am Tag zuvor immer wieder einzelne lockere Schollenfelder gesichtet worden waren. Der Übergangsbereich vom Zirkumpolarstrom zum Weddellwirbel zwischen 56° und 59°S machte sich durch zahlreiche Eisberge bemerkbar, deren Häufigkeit weiter südlich wieder deutlich abnahm. Am nördlichen Rande des Weddellwirbels nahmen wir eine dritte Verankerung auf. Auf unserem weiteren Weg nach Süden kreuzte eine Gruppe meteorologisch/ozeanographischer Bojen unseren Kurs, von denen wir so viele wie möglich aufnehmen sollten. Da die Bojen im Eis sehr schlecht zu sehen und die Positionen zum Teil sehr ungenau waren, gestaltete sich die Suche schwieriger und zeitaufwendiger als erwartet, so daß wir nur bei einer Boje erfolgreich waren. Bei 65° 00'S, 8° 48'W erfolgte die erste biologische Station mit dem Multinetz. Das CTD-Profil, das an dieser Station aufgenommen wurde, zeigte Temperaturen von 0,9°C im Maximum des Warmen Tiefenwassers, das damit deutlich wärmer als in früheren Jahren war. Während bei unserer Abreise der Eisgürtel in den Eiskarten noch sehr geschlossen und weit nach Norden reichend dargestellt worden war, beobachteten wir auf unserem Weg nach Süden einen schnellen Zerfall der Eisbedeckung, der uns über weite Strecken eine nahezu vom Eis unbehinderte Fahrt ermöglichte.

Vor der Küste öffnete sich eine weite Fläche, die vollständig frei von Meereis war, die Küstenpolynja. In der Nacht zum 16. Dezember erreichten wir die Atkabucht und brachen uns im Festeis einen Liegeplatz. Bei ausgezeichnetem Wetter begann am frühen Morgen die Entladung zur Versorgung der Neumayer-Station, wo wir das wissenschaftliche und technische Überwinterungspersonal mit dem notwendigen Ausrüstungs- und Versorgungsmaterial abgesetzten. Als Sommergäste blieben logistisches Personal und wissenschaftliche Arbeitsgruppen an der Station, die

Fig. 7.1.1: Die Fahrtroute der "Polarstern" während ANT X/7.
Cruise track of "Polarstern" during ANT X/7.

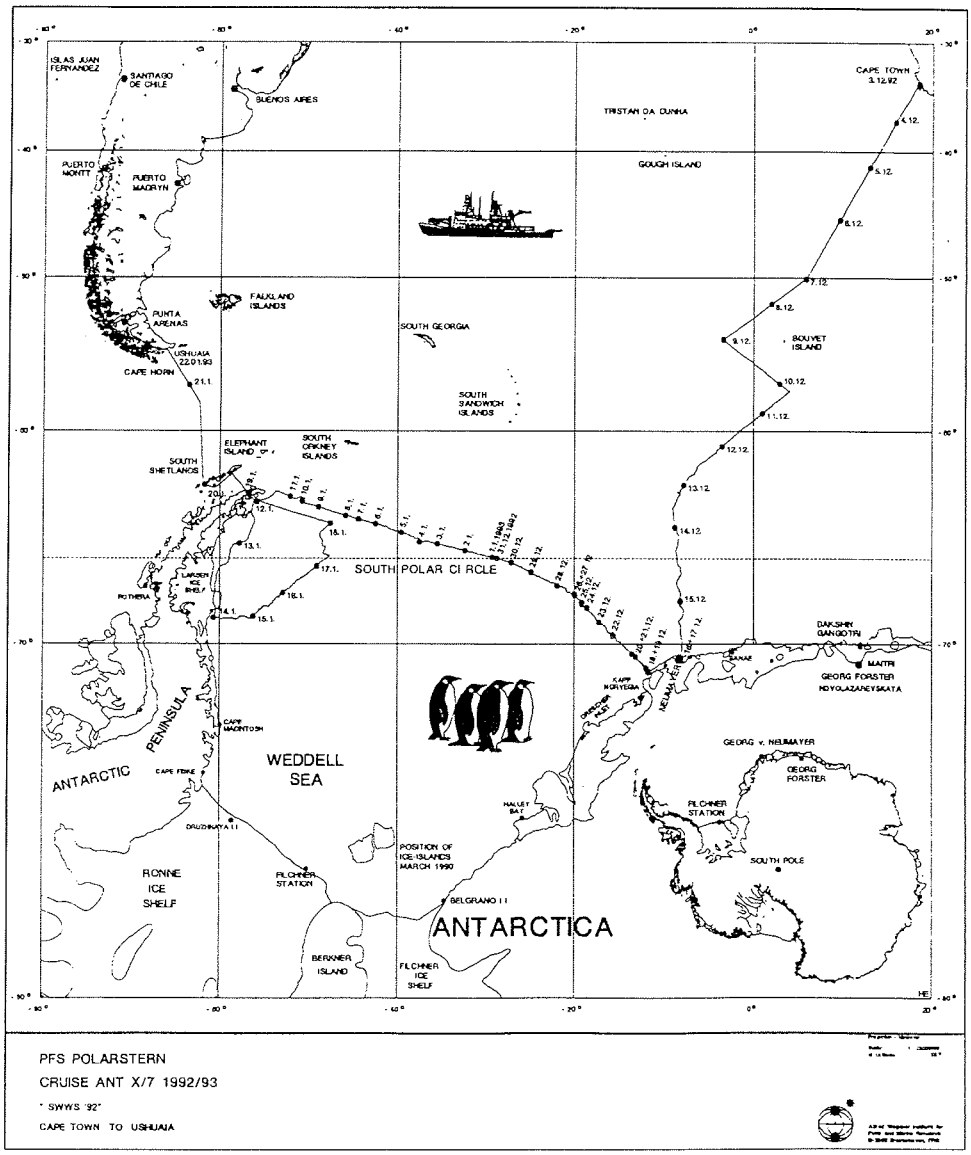

Eisbohrungen betrieben und einen Radar-Eisdickenmesser erprobten. Zusätzlich waren Baumannschaften mitgekommen, um die Arbeiten an der neuen Station abzuschließen und die alte abzubauen. Da die schweren Tankcontainer nicht durch den tiefen Schnee auf dem Festeis transportiert werden konnten, mußten wir zur Treibstoffübergabe an die 26 m hohe Schelfeiskante verholen. Viele von uns konnten die Zeit der Entladung zu einem Besuch in der Neumayer-Station und der Pinguin-Kolonie nutzen.

Noch in der Nacht zum 19. Dezember verließen wir die Atkabucht, um in der Küstenpolynja weiter nach Südwesten zu versegeln, wo wir am nächsten Morgen die wissenschaftlichen Arbeiten aufnahmen. Hier erreichten wir vor einem Inlet im Schelfeis bei 71°07'S, 11°25'W, wenige Meilen nordöstlich von Kapp Norvegia, den südlichsten Punkt unserer Reise (Abb. 7.1.1). Das wissenschaftliche Grundprogramm im zentralen Weddellmeer zwischen Kapp Norvegia und der Joinvilleinsel bestand in der Messung von Vertikalprofilen der Temperatur, des Salzgehalts und des Gehalts an Spurenstoffen im Meerwasser an 57 hydrographischen Stationen. Zusätzlich wurden 18 Strömungsmesserverankerungen nach zweijähriger Meßdauer aufgenommen und 9 neu ausgelegt. Die Verankerungen dienen der Aufzeichnung langfristiger Zeitreihen der Strömungsgeschwindigkeit und -richtung, sowie der Temperatur. In zwei Verankerungen waren Sedimentfallen eingebaut, die absinkende Partikel auffangen. Eisecholote, die Zeitreihen der Eisdicke über der Verankerungsposition messen, wurden in sechs Verankerungen eingesetzt.

Die Verankerungsaufnahme gestaltete sich schwieriger als erwartet, da die akustischen Auslöser in den Verankerungen nicht ordnungsgmäß funktionierten. So waren die Antwortsignale nach dem Auslösen nicht zu empfangen, was den Einsatz von akustischen Peilgeräten unmöglich machte. Nur wegen der günstigen Eisverhältnisse traten durch diesen Umstand keine Verluste auf, da mit Ausnahme einer Verankerung, die erst nach mehrstündiger Suche im Eis gefunden wurde, alle zumindestens teilweise im freien Wasser an der Oberfläche auftauchten. Bei drei Verankerungen versagten die Auslöser vollständig, so daß sie gedredgt werden mußten, zwei davon mit Erfolg. Beim Hieven einer der gedredgten Verankerungen geriet die Verankerungsleine in den Backbord-Propeller, konnte aber mit Bordmitteln wieder entfernt werden. Drei Versuche, Verankerungen zu dredgen, bei denen schon auf einem früheren Fahrtabschnitt oder mit anderen Schiffen vergeblich Aufnahmeversuche erfolgt waren, verliefen ergebnislos. Der Verlust einer Verankerung auf dem westlichen Schelf muß der Wirkung von Eisbergen zugeschrieben werden. Drei weitere Verankerungen zeigten Berührungsspuren von Eisbergen, wobei aber nur bei einer die Messungen dadurch gestört wurden. Insgesamt gingen von den 79 eingesetzten Geräten 16 verloren. Allerdings registrierten 30 Geräte nur etwa ein Jahr, da sowohl der Stromverbrauch der Geräte als auch die Kapazität der Batterien nicht den Spezifikationen der Hersteller entsprachen.

Mit den ozeanographischen Messungen soll die Zirkulation und die Wassermassenverteilung im zyklonalen Strömungssystem des Weddellwirbels bestimmt werden. Daraus kann der ozeanische Massen- , Wärme- und Salztransport in das und aus dem südliche Weddellmeer berechnet werden, der den Beitrag dieses Meeresgebietes zur Klimawirksamkeit des Ozeans begründet. Entscheidend dafür ist die Bildung des Bodenwassers, die einen tiefen Vertikalaustausch bewirkt und die Speicherfähigkeit des Ozeans für Wärme und gelöste Substanzen reguliert. Die Untersuchungen sind ein Teil der Weddell-Wirbel-Studie, die 1989 begann und zum

World Ocean Circulation Experiment (WOCE) beiträgt. Die vorläufige Auswertung der Verankerungsmessungen zeigt, daß der Massentransport des zyklonalen Weddellwirbels von 30 10^6 m^3s^{-1} weitgehend durch die etwa 500 km breiten Randstöme erfolgt. Im Inneren befindet sich ein antizyklonaler Wirbel mit etwa 3 10^6 m^3s^{-1}. In weiten Teilen des inneren Weddellmeeres erfolgt eine Umkehrung der Stromrichtung mit der Tiefe. Der Austrom des Weddellmeer-Bodenwassers unterliegt einem deutlichen Jahresgang. Längerperiodische Veränderungen werden besonders im Warmen Tiefenwasser sichtbar, dessen Temperaturmaximum 1992 deutlich höher lag als 1990.

Die Kenntnis der physikalischen Bedingungen stellt die Grundlage der chemischen, biologischen und biogeochemischen Arbeiten dar. Die chemischen Untersuchungen befaßten sich mit den im Meerwasser gelösten anorganischen und organischen Substanzen. Nährstoffe bilden die Voraussetzung für den biologischen Stoffkreislauf. Deshalb wurden die Verteilung von Nitrat, Nitrit, Ammonium, Silikat und Phosphat in der Wassersäule bestimmt. Das Treibhausgas Kohlendioxid war Gegenstand einer Untersuchung, mit der festgestellt werden soll, in welchem Ausmaß dieses Gas im Weddellmeer vom Ozean an die Atmosphäre abgegeben oder aufgenommen wird und wie sich diese Raten räumlich und jahreszeitlich verändern. Die Beurteilung des globalen Kohlendioxidproblems erfordert die Kenntnis des vollständigen Kohlenstoffkreislaufs. Hier stellt der im Ozean gelöste organische Kohlenstoff ein bedeutendes Reservoir dar, zu dem die Huminstoffen zählen. Von ihnen ist noch nicht geklärt, in wieweit sie terrigen sind oder von Meeresalgen gebildet werden. Diesbezügliche Daten sind im Südatlantik äußerst rar und wurden deshalb an den hydrographischen Stationen bestimmt. Einen Bestandteil der organischen Kohlenstoffverbindungen bilden die Sterole, deren gelöster und partikulärer Anteil gemessen wurde.

Die biologischen Programme befassten sich mit der Ökologie des Phyto- und Zooplanktons. In diesem Zusammenhang wurde die Verteilung verschiedener Planktonarten erfaßt, sowie die Produktion und der Stoffumsatz gemessen. Dazu wurde das Phytoplankton aus Wasserproben filtriert, die mit dem Kranzwasserschöpfer der CTD-Sonde genommen wurden. Zum Fang von Zooplankton wurde an 21 Stationen das Multi- und das Bongonetz eingesetzt. An den Organismen aus diesen Fängen erfolgten Untersuchungen der Anpassung unterschiedlicher Organismen an antarktische Bedingungen, die durch die Lebensweise und durch physiologische Eigenschaften erfolgen kann. Um die Verfügbarkeit von Nährstoffen im Stoffkreislauf zu bestimmen, ist nicht nur der Aufbau organischer Substanz, sondern auch der Abbau durch Bakterien von Bedeutung, der von einer mikrobiologischen Arbeitsgruppe behandelt wurde. Die Abschätzung der Wirkung zunehmender UV-B Strahlung durch die Abnahme der Ozonschicht auf das Phytoplankton und die im Wasser lebenden Bakterien gab diesen Arbeiten einen aktuellen Bezug. Die Eindringtiefe der Strahlung unterschiedlicher Wellenlängenbereiche wurde an 19 Positionen gemessen.

Bei mäßigem Wind, Temperaturen um den Gefrierpunkt und einer geschlossenen Wolkendecke war das Eis weich und brüchig. Bei 64°35'S, 44°25'W hatten wir auf unserem Schnitt am 7. Januar die westliche Eisgrenze erreicht, die auf kurze Entfernung den Übergang von 90% auf 10% Eisbedeckung mit sich brachte. Schon 20 Meilen vor dem Eisrand schien das Meer zu atmen. Im gleichförmigen Rhythmus der stark gedämpften Dünung hoben und senkten sich die Eisschollen und kündigten den im dichten Nebel unsichtbaren Eisrand an.

Die Verknüpfung der physikalischen und biologischen Daten hat gezeigt, daß die jahreszeitlich bedingte Entwicklung der pflanzlichen Biomasse im östlichen, zentralen und westlichen Weddellmeer unterschiedliche Stadien erreicht hatte. Diese drei Bereiche des Weddellmeeres wurden durch zwei Gürtel dichter Eisbedeckung getrennt, deren Lage durch das Windfeld und die Zirkulation des Weddellwirbels bestimmt wurde. Hier im Packeisbereich konnte im Schatten der mit einer dicken Schneeschicht bedeckten Schollen die Entfaltung der Frühjahrsblüte noch nicht einsetzen. Außerhalb dieses Gürtels, wo nach dem Tauen des Eises durch Schmelzwassereintrag und Erwärmung eine Stabilisierung der Wassersäule eingetreten war, die es den Algen ermöglicht hat, im lichtdurchfluteten Teil der Wassersäule zu verbleiben, hat sich in der bereits seit Anfang Dezember geöffneten östlichen Küstenpolynja eine üppige Algenblüte von Diatomeen und *Phaeocystis* entwickelt. Im Zentrum des Weddellmeeres war die Entwicklung noch nicht so weit fortgeschritten. Das Abgrasen durch eine Vielzahl Zooplankter, sowohl Einzeller als auch Ruderfußkrebse, erschwerte hier zusätzlich die Algenentwicklung. Im Westen hingegen hatten sich bereits seit längerem weite Flächen freien Wassers gebildet, so daß die Diatomeenblüte ihren Höhepunkt überschritten hatte und nach dem Abgrasen durch die Zooplankter von einer reinen *Phaeocystis*- Blüte mit gewaltigem Ausmaß in Dichte und Ausdehnung verdrängt wurde.

Nach dem Abschluß der Arbeiten auf dem Hauptschnitt bot sich nun noch die Möglichkeit, die außergewöhnlichen Eis- und Wetterverhältnisse zum Vorstoß nach Süden entlang des Larsen Schelfeises zu nutzen (Abb. 7.1.1). Während sich in normalen Jahren der Eispanzer im südwestlichen Weddellmeer kaum öffnet, waren in diesem Jahr weite Gebiete mit weniger als 50% Eis bedeckt. Dies ist umso erstaunlicher, da zu Beginn unserer Reise der antarktische Eisgürtel noch dicht geschlossen war und überdurchschnittlich weit nach Norden gereicht hatte. Es wird ein Teil der Auswertung unserer Meßdaten sein, zu verstehen, in wie weit der rasche Rückgang des Eises durch die ruhigen und milden Wetterverhältnisse bedingt war, oder ob die ozeanischen Bedingungen einen wesentlichen Beitrag dazu geleistet haben.

Unter den günstigen Eisbedingungen konnten wir 50 Meilen weiter nach Süden vordringen als Kapitän Larsen, der 1893 dieses Schelfeis im Osten der Antarktischen Halbinsel entdeckt hatte. Als wir auf unserem Weg nach Süden die argentinische Station "Marambio" auf Seymour Island passierten, nutzen wir die Gelegenheit, die internationalen Kontakte in der Antarktis zu stärken und gaben den argentinischen Stationsbewohnern einen Empfang an Bord. Bei der Fortsetzung unserer Fahrt in der Küstenpolynja überraschten uns Gebiete mit extrem hohen Wassertemperaturen von über 2°C, die zusammen mit der schon stark gealterten Planktonblüte zeigten, daß hier im Südwesten schon vor längerer Zeit das Frühjahr eingezogen war. Bei 69°S hatten wir am 14. Januar den südlichsten Punkt im westlichen Weddellmeer erreicht, der mit der noch zur Verfügung stehenden Zeit zu vereinbaren war, und begannen von der Schelfeiskante aus einen Schnitt mit 20 CTD- und 4 Biologie-Stationen nach Nordosten (Abb. 7.1.1), auf dem wir die Unterschiede der physikalischen, chemischen und biologischen Bedingungen im Vergleich zum nördlichen Arbeitsgebiet bestimmen können. Hierbei ist die meridionale Veränderung des Ausstroms von Weddellmeer-Bodenwasser, das am Kontinentalabhang nach Norden geführt wird, von besonderem Interesse. Nun besitzen wir Messungen, die etwa auf halben Weg zwischen dem wahrscheinlichen Entstehungsgebiet dieser Wassermasse, dem Filchner-Ronne Schelfeis, und der Joinvilleinsel liegen. Daraus können wir die Inten-

sität der Vermischung mit den umliegenden Wassermassen ableiten. Die vorläufige Untersuchung der Eigenschaften und der Verteilung der Wassermassen auf dem Larsen-Schnitt und dem Hauptschnitt deutet darauf hin, daß dem nach Norden strömenden Weddellmeer-Bodenwasser ein bedeutender Anteil von Wasser des Larsen Schelfs zugemischt wird.

Nachdem der erste Teil unserer Reise durch die strenge Routine einer mehrfachen Wiederholung im Rahmen der Weddell-Wirbel-Studie bestimmt war, hatten wir nun die Möglichkeit, Entdeckerfreude zu empfinden, als wir weiße Stellen auf der Karte erforschten, an denen nicht einmal die Bodentopographie bekannt war, geschweige denn die ozeanographischen, chemischen und biologischen Bedingungen. Um auch einen Eindruck vom benthischen Leben vor dem Larsen Schelfeis zu erhalten, haben wir drei Hols mit dem Agassiz-Trawl ausgeführt.

Die Lage dieses Schnittes hatten wir auf der Grundlage von Satellitenkarten der Eisbedeckung gewählt, die wir vom kanadischen Atmospheric Environment Service, Ice Branch, übermittelt bekommen hatten. Sie zeigten ein Minimum zwischen zwei Bereichen mit vollständiger Eisbedeckung. Diese Verteilung wurde weitgehend bestätigt, so daß wir erst wieder bei 66°25'S, 47°55'W auf dichtes Eis trafen, wo wir nach Nordwesten abdrehten (Abb. 7.1.1), um bei 64°48'S, 47°35'W, etwa 40 Meilen südlich unseres Hauptschnittes, die Stationsarbeiten einzustellen.

Die Rückreise nach Südamerika führte uns noch durch den Antarctic-Sund nach King George Island, wo wir die argentinischen Station "Jubany", die nun auch von deutschen Wissenschaftlern genutzt wird, besuchten, um dort eine Räumschaufel abzuliefern. Der gegenseitige Besuch auf der Station und auf "Polarstern" velief turbulent, da gleichzeitig mit uns auch das spanische Forschungsschiff "Hesperides" in der Maxwellbucht eintraf, und wir innerhalb kurzer Zeit ein sehr herzliches Besuchsprogramm mit den argentischen und spanischen Besatzungsmitgliedern, Wissenschaftlerinnen und Wissenschaftlern, sowie den deutschen Gastforscherinnen und Gastforschern auf der Station und dem spanischen Schiff abwickelten. Kurze Zeit vorher hatten wir eine Nachricht von der "Hesperides" erhalten, die uns darüber informierte, daß die einzige CTD-Sonde an Bord ausgefallen sei, und nun das gesamte Programm gefährdet wäre. Da unser eigenes Programm abgeschlossen war, konnten wir helfen, indem wir eine CTD-Sonde übergaben.

Vorbei an Deception Island erreichten wir bei strahlendem Sonnenschein die Drakestraße, wo während der Passage nach Südamerika XBT-, ADCP-, und COMED-Messungen vom fahrenden Schiff aus durchgeführt wurden. Am 22. Januar 1993 lief "Polarstern" in Ushuaia ein.

1. Itinerary and summary

E. Fahrbach (AWI)

On 3 December 1992 the R.V. "Polarstern" left Cape Town to cross the Southern Ocean towards the Weddell Sea (Fig. 7.1.1). Oceanographic measurements from the moving ship started immediately on the continental shelf with XBT (Expendable Bathythermograph) and ADCP (Acoustic Doppler Current Profiler) profiles. Additionally, the COMED-system to measure mixed layer temperature, salinity and the concentration of chlorophyll-a and humic substances as well as Raman- and Mie-

backscattering was activated. The measurements showed a warm Agulhas-ring and the Subtropical, Subantarctic and Polar Fronts during the transect across the Antarctic Circumpolar Current. The first iceberg was sighted at 44°45'S, 10°23'E on 6 December and the Polar Front was crossed on 7 December at 48°20'S, 07°20'E. Two moorings with sediment traps were recovered and redeployed in the area of the Antarctic Polar Frontal Zone. At the mooring positions the first profiles with the CTD-sonde (conductivty, temperature, depth) were measured. The ice edge was reached at 58°24'S, 02°15'E. The transition zone from the Antarctic Circumpolar Current to the Weddell Gyre was marked by a belt of frequent icebergs between 56° and 59°S. A third mooring was recovered in the northern Weddell Gyre boundary. On the way further south, towards Atka Bight we searched for some meteorological buoys and recovered one of them. At 65°00'S, 08°48'W, the first biological station was carried out with a multinet. The CTD-profile obtained at that station revealed a surprisingly high temperature of 0.9°C in the temperature maximum of the Warm Deep Water. Even if the ice belt extended extremly far to the north when we left Cape Town, it decayed dramatically during our way to the south with the consequence that we could proceed rather undisturbed by the ice and reached the wide coastal polynya on 16 December.

At the Neumayer-Station overwintering personnel and building crews disembarked to finish the new station and to dismantle the old one. Additionnal groups, which carried out drilling programmes on the shelf ice with a hot water and an electrically heated system and the testing of an instrument to measure ice thickness by radar, stayed at the station. Supply goods and equipment for the next overwintering period were deposited. During the night to 19 December we left the Atka Bight and followed the coastal polynya to the southwest.

The basic scientific program in the Weddell Sea, on a transect from Kapp Norvegia to Joinville Island (Fig. 7.1.1), consisted of the measurement of vertical profiles of temperature, salinity and natural trace substances at 57 hydrographic stations. On that transect 18 moorings with 79 instruments, current meters, thermistor chains, water level recorders and sediment traps were recovered and nine moorings were redeployed. Six upward-looking sonars are presently installed to measure ice thickness and five were recovered. The recovery was hampered by the malfunction of acoustic releases. The ones deeper than 1500 m meters and moored for two years did not respond with enough power to be acoustically ranged. Three of them did not release at all. Due to the favorable ice conditions and various dredging operations all but three moorings were recovered with a total loss of 16 instruments.

The measurements aim to determine the circulation and the water mass distribution in the Weddell Gyre with the transports of mass, heat and salt. The data allow to estimate the rate of bottom water formation in the Weddell Sea which controls to a large extent the vertical exchange and consequently the ability of the ocean to store heat and dissolved substances. Bottom water formation determines the contribution of the Weddell Sea to the effect of the world ocean on climate variations. The investigations are part of the Weddel Gyre Study which began in 1989 in the framework of the World Ocean Circulation Experiment (WOCE). The preliminary data show that the mass transport of the cyclonic gyre of 30 10^6 m^3s^{-1} is mainly determined by the 500 km wide boundary currents. In the interior an anticyclonic gyre transports about 3 10^6 m^3s^{-1}. In most part of the gyre the current direction reverses with depth. The outflow of the Weddell Sea Bottom Water in the west is subject to a significant seasonal

cycle. Longer period changes are especially visible in the temperature field. The most obvious variation was measured in the maximum temperature of the Warm Deep Water which increased significantly from 1990 to 1992.

The knowledge of the physical conditions provides the basis for chemical, biological and biogeochemical investigations. The biogeochemical programs referred to cycles of different anorganic and organic compounds in sea water and the exchange of carbon dioxide between ocean and atmosphere. The biological work focused on phyto- and zooplankton ecology. For this purpose 21 biological stations with multi- and bongonet catches were carried out. Distribution of microbial biomass and respiratory activity was studied. Dissolved organic carbon and humic substances as well as dissolved and particulate sterols were measured. Alltogether these programs contribute to a better understanding of the global carbon cycle and are to be viewed in the context of the Joint Global Ocean Flux Study (JGOFS). Special emphasis was given to the investigation of the effect of increasing UV-B radiation on Antarctic marine organisms.

With moderate winds, air temperatures at the freezing point and overcast sky we reached on 7 January the western ice edge at 64°34'S,44°25'W where the ice cover decreased from 90 to 10% within a short distance. The ice cover was split in two large bands which were separated by a rather open area in the center of the gyre and surrounded by the wide eastern and western polynyas. This structure was reflected in the hydrographic conditions and the status of the biological systems. Whereas in the area of the ice belt winter conditions still prevailed, the open areas, where light was available and the water column was stabilized by warming and melt water input, rich blooms had developed. In the eastern coastal polynya an advanced bloom of diatoms and *Phaeocystis* was observed. The one in the center was much less intense and obviously affected by grazing. In the west, where spring conditions prevailed since several weeks, the maximum of the diatom bloom was passed due to intensive grazing and a strong *Phaeocystis* bloom dominated the system.

The station work on the main transect stopped east of Joinville Island. Due to the favourable ice conditions time was still available to take advantage at the unique conditions and to proceed to 69°S along the Larsen Ice Shelf (Fig. 7.1.1), 50 nautical miles further south than C. A. Larsen when he explored this ice shelf in 1893. On the way we passed the Argentine Station "Marambio" on Seymour Island, where we could cultivate the international relations by a reception on board of "Polarstern". The shelf was cut by a series of depressions to a depth of 600 m which seemed to steer the cross shelf circulation. Sea surface temperatures of up to 2°C were observed in the polynya.

From 64°34'S,44°25'W we directed a transect with 20 CTD and four biological stations towards the northeast (Fig. 7.1.1). On the shelf three hauls with the Agassiz Trawl were carried out. The location of the transect was determined according to SSM/I (Special Sensor Microwave/Imager) satellite data of the ice cover as obtained from the Ice Centre of the Atmospheric Environment Service, Canada. It was in accordance with the satellite data, that we met heavy ice conditions only around 66°25'S,47°55'W where we were forced to turn northwest and to finish the transect at 64°48'S,47°35'W at about 40 nautical miles from our main transect. The hydrographic conditions on that transect indicate by low saline water overlying a thin near

bottom higher saline layer, the admixture of Larsen Shelf water to the northward flowing Weddell Sea Bottom Water.

From the end of the transect "Polarstern" proceeded through the Antarctic Sound to King George Island where we deposited material at the Argentine "Jubany" Station which is now used jointly with German scientists. In the Maxwell Bight we met the Spanish R.V. "Hesperides" which was working in the Bransfield Strait and we transferred one of our CTDs. On our way to the Drake Passage we passed by Deception Island where we continued the oceanographic work from the moving ship across the Antarctic Circumpolar Current with XBT, ADCP and COMED measurements. On 22 January 1993 "Polarstern" arrived at the port in Ushuaya.

2. Physical oceanography

2.1 Water masses and circulation in the Weddell Sea

T. Boehme, J. Corleis v. d. Voet, E. Fahrbach, H. Fischer,
R. Hamann, L. Kolb, A. Latten, G. Rohardt, E. Schütt, G. Seiß,
V. Strass, H. Witte, F. Zwein (AWI)

Objectives

The physical oceanography work was aimed to investigate the water mass distribution and circulation in the Weddell Sea in order to understand the influence of ocean, ice and atmosphere on the formation of water masses which leave the Weddell Gyre and affect the characteristics of the bottom water of the world oceans. The activities during ANT X/7 are part of a multiyear program, the Weddell Gyre Study, which contributes to the World Ocean Circulation Experiment (WOCE). During this programme, a hydrographic section between the northern tip of the Antarctic Peninsula and Kapp Norvegia (Fig. 7.1.1) was repeated four times. The repetition of the same section during different seasons and years allows to measure longer term mean conditions of water mass characteristics and to assess the seasonal as well as the interannual variability. The programme was initiated in 1989 with a hydrographic survey in late winter during which a set of seven current meter moorings was deployed. A second survey in early spring followed in 1990 during which the first set of moorings was recovered and a new set of 21 moorings was deployed. Early winter conditions were observed in 1992. However, due to the severe ice conditions during that cruise the section could not be covered completely. The present cruise was aimed to recover the 21 moorings, to deploy a new set of 9 moorings and to obtain a summer survey.

The data from the moored current meters are used to describe the large scale current patterns of the Weddell Gyre and to estimate its volume transport. This can only be done with measurements from moored current meters, because of the contribution of the barotropic current field, which, for the time being, can only be derived from direct measurements as there is no indication on an appropriate reference level. Furthermore, intensive current fluctuations require long time series to determine statistically significant averages representative for those circulation patterns which are relevant to water mass formation. From the mass transport measured with the moored current meters and the water mass characteristics obtained during the hydrographic surveys, we can estimate heat and salt transports across the transect. The differences in

volume between the water masses which are advected into the southwestern Weddell Sea and the ones which leave the area to the north reflect the formation of water masses south of the transect.

Fig. 7.2.1 Location of the CTD-profiles during the "Polarstern"-cruise ANT X/7

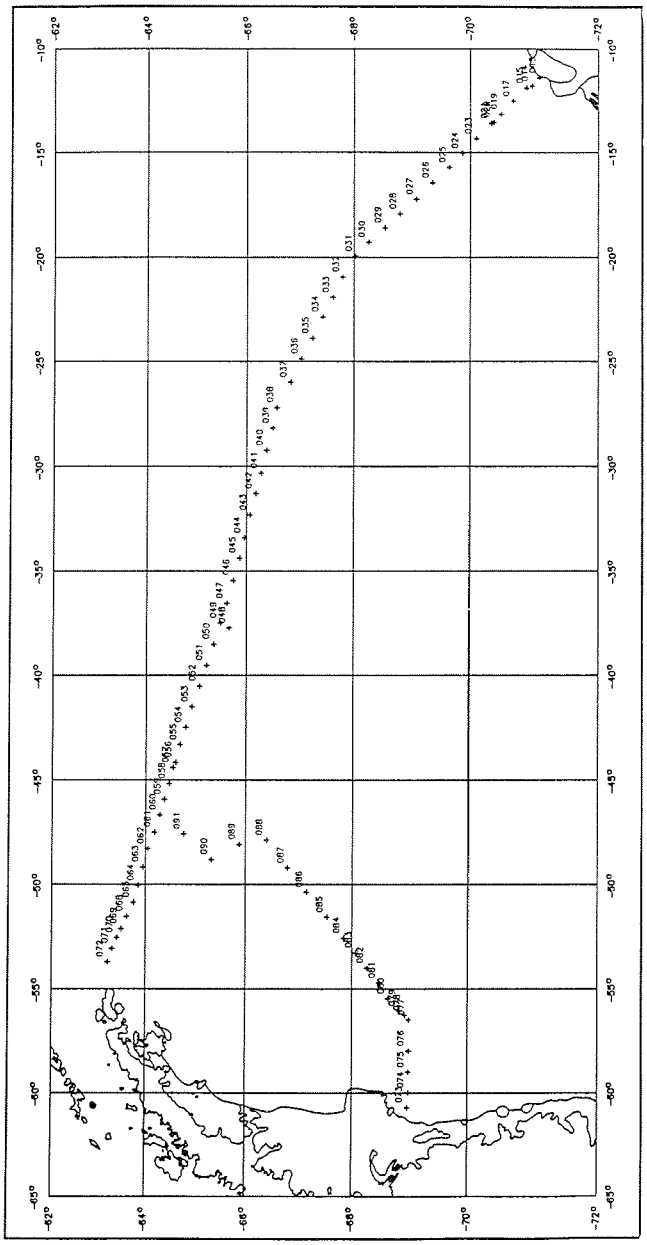

Fig. 7.2.2 The means (triangles) and the standard deviations (stars) of the salinity differences in 10^{-3} PSU between bottle samples and CTD readings as well as the number of samples for each vertical profile (dots).

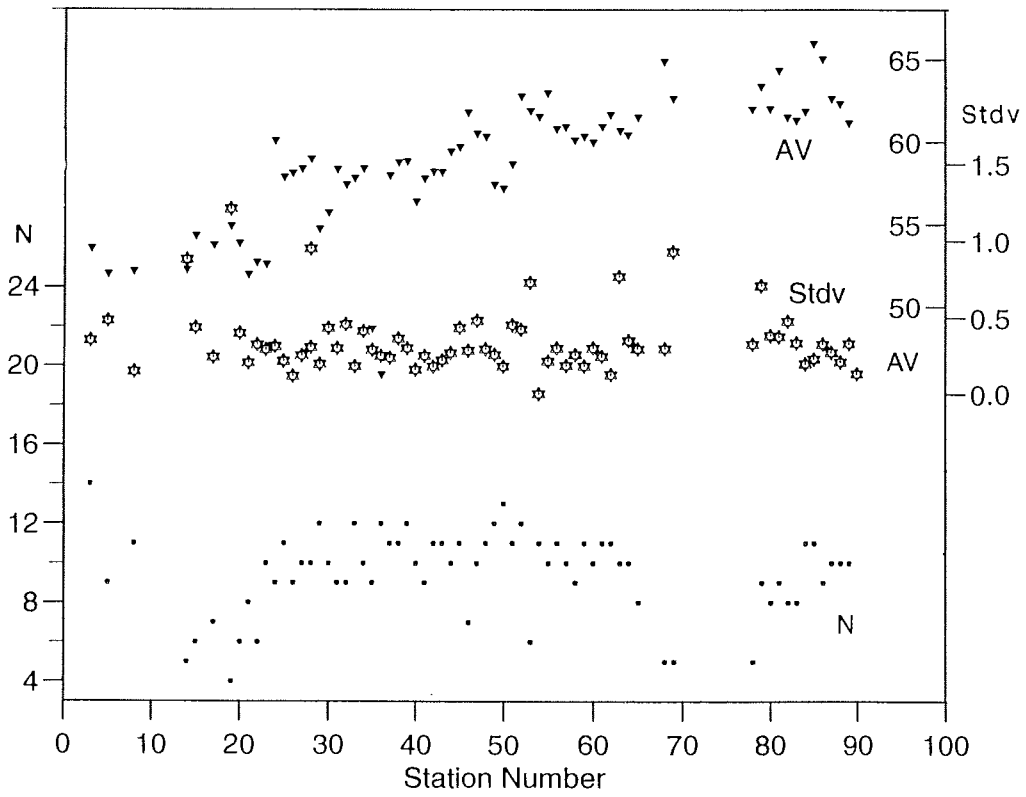

Work at sea

The distribution of water mass characteristics along the hydrographic section from Kapp Norvegia to Joinville Island at the northern tip of the Antarctic Peninsula (Fig. 7.2.1) was measured with 57 CTD-profiles (Conductivity, Temperature, Depth) and discrete samples for temperature, salinity, oxygen, nutrients and trace substances. A second transect with 20 stations was made from the edge of the Larsen Shelf Ice at 69°S60°42'W towards the northeast (Fig. 7.2.1). In order to measure during the available time the characteristics of the Weddell Sea Bottom Water as far south from the main section as possible, the location of the section was chosen to avoid areas with heavy pack ice.

The CTD-measurements were carried out with a NB Mark III sonde connected to a General Oceanics rosette water sampler with 24 12-liter bottles. The quality of the CTD-data relies on the laboratory calibrations of the temperature and pressure sensors made before the cruise at the Scripps Institution of Oceanography. The performance of the instrument during the cruise was controlled by use of SIS digital thermometers and pressure meters as well as Gohla mercury reversing thermometers. The pre-cruise temperature and pressure calibration values were applied to the measurements on board. The conductivity readings of the CTD were corrected by means of salinity measurements from the rosette water samples. The salinity of the samples was determined with a Guildline Autosal 8400 A salinometer in reference to I.A.P.S.O. Standard Seawater. The salinities are given in PSU and calculated by use of the UNESCO Practical Salinity Scale (PSS78). The means and the standard deviations of the salinity differences between bottle samples and CTD readings for each profil are shown together with the number of samples for each profile in Fig. 7.2.2. Due to the stratification of the water column the scatter of the differences is higher in the upper levels. Therefore only differences in levels deeper than 500 m are used and displayed in Fig. 7.2.2 to get an impression of the qualitiy of the instruments and processing. The preliminary data presented in this report are corrected by a constant offset of 0.0588. The accuracy of the preliminary data was estimated to 4 mK in temperature, 4 dbar in pressure and 0.005 in salinity. The final data will be available after the post cruise laboratory calibration. The salinity correction will take into account the slight time drift which was observed.

During the cruise the concentration of dissolved oxygen was measured by means of a computer controlled SIS Winkler-titrator from 1923 water samples taken at 81 stations. The precision of the measurements was estimated by means of three calibration stations where all water bottles were closed in the same depth and 24 samples were taken. The standard error of each station ranged between 0.04 and 0.09 µM with a standard deviation from 0.19 to 0.44 µM corresponding to a precision of 0.1 to 0.2%. For the continous control of the precision 238 double samples were taken from the same bottle during the cruise.

On the main section from Kapp Norvegia to Joinville Island 18 of 21 moorings were recovered (Fig. 7.2.3, Tab. 7.2.4) and 9 of them were exchanged (Tab. 7.2.5). The moorings to recover were equipped with 55 Aanderaa current meters (RCM4, RCM5, RCM7, RCM8) as well as six Aanderaa thermistor cables and two Aanderaa water level recorders. In the near bottom layer nine EG&G acoustic current meters were used (ACM-2). On six moorings, upward-looking sonars (ULS) built by the Christian Michelsen Institute, were installed to measure the ice thickness. One mooring carried an acoustic Doppler current profiler (ADCP) from RD Instruments. The locations of the instruments in the moorings are shown in Fig. 7.2.6.

The recovery of the moorings was hampered by the malfunction of the acoustic releases. In water depths greater than 1500 m no reply signal could be received from the moored releases neither after interrogating nor after releasing, even when the instruments were returned to the surface and floating in sight of the ship in a distance of a few hundred meters. The missing communication link made it impossible to use the available ranging and bearing systems. Only due to the favourable ice conditions, serious losses did not occur. Normally some floats reached the surface in open water between the ice floes and could be located visually. Only one mooring was

completely hidden under the ice after its release and was found only after some hours of searching.

Five times a mooring did not appear at the sea surface after being acoustically released, and dredging had to be tried. In three cases dredging was at least partially successful. The dredged moorings could not be recovered completely, from one only the ground weight and the release was obtained. One mooring was lost due to the rupture of the Kevlar dredging cable, which was used in order to increase the cable length to pick up the mooring with the release. The successful dredging indicates that unreliable acoustic releases are the most likely reason for the failure. The mooring KN4 and two moorings of the University of Southern California which were acoustically released on earlier cruises were dredged unsuccessfully.

Mooring 215 in a water depth of 448 m was most likely lost by contact with icebergs. It could neither be dregded nor acoustically ranged or released in spite of the shallow depth. Three other moorings had obviously been touched by icebergs, but only mooring 206-2 was seriously affected by the loss of the uppermost floats. Because the risk of damage by icebergs had to be accepted in order to obtain ice thickness and upper layer current measurements, moorings and instruments were designed to reduce the resistance to an iceberg in case of contact. The ULSs in 150 m depth were protected by a conical floatation collar and the main buoyancy of the mooring was only in 250 m depth to allow the upper part of the mooring to be depressed by icebergs. The recovery rate of five out of six ULSs proved that the taken precautions were efficient.

As a consequence of three complete and two partial losses of moorings, we lost 15 current meters, one ULS and one water level recorder. From 59 recovered instruments, three were deloyed only for one year and worked reliably, but only 18 of the ones deployed for two years recorded longer than 600 days, whereas 30 stopped after approximately one year due to the mismatch of power consumption and battery power, and eight instruments failed completely due to loss of memory or water intrusion. The five recovered ULS had to be returned to the Christian Michelsen Institute to read out the data due to a malfunction of the communication link.

Tab.7.2.4: Moorings recovered during "Polarstern"-cruise ANT X/7.

Mooring	Latitude (S) Longitude (W)	Deployment Date, time, (UTC)	depth (m)	Instrument Type	No	Depth (m)	Record length (days)
214/3	71°03.3'	14.02.92	380	AVTCP	9763	210	307
	11°44.1'	10:42		AVT	9179	320	307
				WLR	1154	380	244
KN4	70°59.5'	15.12.90	892	S	860019	328	lost
	11°46.9'	09:55		AVTP	9209	333	lost
				S	860020	782	lost
				AVTPC	9210	810	lost
				UCM		811	lost
212/2	70°54.7'	14.12.90	1555	ULS	12/90	135	736
	11°57.8'	07:34		AVTP	8367	250	736
				AVTC	9401	760	384
				AVT	9402	1505	no data
211/2	70°29.7'	14.12.90	2450	AVP	10004	340	397
	13°08.9'	22:17		TK	1572		
				ATR	1104	600	736
				AVTP	8396	1090	736
				AVT	9999	2296	lost
				AVT	9392	2402	lost
226	70°22.8'	13.12.90	2900	AVP	10003	190	373
	13°32.5'	00:57		AVP	9998	940	397
				AVTC	9207	2850	433
225	70°19.1'	12.12.90	4330	AVP	10002	270	100
	13°39.6'	18:19		AVTP	9783	1130	319
				AV	9997	2630	375
				AVT	9782	4280	408
210/2	69°39.6'	11.12.90	4750	ULS	10/90	151	736
	15°42.9'	16:50		AVTP	9201	270	392
				TK	1571		
				ATR	1103	520	741
				AVP	9995	1010	382
				AVT	9391	2521	no data
				ACM-2	1297	4694	no data
224	68°49.7'	10.12.90	4740	AV	9770	4240	330
	17°54.5'	13:38		ACM-2	1291	4690	698
223	67°59.8'	09.12.90	4885	AVTPC	9205	251	lost
	19°57.6'	17:24		AVTPC	9218	1010	lost
				AVT	9208	2520	lost
				ACM-2	1290	4834	lost
222	67°03.6'	07.12.90	4840	AV	9769	4340	398
	24°52.1'	22:54		ACM-2	1282	4790	699
209/2	66°37.3'	03.12.90	4860	ULS	14/90	147	lost
	27°07.1'	20:50		AVTP	9202	279	lost
				AVTPC	9216	1015	lost
				AVTPC	9217	2526	lost
				ACM-2	1289	4810	703
221	66°16.6'	02.12.90	4750	ADCP	378	212	762
	30°17.8'	10:49		AVTPC	9195	220	453
				TK	1426		
				ATR	943	470	628
				AVTP	9214	960	415
				AVT	9215	2470	372
				ACM-2	1288	4700	703
220	65°58.2'	30.11.90	4800	AV	9767	4300	396
	33°20.3'	15:43		AVT	9768	4748	no data

Tab.7.2.4 (cont'd): Moorings recovered during "Polarstem"-cruise ANT X/7.

Mooring	Latitude (S) Longitude (W)	Deployment Date, time, (UTC)	depth (m)	Instrument Type	No	Depth (m)	Record length (days)
208/2	65°38.1'	29.11.90	4710	ULS	11/90	141	no data
	36°30.2'	18:27		AVTPC	9194	230	418
				AVT	9213	987	84
				S	890106	1070	
				AVT	9191	2475	426
				S	890108	4100	
				ACM-2	1285	46600	704
219	65°39.9'	28.11.90	4730	AVT	9187	4230	389
	37°42.5'	13:36		AVT	9188	4680	429
				AVT	9190	4722	no data
218	64°48.9'	25.11.90	4650	AVTP	10005	225	no data
	42°29.3'	21:15		TK	1427		
				ATR	944	475	630
				AVTP	9212	960	433
				AVT	9186	2470	423
				ACM-2	1284	4600	659
217	64°25.1'	24.11.90	4390	ULS	13/90	110	736
	45°51.0'	21:26		AVTPC	9192	220	427
				S	890107	780	
				AVTC	9211	985	no data
				AVT	9185	2480	no data
				ACM-2	1281	4340	708
216	63°57.0'	24.11.90	3480	AVT	9182	2970	427
	49°09.2'	00:34		AVT	9184	3430	451
207/2	63°45.1'	23.11.90	2460	ULS	9/90	165	736
	50°54.3'	06:52		AVTPC	9206	300	391
				TK	1569		
				ATR	1100	550	685
				AVTPC	8395	1010	716
				AVT	8417	2150	664
				TK	1570		
				ATR	1102	2400	666
				AVT	8418	2410	740
206/2	63°29.6'	22.11.90	950	AVTP	8402	260	210
	52°06.3'	14:54		AVTP	9786	900	390
215	63°19.9'	21.11.90	448	AVTP	10001	291	lost
	52°59.1'	20:14		AVTP	9996	396	lost
				WLR	1155	447	lost

Abbreviations

ACM-2	Acoustic current meter, Neil Brown
ADCP	Acoustic doppler current meter
ATR	Recording unit for thermistor cable
TK	Thermistor cable
AVTPC	Aanderaa current meter with temperature. pressure and conductivity sensor
S	Sediment trap
ULS	Upward looking sonar
WLR	Water level recorder

Tab. 7.2.5: Moorings deployed during "Polarstern"-cruise ANT X/7

Mooring	Latitude Longitude	Date Time (UTC)	Water Depth (m)	Type	Instrument Ser. No.	Depth (m)
214/4	71°03.2'S	18.12.92	360	AVTP	9193	210
	11°43.9'W	13.13		AVTC	8401	310
				WLR	100312	360
212/3	70°54.55'S	20.12.92	1540	ULS	28/91	140
	11°57.89'W	07.25		AVTCP	10487	230
				AVTCP	10488	740
				AVT	10493	1500
210/3	69°38.46'S	23.12.92	4750	ULS	5/92	130
	15°43.58'W	03.05		AVTPC	10489	250
				AVTPC	10490	1030
				AVTPC	9920	2530
				AVT	10494	4700
209/3	66°37.43'S	31.12.92	4860	ULS	2/92	135
	27°07.22'W	03.27		SC	1167	150
				AVTPC	10491	150
				TK	1572	
				ATR	1104	400
				AVTPC	10492	1020
				AVT	10496	2530
				AVT	10498	4810
208/3	65°37.60'S	03.01.93	4766	ULS	29/91-24	140
	36°29.38'W	22.40		AVTPC	10872	250
				AVTPC	9785	1040
				S	860009	1120
				AVT	10499	2530
				S	860012	4165
				AVT	10503	4725
217/2	64°25.10'S	08.01.93	4420	ULS	3/92-26	145
	45°50.97'W	14.25		SC	166505	150
				AVTPC	10873	240
				AVT	10540	1010
				AVT	9782	2510
				AVT	9561	4370
207/3	63°45.05'S	10.01.93	2498	ULS	4/92-27	150
	50°54.32'W	11.28		AVTPC	9200	326
				ATR	943	
				TK	1420	580
				AVTPC	9204	1040
				AVTP	9783	2190
				ATR	1103	
				TK	1571	2430
				AVTC	9207	2450
206/3	63°29.55'S	11.01.93	960	AVTP	8370	245
	52°06.27'W	14.05		S	890106	315
				S		875
				AVT	8367	915
215/2	63°19.89'S	12.01.93	450	AVT	9201	400
	52°59.07'W	00.07		WLR	1154	450

Abbreviations

ATR Recording unit for thermistor cable, TK Thermistor cable
AVTPC Aanderaa current meter with temperature, pressure and conductivity sensor,
S Sediment trap, SC Seacat
ULS Upward looking sonar
WLR Water level recorder

Fig. 7.2.3: Location of the moorings in the central Weddell Sea on the transect between Kapp Norvegia and Joinville Island which were to recover during ANT X/7.

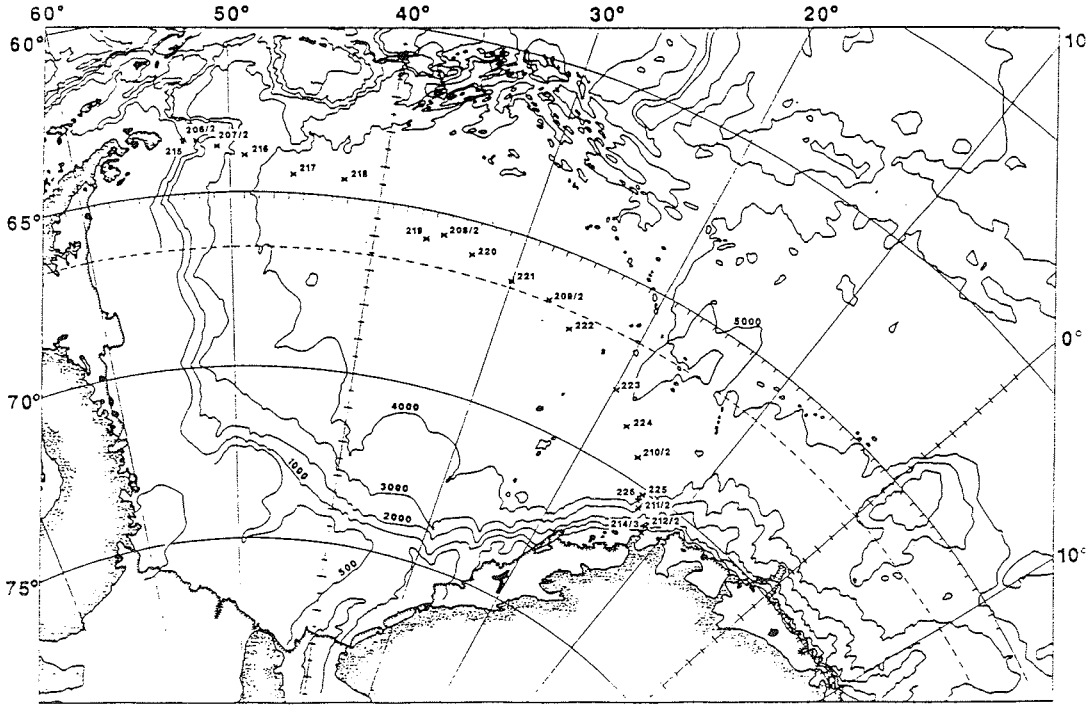

Fig. 7.2.6: Locations of the instruments in the moorings: Aandraa current meters (dots), ACM-2 (squares), Aanderaa thermistor cables (bars), Aanderaa water level recorder (triangle), upward looking sonars (rhombs), sediment traps (open triangles), ADCP (open circle).

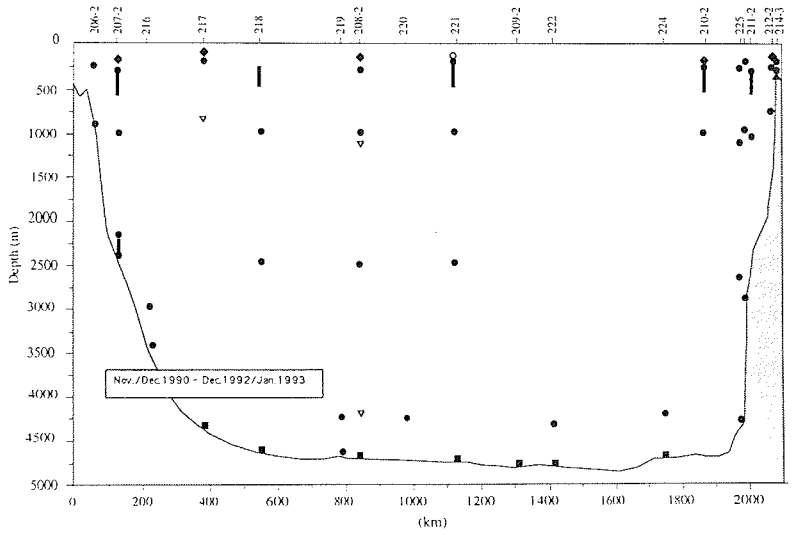

XBT sections were carried out during the crossing of the western ice edge (Tab. 7.2.7) and off the Larsen Ice Shelf (Tab. 7.2.8.). Because the XBTs had a high failure rate, most likely due to the low water temperatures, the sections have large gaps.

Tab. 7.2.7: XBTs launched during the crossing of the ice edge

No.	Date	Time (UTC)	Latitude	Longitude	Depth (m)
157	07.01.93	22:03	64°29'S	45°11'W	4502
156		21:51	64°30'S	45°08'W	4499
155		21:45	64°30'S	45°06'W	4498
154		21:30	64°31'S	45°01'W	4489
153		21:15	64°32'S	44°56'W	4505
152		21:00	64°33'S	44°50'W	4498
151		20:45	64°33'S	44°44'W	4496
150		20:30	64°34'S	44°39'W	4516
149		20:17	64°35'S	44°34'W	4500
148		20:13	64°35'S	44°33'W	4572
147		20:10	64°35'S	44°31'W	4569

Tab. 7.2.8: XBTs launched during the transit from Joinville Island to the Larsen Ice Shelf

No.	Date	Time(UTC)	Latitude	Longitude	Depth (m)
160	14.01.93	23:30	67°12'S	60°21'W	401
167		01:31	67°35'S	60°30'W	487
168		01:36	67°36'S	60°31'W	491
170		01:48	67°39'S	60°32'W	503
174		02:24	67°46'S	60°32'W	537
175		03:19	67°57'S	60°31'W	577
177		03:34	68°00'S	60°34'W	590
178		03:49	68°02'S	60°35'W	607
183		05:43	68°24'S	60°41'W	564
186		07:03	68°38'S	60°29'W	400
187		07:32	68°44'S	60°27'W	251
191		08:40	68°54'S	60°41'W	299
192		09:05	68°59'S	60°43'W	289

Preliminary results

The sections of potential temperature, salinity and oxygen between Kapp Norvegia and Joinville Island (Fig. 7.2.9, 7.2.10, 7.2.13) show the typical water masses of the central Weddell Sea. The near surface layer is characterized during the summer by temperatures significantly above the freezing point, relatively low salinity and high oxygen concentrations. The Winter Water layer below it is obvious at a temperature minimum. In the section plots small scale structures and extreme values do not appear in the near surface and near bottom layers due to the applied smoothing procedures. The Winter Water is separated from the Warm Deep Water by a shallow thermo- and halocline. Its depth increases to several hundred meters from the open water towards the coast, above the upper continental slope in the east and the west. Due to its origin from the Antarctic Circumpolar Current the Warm Deep Water causes a temperature and salinity maximum as well as an oxygen minimum. The Warm

Deep Water is most pronounced near the eastern and western boundaries. The deeper parts of the water column are filled by Antarctic and Weddell Sea Bottom Waters, separated by the potential temperature of -0.8°C. The newly formed Weddell Sea Bottom Water is most prominent at the western continental slope where the deepest temperatures and highest oxygen concentrations are found. On the continental slope off the Larsen Ice Shelf, between 1500 and 2500 m, a colder and saltier layer of only a few meters thickness is found under the lense of cold and fresh Weddell Sea Bottom Water (Fig. 7.2.11, 7.2.12). If the saline near bottom layer represents flow from the area of the Larsen Ice Shelf or water from the outflow of the Filchner Depression will be investigated in the course of the future analysis by use of all available parameters, in particular the stable isotop ^{18}O. On the shelf, in front of the Larsen Ice Shelf, depressions of up 600 m depth (Fig. 7.2.15) could guide the flow to the deep sea. Significant variability of sea surface temperature and salinity are indicative of cross shelf flow, however, no supercooled water can be detected in the XBT records (Fig. 7.2.16).

Comparison of the near surface water mass characteristics observed during the present cruise, with the ones measured during ANT IX/2 from 17 November to 31 December 1990 and ANT VIII/2 from 6 September to 30 October 1989, reveals the seasonal progress by the development of the summer surface water layer with increasing temperatures and decreasing salinities (Fig. 7.2.17) from late winter through spring to summer. However, as the present cruise occurred only two to four weeks later than ANT IX/2, not only seasonal change contributes to the differences, but interannual variability has also to be taken into account. It is obvious from the ice conditions that the present observations are subject to significant interannual variations. This is supported by the conditions in the Winter Water and Warm Deep Water layers (Fig. 7.2.18) which are significantly warmer during the present survey than in 1990.

The measurements from the moored current meters reveal the large scale circulation pattern of the Weddell Gyre. The record long average flow across the transect from Kapp Norvegia to Joinville Island is shown in Fig. 7.2.19. The structure of the cyclonic gyre is determined by the western and eastern boundary currents with annual mean speeds of up to 16 cm/s in the east and 11 cm/s in the west. The volume transport of the boundary currents which are approximately 500 km wide amounts to 25 $10^6 m^3/s$. The interior of the Weddell Sea circulation consists of an anticyclonic circulation cell of about 1000 km diameter. There, the current has an important component in the direction of the transect. Therefore, the annual mean speeds amount to 1 cm/s, whereas the flow across the transect is smaller than 0.5 cm/s. The transport of the interior anticyclonic gyre amounts to 3 $10^6 m^3/s$. The vertical distribution of the current indicates a significant barolinic component. Almost in the whole basin the flow reverses in the near bottom layers. This flow pattern suggests that the newly formed Weddell Sea Bottom Water leaves the southern part of the the basin in the west. Partly, it recirculates in the interior supporting a secondary outflow in the east.

Fig. 7.2.9: Vertical section of potential temperature measured during ANT X/7 between Kapp Norvegia and Joinville Island.

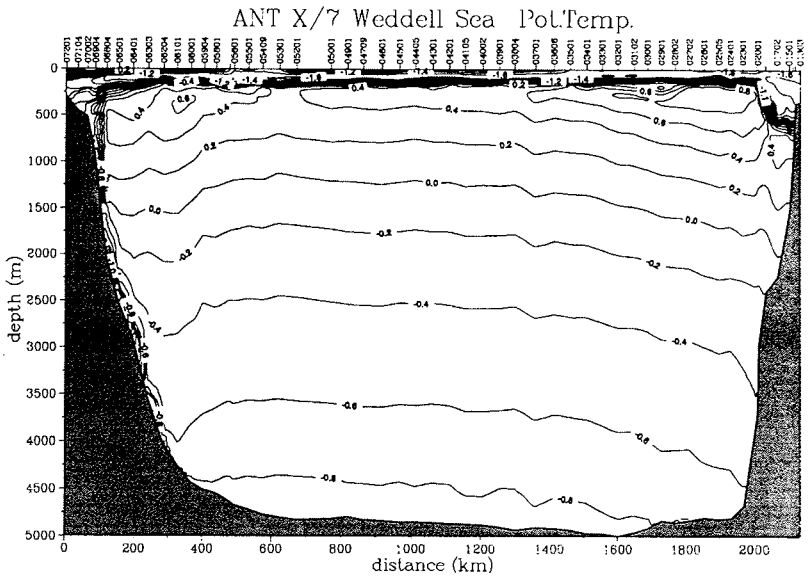

Fig. 7.2.10: Vertical section of salinity measured during ANT X/7 between Kapp Norvegia and Joinville Island.

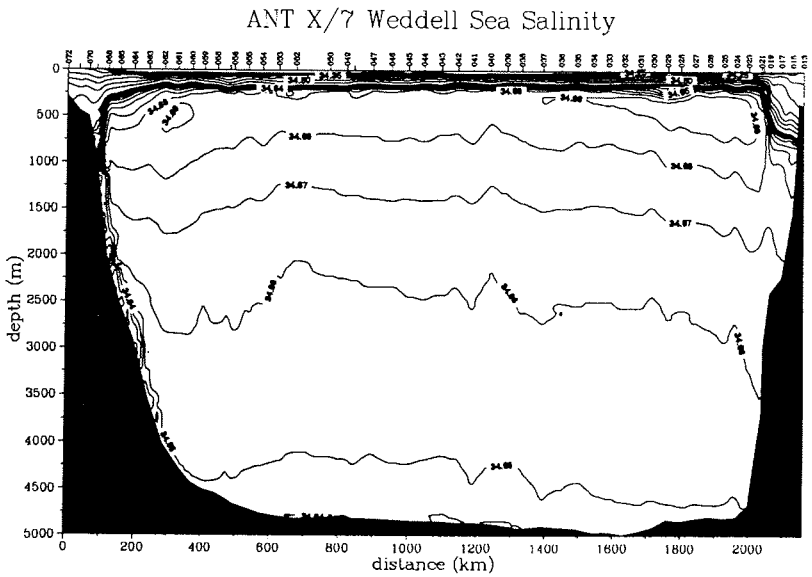

Fig. 7.2.11: Vertical section of potential temperature measured during ANT X/7 from the Larsen Ice Shelf to the northeast.

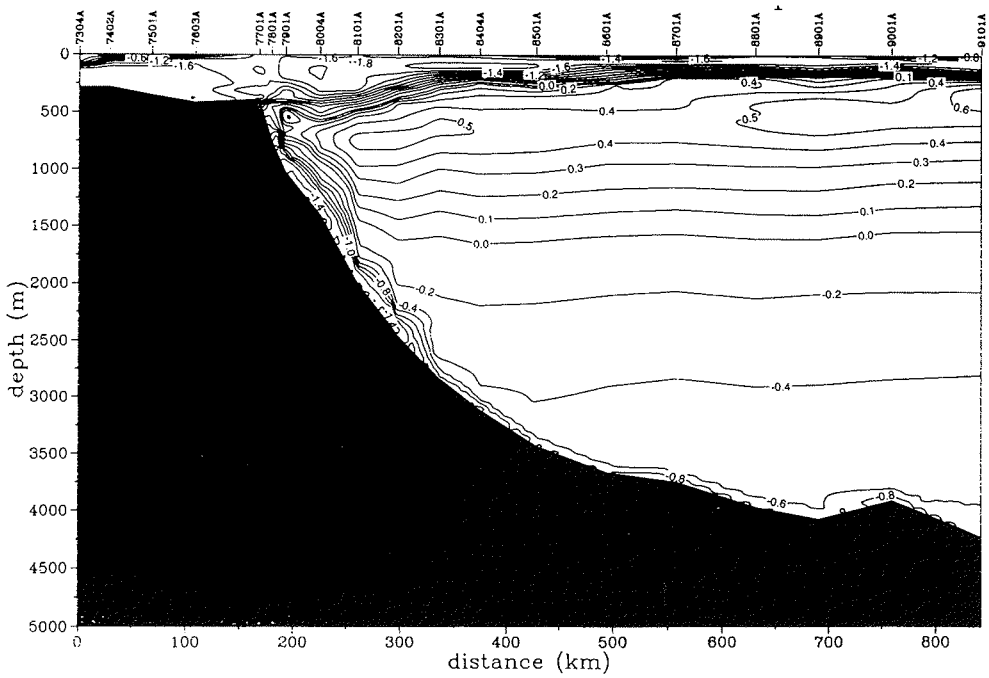

Fig. 7.2.12: Vertical section of salinity measured during ANT X/7 from the Larsen Ice Shelf to the northeast.

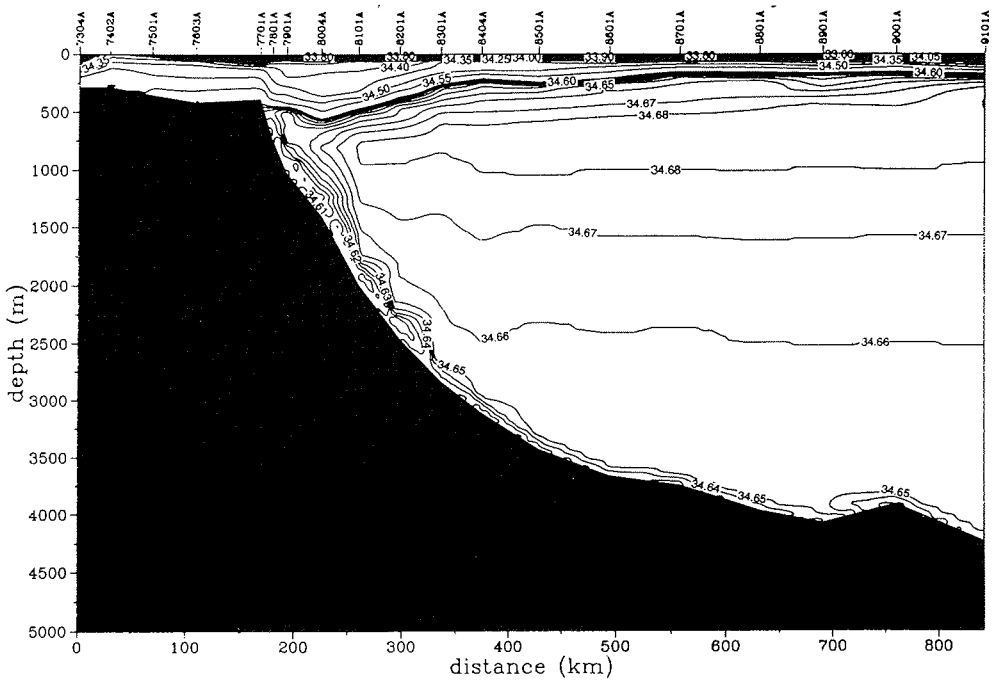

Fig. 7.2.13: Vertical section of dissolved oxygen measured during ANT X/7 between Kapp Norvegia and Joinville Island.

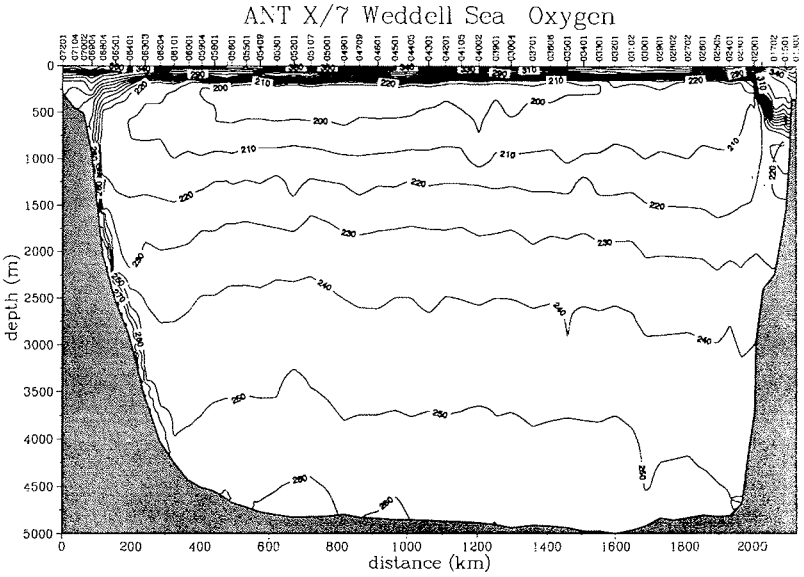

Fig. 7.2.14: Vertical section of dissolved oxygen measured during ANT X/7 from the Larsen Ice Shelf to the northeast.

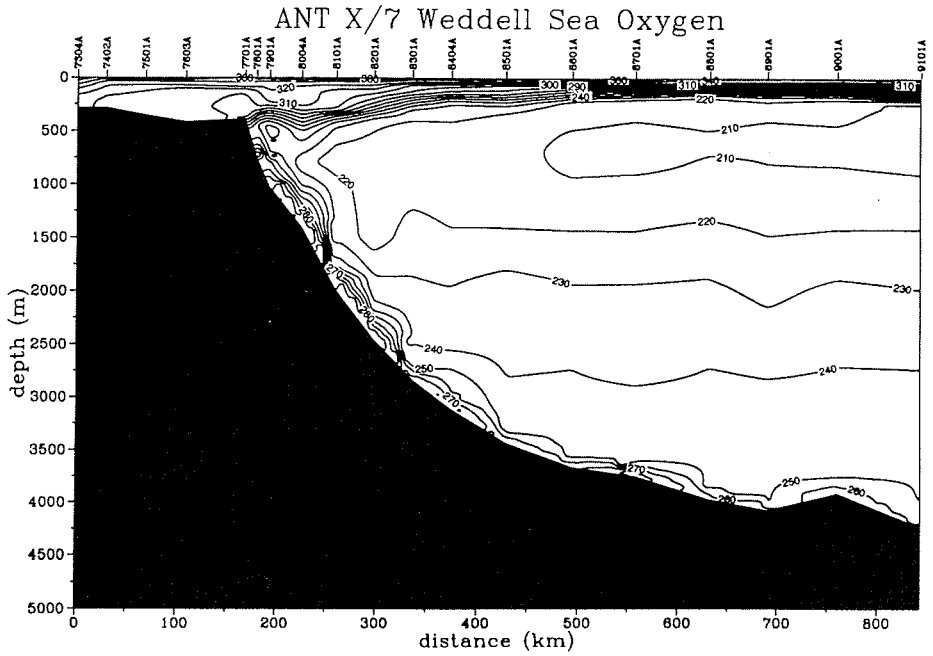

Fig. 7.2.15: Water depth and near surface temperature and salinity in PSU on the Larsen Shelf along the track line shown on Fig.7.1.1.

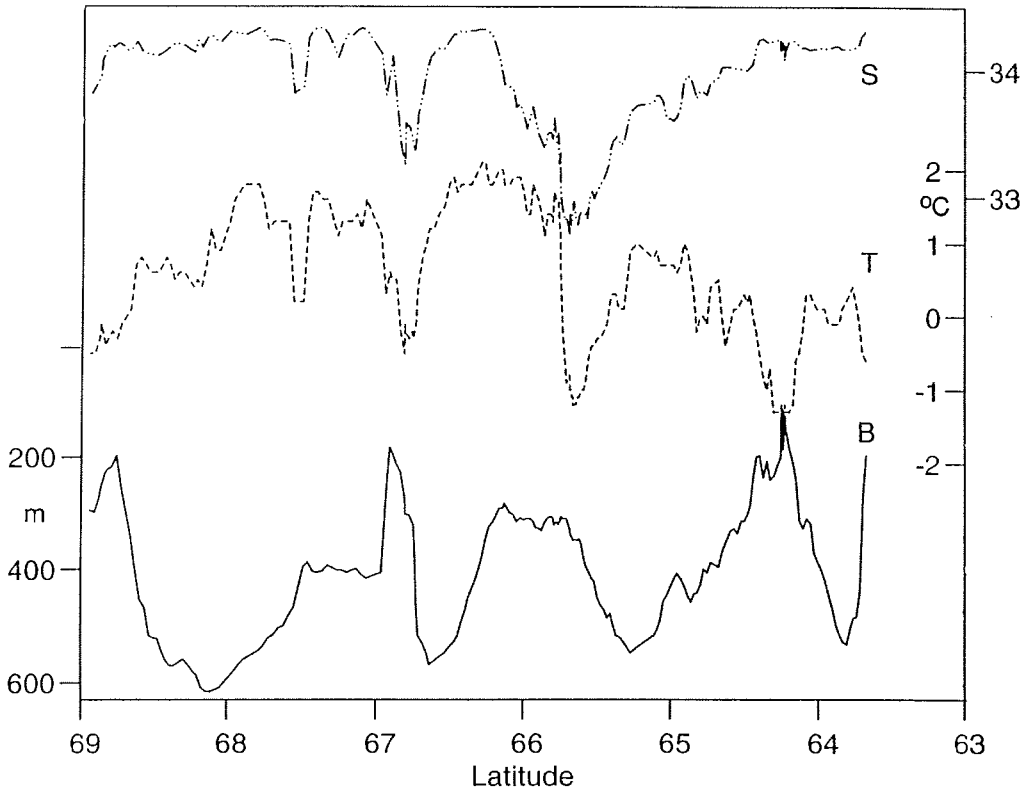

The average current system is subject to intensive fluctuations. Whereas the seasonal cycle dominates the variability of the eastern boundary current, it is barely visible in the west (Fig. 7.2.20). However, the temperature of the outflowing Weddell Sea Bottom water is subject to a clear seasonal cycle. In the interior only higher frequency fluctuations are present. The currents do not show a significant longer term trend, while the records of the thermistor cables (Fig. 7.2.20) indicate an increase of the maximum temperature in the Warm Deep Water layer during the two years of the observation period. This is consistent with the CTD measurents. Simultaneously, the temperatures of the outflowing Weddell Sea Bottom Water decrease (Fig. 7.2.20). The correlation of the observed seasonal and interannual variability of the oceanic circulation and temperatures with the fluctuations of the atmospheric driving forces and ice conditions will be investigated when the complete data sets will be available.

Fig. 7.2.16: XBT-section across the southernmost depression on the Larsen Shelf. For exact location see Table 2.4.

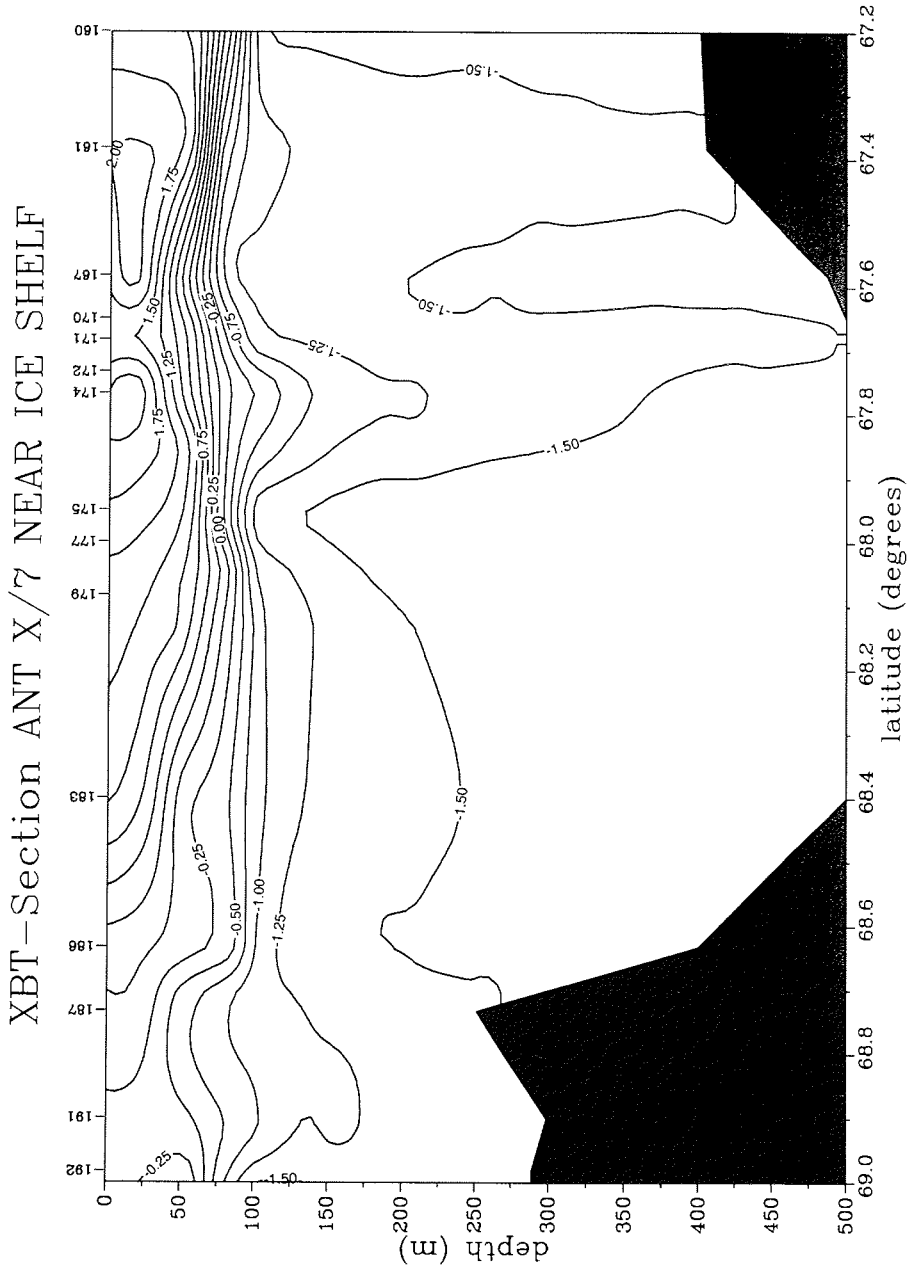

Fig. 7.2.17: Near surface temperature (top) and salinity in PSU (bottom) on the transect between Kapp Norvegia and Joinville Island during summer (ANT X/7,1), early winter (ANT X/4, 2), late winter (ANT VIII/2, 3), and spring (ANT XI/2, 4).

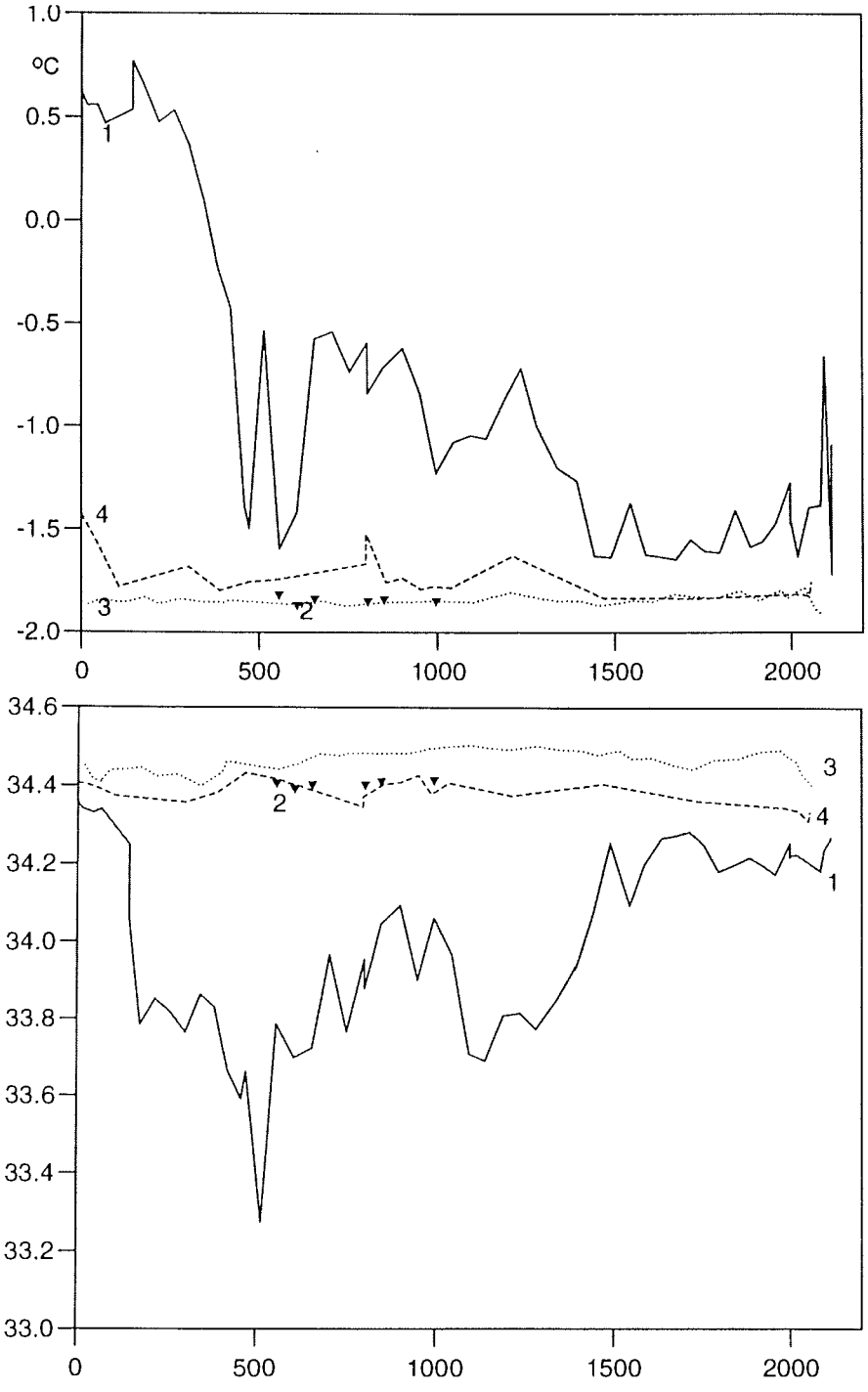

Fig. 7.2.18: Temperature in the minimum of the Winter Water (top) and the maximum of the Warm Deep Water (bottom) on the transect between Kapp Norvegia and Joinville Island during ANT XI/2 and ANT X/7.

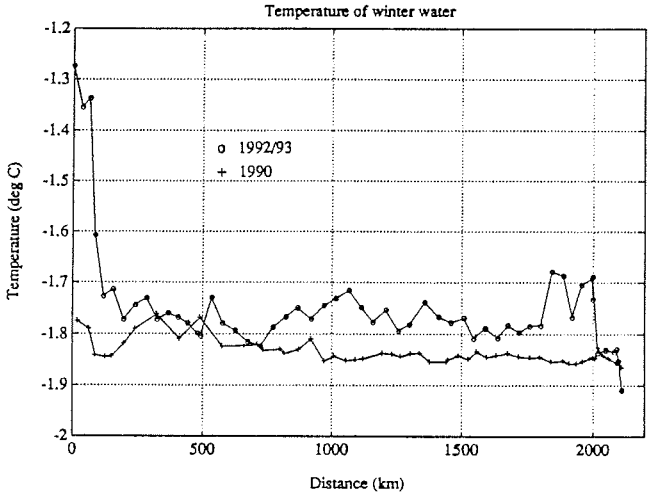

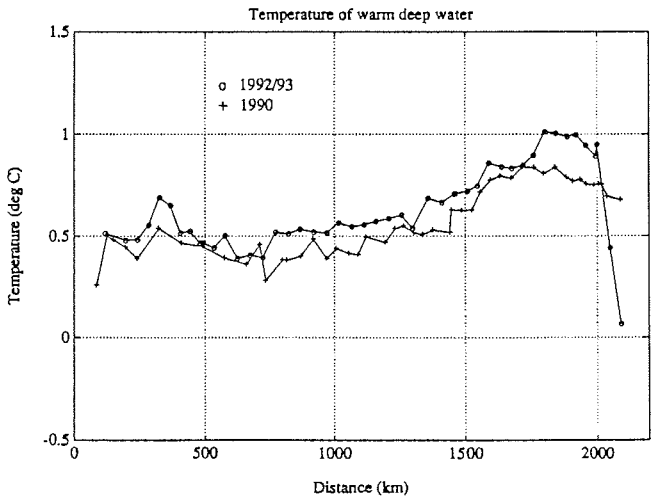

Fig. 7.2.19: Mean flow in cm/s across the transect between Kapp Norvegia and Joinville Island from the measurements with moored current meters averaged approximately over one year.

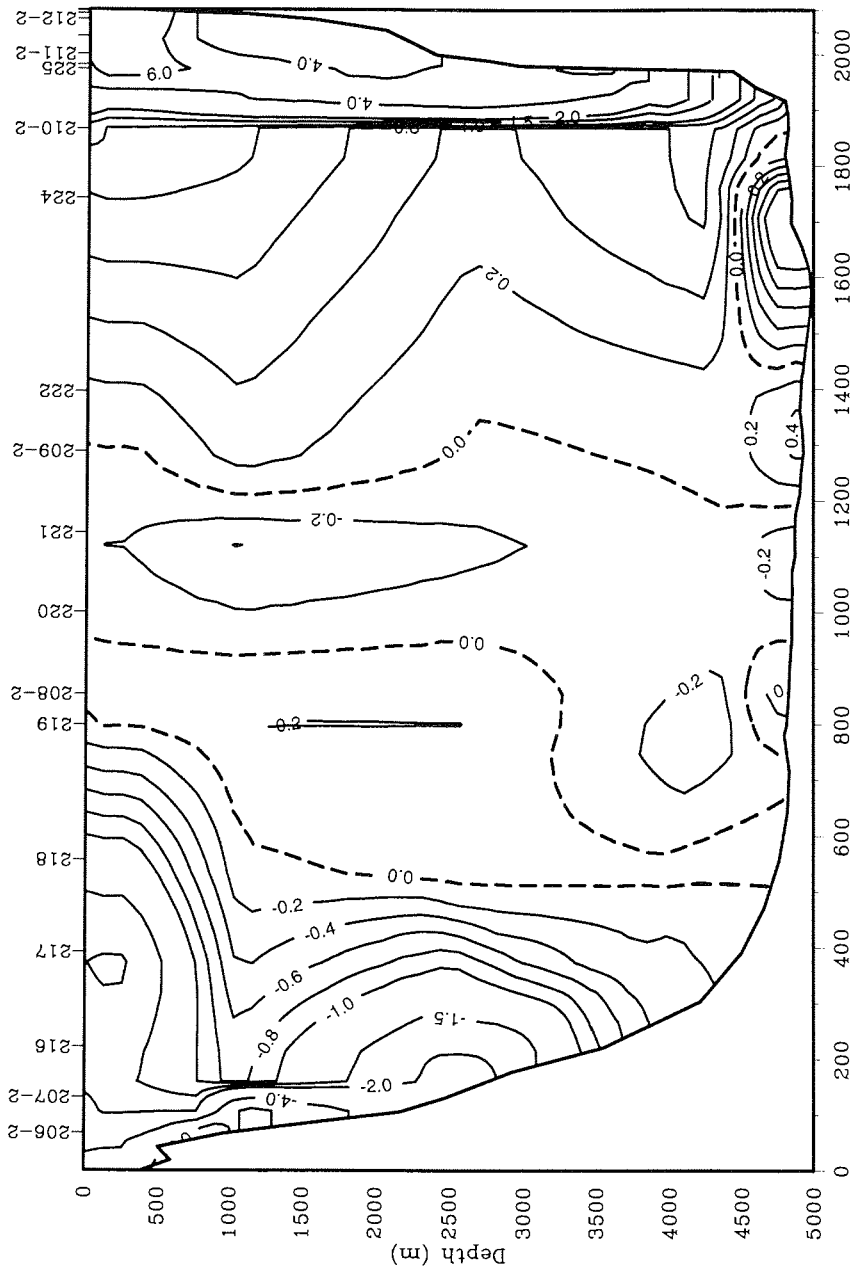

Fig. 7.2.20: Time series of moored current meters in the eastern (top) in 250 and 1090 m and the western boundary currents in 1010 and 2410 m depth (bottom).

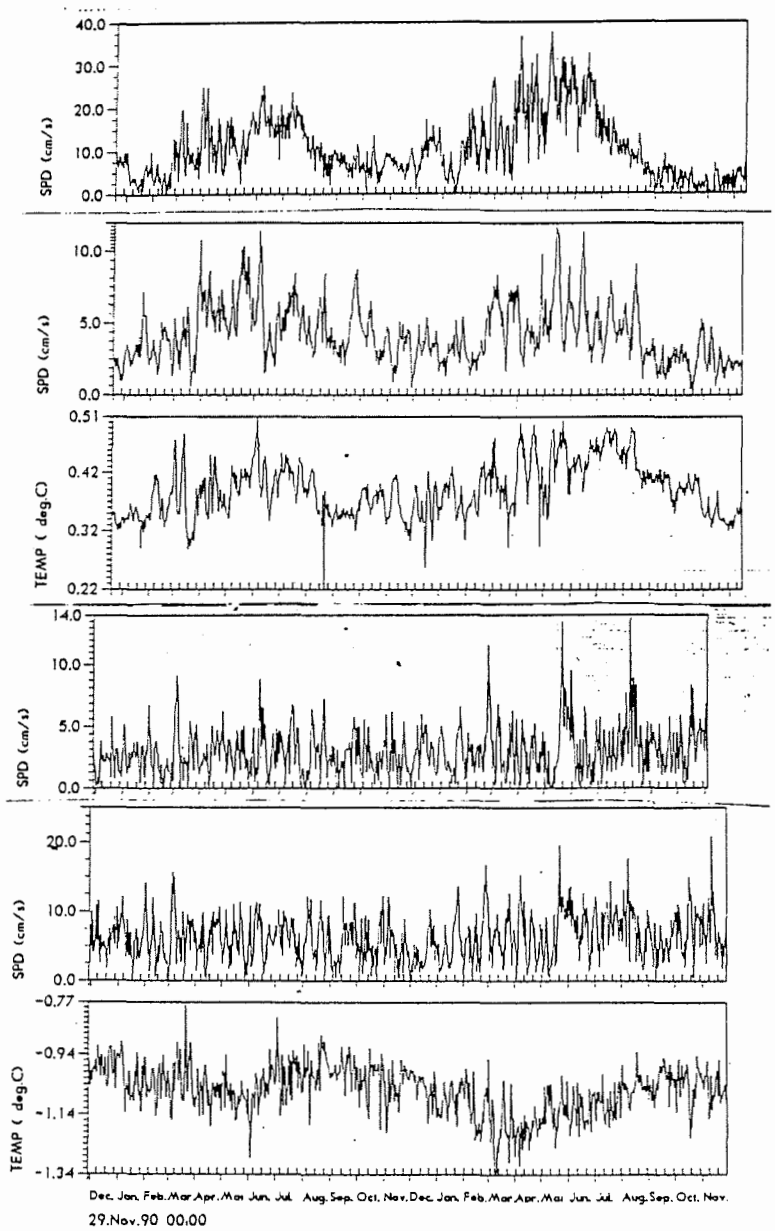

Fig. 7.2.21: XBT section from Cape Town to the Atka Bight carried out during ANT X/7.

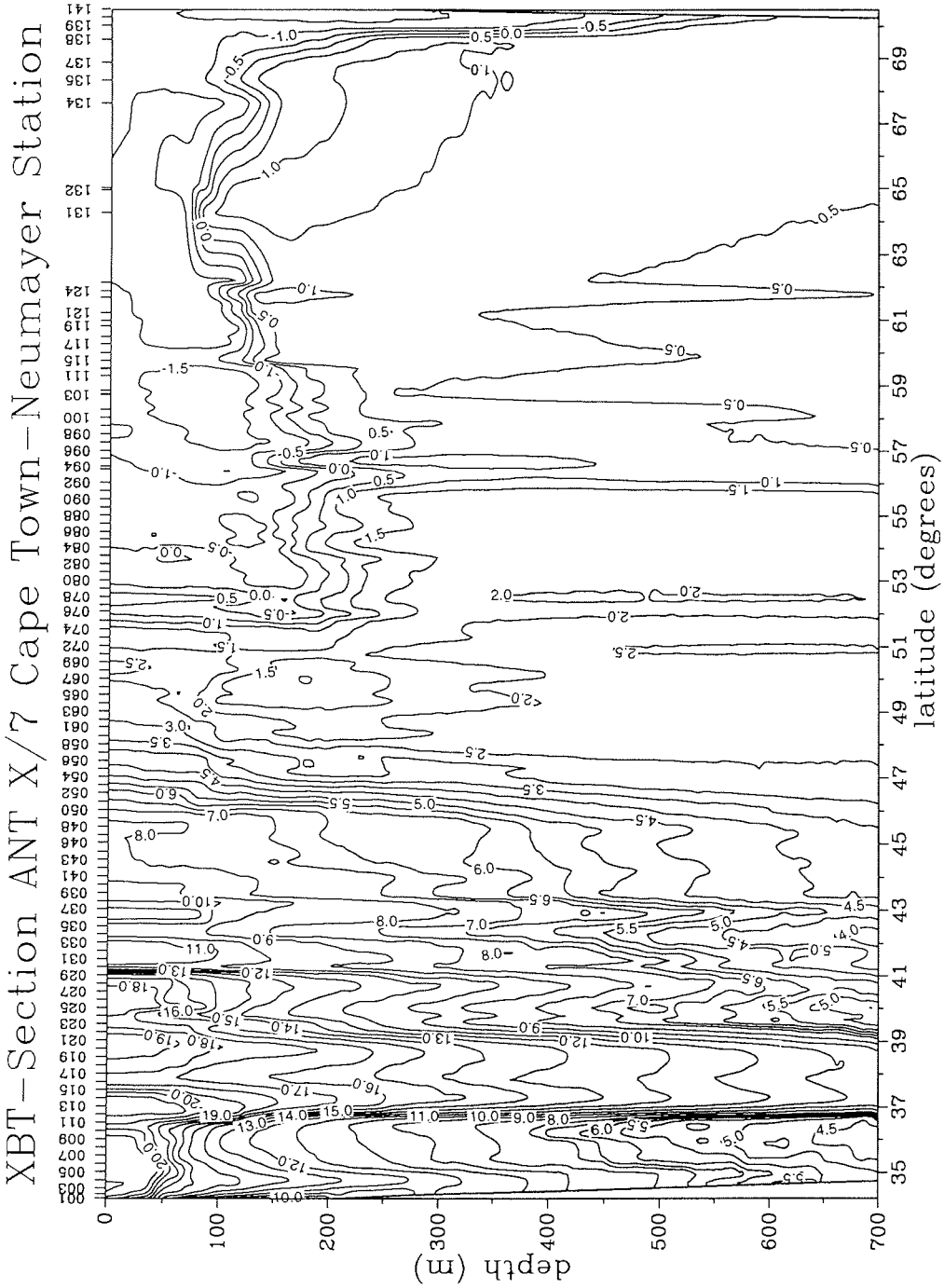

Fig. 7.2.22 XBT section across Drake Passage carried out during ANT X/7

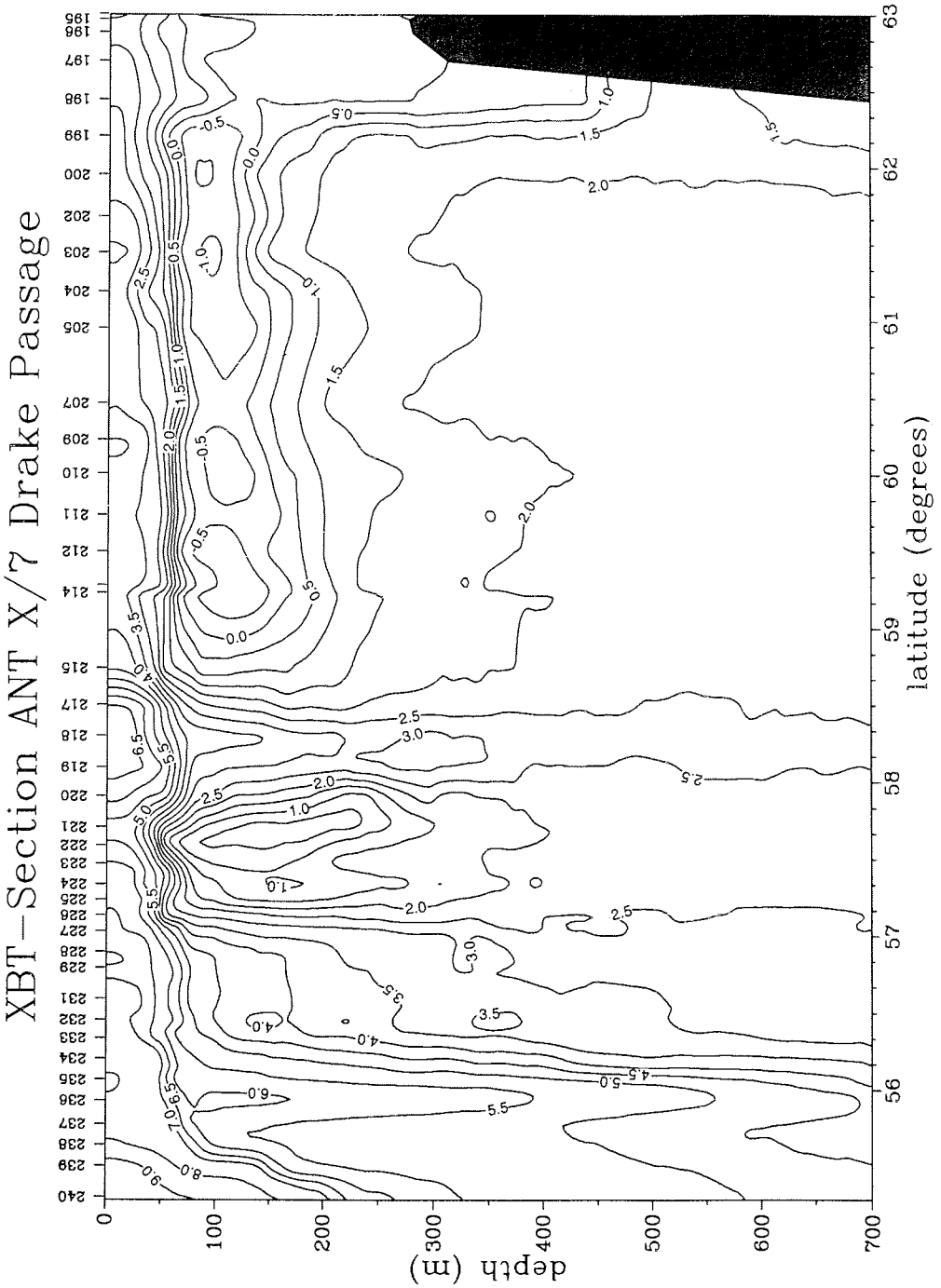

2.2 Structure of the Antarctic Circumpolar Current

T. Boehme, J. Corleis v. d. Voet, M. Damm, E. Fahrbach, H. Fischer, R. Hamann, L. Kolb, A. Latten, G. Seiß, V. Strass, M. Tibcken, H. Witte, F. Zwein (AWI)

Objectives

The Antarctic Circumpolar Current is the connection between three ocean basins. Its major transport occurs in oceanic fronts, the Subtropical, the Subantarctic and the Polar Front. In the area of our observations the boundary between the Antarctic Circumpolar Current and the Weddell Gyre is of special interest. In spite of the dominant zonal component of the mean current, significant meridional transports occur which are to a large extent caused by mesoscale fluctuations. These fluctuations are of interest also to the dynamics of the current, because they are transferring the momentum from the surface to the deep water. Measurements in the Antarctic Circumpolar Current, made repeatedly underway and by moored current meters, aim at obtaining better statistics of the fluctuations and the fronts.

Work at sea

On the way to and from the major working area 166 XBTs (Tab. 7.2.25 and Tab. 7.2.26) were launched and current profiles were measured with a vessel mounted acoustic Doppler sonar current meter (VM-ADCP) to gather information on the variability of the Antarctic Circumpolar Current. In the area of the Antarctic Polar Frontal Zone and the northern boundary of the Weddell Gyre three current meter moorings were recovered and two were deployed (Tab. 7.2.23 and Tab. 7.2.24). The COMED system was recording temperature, salinity, Raman- and Mie-backscattering, fluorescence and chlorophyll in the ice free parts of the transects. On the transect across the Drake Passage, the VM-ADCP measurements are degraded due to the failure of the ship's pitch and roll platforms.

Preliminary results

The data from the XBTs show the typical structure of the Circumpolar Current with the associated fronts on the southbound transect from Cape Town to Antarctica (Fig. 7.2. 21) and in Drake Passage (Fig. 7.2.22). A statistical analysis is only possible in connection with the data from previous and further cruises.

Tab. 7.2.23: Moorings recovered on the way from Cape Town to the Neumayer-Station during "Polarstern"-cruise ANT X/7.

Mooring	Latitude Longitude	Deployment Date, time, (UTC)	depth (m)	Type	Instrument No	Depth	Record lenght (days)
PF5	50°06.0S'	14.05.92	3700	AVTCP	10487	160	206
	05°55.4'E	11.58		S	860009	575	
				AVTCP	10488	650	206
				AVT	10493	1460	206
				AVT	10494	2930	206
				S	860012	3125	
				AVT	10495	3660	91
BO_2	54°20.8'S	12.05.92	2670	AVTCP	10489	190	210
	03°23.6'W	13.12		AVTCP	10490	390	210
				S	860038	430	
				AVT	10496	1480	210
				S	890009	2160	
				AVT	10497	2600	210
400/1	57°37.8'W	10.05.92	4410	AVTCP	10491	180	213
	04°02.3'E	13.03		AVTCP	10492	380	213
				S		425	213
				AVT	10498	1470	
				AVT	10499	2970	213
				S		3015	
				AVT	10503	4360	213

Tab. 7.2.24: Moorings deployed on the way from Cape Town to the Neumayer-Station during "Polarstern"-cruise ANT X/7

Mooring	Latitude Longitude	Date Time (UTC)	Water Depth (m)	Type	Instrument Ser. No.	Depth (m)
PF6	50°05.50'S	07.12.92	3778	AVTP	9765	190
	05°51.20'E	18.05		S		609
				AVTC	9400	687
				AVT	9564	1485
				AVT	9181	2994
				S		3043
				AVT	9784	3733
BO3	54°19.91'S	09.12.92	2734	AVTP	9766	230
	03°20.57'W	11.44		AVTPC	7727	437
				S		490
				AVT	9183	1539
				S		2239
				AVT	8037	2687

Abbreviations

AVTPC	Aanderaa current meter with temperature. pressure and conductivity sensor
S	Sediment trap

Tab. 7.2.25: XBTs launched during the transit of the Antarctic Circumpolar Current from Cape Town to Atka Bight

No.	Date	Time (GMT)	Latitude	Longitude	Depth (m)
1	03.12.92	16:43	34°12'S	18°05'E	218
2		17:20	34°20'S	18°00'E	276
3		18:17	34°30'S	17°53'E	400
4		19:33	34°45'S	17°44'E	1740
5		20:57	35°00'S	17°33'E	2605
6		22:21	35°15'S	17°24'E	2975
7		23:50	35°30'S	17°12'E	3506
8	04.12.92	01:22	35°45'S	17°01'E	4071
9		02:56	36°00'S	16°51'E	4291
10		04:34	36°15'S	16°41'E	4383
11		06:15	36°30'S	16°31'E	4477
12		08:05	36°45'S	16°17'E	4572
13		10:15	37°00'S	16°02'E	4646
14		11:35	37°15'S	15°54'E	4687
15		12:55	37°30'S	15°46'E	4746
16		14:20	37°45'S	15°36'E	4784
17		15:45	38°00'S	15°27'E	4822
18		17:10	38°15'S	15°16'E	4784
19		18:34	38°30'S	15°05'E	4795
20		19:59	38°45'S	14°55'E	4794
21		21:20	39°00'S	14°45'E	4727
22		22:40	39°15'S	14°35'E	4698
23	05.12.92	00:10	39°30'S	14°22'E	4743
24		01:38	39°45'S	14°10'E	4671
25		03:01	40°00S	14°00'E	4174
26		04:34	40°15'S	13°48'E	4764
27		05:59	40°30'S	13°37'E	4865
28		07:22	40°45'S	13°26'E	4864
29		10:18	41°00'S	13°12'E	4538
30		11:38	41°15'S	13°01'E	4877
31		13:05	41°30'S	12°51'E	6308
32		14:28	41°45'S	12°40'E	3398
33		15:49	42°00'S	12°31'E	5113
34		17:17	42°15'S	12°18'E	3582
35		18:40	42°30'S	12°08'E	4390
36		19:15	42°34'S	12°04'E	4689
37		21:45	43°01'S	11°43'E	4718
38		23:05	43°13'S	11°34'E	4666
39	06.12.92	00:35	43°28'S	11°22'E	4981
40		02:05	43°45'S	11°10'E	4440
41		03:20	43°58'S	10°58'E	4363
42		04:50	44°15'S	10°47'E	4669
43		06:16	44°28'S	10°35'E	4852
44		07:38	44°45'S	10°21'E	4660
46		09:01	45°01'S	10°10'E	4711
47		10:12	45°15'S	9°59'E	4769
48		11:38	45°30'S	9°45'E	4495
49		12:46	45°43'S	9°35'E	4545
50		14:07	46°00'S	9°23'E	4645
51		15:21	46°15'S	9°11'E	4684
52		16:50	46°33'S	8°55'E	4353
53		17:44	46°43'S	8°47'E	3704
54		18:59	47°00'S	8°33'E	3506
55		20:13	47°15'S	8°21'E	1714

Tab. 7.2.25 (cont'd): XBTs launched during the transit of the Antarctic Circumpolar Current from Cape Town to Atka Bight

No.	Date	Time (GMT)	Latitude	Longitude	Depth (m)
56		21:26	47°30'S	8°07'E	2622
57		22:40	47°45'S	7°56'E	3083
58		23:54	48°00'S	7°44'E	4170
59	07.12.92	01:06	48°15'S	7°30'E	2224
61		02:26	48°32'S	7°16'E	3527
62		03:34	48°45'S	7°04'E	3907
63		04:46	49°00'S	6°52'E	3629
64		06:00	49°15'S	6°39'E	3442
65		07:10	49°30'S	6°27'E	2953
66		08:20	49°44'S	6°14'E	3630
67		09:35	50°00'S	5°58'E	3708
68		22:28	50°15'S	5°31'E	3610
69	08.12.92	00:43	50°30'S	5°00'E	3397
71		03:01	50°45'S	4°28'E	3312
72		05:15	51°00'S	3°54'E	3454
73		07:15	51°15'S	3°25'E	3404
74		09:01	51°30'S	2°54'E	3423
75		11:00	51°45'S	2°19'E	3001
76		13:10	52°02'S	1°41'E	2778
77		14:43	52°15'S	1°15'E	2510
78		16:28	52°30'S	0°43'E	2834
79		18:26	52°45'S	0°09'E	2785
80		20:19	53°00'S	0°22'W	2461
81		22:14	53°15'S	0°54'W	2403
82	09.12.92	00:01	53°30'S	1°26'W	2836
83		01:48	53°45'S	2°00'W	2124
84		03:45	53°59'S	2°35'W	2723
85		05:30	54°15'S	3°12'W	2461
86		15:42	54°30'S	2°59'W	2758
87		17:36	54°45'S	2°30'W	2587
88		19:30	54°59'S	1°56'W	1948
89		21:20	55°15'S	1°25'W	3979
90	10.12.92	23:35	55°30'S	0°51'W	3351
91		01:10	55°45'S	0°11'W	3881
92		03:25	56°00'S	0°17'E	3481
93		04:58	56°13'S	0°47'E	3770
94		07:07	56°30'S	1°26'E	4140
95		09:02	56°44'S	1°59'E	4317
96		10:28	56°55'S	2°24'E	4324
97		12:44	57°15'S	3°07'E	4429
98		14:43	57°30'S	3°45'E	4410
99	11.12.92	22:53	57°45'S	3°44'E	4828
100		01:31	58°00'S	3°10'E	3386
101		04:10	58°15'S	2°36'E	4896
102		05:43	58°23'S	2°18'E	4771
108		10:48	58°50'S	1°17'E	4939
109		13:36	59°00'S	0°53'E	5212
111		16:30	59°17'S	0°12'E	5202
112		19:34	59°30'S	0°16'W	5240
113		19:40	59°30'S	0°18'W	5345
115		23:02	53°45'S	0°59'W	5010
116	12.12.92	01:46	60°00'S	1°31'W	5360
117		04:16	60°15'S	2°03'W	5260
118		07:20	60°28'S	2°38'W	5376
119		11:47	60°48'S	2°58'W	5145
120		14:06	60°58'S	3°51'W	5312

Tab. 7.2.25 (cont'd): XBTs launched during the transit of the Antarctic Circumpolar Current from Cape Town to Atka Bight

No.	Date	Time (GMT)	Latitude	Longitude	Depth (m)
121		16:36	61°12'S	4°10'W	4782
123		23:42	61°40'S	5°26'W	5277
124	13.12.92	02:24	61°51'S	6°01'W	5290
125		04:41	62°07'S	6°21'W	5275
126		06:50	62°19'S	6°36'W	5250
128		09:07	62°26'S	7°04'W	4875
131	14.12.92	05:57	64°15'S	8°55'W	5161
132		09:57	64°56'S	8°50'W	5100
133		14:00	65°00'S	8°41'W	5087
134	15.12.92	08:11	67°37'S	8°28'W	4889
135		12:08	68°19'S	8°10'W	4334
137		14:46	68°51'S	7°52'W	3630
138		18:36	69°34'S	8°07'W	3015
139		20:39	70°00'S	7°58'W	1546
140		21:47	70°15'S	7°59'W	1675
141		22:51	70°30'S	8°07'W	269
142	18.12.92	03:49	70°30'S	8°59'W	435
143		05:28	70°38'S	9°38'W	455
144		05:38	70°39'S	9°42'W	457
145		06:49	70°44'S	10°09'W	360
146		08:55	70°53'S	10°57'W	290

Tab. 7.2.26: XBTs launched during the transit of the Antarctic Circumpolar Current in the Drake Passage

No.	Date	Time (GMT)	Latitude	Longitude	Depth (m)
194	20.01.93	10:09	63°02´S	60°43´W	286
195		10:59	62°58´S	61°13´W	277
196		12:02	62°53´S	61°45´W	280
197		12:57	62°42´S	61°56´W	313
198		13:58	62°27´S	61°59´W	790
199		14:56	62°13´S	61°59´W	1884
200		15:59	61°58´S	62°00´W	3530
201		16:57	61°43´S	62°01´W	4316
202		17:06	61°42´S	62°02´W	4244
203		18:02	61°28´S	62°02´W	3734
204		19:00	61°13´S	62°04´W	3561
205		20:00	60°59´S	62°05´W	3845
207		22:06	60°30´S	62°08´W	3814
209		23:08	60°16´S	62°10´W	3800
210	21.01.93	00:06	60°03´S	62°11´W	3755
211		01:01	59°47´S	62°13´W	4144
212		02:00	59°33´S	62°14´W	4032
213		02:59	59°20´S	62°14´W	3936
214		04:02	59°17´S	62°15´W	3846
215		05:08	58°48´S	62°17´W	3253
217		06:06	58°34´S	62°18´W	3016
218		06:57	58°22´S	62°20´W	3476
219		07:56	58°10´S	62°32´W	3056
220		08:59	57°59´S	62°47´W	3651
221		10:01	57°47´S	62°59´W	3823
222		11:00	57°40´S	63°07´W	3623
223		12:00	57°33´S	63°16´W	3622
224		13:01	57°25´S	63°24´W	3747
225		13:59	57°19´S	63°33´W	3910
226		14:56	57°13´S	63°41´W	4186
227		15:49	57°07´S	63°47´W	4032
228		16:52	56°59´S	63°46´W	3973
229		18:01	56°53´S	64°06´W	3946
231		19:05	56°41´S	64°15´W	4146
232		20:03	56°33´S	64°25´W	1890
233		21:03	56°26´S	64°34´W	3112
234		21:59	56°18´S	64°43´W	2643
235		22:59	56°10´S	64°53´W	3283
236		23:59	56°02´S	65°03´W	3910
237	22.01.93	01:00	55°53´S	65°12´W	3651
238		01:58	55°45´S	65°19´W	2768
239		02:59	55°37´S	65°27´W	3230
240		04:02	55°25´S	65°41´W	1819

3. Marine chemistry

3.1 Distribution of nutrients in the Weddell Sea

P. Ahlers, K.-U. Richter, S. Schröder (AWI)

Objectives

The near surface layers, in particular the Winter Water, of the Weddell Gyre are supplied with nutrients by entrainment and upwelling of Warm Deep Water. Therefore, macronutrients are generally not considered as limiting factors for phytoplankton production in the Weddell Sea. Our objective was to measure the distribution of the nutrients on a transect through the Weddell Gyre from Kapp Norvegia to the Antarctic Peninsula and on a second transect from the Larsen Ice Shelf to the northeast.

Work at sea

Water samples were collected with the oceanographic rosette sampler and analyzed on a Technicon Autoanalyzer-II-System. Nitrate was determined as nitrite after reduction with cadmium and reaction with sulphanilamide and N-(1naphtyl)-ethylendiamin dihydrochloid as red coloured azodye at 520 nm. Ammonium was measured as blue coloured indophenole at 630 nm after the reaction with phenolate and hypochlorite under alcaline conditions (Berthelot reaction). For the determination of silicate and phosphate the compounds react with ammonium molybdate by forming a blue molybdate-complex that was measured at 660 nm respectively at 880 nm.

Preliminary results

As an example for the distribution of nutrients in the different water masses of the Weddell Sea the concentration of silicate is shown on the transect from Kapp Norvegia to Joinville Island (Fig. 7.3.1). The near surface layers are characterised by a strong vertical gradient due to nutrient consumption by phytoplankton in the euphotic zone. In the deeper layers of the Warm Deep Water and the Antarctic Bottom Water the concentration values between 120 and 130 µM vary only slightly with two exceptions. Silicate values higher then 130 µM indicate the inflow of silicate enriched Antarctic Bottom Water from the Enderby Basin near the eastern continental slope below 4000 m depth. At the western continental slope a distinct silicate minimum below 1500 m depth is related to the Weddell Sea Bottom Water. It is most pronounced with values of less than 95 µM between 2000 and 3000 meters depth. The low silicate concentrations near the bottom extent almost over the total Weddell Basin and indicate the spreading of the Weddell Sea Bottom Water. The nitrate values show comparable structures with a strong gradient in the near surface layers and the influence of the Weddell Sea Bottom Water (Fig. 7.3.2). A nutrient maximum is related to the Warm Deep Water which is more pronounced in the western part of the gyre (Sta. 44 - 61) with maximum nitrate concentrations higher then 35 µM between 300 and 1000 m. In the Weddell Sea Bottom Water the concentration decrease to values below 33 µM.

Fig. 7.3.1 : Silicate distribution on the transect from Kapp Norvegia to the Joinville Island (in µM Si).

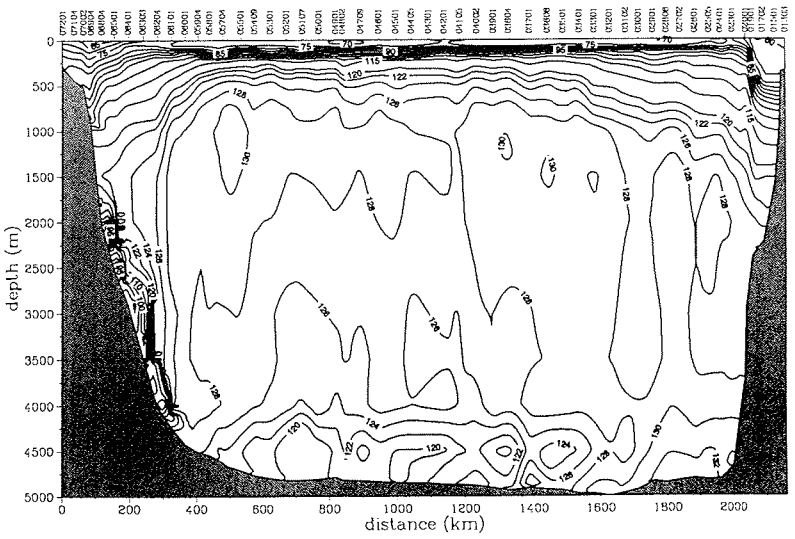

Fig. 7.3.2 : Nitrate distribution on the transect from Kapp Norvegia to Joinville Island (in µM NO_3-N).

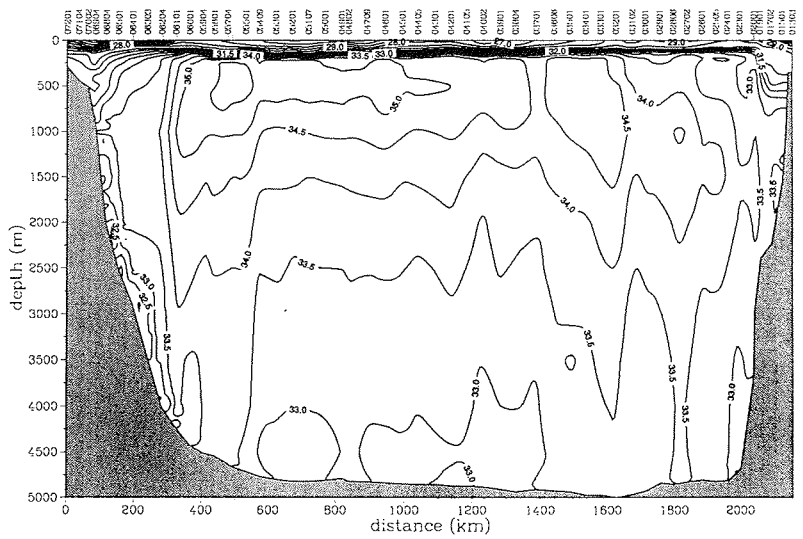

The surface values of nitrate, silicate and phosphate reflect the biological conditions (Fig. 7.3.3). Due to the extensive bloom of large phytoplankton stocks in the coastal polynya off Kapp Norvegia (Sta. 13 to 23) and off the Antarctic Peninsula (Sta. 61 to 64), nutrients were remarkably depleted. The silicate concentration reached values of less than 58 µM in the eastern bloom and 62 µM in the western one. Similar minima are found in the nitrate and phosphate concentrations for both bloom areas with nitrate values of 19.8 µM in the east and 16.7 µM in the west and with phosphate values of 1.43 µM and 1.12 µM respectively. A slight depletion at approximately 700 km from the western boundary, at the Sta. 47 to 49, can be related to a third bloom area. In contrast to the bloom areas, the nutrient concentrations are high elsewhere (Sta. 24 to 44). The concentrations range from 70 µM to 77 µM for silicate, from 26.2 µM to 30.0 µM for nitrate and from 1.77 µM to 1.99 µM for phosphate.

3.2 Carbon dioxide chemistry in the Weddell Sea

J.M.J. Hoppema, I. Schweimler (AWI)

Objectives

Carbon dioxide is a widely known greenhouse gas, whose concentration in the atmosphere has increased because of anthropogenic causes. The oceans are the most important sink of anthropogenic CO_2 and among those the polar oceans are thought to be pivotal. For the Southern Ocean the details of the possible uptake of CO_2 are still unclear. Particular attention will be given to the following points:

1. Partial pressures of CO_2 in sea water and atmosphere. The difference between those two is the driving force for the exchange of CO_2 between both reservoirs, which will be used to estimate the sink (or source) function of the Weddell Sea.
2. Factors governing the CO_2-system. For this purpose the total-CO_2 and alkalinity will be correlated with other properties such as salinity, oxygen, nutrients etc.
3. Total-CO_2 and alkalinity are unique properties of water masses. Their potential as a tracer will be investigated.
4. Differences between the present measurements and those in winter, which were performed during June and July 1992 in the Weddell Sea, will be analyzed.

Work at sea

CO_2 dissolved in sea water is actually part of a system of chemical equilibria, where the main component is the bicarbonate ion. Because of this it is not trivial to measure CO_2, but rather one has to determine the CO_2-system. Knowing two measurable quantities of the system enables to calculate all other system parameters. During this cruise, measurements were done of three parameters, notably, total-CO_2 (TCO_2), which is all inorganic carbon, total alkalinity and the partial pressure of CO_2 (pCO_2). In addition, the pCO_2 of air was measured.

Fig. 7.3.3 : Concentrations of silicate (a), nitrate (b) and phosphate (c) in the near surface layers of the transect from Kapp Norvegia to Joinville Island.

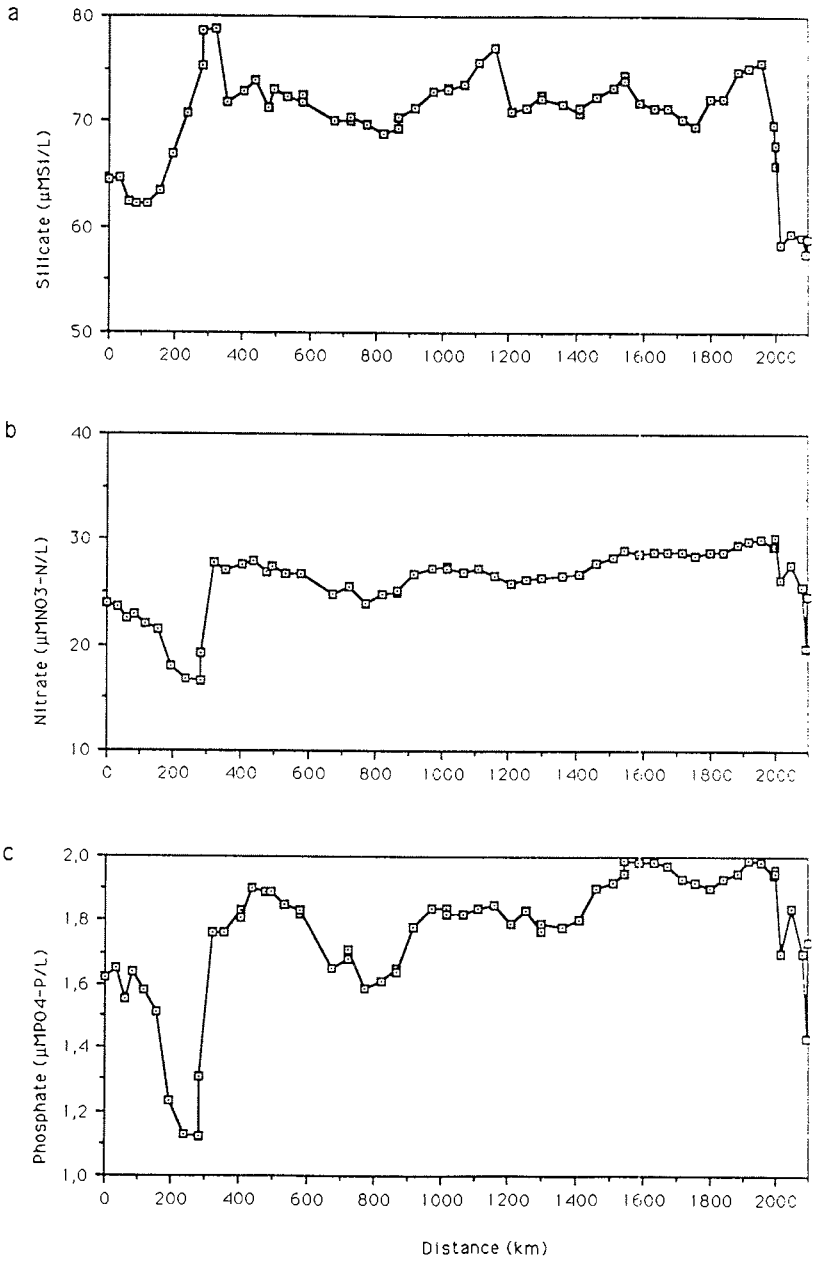

On almost all stations, where water was collected with the CTD-Rosette sampler TCO_2 was determined with a standard coulometric method. Thus complete depth profiles were obtained for TCO_2. Alkalinity was measured by means of a rapid potentiometric titration with open vessel. The alkalinity will be calculated from the titration data using the Gran method. As for TCO_2, samples were analyzed for alkalinity at almost all CTD-stations, but at about half of the stations only the surface layer until 200 m was sampled. In between stations semi-continuous measurements for pCO_2 were done. The water was taken in from about 9 m below the surface and continuously sprayed into an equilibrator where it was brought to equilibrium with air. Via a chemical dryer this air was pumped through a non-dispersive InfraRed Analyzer (Li-cor) where the absortion caused by CO_2 was recorded. In the same way the CO_2 concentration of marine air from approxmately 20 m above sea level was obtained.

Fig. 7.3.4: TCO_2-depth profile in the central Weddell Sea

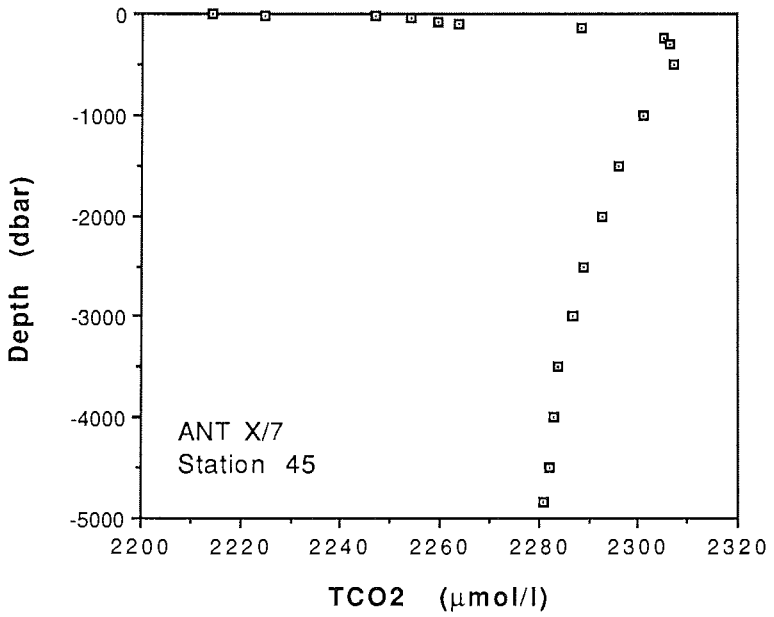

Preliminary results

Fig. 7.3.4 shows a depth profile of TCO_2 of a station in the centre of the Weddell Gyre. It has to be kept in mind that data are indeed preliminary and further processing has to be done. This can change the figure slightly, but will not significantly affect the shape of the profile. The profile shows a CO_2 depletion in the surface layer compared

to the deep and bottom waters, which is mainly biologically mediated. At about 500 m there is a TCO_2 maximum, indicating the depth where the Warm Deep Water exerts its largest influence. The depth of the TCO_2 maximum in the Weddell Sea is not constant. In the surface layers a large variation of the TCO_2 content was observed, with generally high values in the centre of the Weddell Gyre and values up to 100 µmol/l lower in the western Weddel Sea. The TCO_2 values in the central Weddell Sea were comparable to values measured in the winter. The continuous pCO_2 measurements confirmed this trend in the TCO_2 data. In the central Weddell Sea the pCO_2 of the sea water was always close to atmospheric values, whereas in the western Weddell Sea there was always undersaturation of CO_2 with respect to the atmosphere, with values decreasing to approximately 150 ppm.

3.3 Organic carbon and humic substances in the Weddell Sea

A. Skoog, M. Wedborg (AMK)

Objectives

Dissolved organic matter (DOM) in the ocean is the largest organic carbon reservoir in the global carbon cycle. It may be of importance as a sink of atmospheric carbon dioxide. Substantial quantities of DOM, mainly in the form of humic substances (HS), are added to the ocean by the rivers. The fate of this DOM, which is often referred to as biologically refractory, is uncertain. In the literature it has been reported that structural units, typical of terrestrial vascular plants are present in HS from the deep ocean, and that the marine HS can be quite old, between 5,000 and 10,000 years. This suggests that terrestrial DOM may be of significance as a part of the marine HS. The objective of this project was to increase the scarce information on total/dissolved organic carbon (TOC/DOC) and HS in the open ocean. The Weddell Sea is of special interest because the direct influence from the Antarctic continent is assumed to be negligible, while the biological productivity in the water column can be high.

Work at sea

Water samples for determination of TOC/DOC and HS were taken at all but ten CTD stations. TOC/DOC was determined by the high temperature catalytic oxidation method, and HS by fluorescence spectrophotometry, excitation 350 nm, emission 450 nm. The samples were normally processed within a few hours after sampling. HS were isolated on Amberlite XAD-2 columns, mainly for the purpose of estimating the fraction of TOC/DOC that is present as HS.

Preliminary results

The concentrations of TOC/DOC and HS found in the Weddell Sea were slightly lower than those from the Atlantic water in the deep Skagerrak, approximately 40 to 50 mM of TOC/DOC and 0.2 to 0.7 mg/l (as quinine sulphate equivalents, QS) of HS. For TOC/DOC, the concentration normally increased towards the surface, whereas for HS the lowest concentrations were in most cases found at the surface, and a maximum at approx 500 to 1000 m. At a few stations, some of which had a high biological productivity (e.g. Sta. 14 and 62, 72 to 76), the HS profile showed an increase at the surface but the TOC profiles for the stations with a high biological productivity were not notably different from those of the other stations (Fig. 7.3.5).

Fig. 7.3.5 TOC and fluorescence at stations 14, 62 and 84

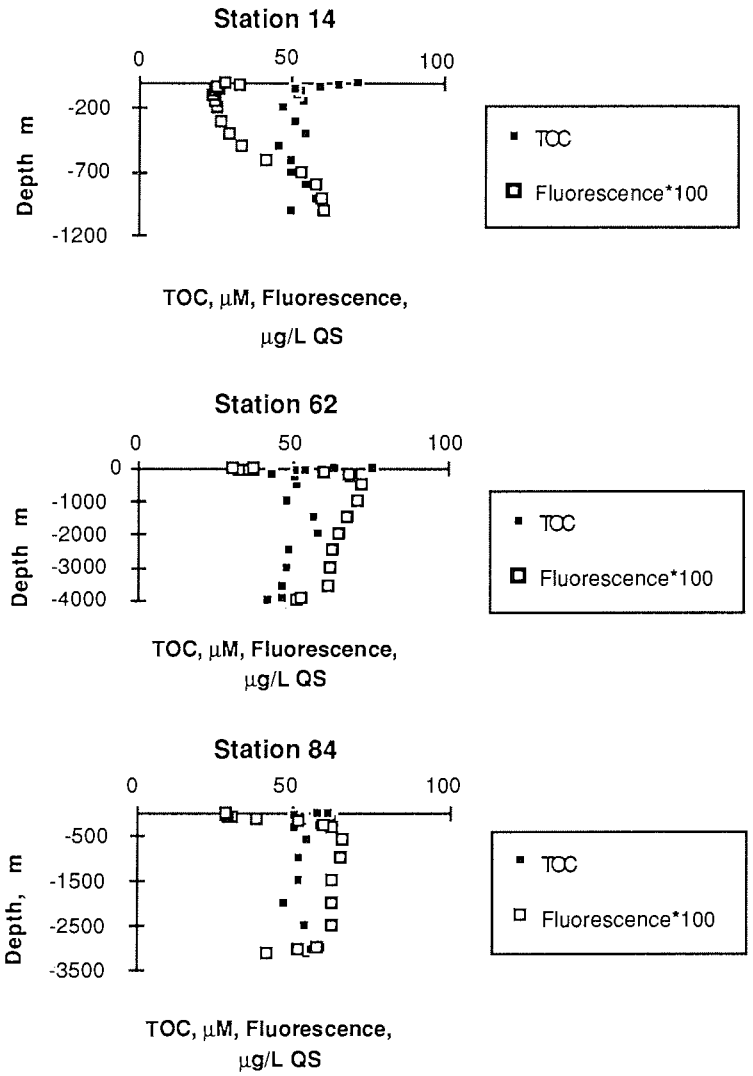

stations (Fig. 7.3.5). For stations 79 to 85 the HS profiles resembled that of Sta. 62, with a marked decrease near the bottom, but without the increase at the surface (Fig. 7.3.5). The concentrations of TOC and HS in brown ice were found to be two to ten times as high as in the water column.

3.4 Dissolved and particulate sterols in the Weddell Sea

G. Hanke (AWI)

Objectives

Investigations of sterols in the Weddell Sea aim to understand transport and turnover of dissolved organic compounds in the oceans and contribute to the understanding of the global carbon cycle. The correlation of the distributions of oceanographic data with the ones of dissolved and particulate phytosterols will be used to follow their fate in the water column. Deep and bottom water formation in the Weddell Sea is of special interest, because it could provide a transport mechanism of organic compounds into the deep sea, by-passing the usual particle-bound path.

Sterols were selected for this study due to their high structural diversity and widespread occurence allowing the comparison of sterol patterns in different samples. In addition some of the sterols are produced only by certain groups of organisms, which makes them useful as biomarkers.

For the Antarctic environment the input of ice algae in the sea during the seasonal sea ice melting is important to initiate algal blooms, but could be as well a direct source of dissolved organic compounds to the sea.

Work at sea

During ANT X/7 20 liter water samples were filtered through glasfiber filters and extracted with n-Hexane in glas bottles. The filters and extracts are returned to Bremerhaven for the later evaporation, derivatization and Gas Chromatographic/ Mass Spectrometric analysis. Five surface water samples were collected on the way from Cape Town to the ice edge in the Polar Frontal Zone to complement data from a previous cruise (ANT X/1b), and to correlate the gradients of dissolved organic compounds to oceanographic frontal zones. Two stations, with six depth levels each, were sampled as test stations and to compare the conditions found in the Weddell Sea with the ones of the circumpolar water belt. On the main transect through the Weddell Sea 63 water samples with 20 l were taken at 11 biological stations at 6 depth levels. On three stations of the Larsen Ice Shelf section 15 samples were collected. For the further evaluation of the sampling method 12 surface samples were taken. To investigate the role of the melting sea ice as a source of dissolved and particulate organic matter for the water column eight samples of brown ice were obtained with a steel basket. The ice was molten in a steel drum, the melt water filtrated and the organic compounds extracted.

During the stay at the Neumayer-Station six snow samples were collected on the ice shelf at about 25 km southeast of the Station for the analysis of organic trace compounds. Special care was given to the sampling procedure to avoid contamination. Thus only specially cleaned tools and steel containers were used. Oversuits were used during sample collection to prevent input of particles from the clothes. The snow was transported to Bremerhaven at -30°C for extraction and further analysis by Gas-Chromatography/Mass Spectrometry.

3.5 Lipid investigations

K. Fahl (AWI)

Objectives

The main goals were the investigations on the lipid metabolism of endemic Antarctic copepods, mainly the three species *Calanoides acutus*, *Calanus propinquus* and *Metridia gerlachei*. The herbivorous or omnivorous copepods incorporate the polyunsaturated fatty acids of the phytoplankton into the storage and the membrane lipids. With the aid of these highly unsaturated fatty acids as markers, it is possible to obtain more informations on physiological adaptations to the environment and the food supply. Additional investigations on the lipid metabolism on Antarctic shrimps (*Notocrangon antarcticus* and *Chorismus antarcticus*) and three specimens of Mysidaceans, a closely related crustacean group, were made. The results of this cruise will be compared with the data gathered during the winter cruise in June and July 1992 in order to detect seasonal and geographical variations.

Work at sea

All animals were caught with a bongo- or multinet on different stations. The investigations made during the cruise consist of four parts:

- Feeding of the different copepods species and developmental stages with radioactively-labeled phytoplankton material (use of $NaH^{14}CO_3$) to investigate the lipid's turnover.

- The same experiment was carried out with four specimens of benthic shrimp larvae, three *Notocrangon antarcticus* and one *Chorismus antarcticus* captured on the continetal shelf and kept in tanks. Before the feeding experiments, the stage of larval development was analysed by morphological structures of the telson by Dr. Matthias Gorny.

Except for one Zoea II of *Notocrangon antarcticus* all larvae caught were newly hatched. Additionally, the three specimens of Mysidaceans were fed under the same conditions.

- Feeding experiments with non-labeled algae with a food supply differing from the natural conditions to obtain information about the flexibility of the feeding behaviour of the copepods.

- Additionally, from nearly every station zooplankton samples were caught to investigate the fatty acid and fatty alcohol composition by gas chromatography directly on board the ship.

Preliminary results

The validation of the experiments will be carried out in Bremerhaven, because the analysis of the radioactive material can not be conducted on board.

4. Marine biology

4.1 Phytoplankton blooms and species composition in the Weddell Gyre

M. Baumann, L. Goeyens, S. Jesse, L. Riegger, R. Röttgers, M. Tibcken (AWI), F. Brandini (CBM),

Objectives

The Weddell Gyre Study provide the opportunity to investigate the spatial variation of the seasonal phytoplankton development along a transect of from Kapp Norvegia to the tip of the Antarctic Peninsula. It is observed in the Indian and parts of the Pacific sector of the southern Ocean, but not in the Weddell Sea, that the phytoplankton blooms propagate meridionally when the growth season progresses zonally. It is the aim of our study to investigate, if the large scale cyclonic circulation inhibits the development of phytoplankton blooms in the Weddell Sea by hampering light penetration in the pelagic environment by its effect on the extend of the pack-ice cover. Because poor light conditions associated with low near surface temperatures cause low phytoplankton production, phytoplankton blooms (i.e. more than 1 µg Chl.*a*/l) were only observed when solar irradiance (due to relatively little ice coverage), water temperature and stability of the water column were higher than normal. The development of a bloom is not only related to the physical parameters, but as well to the size distribution of the biomass. While in the low productive areas most of the autotrophic biomass is concentrated in the less than 10 µm size-fraction, the blooms are mostly dominated by macrosize cells, usually diatoms and *Phaeocystis* colonies. The development of these blooms and the consequences for the higher trophic levels are still not understood. Additionally the effect of UV-radiation on the phytoplankton growth is investigated.

Work at sea

At 32 stations along the transect the light penetration was measured with the secchi disc. At those stations phytoplankton samples were taken from the rosette water sampler and the net. The water samples were obtained from the surface to a maximum depth of 300 m. The water was filtered through GF/F filters for fluorometric determinations of Chl.*a* (Turner design fluorometer) which were carried out on board immediately after sampling. Samples for particulate organic carbon and nitrogen were also collected. The measurements will be done in Bremerhaven, using a Carlo Erba 1500 CHN Analyzer. Additional water samples were fixed with formaline for the later determination of cell counts using Utermöhl sedimentation techniques and the use of an inverted microscope. The vertical net hauls were performed from 50 m (or 25 m) to surface according to the abundance of phytoplankton using a 20 µm mesh Apstein conical net. Samples were immediately examined in vivo under a Zeiss inverted microscope equipped with video system for a general characterization of the microplankton composition at each station. Detailed taxonomic studies will have to be performed later with the preserved material. At all stations experiments for comparing the carbon uptake rate with and without exposure to natural UV-light were performed in a deck incubator, cooled with running sea water, using quarz and glass bottles. Additionally, photosynthesis light curves were measured in the surface samples using a laboratory incubator at standard light conditions between 4 and 400 µmol m^{-2} s^{-1}.

Fig. 7.4.1: Secchi depths, given in meter during ANT X/7.

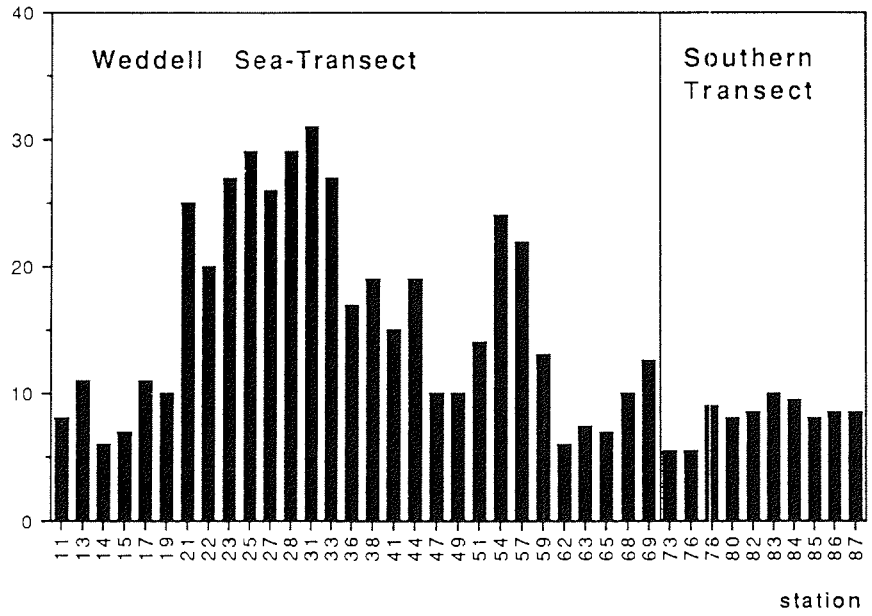

Fig. 7.4.2: The distribution of Chl.*a* along the vertical transect from Kapp Norvegia to Joinville Island.

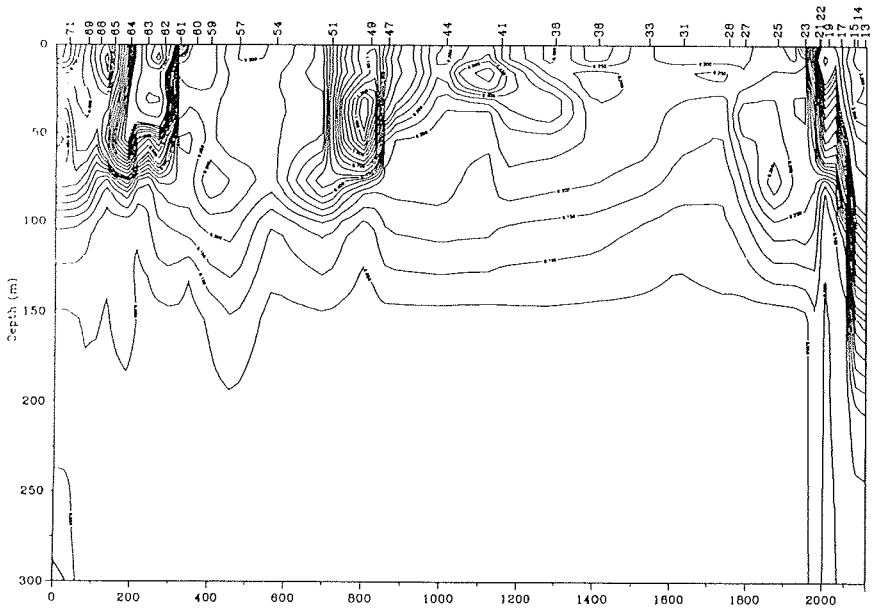

Preliminary results

Water transparency (Secchi depth) and integrated chlorophyll at each station show a clear inverse correlation (Fig. 7.4.1). The distribution of chlorophyll along the transect shows that the bulk of chlorophyll biomass was concentrated in the upper 50 m of the water column, except at the eastern shelf of Kapp Norvegia, where significant chlorophyll concentrations were detected to a depth of 100 m (Fig. 7.4.2). The continuous record of surface "in vivo" chlorophyll concentrations (Fig. 7.4.3) resolves the extention, fine scale variabilty and magnitude of the blooms better than the samples. The discrete values obtained at stations by the "in vitro" technique agree well with the continuous data. Three intensive blooms and a minor one were detected. The first bloom was located in the large coastal polynya off the eastern shelf off Kapp Norvegia between Sta. 13 and 23 with maximum chlorophyll concentrations above 5 mg m^{-3}. The bloom was formed by *Phaeocystis* colonies and a very diverse diatom assemblage (*Thalassioaira* spp., *Nitzschia* spp., *Proboscia* spp., *Chaetoceros* spp., etc.). The second bloom occupied a large area in the interior of the gyre reaching its maximum Chl.*a* concentration of 1.76 mg m^{-3} at Sta. 49. It consisted mainly of diatoms and the silicoflagelate *Distephanus speculum*. In the area of this bloom the ice cover was made of the remainders of strongly melted pressure ridges. The third "western" bloom occurred in slope waters off Joinville Island between Sta. 61 and 64. It was mostly dominated by *Phaeocystis* colonies although a few diatoms (*Nitzschia cylindrus, N.* cf. *seriata, N. longissima, Chaetoceros* spp., *Thalassiotrix* spp., *Corethron* spp. etc.) were also present. Maximum chlorophyll concentrations reached 4.23 mg m^{-3} at the surface between Sta. 62 and 63. A less intense bloom was observed in shelf waters off the coast of the Antarctic Peninsula. This bloom was almost totally dominated by*Corethron criophyllum* with chlorophyll concentrations of 1.05 mg m^{-3}. The blooms were separated by areas of varying ice cover. The net phytoplankton assemblages consisted mainly of diatoms and silicoflagelates. *Phaeocystis* was scarcely observed. The heterotrophic community, mainly formed by copepods, heterotrophic dinoflagelates and ciliates, was probably grazing actively as confirmed by the great abundance of pellets and minipellets of probable protozoan origin in the net samples.

Some results of measurements on the influence of UV-radiation on carbon uptake are given in Fig. 7.4.4. In all cases primary production was reduced under the influence of UV-light between 13 and 40%. The different rates were independant from total phytoplankton biomass, however the analyses of phytoplankton net samples indicate that species composition might play a role. Laboratory experiments with unialgal cultures in Bremerhaven will provide more information on this.

The assimilation numbers derived from the photosynthesis light curves ranged from 0.7 to 2 mg C (mg Chl.*a* h)$^{-1}$, the slope of the linear part of the P/I curve from 0.008 to 0.03 mg C (mg Chl.*a* h)$^{-1}$ (µmol m^{-2} s^{-1})$^{-1}$. A typical P/I curve is given in Fig. 7.4.5 (Sta. 36). One must be aware that the values represent the reaction of a whole phytoplankton community whose members may be very different in their physiological behaviour, and therefore the field results can only be understood after additional experiments in Bremerhaven with unialgal cultures of dominant phytoplankton species.

Fig. 7.4.3 Continous recording of surface chlorophyll by the "in vivo" fluorescence measured by a Turner fluorometer (line) and the "in vitro" measurements of the surface values.

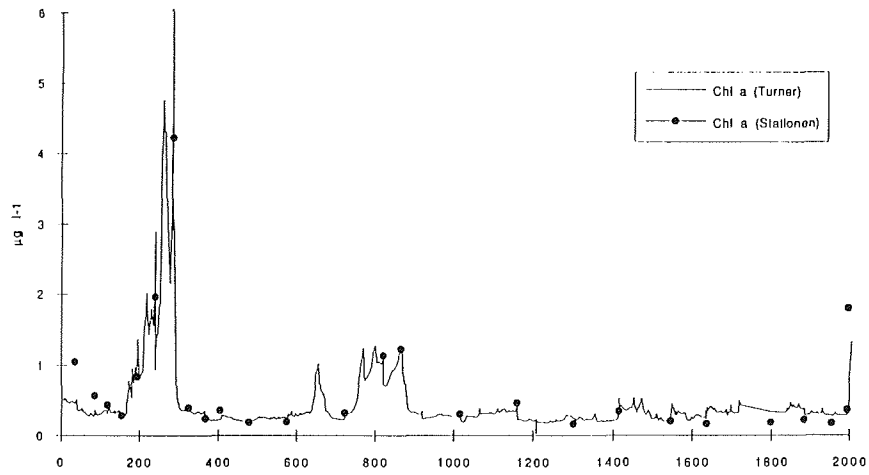

Fig. 7.4.4 Comparison of primary production with (quarz) and without (glass) the exposure to natural UV-irradiance

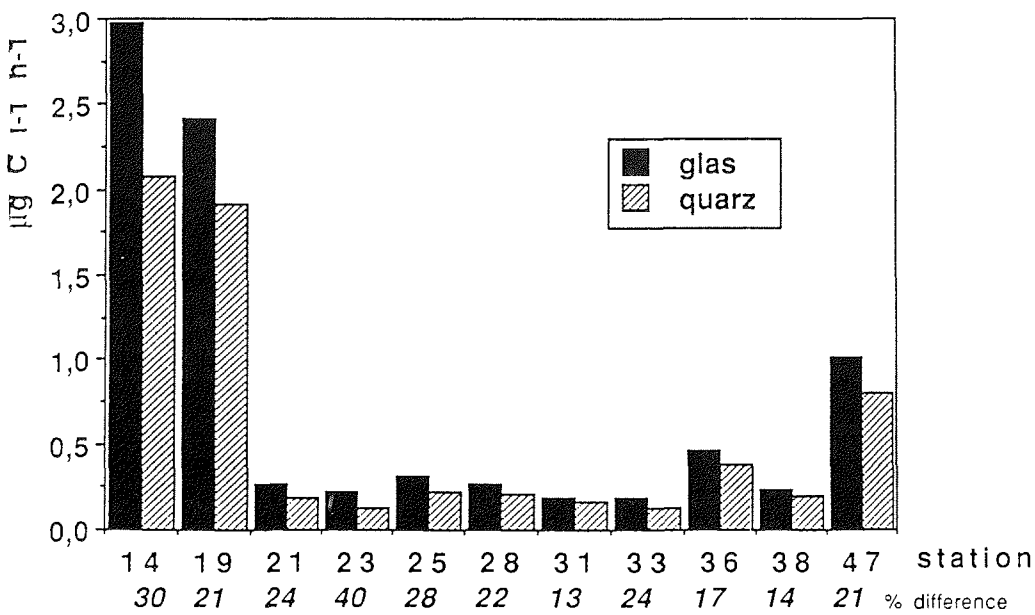

Fig. 7.4.5 Photosynthesis light curve (P/I), Sta. 36 as a typical example

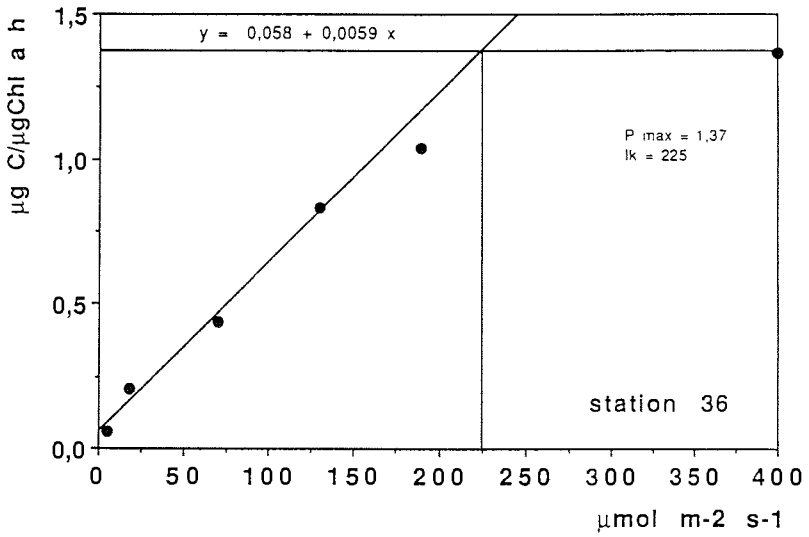

4.2 Nitrate, nitrite and ammonium assimilation by primary producers

M. Baumann, L. Goeyens, S. Jesse, R. Röttgers (AWI), F. Brandini (CBM), F. Dehairs (VUB)

Objectives

Previous investigations made clear that rates of nitrogen assimilation during primary production change regionally as well as seasonally in the Southern Ocean. It was observed that the marginal ice zone (MIZ) in the Scotia-Weddell Confluence area and the coastal and continental shelf zone (CCSZ) in Prydz Bay exhibited enhanced nitrate uptake in the beginning of the season, followed by a predominance of ammonium uptake (f-ratios < 0.5). Open ocean zones (OOZ) of the Scotia Sea and the Indian sector of the Southern Ocean and closed pack ice zones (CPIZ) of the Weddell Sea, on the other hand, are characterized by smaller nitrate uptake rates with a consistent predominance of nitrate uptake though (f-ratio > 0.5). Production based on ammonium uptake (as observed in the MIZ and CCSZ) is generally triggered by elevated ammonium concentrations. This reflects intensive recycling of nitrogen in the upper water column, and therefore the fraction of primary production left for export to the deeper ocean (and the sediments) is comparatively small.

organic matter. Ammonium based primary production, on the contrary, is regenerated in-situ. However, the appearance of enhanced ammonium pools reflects the remineralization of similarly large pools of organic matter and requires the channelling of primary production towards an in-situ recycling system. In those environments a significant fraction of nitrate uptake must be fueling recycled production.

One objective of this study is to investigate the role of the nitrogen signature in Antarctic surface waters on the nutrient (nitrogen) uptake regime. Can ammonium exert a significant effect on the nitrogen utilization by Antarctic phytoplankton, living in a sea of nitrate? A second objective is to study the spatiotemporal variability in nitrogen signature and in nitrogen uptake regime, and to compare these aspects with the simultaneous ammonium remineralization process.

Work at sea

The total amount of nitrate, removed from the upper layer of the water column by autotrophic assimilation, is estimated from the nitrate depletion or the integrated differences between the nitrate concentration in the Winter Water and the ones in the overlying water. Ammonium availabilities, the percentages of the ammonium nitrogen in the total inorganic nitrogen pool, mirror the excess of ammonium production by heterotrophic activity. Absolute and specific uptake rates for nitrate, nitrite and ammonium were determined using ^{15}N labelled nitrogenous nutrients. Only surface samples were taken and incubated in an on-deck incubator, kept at surface water temperature by flow-through of surface sea water. Ammonium remineralization rates are measured by the isotope dilution technique. Therefore, ammonium is extracted from the sea water matrix using a micro-diffusion technique. ^{15}N enrichment in all collected samples (particulate organic matter and ammonium) will be determined by emission spectrometry in the home lab.

4.3 Seasonal variability of specific nitrogen uptake rates in the Southern Ocean ice edge zones

M. Baumann, L. Goeyens, S. Jesse and R. Röttgers (AWI), F. Brandini (CBM)

Objectives

The nitrogen signature of Southern Ocean surface waters emphasizes a ubiquitous abundance of nitrate and localized high ammonium concentrations. The nitrate concentrations range from approximately 31 µmol N l^{-1}, as observed in upwelling water of the Antarctic Divergence, to half this concentration in stabilized surface water lenses of the marginal ice zone. For well-sheltered waters in the immediate vicinity of shelf ice edges enhanced removal and even complete exhaustion are observed. The ammonium availability is generally high in ice edge areas, where it can represent >10% of the inorganic nitrogen pool. It is comparingly low in open ocean zones of the Antarctic Circumpolar Current (ACC), where its concentrations hardly represent 1% of the inorganic nitrogen. Moreover, several investigations reveal that the Indian sector of the ACC displays poor to very poor biomass build-up and primary production, whereas the Scotia Sea exhibits somewhat higher values. Nevertheless, phytoplankton blooms worthy of the term are in general related to typical ice edge regions.

Poorly productive habitats obviously exhibit functional oligotrophy: the nitrate load is sufficiently high but new production fails to reach high levels appropriate to the nutrient status of the sea. Usually blooms do not occur and nitrate concentrations are never exhausted. These features are common for "high nutrient, low chlorophyll" (HNLC) areas, as occurring in central North and eastern equatorial Pacific waters also. According to Dugdale and Wilkerson (1991), the functional oligotrophy is related to low specific nitrate uptake rates: the ecosystem evidences a poor capacity to exploit the luxurious nitrate abundance. Low specific nitrate uptake rates characterize the open ocean zone (OOZ) of the ACC.

In contrast to the oligotrophic regions of the Southern Ocean, oceanographic processes in ice edge regions stimulate elevated primary production, which is subsequently assimilated in the localized food web to support the observed elevated stocks of higher trophic levels. Typical MIZ habitats display higher specific nitrate uptake rates during early spring but decreasing values with increasing seasonal maturity, even when the nitrate pool is not exhausted.

Since it was observed that decreasing specific nitrate uptake rates coincide with strikingly enhanced ammonium pools in the water, the variable effects of the presence of ammonium on the nitrate uptake behaviour of Antarctic phytoplankton was investigated.

Work at sea

Surface samples, taken in areas with dense phytoplankton blooms, were spiked with different amounts of ammonium and incubated with ^{15}N-labelled nitrate in order to investigate the effects of ammonium on the nitrate uptake rate.

Characteristics of the samples were determined by nutrient, POC, PON, and chlorophyll concentrations as well as by species composition. The ^{15}N methodology was applied for measuring uptake rates of nitrate and ammonium.

4.4 Mesopelagic barite accumulation and export production

F. Dehairs (VUB), L. Goeyens, R. Röttgers (AWI)

Objectives

As the role of the Southern Ocean in the global biogeochemical carbon cycle is currently a leading concern in oceanographic research, this study aims to define the specific effect of dissolved inorganic nitrogen on the primary production's development and fate. The inherent consequences of the nitrogen utilization by primary producers is investigated in view of determining the fate of the produced organic matter. In addition to investigations on the variability in inorganic nitrogen uptake for primary production as well as on the variability in the amounts of organic nitrogen channelled towards in-situ regeneration, this part of the programme focuses on the fraction of primary production leaving the upper layer as vertically settling material.
There exists increasing evidence that barium sulphate (barite) microcrystals, precipitating in the oceanic environment as a result of biological activity, carry a potential for tracing productivity, both, at geological and seasonal time scales. The

process involved in pelagic barite formation appears to be decay of organic matter inside micro-environments, such as mixed biogenic aggregates. Dissolution and heterotrophic oxidation may eventually eliminate most of the micro-environment components, except for the barite crystals, which only dissolve very slowly in the undersaturated sea water. Its semi-conservative character imparts to the accumulated barite a potential as tracer of past productivity.

During recent studies in the Southern Ocean we have observed interesting correlations between mesopelagic barite accumulations and the type of production prevailing in the investigated area. In environments, where during the ongoing season the phytoplankton community switched from predominantly nitrate based production to ammonium based production, the largest fraction of the organic matter was recycled in the upper water column and no significant mesopelagic barite accumulation occurred. The marginal ice zone (MIZ) in the Scotia-Weddell Confluence area and the coastal and continental shelf zone (CCSZ) in Prydz Bay were such environments. On the contrary, in open ocean zones (OOZ), eventually covered by sea ice in winter, and in the closed pack ice zone (CPIZ), nitrate based production prevailed all over the season and subsurface accumulation of barite is common. Despite the fact that total productivities in OOZ and CPIZ areas are in general significantly lower than in the MIZ and the CCSZ, the enhanced concentrations of mesopelagic barite suggest significant export of production to occur in these environments.

Work at sea

Depending on the suspended matter load, between 5 and 22 l of sea water were filtered on Nuclepore membranes of 0.4 µm porosity. In the home laboratory they will be digested using a $LiBO_2$ fusion method with redissolution in HNO_3. The final solution is anlysed for Ba, but also for Sr, Ca, Si and Al content by inductively coupled plasma - optical emission spectrometry (ICP-OES) and ICP-mass spectrometry (ICP-MS).

4.5 Impact of UV irradiance on nitrogen assimilation and pigmentation of Antarctic phytoplankton and ice algae

G. Döhler (BIF)

Objectives

The main topic of this study is to obtain information of UV irradiance damaging effects on the nitrogen metabolism, cell components and growth of phytoplankton and ice algae from Antarctica. The response of several Antarctic microalgae to UV irradiance of different wavebands and the adaptation strategies via special protecting mechanisms are included, too.

Work at sea

The activities during the cruise have been:

- -collection of phytoplankton by Apstein-net
- -collection of phytoplankton by rosette-sampler at different depth
- -collection of ice algae from ice lumps

-^{15}N experiments in the laboratory container and on the deck

Samples of phytoplankton or ice algae from several stations were exposed to UV radiation in special plexiglas vessels (UV transparent and non-transparent) at 2°C under controlled laboratory conditions. The different UV doses were obtained by changing the distance to the vessels or by the exposure time. The UV intensities during the experiments are comparable and significantly lower as the ones of a sunny day. Philips lamps (TL 20W/12) and cut-off filters (WG 295, WG 305 and WG 320) have been used. Samples were collected after different photosynthetic periods by a syringe, filtrated onto Whatman filters and heated 2 h at 60°C. ^{15}N analysis will be carried out in Frankfurt a. M. with an atomic emission spectrometer (Jasco N150). In addition, samples were collected for estimation of the pool sizes by HPLC (high performance liquid chromatography), the ^{15}N incorporation into free aminoacids and the pigmentation. Out door experiments were carried out under "natural " conditions on deck of the ship. Phytoplankton and ice algae samples from several stations were collected for cultivating purposes at home. Several pure cultures of Antarctic diatoms were used too.

Preliminary results

Measurements of ^{15}N enrichment and analysis by HPLC can be performed in the home laboratory only. Therefore, no results are available at present. However, we can expect an UV damage of ^{15}N-ammonium and ^{15}N-nitrate uptake in dependance on the UV wavebands and the exposure time. UV-B of shorter wavelength might lead to a stronger reduction of the uptake rates and to a variation in the pattern of free aminoacids. On the other hand, differences in the response to UV radiation might exist in dependance of the composition of the phytoplankton assemblages. The impact of UV irradiance on cell components and growth are planned to be investigated under laboratory conditions at home.

4.6 Light attenuation (PAR, UV-A, UV-B) and mircrobial biomass in the Weddell Sea

J.H. Vosjan, A.L.H.H. van Balen (NIOZ)

Objectives

For the primary production in the sea the penetration of photosynthetically available radiation (PAR) is of the utmost importance. Besides this PAR (wavelength between 400-700 nm), radiations with other wavelength affect life in the sea e.g. the UV-A (wavelength between 315-400 nm) as an inhibitary radiation for photosynthesis and the UV-B also as a very detrimental radiation for various groups of organisms. The shorter the wave length the more toxic for biological systems. Especially studies about the middle UV radiation (UV-B) are interesting, because this kind of radiation is increasing on the earth surface since the decrease of the ozone shield in the stratosphere.

The aim of our study is to describe the penetration of PAR, UV-A and UV-B in the Weddell Sea water on the transect between Kapp Norvegia and Joinville Island. The attenuation of these wave length bands in the water column was determined and will be correlated with the amount of suspended microbial biomass.

The results will be compared with measurements by means of the same radiation sensors which we made in other regions e.g. in coastal waters of the Antarctic Peninsula low in humic substances and in coastal waters off the Netherlands rich in suspended material and humic acids. The knowledge of the attenuation of radiation in that waveband is of importance for studies on the effects of that radiation on the aquatic ecosystems. Also for our experimental work about the effects of UV-B radiation on marine microorganisms we need to know the natural doses of irradiation these organisms get under natural circumstances.

Work at sea

International light detectors of PAR (band between 300 and 800 nm), of UV-A (band between 300 and 400 with maximum at 360 nm) and of UV-B (band between 260 and 350, with a maximum at 290 nm) were lowered in the upper 30 m of the water column and one set of sensors was situated in a container with water at the ships deck, to correct for changes in the sunlight intensity during the measurements. The sensors for lowering in the sea were connected with a depth sensor and the data collected in a li-cor data logger. At 17 stations a vertical profile of the under water light have been measured. The concentration of suspended microbial biomass and their activity was estimated in the upper water layers of the same stations.

Fig. 7.4.6: The 1% depth of PAR, UV-A and UV-B on the transect from west to east.

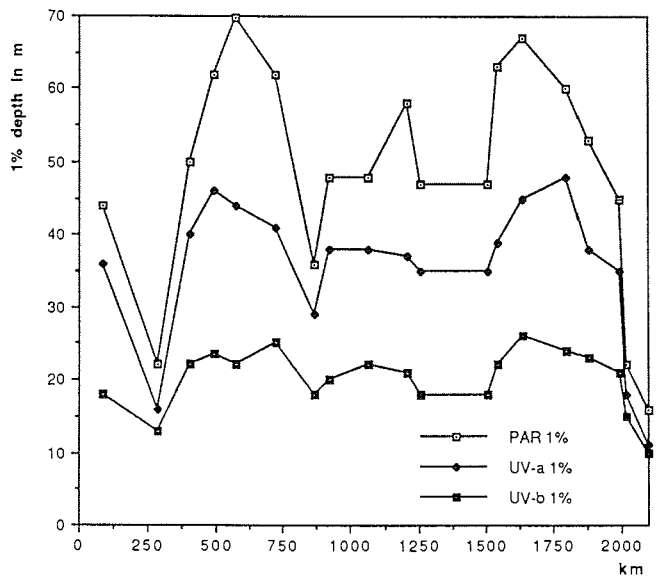

Primary results

The lowest light penetrations were measured in the regions rich in biomass, in the spring bloom in the eastern polynya (Fig. 7.4.6). There, the 1% level of PAR was reached at 16 m depth, the 1% level of UV-A at 11 m and of UV-B at 10 m depth. Deep penetration depths were found at Sta. 31 and 54, here the 1% depths of PAR were respectively 67 and 70 m, of UV-A 45 and 44 m and of UV-B 26 and 22 m. The correlation found between the light penetration and the biomass concentration is the best for the sensor with the narrowest wave length band, the UV-B.

For PAR 1% depth in m = 73.15-1.53 (mg ATPm^{-2}) R= 0.67
For UV-A 1% depth in m = 50.81-0.96 (mg ATm^{-2}) R= 0.65
For UV-B 1% depth in m = 27.46-0.46 (mg ATPm^{-2}) R= 0.75

4.7 Microbial biomass and respiratory electron transport system activity (ETS-A) in the Weddell Sea

J.H. Vosjan, A.L.H.H. van Balen (NIOZ)

Objectives

The knowledge of respiration rates in marine ecosystems provides information on the carbon cycle, oxygen consumption, carbon dioxide production and the energy flow in the studied area. The information also could be used in calculations of the ages of water masses. If the amount of consumed oxygen and the oxygen consumption rate are known, than with some speculative assumptions the age of a water mass could be calculated.

The respiration reaction in which oxygen is consumed is the opposite reaction of the photosynthesis in which oxygen is produced. In contrast to the primary production, which only can occur in the euphotic zone, the respiration reaction occurs in all depth, from surface to the deepest deep sea. This oxygen consumption is mainly due to the respiratory activity of microorganisms. However the rates are, especially in deep sea and in cold waters very low and difficult to measure. Also the scarce biomass in deeper waters is hard to estimate.

With a precise photometrically Winkler titration the oxygen consumption of surface waters can be measured, after incubation for some days at low temperatures. However the respiration rate in deeper waters cannot be measured directly. Packard introduced for this an alternative method by measuring the activity of the respiratory electron transport system (ETS-A). This method we applied successfully in earlier expeditions to tropical and Antarctic regions. Another alternative method to calculate the respiration rate of an ecosystem is to estimate the biomass and calculate from this the respiration rate. The microbial biomass was estimated by measuring the ATP (adenosine-tri-phosphate), as a relative measure for the in-situ microbial biomass.

The aims of the research are to:
-describe the horizontal and vertical distribution of ETS-A in a transect over the Weddell Sea.
-estimate on the same transect the ATP (biomass) concentration.

-estimate the ratio between the ETS-A and the real respiration rate, this only can be done for surface waters.

Fig. 7.4.7: ATP(mg m^{-2}) in the upper 50 m of the water column on the transect from west to east.

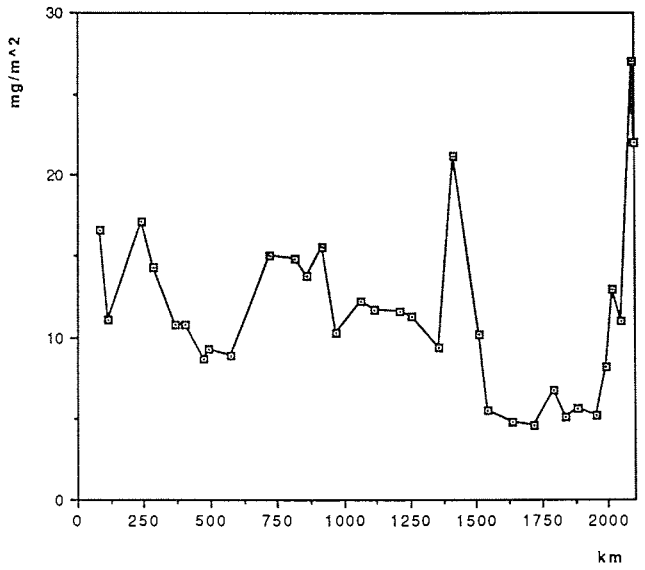

Fig. 7.4.8: ETS-activity (mmol m^{-2} d^{-1}) in the upper 50 m of the water column on the transect from west to east.

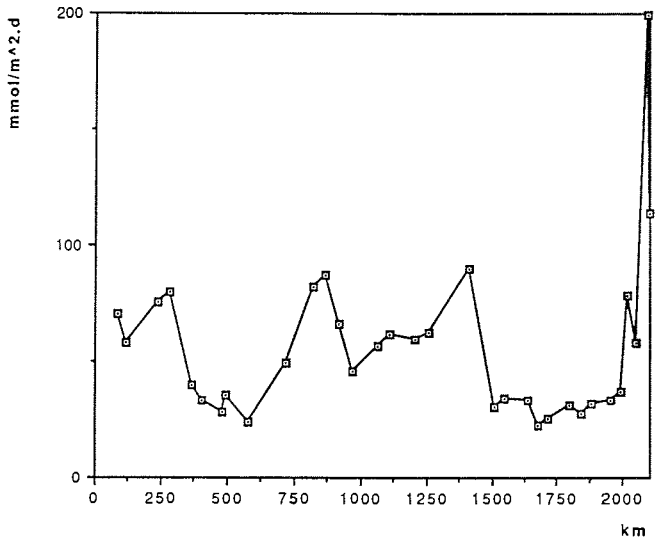

Work at Sea

The vertical profiles of ATP and ETS-A distribution have been determined at 35 stations at eight depths from surface to bottom. At some stations the oxygen consumption rate in surface water was estimated by incubation experiments. Several samples were fixed with formaldehyde to study the microbial biomass by epifluorescence microscopy at the home laboratory.

Preliminary results.

The vertical profiles show that most biomass and activity is in the upper 50 m of the water column. Values of about 300 ng ATP l^{-1} and of about 100 nmol $l^{-1}h^{-1}$ ETS activity at in-situ temperature were observed. High values observed in the bloom off the eastern ice shelf were 750 ng ATP l^{-1} and 200 nmol $l^{-1}h^{-1}$ ETS-A. The horizontal dristribution along the transect show high values in the beginning, about 25 mg ATP m^{-2} over a water column of 50 m and the lowest values were found in the stations 23 to 33, here the values were about 5 mg ATP m^{-2}. Sta. 36 shows a high value and in the western part of the transect from Sta. 39 to 69 values were between 10 and 15 mg ATP m^{-2} (Fig. 7.4.7, 7.4.8).

4.8 Population dynamics of calanoid copepods within the Weddell Sea

F. Kurbjeweit, S. Günther, M. Gorny (AWI)

Objectives

Dominant calanoid copepods in the Weddell Sea are *Calanus propinquus, Metridia gerlachei, Microcalanus pygmaeus,* and *Stephos longipes.* It was the aim of this study to determine the abundance and the distribution in space and time of those species in summer. In connection with data from other cruises, we investigate the seasonal change of the population structure and the influence of biotic and abiotic parameters as food and water masses on the reproduction. The time dependance of the reproduction rate of these copepods is of importance, because of the short duration of primary production in the Weddell Sea. Additional biochemical parameters as lipid content, dry weight and C/N ratio will help to describe the life cycles of these copepods and their importance as secondary producers in the pelagic system. An additional study refers to the development of shrimp larvae.

Work at Sea

The distribution and abundance of dominant copepods in the upper 1000 m of the water column was examined at 20 stations by means of a multiple opening and closing net (100 µm mesh size; 0.25 m^2 opening area) on a transect from Kapp Norvegia to the northern tip of the Antarctic Peninsula. One additional catch was carried out west of Maud Rise and four catches on a transect in the western part of the Weddell Sea off the Larsen Shelf Ice. Samples from five depth strata were preserved in 4% buffered formaldehyde for future investigation of stage distribution of the four dominant copepod species, their gonad development and the determination of weight-length relationships.

The bongonet (100 µm mesh size; 60 cm ø) was lowered at the same stations to 500 m or 1000 m, to obtain undamaged females for reproduction experiments and lipid analysis. If available, up to 50 females of the four copepod species were incubated on all 24 stations under in situ conditions in surface water.

The influence of the food on the reproduction was investigated with females of *Calanus propinquus*, *Metridia gerlachei* and *Microcalanus pygmaeus*. They were starved in 0.2 µm Nucleopore filtered sea water for up to two weeks before they were fed with high concentrations of diatoms as *Thalassiosira tumida* to determine, if reproduction depends on the quantity of the available food, and to measure the time required by the copepods to generate eggs after the onset of feeding. The influence of the quality of the food was investigated by feeding with different algae as *Thalassiosira antarctica* and *Nitzschia linearis*. Additional information on the reproductive success and potential of the copepods will be derived from samples for measuring dry weight, C/N-ratio content and lipids. The measurements will be done in Bremerhaven.

Samples of ice cores and water under the ice were collected to investigate faunal and floral composition within and beneath the ice and the dependence from abiotic parameters. Due to the advanced melting of the ice, this was only possible on two floes.

Preliminary results

a) Distribution and abundance of zooplankton

Copepodite stages CV and adults of *Calanus propinquus* were dominant in the eastern part of the Weddell Gyre in the upper 100 m (surface waters) and were less frequent in the western part. Besides *Calanoides acutus Metridia gerlachei* was the generally most abundant large calanoid copepod species, dominated by females and less CV. At stations were blooms of *Phaeocystis antarctica* (st. 13, 15, 62) or *Corethron criophyllum* (st. 71) were observed, it was the only large copepod species in the water column, but only present in low numbers. *Microcalanus pygmaeus*, a small calanoid copepod of about 0.6 mm in length (adult females), was frequent at the offshore stations, the numbers increased with water depth to a maximum at 500 m. On the shelf it was rare or almost absent. Copepodite stages CIV to CVI dominated the populations. The other small copepod species *Stephos longipes* was only found on the eastern shelf in significant numbers, namely at the first two stations 13 and 15, where it lived as a cryopelagic species in the water column and the sea ice. On the western shelf off the Antarctic Peninsula it was missing, presumably it migrated to greater depths in the course of the seasonal development. The population consisted mainly of female and male adults and CV. This population structure resembles the one observed during the spring of 1990. At almost all stations cyclopoid copepods of the genera *Oncaea* spp. and *Oithona* spp. were predominant in the micro- and smaller meso-zooplankton size classes. Radiolarians were important in offshore waters in depths greater than 200 m, being a potential trap for most of the other zooplankton organisms.

b) In situ egg production of copepods

In situ egg production experiments over 48 hours in ambient surface water with females of *Calanus propinquus*, *Metridia gerlachei* and *Microcalanus pygmaeus* did not show an obvious correlation between the mean egg production rates and the Chl.*a* at the surface or integrated to a depth of 300 m (Fig. 7.4.9). There is an indication, that the egg production of the first two species was related to the

Fig. 7.4.9: Mean egg production rates of *Calanus propinquus, Metridia gerlachei* and *Microcalanus pygmaeus* in in-situ incubations in comparison with a) surface Chl.*a* and b) integrated Chl.*a* for the upper 300 m.

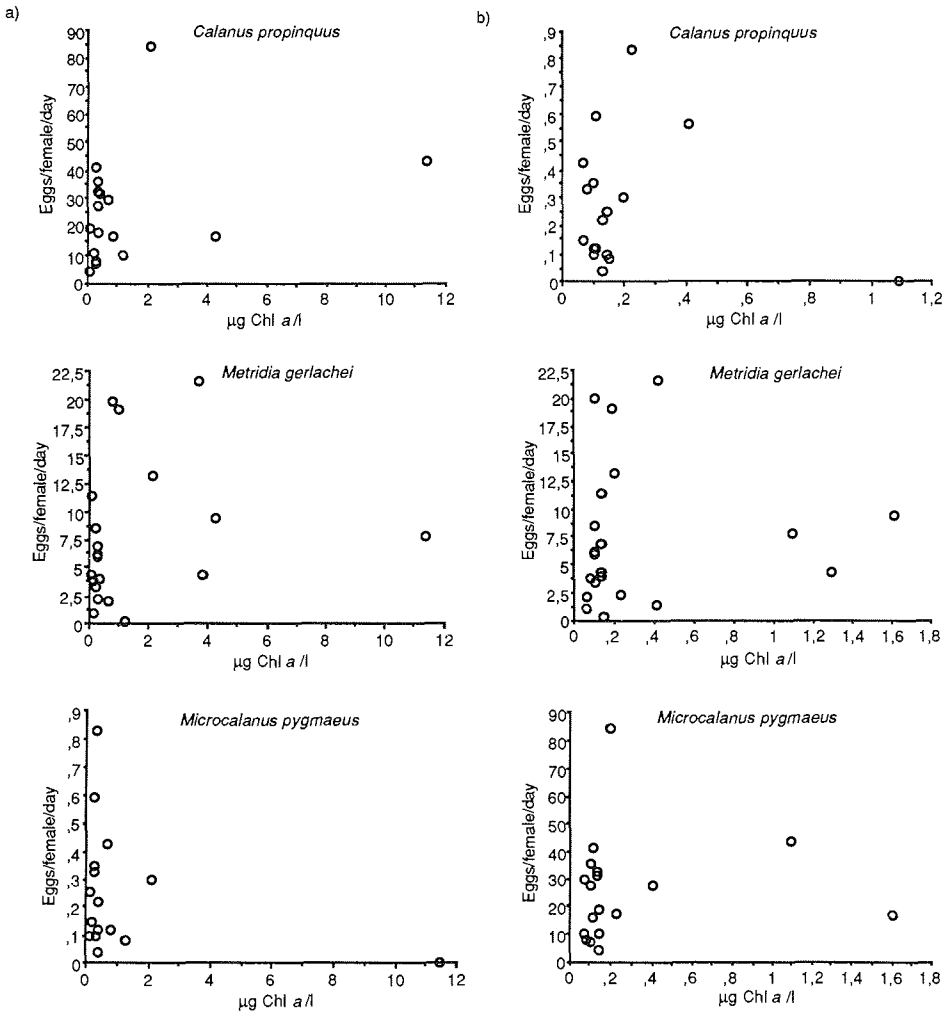

Fig. 7.4.10: Comparison of ice coverage (filled bars) and in situ egg production (open bars) of a) *Calanus propinquus* and b) *Metridia gerlachei* on the main transect from Kapp Norvegia in the southeast of the Weddell Sea to the tip of the Antarctic Peninsula.

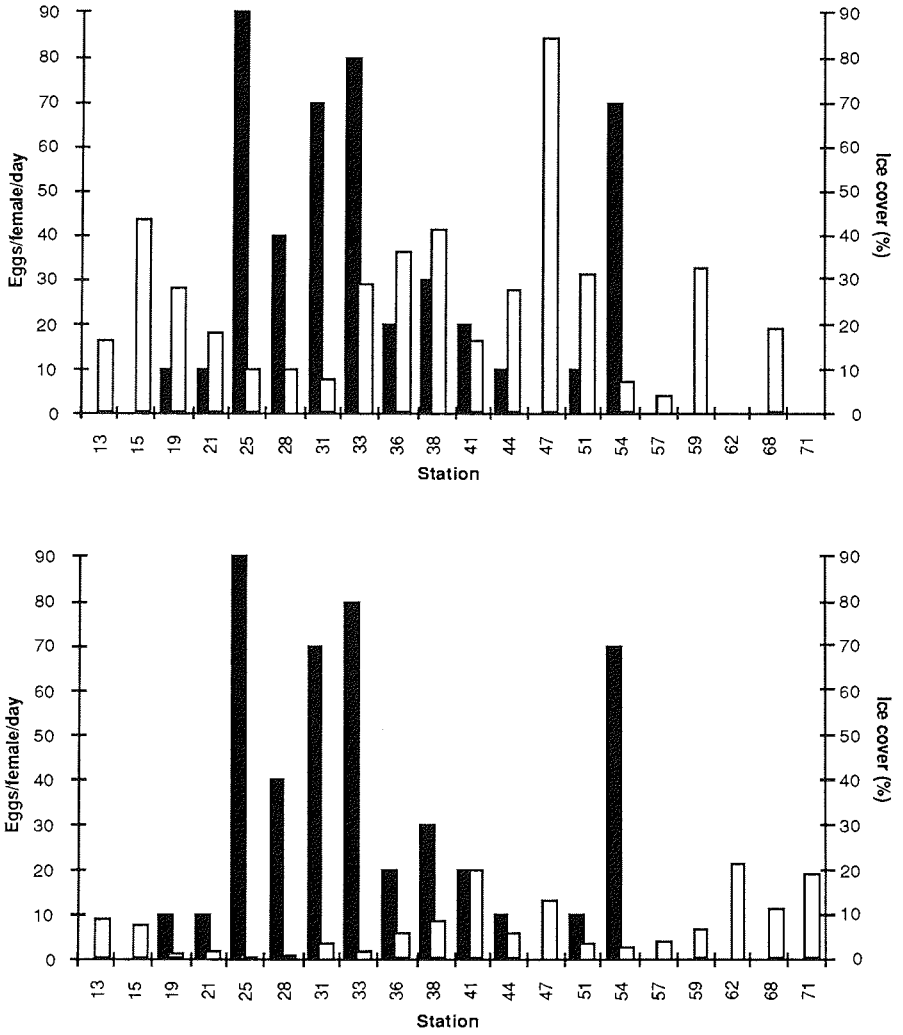

hydrographic and the ice conditions (Fig. 7.4.10). Highest egg production rates were found on both shelfs and in the centre of the Weddell Gyre where ice coverage was low or absent. *Stephos longipes* did not reproduce on the eastern shelf (Sta. 13 and 15). A multifactorial analysis will be used to determine the dominant biotic and abiotic factors which affect the egg production.

Since *Microcalanus pygmaeus* is a mesopelagic copepod species whose distribution maximum ranges between 200 and 500 m, ice or Chl.*a* is not expected to affect its reproduction. The depth range of its distribution is consistent with the first preliminary lipid analyses of this copepod which show a completely different lipid composition from those of the typical herbivorous copepods as *Calanoides acutus* or *Calanus propinquus*.

c) Starvation experiments

During the starvation experiments with *Calanus propinquus* and *Metridia gerlachei*, it was not possible to enhance production by feeding either with *Porosira* sp. or *Thalassiosira tumida* for a period of up to two weeks, after two weeks of starvation.

Fig. 7.4.11: Egg production of *Calanus propinquus* under superabundant food concentrations (≈ 10 µg Chl.*a* l^{-1}) of *Thalassiosira tumida*. Arrows indicate times of supply of food.

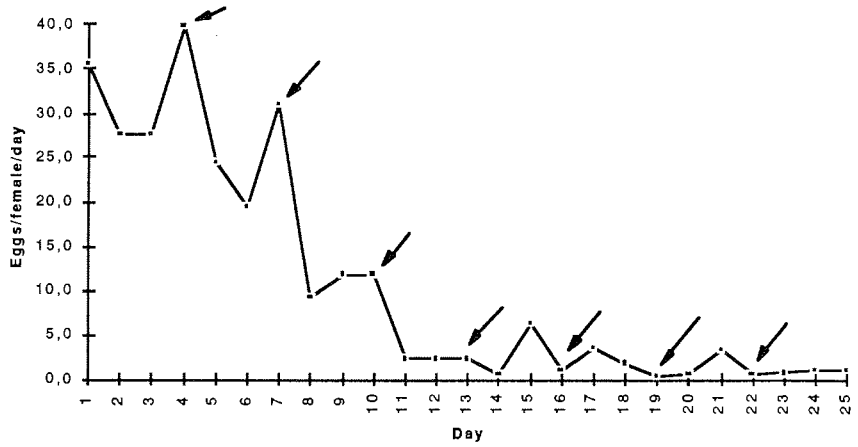

d) Superabundant food

In another set of experiments *Calanus propinquus* needed approximately three days to respond to offered food by egg production. Later in the experiment the response to feeding was less clear and it was not possible even under high Chl.*a* concentrations (≈ 10 µg Chl.*a* l^{-1}) of *Thalassiosira tumida* to keep the production on a high level (Fig. 7.4.11).

e) Distribution and occurrence of shrimp larvae

Larvae of decapods were generally rare. Off Kapp Norvegia, on the continental shelf, two hauls with the bongonet yielded three specimens of *Notocrangon antarcticus* and one larvae of *Chorismus antarcticus* (Sta. 13). Between 200 and 600 m depth adults of these benthic shrimp species are common in the eastern Weddell Sea. In the inner Weddell Sea one haul with the multinet contained one juvenile specimen of the

pelagic shrimp *Acantephyra pelagica* (Sta. 51). The low density of shrimp larvae in the eastern Weddell Sea is due to the small number of eggs produced by the females. Female fecundity is reduced, compared to shrimp populations in the Sub-Antarctic off South Georgia.

4.9 Sampling of benthic shrimps (Decapoda, Natantia) and macrozoobenthos off the Larsen Ice Shelf in the western Weddell Sea

M. Gorny (AWI)

Objectives

Decapods are represented in the eastern Weddell Sea only by nine species of shrimps. *Notocrangon antarcticus* and *Chorismus antarcticus* are the common species between 100 and 600 m depth on the continental shelf. Compared to the populations living north of the Antarctic Peninsula, off South Georgia, the populations from the Weddell Sea showed delayed maturity and reduced fecundity. Therefore it is planned to extend the comparison to the populations living in the western Weddell Sea.

In the past, investigations of macrozoobenthos were concentrated on the continental shelf and slope in the eastern and southeastern part of the Weddell Sea. The hauls taken during ANT X/7 should provide first informations about the species composition in the western Weddell Sea.

Work at sea

Three successfull hauls with the Agassiz Trawl (mesh size in the cod end: 10 mm) were taken between 292 and 422 m depth. All hauls contained a large amount of mud and had to be sieved. Invertebrates and fishes were picked out of the total catch. Additionally, from each catch a subsample of 10 l was taken at random, and sorted out in the laboratory. All material was preserved in 4% formalin.

Preliminary results

The material yielded 26 groups of invertebrates (Tab.7.4.12) and a total number of five fishes. Ophiuroids were dominant at all three stations, whereas sponges were rare, and occurred only in small sizes. Within the crustaceans, isopods and decapods were the dominant taxa. Decapods were represented by 38 specimens of *Notocrangon antarcticus*, one of them carrying eggs on the pleopods. Reptant decapods were absent. The gonadal development and growth parameters of *N. antarcticus* will be analysed by detail in Bremerhaven.

Tab. 7.4.12 Occurrence of macroinvertebrates in Agassiztrawl (AGT) catches.

Station	73	74	76
AGT No.	1	2	3
Depth range (m)	294-296	292-292	417-422
Hexactinellida		-	-
Demospongia	-	-	-
Actinaria	-	-	-
Zoantharia			
Scleractinia		-	-
Stylasteroidea			
Hydroidea	-	-	+
Alcyonaria			
Pennatularia		-	-
Gorgonaria			
Bryozoa	-	-	-
Brachiopoda	-	-	-
Turbellaria			
Nemertini			
Echiurida			
Priapulida			
Sipunculida		-	-
Polychaeta			
Errantia		-	-
Polychaeta			
Sedentaria			
Aplacophora			
Polyplacophora			
Prosobrancia	-	-	-
Ophisthobranchia			
Scaphopoda		-	-
Bivalvia	-	-	-
Cephalopoda	-	-	-
Pycnogonida	-	-	-
Decapoda	-	+	-
Mysidacea			
Cumacea			
Isopoda	-	+	-
Amphipoda	-	-	-
Cirripedia	-		
Crinoidea	-	+	-
Asteroidea	-	-	-
Ophiuroidea	+	+	+
Echinoidea			
Regularia	-	+	+
Echinoidea			
Irregularia			
Holothuridea	-	-	-
Pterobranchia			
Ascidiae		-	-

no sign = absent
(-) = rare
(+) = common
(o) = very common

4.10 Epontic organisms on recovered moorings

M. Baumann, S. Jesse, R. Röttgers (AWI)

The following animal species could be determined on recovered moorings:

Octocorallia	Pennatularia	*Umbellula pallida*
Kamptozoa		*Loxosomella compressa*
Hydrozoa	Cnidaria	
	Synthetiida	*Staurotheca* sp.
	Sartulariidae	*Symplectoscylus*
Ascidiacea	Molgulidae	*Parengyrioides aernbaceae*

4.11 Ice-core Drilling

M. Baumann, M. Gorny, S. Günther, F. Kurbjeweit, L. Riegger (AWI)

Objectives

It was planed to drill several ice-cores along the transect to determine the species composition of ice-algae and microzooplankton together with the abiotic parameters nutrient and chlorophyll concentration, temperature and salinity. With additional samples we wanted to start experiments with ice algae of the melted ice cores to determine the fatty acid composition and the UV-B adaptation of the algal-community. For these experiments we needed ice cores with a thick brown layer, otherwise the biomass is too low to determine the biotic parameters. Furthermore, it was planned to use the under-ice pump to determine copepod species living in the water layer under the ice.

Work at sea

The melting of the ice had advanced so far that we found only at one station floes on which we were able to drill without risk. Only at one of these floes we found ice with a thin brownish layer. Therefore we measured only the abiotic parameters of the cores and fixed the organisms with formalin for further investigations in Bremerhaven. The under-ice pump was used at that station as well and samples were fixed.

Preliminary results

The data measured from core AN 107930052 are given in Tab. 7.4.13.

Station No.:	S	65°07.22´	Date	Core No.:		Snow temp.	Snowboard
51	W	40°43.18´	05/01/93	AN 107930052		0.2°C	10 cm
Depth [cm]	Temp. [°C]	Salinity [ppt]	Chlorophyll [µg/l]	PO4 [µg/l]	NO3 [µg/l]	NO_2 [µg/l]	Si [µg/l]
0 - 10	0.0	0.2	00.46	0.02	0.14	0.06	0.53
10 – 17	0.0	0.4	00.69	0.02	0.08	0.04	0.39
17 – 37							
37 – 47	-0.4	2.8	10.20	0.33	0.04	0.05	189
47 - 57	-0.4	2.7	08.84	0.05	0.02	0.08	0.62
57 - 67	-0.5	2.5	14.64	0.25	0.02	0.05	0.06
67 - 77	-0.6	2.7	20.83	0.53	0.02	0.08	1.75
77 - 87	-0.8	3.4	23.92	0.34	0.45	0.09	0.34
87 - 97	-0.9	3.4	40.51	0.07	0.43	0.13	9.80
97 - 107	-0.9	2.6	08.40	0.06	0.64	0.10	3.54
107 - 116	-1.1	3.1	11.44	0.05	1.07	0.09	4.14

5. Weather conditions

W. Seifert, H. Sonnabend (DWD)

During the first week of December the South Atlantic high-pressure-centre was situated relatively far north, near 25°S. Therefore a strong westerly flow formed an intensive frontal zone with a well developed gale centre southwest of Bouvet Island. It forced warm wave depressions from subtropical latitudes and secondary lows moving form the Drake Passage eastward in its steering circulation systeme which maintained the baroclinic structure. "Polarstern" passed the rear of the gale centre with southwesterly gales and wave heights up to 5 m. Reaching the sea-ice-belt the sea state weakend in spite of crossing cold fronts with snow showers and gusty conditions.

By mid-December the circulation pattern changed. The development of an intensive gale centre at the Antarctic Peninsula and the southeastern Weddell Sea generated a high pressure ridge over the eastern Weddell Sea with a descending air flow and rapidly decreasing cloud cover giving rise to sunny sky with light to moderate southerly winds during the stay at the Neumayer-Station.

During the following week the high pressure ridge moved northward while secondary lows formed at the western flank of the low east of Bouvet Island near 20°E. Wave depressions embedded in the southwesterly flow produced gusty flurries. The weak anticyclonic southwesterly flow, locally interrupted by small embedded mesoscalic waves persisted until 10. January 1993. The development of such waves is frequently observed in the Weddell Sea. It is caused by the vertical transport of mass and water vapour over regions with no or weak ice cover and water temperatures higher than -1°C. The typical range of the mesoscale waves is 200 to 500 km. They form a vortex with frontal structures and the associated wind and weather conditions.

Towards mid-January, the high pressure system weakened and one of the mesoscale lows moved from the Filchner Shelf westnorthwestwards under the influence of an upper secondary trough as part of the northeastern Antarctic low pressure system. It developed to a gale centre and became stationary two days later northeast of the Antarctic Sound with a core pressure below 975 hPa. At its rear the southerly winds increased to gale force Bft 8 to 9 with gusty snow showers and sea heights in open waters up to 3 m. The southerly winds were forced as barriere winds by the Antarctic Peninsula from southwest to northeast. By 15 January the low filled slowly up, while a high was moving from the southern Pacific across the Antarctic Peninsula to the western Weddell Sea inducing a weak pressure gradient with light southeasterly winds.

During the last five days of the cruise an intensive storm centre formed far northwest of the Drake Passage with eastward moving secondary lows developing at the occlusion point off the Drake Passage. With strong northerly winds and gusty snow showers "Polarstern" crossed the Antarctic Sound and reached the "Jubany" station under a following high pressure ridge. Another intensive gale centre west of the Drake Passage produced a stormy secondary low moving quickly east with northeasterly gales force Bft 8 and waves up to 3.5 m. In a following ridge the wind decreased to force 4 Bft but the visibility became rather poor.

Fig. 7.5.1: Statistics of wind force (top) and direction (bottom) during ANT X/7 and ANT IX/2

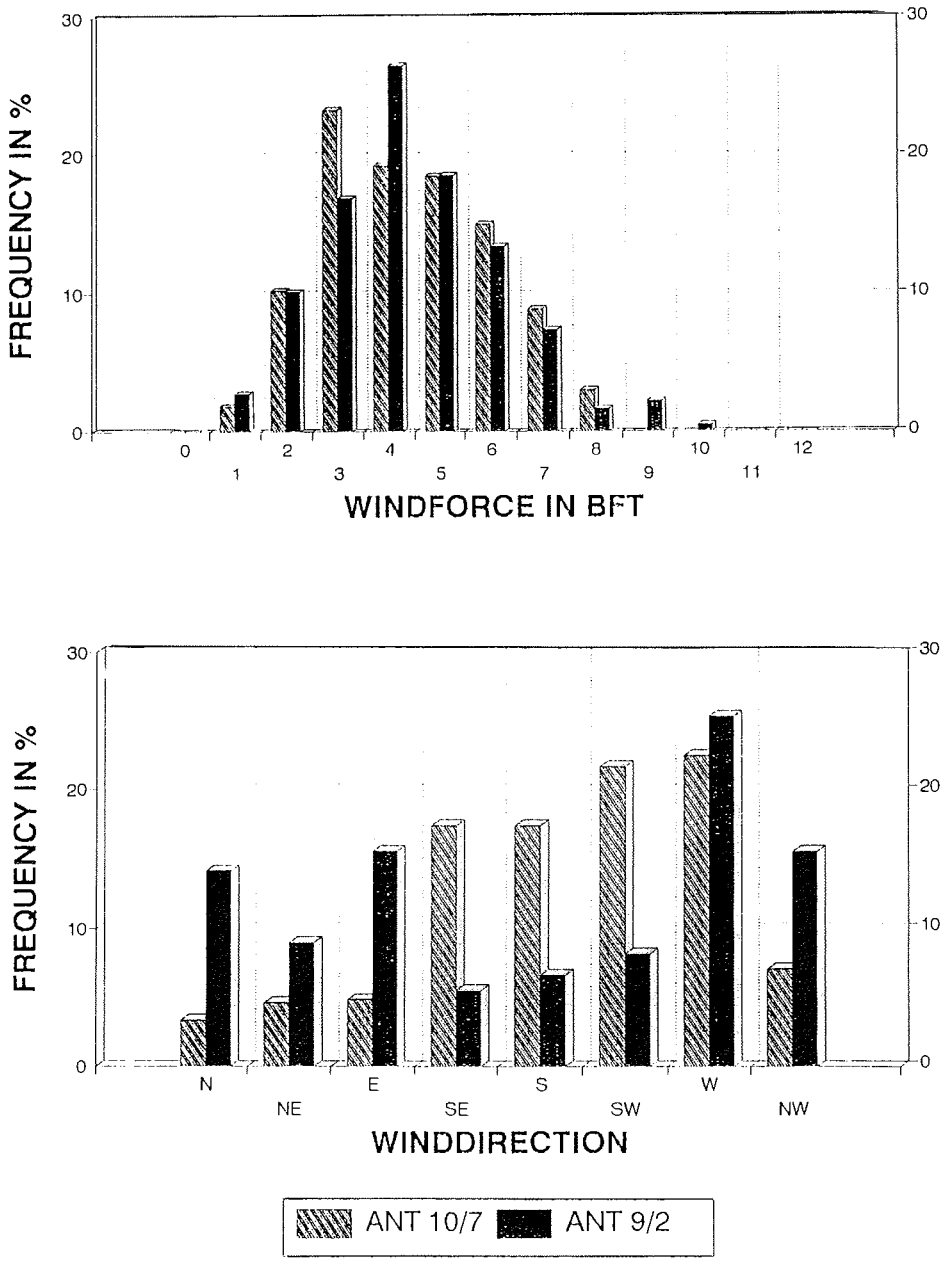

Fig. 7.5.2: Schematic representation of the surface pressure field as long term average for January (top) and during ANT X/7 (bottom)

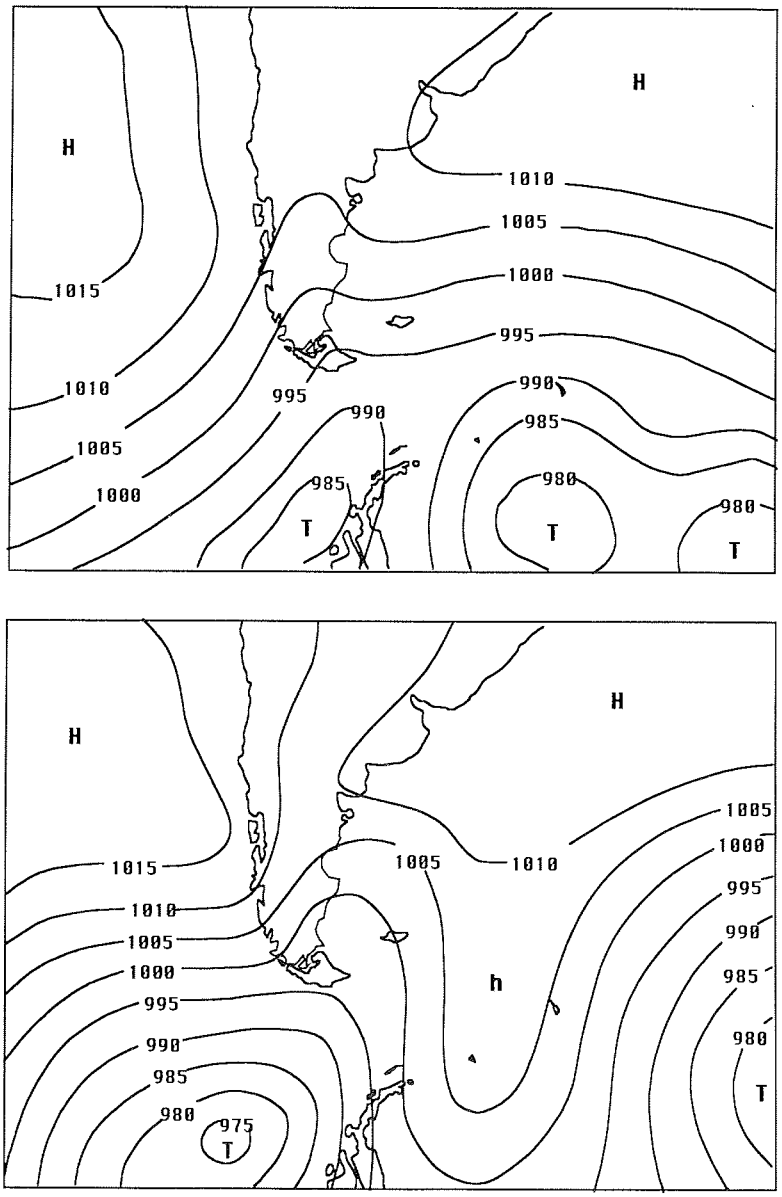

The meteorological conditions were favourable to achieve the objectives of the cruise. The wind statistics show that 70% of all observations were below force 6 Bft (22 kt). The predominant wind directions were southerly to southwesterly in contrast to other years as 1990 when during ANT IX/2 easterly directions were frequently observed (Fig. 7.5.1). The zonal wind component averaged along the main transect was approximately 5 kt, while the longtime mean value for December and January averaged along 65°S over the same longitudes is -2 kt, representing easterly wind components. The circulation seemed to differ from the typical pattern with a dominant low over the western Weddell Sea which would produce easterly winds south of 65°S due to the frequent formation a high pressure ridge over the Weddell Sea (Fig. 7.5.2). From the time series of surface air temperature, surface pressure and wind direction it appears that the wave depressions were triggered convective processes and not by advection.

6. Ice conditions

T. Boehme, E. Fahrbach, H. Fischer, R. Hamann, L. Kolb, A. Latten, G. Seiß, F. Zwein (AWI)

On 10 December 1992 hourly routine ice observations began with a more detailed observation every three hours. The first iceberg had been sighted at 44°45'S, 10°23'E on 6 December. The ice edge was reached at 58°24'S, 02°15'E. The transition zone from the Antarctic Circumpolar Current to the Weddell Gyre was marked by a belt of frequent icebergs between 56° and 59°S. Even if the ice belt extended extremely far to the north when we left Cape Town, it decayed dramatically during our way to the south with the consequence that we could proceed rather undisturbed by the ice and reached the wide coastal polynya on 16 December. The ice concentration on a transect from Kapp Norvegia to Joinville Island was split in two large scale bands which were separated by a rather open area in the center of the gyre and surrounded by the wide eastern and western polynyas (Fig. 7.6.1, 7.6.2). The western ice edge, where the ice cover decreased from 90 to 10% within a short distance was reached on 7 January at 64°34'S, 44°25'W. From 64°34'S, 44°25'W, we directed a transect towards the northeast according to the satellite data on the ice cover which we obtained from the Canadian Ice Center of the Atmospheric Environment Service. We met heavy ice conditions only at 66°25'S, 47°55'W which forced us to turn northwest and to finish the transect at 64°48'S, 47°35'W at about 40 nautical miles from our main transect. The ice observation record is available on diskette.

7. Acknowledgements

When we left "Polarstern" in Ushuaia, we all felt that we had an extremely successful cruise which was obviously to are large extent due to the most favourable ice and weather conditions and due the outstanding technical facilities of "Polarstern". However, it was obvious to us all, that only the continuous efforts of Master Jonas, his officers and his crew gave us the possibility to use this outstanding instrument. It was not only the active support which helped us to overcome difficult situations, but it was the heartful mood on board which made this cruise not only to a scientifc success, but to a cheerful adventure.

Fig. 7.6.1: Ice concentration in tenth from ship's observations on the transect from Kapp Norvegia (right) to Joinville Island (left).

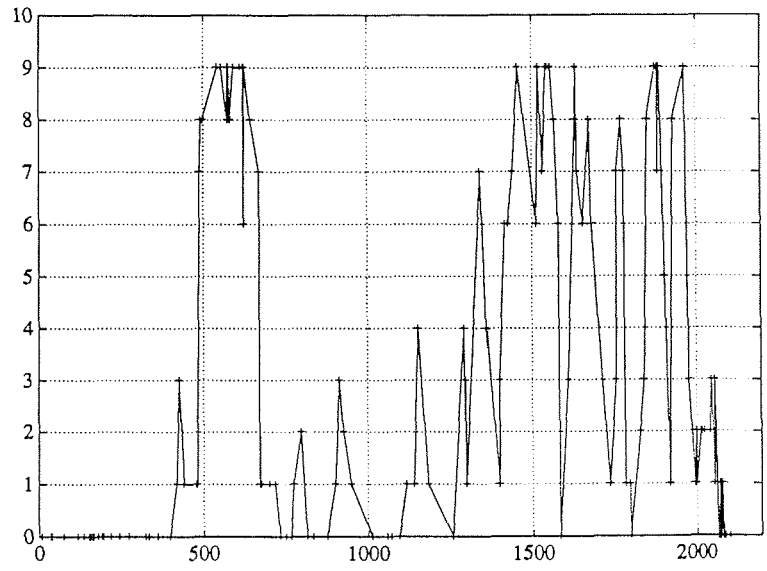

Fig. 7.6.2: Ice map of the NAVY - NOAA Joint Ice Center for the 24 December 1992.

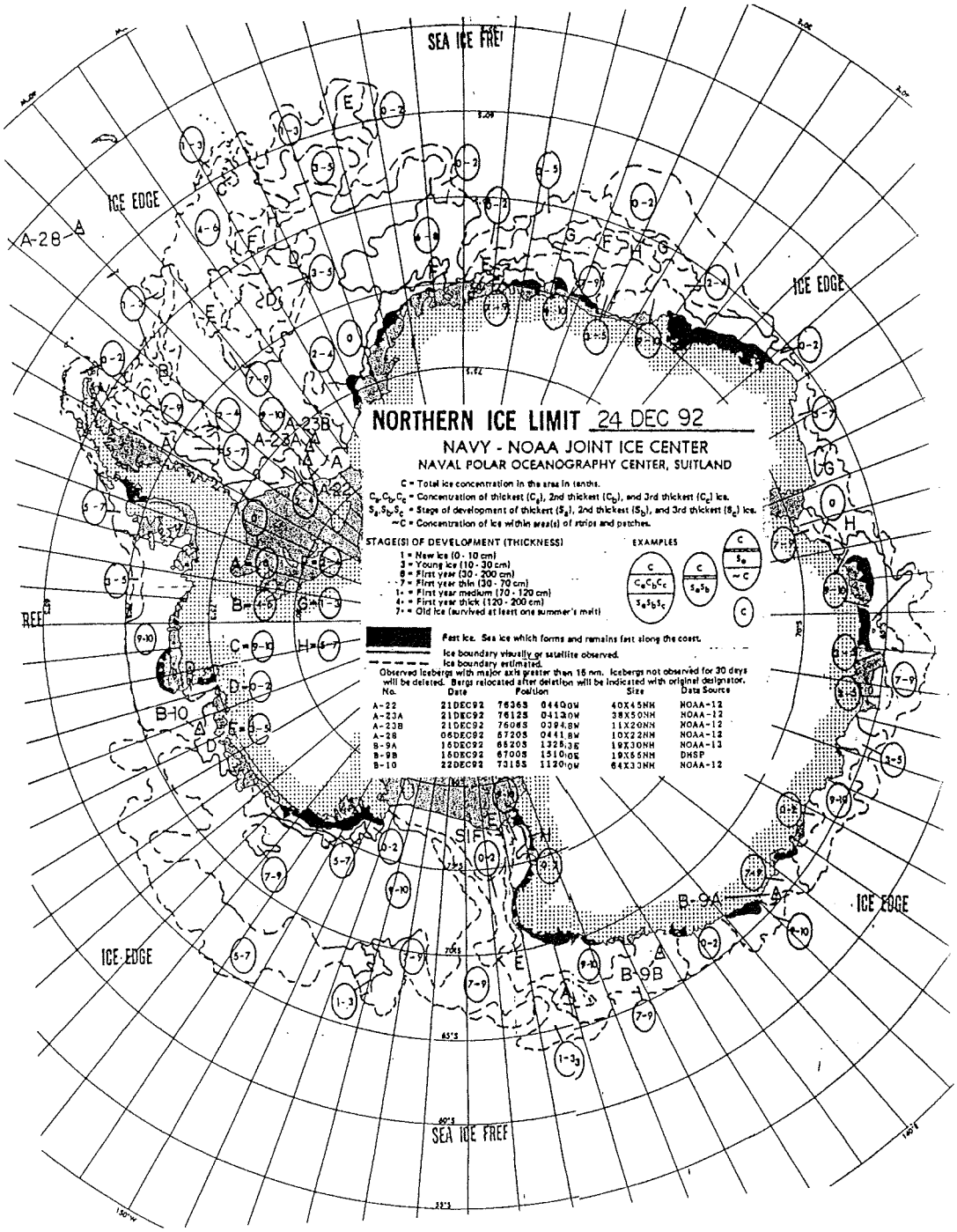

ANT X/8
USHUAIA - BREMERHAVEN 24.01.93 - 22.02.93

1. Zusammenfassung und Fahrtverlauf

Auf ihren fast regelmäßigen Reisen zwischen der Antarktis und dem Heimathafen bietet sich "POLARSTERN" als bewegliches Observatorium für großskalige Prozesse in Ozean und Atmosphäre an. Die meisten auf der Heimreise aus der Antarktis durchgeführten Untersuchungen waren deshalb Teile von langfristig angelegten Beobachtungsprogrammen. Dazu gehörten fast alle chemischen Spurenstoffprojekte, die globale Erfassung des CO_2-Gehalts in Luft und Oberflächenwasser, die Ozonmessungen sowie die Aufnahmen der Temperaturverteilungen in der Deckschicht des Meeres mit XBT- und in der Atmosphäre mit Radiosonden. Ferner kam auf dieser Reise ein neuentwickeltes Schiffslidar-Gerät zu seinem Ersteinsatz. Parallel dazu wurden zahlreiche optische Eigenschaften des Meerwasser gemessen, die sowohl für das neue System als auch für die Satellitenfernerkundung weltweiter Algenverteilungen notwendig sind.

Da die Mehrzahl der Spurenstoffproben unter Reinstraumbedingungen im Labor an Land analysiert werden müssen, kann über erste Ergebnisse nur wenig berichtet werden. Die Konzentration des Ozons in Bodennähe stieg beim Überqueren der Innertropischen Konvergenzzone (etwa am Äquator) sprunghaft auf fast den doppelten Wert an (von 20 auf 35-40 ppb). Die Messungen sollen zur Klärung der Frage beitragen, ob dieser Anstieg hauptsächlich durch die stärkere anthropogene Belastung der Nordhemisphäre oder aber durch natürliche Effekte verursacht wird.
In der Südhemisphäre liegt die Rußbelastung der Luft über dem Ozean unterhalb der Nachweisgrenze des empfindlichen Gerätes. Auf der Nordhalbkugel wurden diese Messungen zeitweise erheblich durch Saharastaub gestört, so daß eine eventuell stärkere Rußbelastung der nördlichen Hemisphäre, die infolge infolge des größeren vom Menschen hervorgerufenen Eintrags auf der Landhalbkugel erwartet wird, wahrscheinlich nicht nachgewiesen werden kann.

Die fortlaufenden Registrierungen der CO_2-Konzentration in Luft und Wasser haben ergeben, daß das Meer zwischen 40° und 30° Süd CO_2 aufnimmt während fluktuierende Übersättigungen zwischen 30°S und 5°N angetroffen wurden.
Das Wasserstoffperoxid, ein wichtiges "Reinigungsmittel" in der Luft, zeigt ein Konzentrationsprofil mit einem breiten Maximum zwischen den Wendekreisen. Seine Konzentration in der sauberen Atlantikluft hängt hauptsächlich von der Sonneneinstrahlung ab. In das Oberflächenwasser gelangt es wohl überwiegend aus der Luft und weniger durch photochemische Reaktionen im Meerwasser, darauf deuten jedenfalls die bisherigen Messungen hin.
Als beachtlicher Erfolg muß schließlich der Ersteinsatz eines Schiffs-Lidar-Gerätes bezeichnet werden, das bereits nach 8 Tagen Installationszeit nahezu im Routinebetrieb gefahren werden konnte.

"POLARSTERN" verließ am 24. Januar 1993 vormittags bei herrlichem Wetter die Reede vor Ushuaia, folgte dem Beagle Kanal und überquerte dann mit nordöstlichen Kursen den Patagonischen Schelf. (Fig. 8.1.1) Der Äquator wurde am 7. Februar auf 26°W überschritten. Nördlich der Insel Texel, nur 110 sm vom Heimathafen entfernt, geriet das Schiff in der Nacht vom 20.2. zum 21.2.93 in einen heftigen NW-Sturm mit

gewaltigen Grundseen auf 24 - 30 m Wassertiefe, die zu beträchtlichen Seeschäden im Wohnbereich und an Deck führten. Selbst 12 m über der Wasserlinie wurde noch Sand vom Nordseeboden gefunden. Das Schiff lief mit 14 Stunden Verspätung in Bremerhaven ein.

1. Summary and itinerary

During her almost regular cruises between Antarctica and the homeport "Polarstern" offers herself as a mobile observatory for large scale processes in ocean and atmosphere. Most of the investigations on this home-cruise, therefore, were parts of long-term observation programmes. This is true for almost all of the chemical projects on trace compounds, the global monitoring of CO_2 in air and water, and the measurements of temperatures in the surface layers of the ocean using XBTs, and radiosondes in the atmosphere. Moreover, this cruise saw the first measurements with a newly developed ship-borne Lidar system. In parallel, numerous optical properties of sea-water were recorded as necessary for the new system as well as for satellite remote sensing of world-wide algae distributions. Most of the trace compounds can only be analysed under clean laboratory conditions. Therefore only few remarks can be made on first results. The concentration of near-surface ozon abruptly increased by a factor of almost 2 (from 20 to 35-40 ppb) while passing the intertropical convergence (near the equator). The measurements will contribute to the question whether this increase is caused by man-made loading or natural effects.

The soot load of the southern-hemispheric air was below the limit of detection of the sensitive detector. In northern hemisphere the measurements were heavily disturbed by the presence of Sahara dust from time to time. Therefore it will hardly be possible to assess the man-made component.
The determinations of CO_2 in air and water show that there is an uptake of CO_2 by the ocean between 40° and 30°S. Fluctuating oversaturations occured between 30°S and 5°N.
H_2O_2, which is an important "cleaning promoter" in air, shows a concentration profile with a broad maximum in between the tropics. Its concentration in the clean air over the Atlantic depends primarily on the sun's radiation. Its presence in surface water appears to result mainly from input from air rather than by photochemical reactions in sea water. Finally, a great success was the first employment of a ship-borne Lidar system. After 8 days of installation time the system could almost be operated on a routine basis.

"Polarstern" left Ushuaia the morning of 24 January 1993. During excellent weather conditions she followed the Beagle Channel and sailed across the Patagonian Shelf with NE course (Fig. 8.1.1). The equator was crossed at 26°W on 7 February. North of the Isle of Texel, only 110 miles away from the home port, the ship met a violent NW-storm with huge breakers on a water depth of 24 to 30 m. In the night from 20th to 21st February considerable damage occured in some cabins and on deck. Even 12 m above the trim line North Sea sand was found on the decks. The ship was late by 14 hours when arriving in Bremerhaven.

Fig. 8.1.1 Cruise ANT X/8 - Atlantic Transect, Ushuaia to Bremerhaven

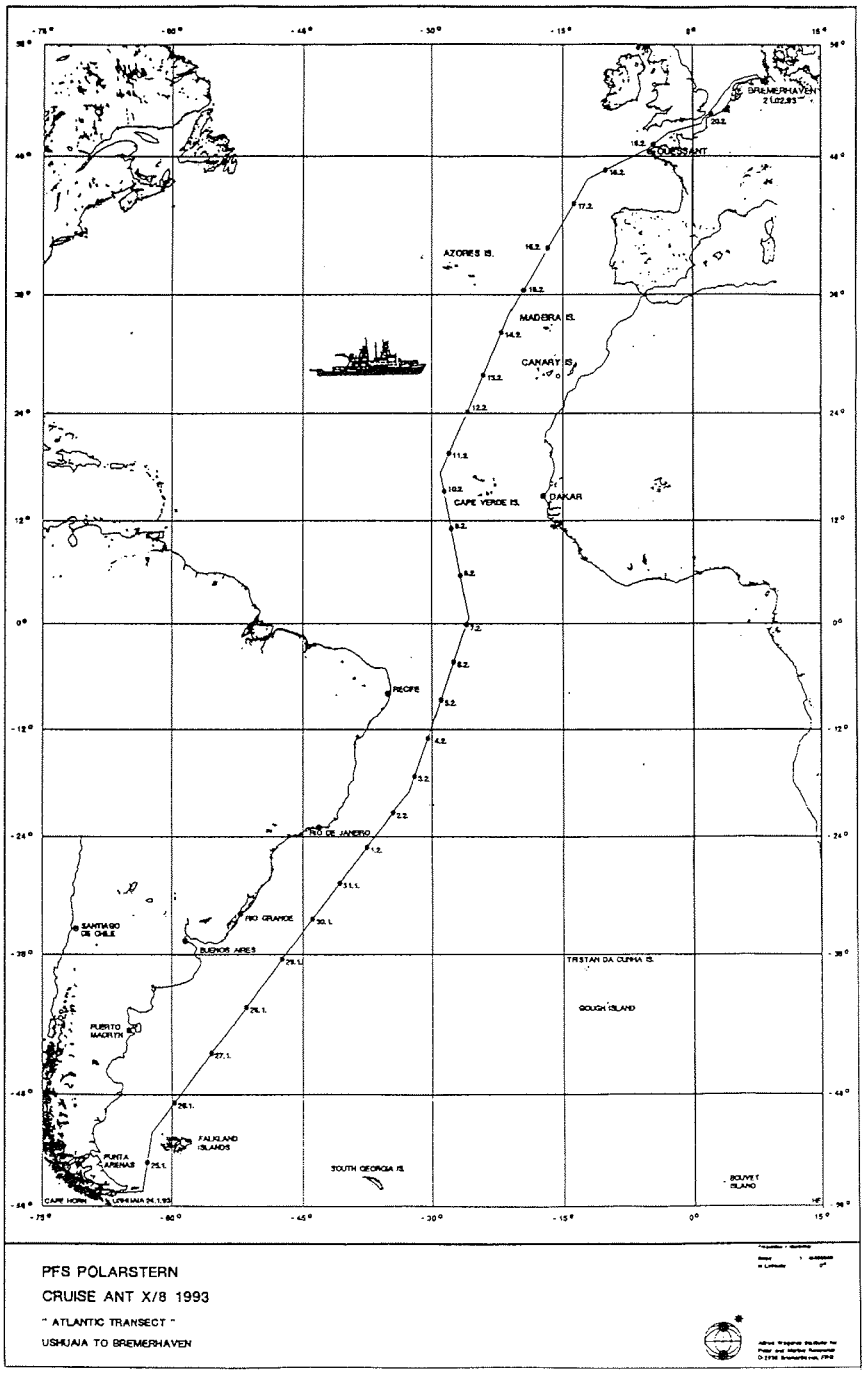

2. Wetter

H. Weiland (DWDS)

Das Wetter in der ersten Woche wurde zunächst bestimmt von einem mehr oder weniger stationären Tiefdrucksystem über der antarktischen Halbinsel. Einzelne Tiefkerne zogen aus dem Seegebiet vor Südwest-Chile über Feuerland ostwärts in Richtung Weddellsee. Damit befand sich die "Polarstern" vorwiegend im Einfluß-bereich nordwestlicher bis westlicher Winde mit Stärken zwischen Bft 4 und 6. An den letzten Tagen des Monats Januar verlagerte sich der Schwerpunkt der zyklonalen Aktivität mehr nach Osten, es entwickelte sich ein Sturmtief östlich von Südgeorgien, während sich hoher Druck über Patagonien aufbaute. In Verbindung mit einem kleinräumigen Tief über Südbrasilien stellte sich ein "sudestada", ein Südostwind vor der La Plata-Mündung ein, der auf der Fahrtstrecke der "Polarstern" zeitweise bis Bft 7 auffrischte. Nach Durchquerung einer Kaltfront trat die Polarstern am Sonntag, dem 1. Febuar in den Breich des südatlantischen Passats ein. Der Wind wehte vor der südbrasilianischen Küste zunächst aus Nordost, drehte später dann über Ost auf Südost. Die Stärke lag einheitlich um die 5 Bft. Am 07.02. wurde um 12:23 Uhr der Äquator überquert. Um 17:00 Uhr durchfuhr die "Polarstern" bei etwa 1°N die ungewöhnlich südlich liegende ITC, verbunden mit einer sprunghaften Winddrehung von Südost auf Nordost. Dabei trat ein Gewitter mit einer sehr hohen Niederschlagsintensität auf. Die dritte Woche wurde bestimmt von einem sehr beständigen Nordostpassat, der unmittelbar nach Durchqueren der ITC am 07.02. einsetzte. Die Stärke lag generell um 5 Bft, nur vorübergehend wurden 6 bis 7 Bft erreicht. Am 10.02. befand sich eine Höhenkaltfront im Fahrtgebiet der "Polarstern", die über der sonst unveränderten Passatinversion lag und ostwärts schwenkte. Sie führte zu örtlichen gewittrigen Niederschlägen. Am 12.02. wurde das Gebiet des Subtropenhochs erreicht. Dabei lagen die Windstärken nur noch um Bft 3. Allerdings erreichte uns eine etwa 4 m hohe lange Dünung aus Nordwest, die auf der Rückseite mehrerer Orkantiefs bei Island im Seegebiet zwischen Grönland und Neufundland gebildet worden war. In den Frühstunden des 14.02. schwenkte die erste atlantische Kaltfront durch. Sie war verbunden mit einem Kaltluftausbruch in der Höhe, der zu einem cut-off-Prozeß führte. Damit bildete sich bei den Azoren ein umfangreiches Tief, nördlich davon eine kräftige Hochzelle, wodurch der Wind sich wieder auf Nordost mit Stärken um Bft 6 einstellte und auf der Strecke bis zum Ärmelkanal erhalten blieb. In diesen Tagen entwickelten sich bei Südgrönland mehrere Tiefs zu Sturmwirbeln und wurden um das Hochdruckgebiet herumgesteuert. Sie zogen von Island in Richtung Baltikum und bauten das mitteleuropäische Hoch ab. Es bildete sich ein Sturmfeld über der Nordsee aus, das bis zum Einlaufen in Bremerhaven erhalten blieb. In den folgenden Abbildungen sind die wichtigsten Wetterparameter dargestellt. (Fig. 8.2.1)

Fig. 8.2.1 Wetterparameter vom 24.01. - 19.02.1993:
a) Windstärke in Bft, b) Windrichtung, c) Luftdruckverlauf, d) Luft- und Wassertemperatur

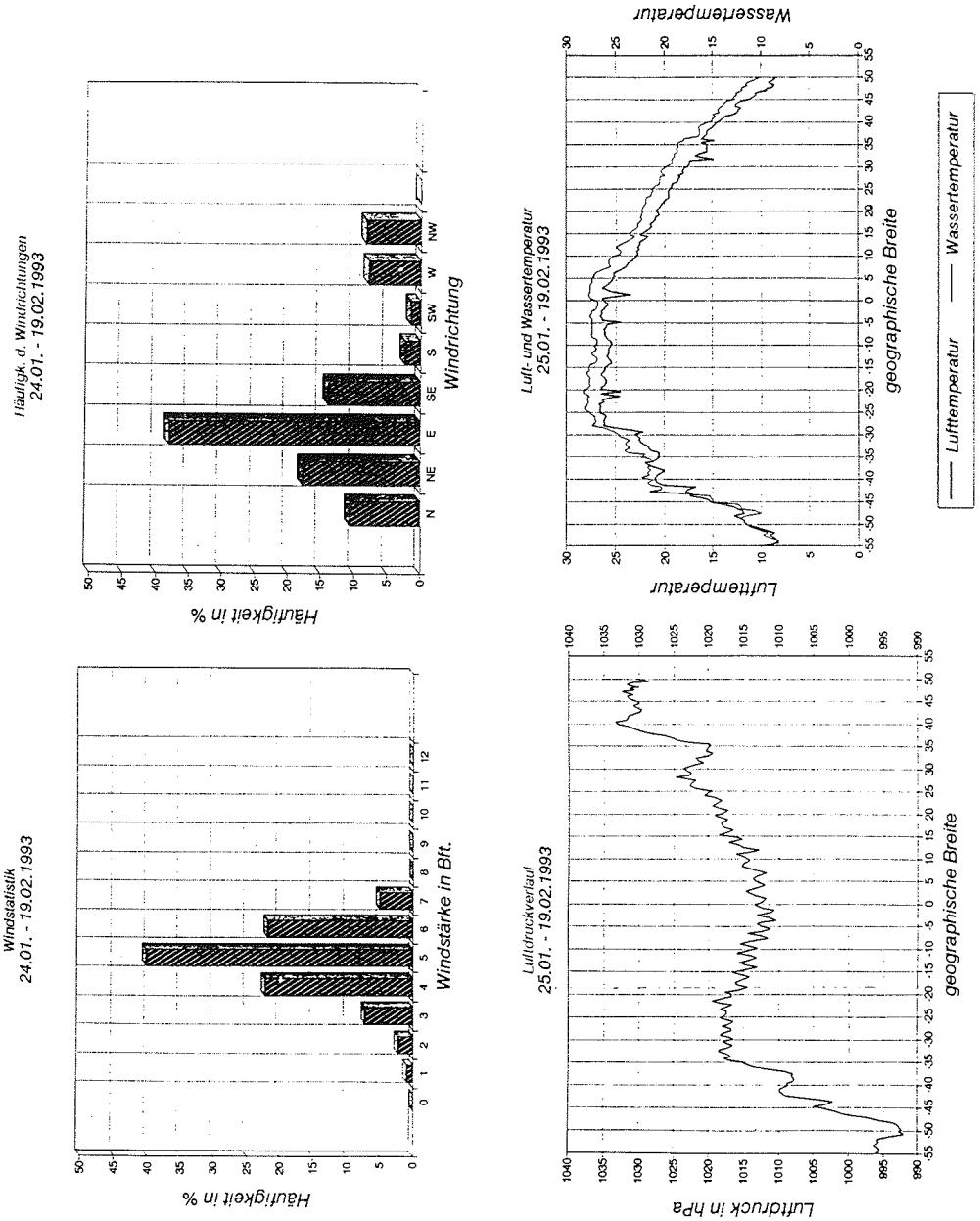

3. Globale Aspekte der Umweltchemie: Ferntransport von organischen Spurenstoffen.

K. Ballschmiter (UUl)

Eine 6-köpfige Gruppe der Abteilung Analytische Chemie und Umweltchemie der Universität Ulm unter Leitung von Prof.Dr. K.Ballschmiter führte umfangreiche Probenahmen zur Bestimmung von organischen Spurenstoffen in der marinen Grenzschicht der Troposphäre und im Oberflächenwasser des Süd- und Nord-Atlantiks durch. Die nachfolgend im einzelnen dargestellten Vorhaben sind Teile eines Gesamtvorhabens, das sich mit dem globalen Verbleib von organischen Xenobiotika unter den Gesichtspunkten von regionalen Quellen, Ferntransport und Transformationen in der Atmosphäre beschäftigt. Xenobiotika sind Stoffe, die in der Natur nicht vorkommen, sondern vom Menschen in die Umwelt eingebracht werden und von Wind- und Meeresströmungen über globale Entfernungen transportiert werden. Besonders interessiert dabei der Austausch zwischen der Nord- und der Süd-Hemisphäre. (K. Ballschmiter, (1992) Transport und Verbleib organischer Verbindungen im globalen Rahmen. Angewandte Chemie 1o4: 5o1-528).

Auf der Fahrtstrecke ANT X/8 von Feuerland nach Bremerhaven wurden 93 Luft- und 61 Wasserproben genommen, um die Verteilung der polychlorierten Biphenyle (PCBs), der halogenierten Phenylmethylether (Anisole), und von Alkylnitraten und halogenierten Kohlenwasserstoffen in der Luft und im Meerwasser entlang der Fahrtroute zu untersuchen. Die Untersuchungen sind u.a. Teile des DFG Vorhabens Ba371,11-2, das Fragen der globalen Aspekte der Umweltchemie zum Thema hat

Bei der hochvolumigen Probenahme von Luft werden 100 - 1000 m^3 angesaugt und über ein Adsorbens geleitet, auf dem die organischen Spurenstoffe, die sich in der Luft befinden, festgehalten werden. Damit sollen u.a. die PCBs wie auch Alkylnitrate bestimmt werden, die in der Troposphäre durch die Reaktion organischer Verbindungen mit Stickoxiden entstehen.

Bei der hochvolumigen Probenahme von Seewasser wird auch durch Adsorption angereichert. Hier werden Glaskartuschen mit einem Adsorbens gefüllt und an die im Schiff eingebauten Seewasserleitungen angeschlossen. Die Ergebnisse dieser Untersuchungen sollen Aufschluß über den Austausch organischer Spurenstoffe zwischen der Meeresoberfläche und der Luft liefern. Außerdem werden neue Adsorbentien für die Extraktion des Wassers getestet.

Doch nicht nur die Verteilung von anthropogenen Stoffen interessiert die Ulmer Arbeitsgruppe. Ein weiteres Vorhaben beschäftigt sich mit halogenierten aromatischen Verbindungen, die auf natürlichem Weg durch Biohalogenierung im Meer entstehen. Auf dieser Reise soll untersucht werden, ob sich die Höhe der Primärproduktion im Atlantik und die Gehalte von halogenierten Anisolen (Phenylmethyl-ether) in der Luft korrellieren lassen. Solch eine Korrelation ist naheliegend; sie konnte bei Untersuchngen auf der Insel Reunion in südlichen Indischen Ozean wahrscheinlich gemacht werden. Einen eindeutigen Beweis sollen die auf dieser Reise gezogenen Luftproben bringen.

Alle Proben werden nach Rückkunft in Ulm unter Reinstraumbedingungen und strengster Blindwertkontrolle aufgearbeitet. Die Ergebnisse sollen mit denen von

früheren Fahrten mit der FS "POLARSTERN" in den Jahren 1985, 1990 und 1991 verglichen werden. Es werden sich so erste Aussagen über die Konstanz oder einen zeitlichen Trend von globalen Transport- und Verteilungsvorgängen machen lassen. Es ist geplant an weiteren Nord-Süd- bzw. Süd-Nord -Traversen der FS "POLARSTERN" über den Atlantik teilzunehmen.

3.1. Quellen von halogenierten Anisolen im Süd- und Nord-Atlantik

U. Führer (UUI)

Um die erwartete biogene Bildung von halogenierten Anisolen (Phenylmethyl-ether mit Brom und Chlor als Substituenten) in den Bereichen erhöhter und hoher Primärproduktion im ozeanischen System zu überprüfen, wurden entlang der Fahrtroute von Feuerland bis zur Biskaya Luftproben mit der High-Volume-Sampling Technik genommen. Als Adsorbens wurde hochgereinigtes und aktiviertes Kieselgel eingesetzt. Es wurden 15 Proben gesammelt, wobei in den gemäßigten Breiten 500 m^3 und in den Tropen 300 m^3 Luft durchgesetzt wurden. In den Tropen ist die Adsorptivität des Kieselgels wegen der hohen Luftfeuchtigkeit und der zusätzlich erhöhten Temperatur vermindert, so daß nur eine geringere Luftmenge gesammelt wurde, um die Wasserbeladung des Adsorbens niedrig zu halten.

Das Kieselgel wurde sofort nach der Probenahme in Glaskartuschen eingeschmolzen, in denen es bereits vor der Probenahme gelagert wurde. Die Proben werden im Anschluß an diese Reise aufgearbeitet und die Gehalte der verschiedenen halogenierten Anisole mittels Kapillargaschromatographie und Elektroneneinfang sowie massenspektrometrischer Detektion bestimmt. Diese Werte sollen mit der Höhe der Primärproduktion im Atlantik verglichen werden.

Besteht für die halogenierten Anisole eine biogene Quelle im Atlantik, so sollte man in den Gebieten mit hoher Primärproduktion auch einen erhöhten Gehalt dieser Verbindungen vorfinden. Entsprechend sollte der Gehalt der halogenierten Anisole in den "Wüstengebieten" des Atlantiks sehr gering sein.

Außerdem wurden mit der gleichen Probenahmetechnik 5 weitere Luftproben um 50°S und im Bereich des Äquators genommen. Allerdings wurden hierbei 1000 m^3 bzw. in den Tropen 800 m^3 Luft extrahiert. Diese Proben sollen die Meßergebnisse früherer Reisen, bei denen der Gehalt an Polychlorierten Biphenylen (PCBs) ermittelt wurde, ergänzen Diese Proben werden in leicht modifizierter Weise ebenfalls im Anschluß an diese Reise aufgearbeitet

3.2. Globale Verteilung von Alkylnitraten in der marinen Grundschicht der Troposphäre

O. Luxenhofer (UUI)

Alkylnitrate sind Ester der Salpetersäure und werden durch photochemischen Abbau von Kohlenwasserstoffen in der Troposphäre gebildet. Die nach der Reaktion mit OH-Radikalen entstehenden Alkylradikale werden nach Sauerstoffanlagerung und Addition von Stickstoffmonoxid zu Alkylnitraten umgesetzt. Vor allem Städte und Industrieregionen stellen durch Verbrennung fossiler Brennstoffe, und den damit

verbundenen hohen NOx- und Kohlenwasserstoffemissionen, eine Hauptquelle für Alkylnitrate dar. Ob Alkylnitrate auch aus Kohlenwasserstoffen biogenen Ursprungs gebildet werden, und wie sie über die geochemischen Kreisläufe global verteilt werden, sollte auf diesem Fahrtabschnitt untersucht werden. Zu diesem Zweck wurden 20 Proben zur Aufarbeitung und Analyse in Ulm gesammelt.

Die Luftprobennahme wurde durch adsorptive Anreicherung von ca. 100 m^3 Luft auf einem hochgereinigten und aktivierten Kieselgel mit Hilfe von High-Volume-Luftsammelturbinen durchgeführt. Um die Adsorption für Alkylnitrate zu erhöhen, wurden dem Kieselgel noch 2% Aktivkohle vom Typ Carbopack B zugesetzt. Die Probenahmeorte auf der FS "POLARSTERN"wurden so gewählt, daß Blindwerte durch das Schiff selbst weitgehend auszuschliessen sind. Der Durchbruch der Alkylnitrate durch die Adsorbensschicht wird durch regelmäßige Verwendung einer zweiten Kieselgelschicht überprüft. Die Proben werden in luftdicht zugeschmolzenen Erlenmeyerkolben bis zur Aufarbeitung im Labor störungsfrei transportiert und gelagert.

3.3. Austausch von polychlorierten Biphenylen zwischen der Grenzschicht der Troposphäre und der Deckschicht im Süd- und Nordatlanik

P. Pagel (UUI)

Polychlorierte Biphenyle (PCBs) sind durch weitgefächerte technische Anwendungen in den letzten Jahrzehnten in großen Mengen in die Umwelt gelangt. Aufgrund ihrer Persistenz und ihrer hohen Fettlöslichkeit besitzen sie eine große Umweltrelevanz. Sie stellen zudem durch das Vorkommen von über einhundert Einzelverbindungen, die über ein weitgefächertes Spektrum an physikalischen Eigenschaften verfügen, ein hervorragendes System von Leitchemikalien zur Untersuchung der molekularen Parameter des globalen Ferntransportes dar.

Auf den Fahrten ANT IX/1 und ANT IX/4 des FS "POLARSTERN" wurden bereits Luftproben genommen und in verschiedenen Breiten teilweise überraschend hohe bzw. niedrige Werte an PCBs festgestellt. Die Verteilung der PCBs zwischen Luft und Wasser sollte gemäß physikochemischen Gleichgewichtsgrößen vorliegen. Gemessene Gehalte im Oberflächenwasser können so zur Klärung der Gehalte in der Luft beitragen.

Aufgrund der Gleichgewichtskonstanten kann man die PCBs in einem Konzentrationsbereich von 0,1 Nanogramm/m^3 erwarten. Es ist daher erforderlich, Wasservolumina von mindestens 1ooo l zu beproben, um ausreichende Mengen des Analyten zu erhalten. Dies wurde realisiert durch Einsatz größerer Mengen eines polymeren Adsorbens (90 g XAD2).
Insgesamt wurden 14 Wasserproben genommen, mit dem Schwerpunkt im Südatlantik und dem Bereich der ITCZ. Die Glaskartuschen wurden an im Schiff vorhandene Seewasserleitungen angeschloßen (Einlaß in 10 m Tiefe). Es konnte beobachtet werden, daß sich Gelbstoff an der Glaswolle und später auch am Adsorbens abschied.

Der Gehalt an Plankton im Wasser schränkte oftmals die Möglichkeit eines großen Wasserflußes ein (100 l/Stunde). Die durchschnittliche Flußgeschwindigkeit betrug

35- 50 l/Stunde, d.h. es wurden 20 bis 24 Stunden für eine Probe gesammelt. Die Adsorbensproben werden in vorgereinigten Glasbehältern unter Seewasser verschlossen zur Untersuchung nach Ulm gebracht. Dort werden sie nach entsprechender Probenvorbereitung mittels Kapillargaschromatographie und massenspektrometrischer Detektion untersucht.

3.4. Bestimmung des Interhemisphären-Transports von leichtflüchtigen Halogenkohlenwasserstoffen (low volume sampling)

Th. Wiedmann (UUl)

Zur Analyse von leichtflüchtigen Halogenkohlenwasserstoffen und anderer leichtflüchtiger Verbindungen (z.B. C1-C8 - Alkylnitrate) in mariner Reinluft wurden während der Atlantiküberquerung ANT X/8 des FS "POLARSTERN" von Ushuaia nach Bremerhaven Luftvolumina von 1 bis 30 Liter gesammelt. Die adsorptive Anreicherung der Spurenstoffe erfolgte überwiegend auf Tenax, einem für die ATD-Technik (Adsorption + Thermische Desorption) bereits bewährten, organischen Polymer. Daneben wurde ein neues Adsorbens auf Kohlenstoffgranulatbasis getestet (Carboxen) und damit acht Proben genommen.
Über den gesamten Streckenabschnitt von Feuerland bis zur Biskaya wurden 50 Luftproben gesammelt, wobei der Schwerpunkt auf die südliche Hemisphäre gelegt wurde. Hier liegen uns vor allem südlich des 30. Breitengrades Süd nur sehr wenig Meßergebnisse vor. Nach Auswertung der Proben in Ulm wird die meridionale Verteilung der leichtflüchtigen Spurenstoffe wichtige Informationen über ihr Verhalten in der Atmosphäre, d.h. über ihre Quellen und Senken, sowie ihre Aufenthaltsdauer in diesem Umweltkompartiment liefern. Wir knüpfen dabei an Untersuchungen im Jahr 1985 an. Damals wurden in ähnlicher Technik Luftproben auf der FS "POLARSTERN" auf ihrer Heimfahrt von Kapstadt nach Bremerhaven gesammelt.
Als Probenahmeort an Bord der FS "POLARSTERN" erwies sich schon 1985 der Bugauslegekran als besonders geeignet, um Blindwerteinflüsse vom Schiff so gering als möglich zu halten. Eine Probe, die achtern in der Abgasfahne genommen wurde, soll einen möglichen Einfluß des Schiffes selbst auf die Spurenstoffgehalte dokumentieren.
Im Bereich 15°S bis 15°N wurden drei Proben mit 120 Liter Luftvolumen gesammelt, um vergleichbare generelle Muster von ECD-aktiven Verbindungen zu erhalten.
Wetter- und Seegangsverhältnisse ließen während der gesamten Fahrt eine kontinuierliche Probenahme zu.

3.5. Hochvolumige Probenahme (2-5 m^3) zur Bestimmung von organischen Spurenstoffen im Seewasser

U. Reuter (UUl)

Auf dem Fahrtabschnitt ANT X/8 der FS "POLARSTERN" wurde Oberflächenwasser unter verschiedenen Aspekten beprobt. Damit wurde an frühere Untersuchungen, u.a. auch auf der FS "POLARSTERN", angeschlossen. Unsere bisherigen Ergebnisse zum Vorkommen von halogenierten organischen Verbindungen im Wasser des Süd- und Nord-Atlantiks sollen damit erhärtet und durch die Untersuchung auf weitere Stoffklasse(n) ergänzt werden. Es wurden erprobte und

neue Sammeltechniken unter Verwendung neuartiger Kohlenstoffmaterialien für die adsorptive Anreicherung eingesetzt.

Die Probennahme erfolgte über die schiffseitig vorhandenen Seewasserleitungen (Klauspumpe mit im Kielbereich liegendem Spargel und Backenquetschpumpe mit Entnahme im Bugbereich). Um größere Mengen der interessierenden Verbindungen zu erhalten, wurde mit gegenüber früher deutlich erhöhten Sammelvolumina gearbeitet. Als Vorgabe war gesetzt worden, aus 2 bis 5 m^3 Seewasser adsorptiv anzureichern. Die notwendigen Wasserflüsse verursachten anfänglich Probleme, die wir aber während der Untersuchungsserie durch technische Maßnahmen begrenzen konnten. Aus den Erfahrungen während der Probenahmen und unseren apparativen Variationen werden wir neue optimalere Anordnungen entwickeln.

Die Untersuchungen bestätigten unsere Vermutung, daß die Bedingungen des Sammelns von Meerwasser mit Süßwasser im Labor nur unzureichend zu simulieren sind.

Die uns interessierenden Verbindungen werden aus dem Meerwasser adsorptiv angereichert. Zur Wasserprobenahme wurden drei verschiedene Adsorbentien eingesetzt, und zwar: XAD 2 Harz, ein poröses organisches Polymer, des weiteren eine spezielle granulierte Aktivkohle und schließlich synthetisches Kohlenstoffvlies.

Es wurden insgesamt 20 hochvolumige Proben gezogen. Die auf Kohlenstoff basierenden Adsorbentien werden in vorgereinigten Glasbehältern unter Seewasser verschlosen nach Ulm gebracht und analog zu den XAD-Adsorbentien (Vorhaben P.Pagel) aufgearbeitet.

4. Ozonsondierungen, Verteilung von H_2O_2 in der marinen Troposphäre und im Oberflächenwasser

R. Weller (AWI)

Die luftchemischen Untersuchungen des AWI befaßten sich mit der Verteilung der Photooxidantien Ozon (O_3) und Wasserstoffperoxid (H_2O_2), sowie von Aerosolen und Rußpartikeln in der marinen Atmosphäre des Atlantischen Ozeans.
Der Schwerpunkt der Arbeiten konzentrierte sich auf die horizontale und vertikale Verteilung von Ozon. Die Ozonkonzentration in Bodennähe wurde kontinuierlich mittels einem auf UV-Absorption basierenden O_3-Analysators aufgezeichnet, während zur Erfassung der vertikalen Ozonprofile ballongetragene, elektrochemische Konzentrationssonden (ECC-Sonden) zum Einsatz kamen. Die Ballone waren mit einer modifizierten Radiosonde (RS 80-15) ausgestattet, die die in situ gemessenen Ozonpartialdrucke zusammen mit der Temperatur, der relativen Luftfeuchte und dem Luftdruck per Funk an die Bodenstation auf Polarstern übertrugen. Täglich wurde eine Ozonsondierung zur Mittagszeit und zusätzlich jeden zweiten Tag eine weitere auch nachts durchgeführt. Die ballongetragenen Sonden erreichten typischerweise eine Gipfelhöhe von 32-36 km, in günstigen Fällen 38 km.
Die Verteilung des Ozons in Bodennähe zeigte in der südlichen Hemisphäre Konzentrationen um 15 ppbv (Fig. 8.4.1). Episodenhaft stiegen die Konzentrationen auf bis zu 30 ppbv und zwar immer dann, wenn westliche Winde Luft kontinentalen Ursprungs zum Meßort transportierten, oder aber beim durchqueren von Gewitterwolken. Während im ersten Fall wahrscheinlich anthropogene Einflüße zu

einer photochemischen Ozonbildung führten, wurde im letzten Fall der verstärkte Austausch troposphärischer mit stratosphärischer Luftmassen durch die bis in die Tropopause reichenden Cumulonimbuswolken verursacht. Abgesehen von diesen Ereignissen lag die Ozonkonzentration der praktisch unbelasteten marinen Troposphäre der Südhemisphäre bei 15 ppbv. Beim Überqueren der Innertropischen Konvergenzzone (ITCZ) stieg mit Erreichen der Nordhemisphäre die durchschnittliche Ozonkonzentration auf 35-40 ppbv. Verantwortlich für diese über doppelt so hohen Ozonkonzentrationen werden zum einen die um 1-2 Größenordnungen stärkere Belastung der Nordhemisphäre mit Stickoxiden (NO_x) gemacht, die über folgenden Mechanismus zu einer Netto - Ozonproduktion führen (M= N_2, O_2):

$$NO_2 + h\nu \rightarrow O + NO \quad (1)$$

$$O + O_2 + M \rightarrow O_3 + M \quad (2)$$

Zum anderen spielen aber auch natürliche dynamische Prozesse eine Rolle: der Austausch troposphärischer mit stratosphärischer Luftmassen ist in der nördlichen Hemisphäre wesentlich höher als in der südlichen Hemisphäre. In der relativ unbelasteten südlichen Hemisphäre sind diese großskaligen vertikalen Advektionsprozesse praktisch die einzige Quelle für troposphärisches Ozon, da photochemische Ozonproduktion aufgrund des niedrigen NOx-Pegels vernachläßigbar ist.
Aus einer vorläufigen Auswertung der Ozonsondierungen ergeben sich folgende Resultate:
1) Auf einigen vertikalen Ozonprofilen sind weitere Maxima der Ozonkonzentration in der Tropopause und der oberen Troposphäre zu erkennen (Fig. 8.4.2). Dies deutet darauf hin, daß ozonreiche Luftmassen aus der unteren und mittleren Stratosphäre in die Troposphäre transportiert wurden; damit korreliert auch ein deutlicher Anstieg im Temperaturprofil in der selben Luftschicht.
2) Häufig war das Ozonprofil in der Troposphäre negativ mit der relativen Luftfeuchte korreliert. Dies läßt auf eine verstärkte photochemische Ozonzerstörung in solchen Schichten schließen:

Fig. 8.4.1 Breitengradabhängigkeit des Ozon-Mischungsverhältnisses.
Δ: Luftmasssen aus belasteten Gebieten Südamerikas.

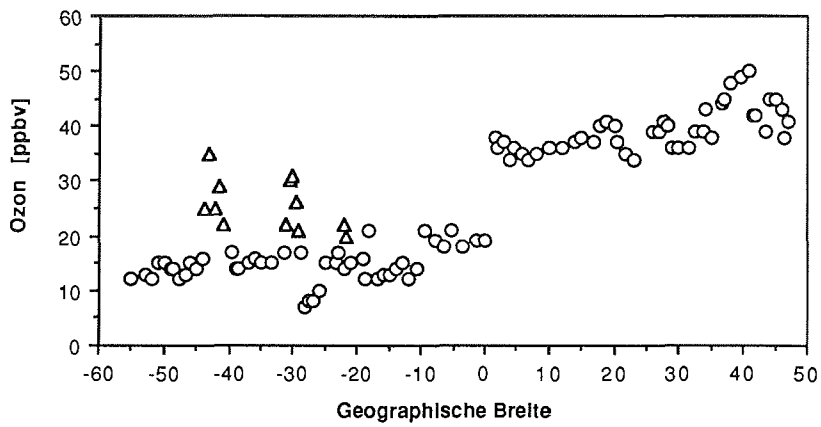

Fig. 8.4.2 Vertikales Ozonprofil vom 14.02.93; Position: 33°06´N / 26°36´W.

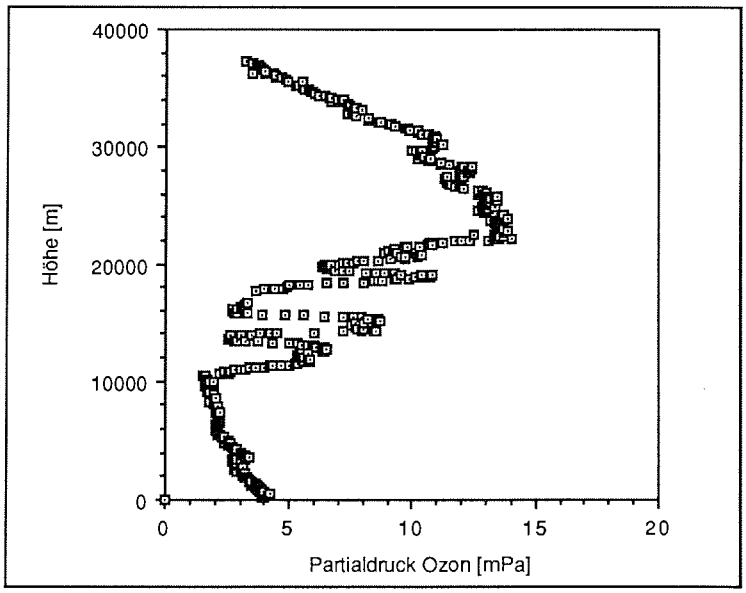

Dabei reagieren die aus der O_3-Photolyse gebildeten elektronisch angeregeten Sauerstoffatome (O^1D) sehr rasch mit H_2O zu OH-Radikalen, die ihrerseits ein weiteres Ozonmolekül zerstören. Die Reaktionen (5) und (6) führen letzlich zu einem katalytischen Ozonabbau. Bei geringem H_2O-Gehalt würden die O^1D-Atome zu Grundzustands O_3P-Atome relaxieren und über Reaktion (9) wieder Ozon produzieren, so daß daraus kein Ozon-Nettoverlust resultiert:

$$O_3 + h\nu \rightarrow O^1D + O_2 \quad (3)$$

$$O^1D + M \rightarrow O_3P + M \quad (8)$$

$$O_3P + O_2 + M \rightarrow O_3 + M \quad (9)$$

Eine detaillierte Auswertung des umfangreichen Meßdatenmaterials muß am AWI in Bremerhaven erfolgen. Die Ozonmessungen sind als langfristig angelegtes Meßprogramm zu sehen. Die Ergebnisse sollen Eingabedaten für mathematische Modellsysteme liefern und zur Klärung der Frage beitragen, ob die doppelt so hohen Ozonbelastungen der nördlichen Hemisphäre hauptsächlich anthropogen oder aber durch dynamische Prozesse verursacht wird.

Die horizontale Verteilung von H_2O_2 in der marinen Troposphäre des Atlantiks und im Oberflächenwasser war ein weiterer Schwerpunkt des Meßprogrammes. Dabei stand die Frage, welches die Hauptquelle für marines H_2O_2im freien Ozean ist, im Vordergrund. Wasserstoffperoxid wurde mittels einer fluorimetrischen Methode quantifiziert, wobei die Konzentration des gasförmigen H_2O_2 kontinuierlich aufge-

zeichnet wurde. Zur Bestimmung des im Oberflächenwasser befindlichen H_2O_2und seines Tagesganges wurden typischerweise 5 Wasserproben am Tag analysiert (Fig. 8.4.3) und insgesamt 3 Tiefenprofile (zweimal bis 200 m Wassertiefe und einmal bis 1000 m Wassertiefe) gemessen (Fig. 8.4.4).
Die gemessenen, breitengradabhängigen Konzentrationen des troposphärischen H_2O_2 bestätigen die Ergebnisse des Fahrtabschnittes ANTX/1: das Konzentrationsprofil zeigt ein breites Maximum zwischen den Wendekreisen mit abfallenden Werten zu höheren Breitengraden: in Reinraumbebieten ist die Wasserstoffperoxidkonzentration hauptsächlich von der Sonnenintensität abhängig. Die Verteilung von H_2O_2 im Oberflächenwasser des Atlantiks zeigt keinen einheitlichen Gang (Fig. 8.4.3). Eine vorläufige Analyse der Meßdaten läßt den Schluß zu, daß die Hauptquelle für marines H_2O_2 im freien Ozean der Eintrag aus der Atmosphäre ist, während H_2O_2 Produktion durch photochemische Reaktionen im Meerwasser eine untergeordnete Rolle spielen. Zusätzlich zu den auf H_2O_2 untersuchten Proben wurden gleichzeitig Wasserproben zur Bestimmung des Gesamtgehaltes an gelöstem Kohlenstoff (DOC) genommen (die Analysen können erst am AWI durchgeführt werden). Photooxidationsprozesse des DOC werden als eine weitere Quelle für marines H_2O_2 angesehen. Eine Korrelation mit den gemessenen H_2O_2 Werten soll einen sichereren Aufschluß bezüglich der Bedeutung dieser Prozesse liefern. Auch der, im Vergleich mit der kontinentalen Troposphäre gemessene, erhöhte Anteil organischer Peroxide in der marinen Troposphäre (zwischen 30 und 40% des Gesamtperoxides, kontinental: zwischen 5 und 10%) ist auf die Tatsache zurückzuführen, daß der Ozean eine mächtige Senke für das wesentlich besser lösliche H_2O_2 ist (die Henry-Konstante ist ca. zwei Größenordnungen höher als die der organischen Peroxide).

Fig. 8.4.3 H_2O_2 Konzentrationen im Oberflächenwasser als Funktion der geographischen Breite

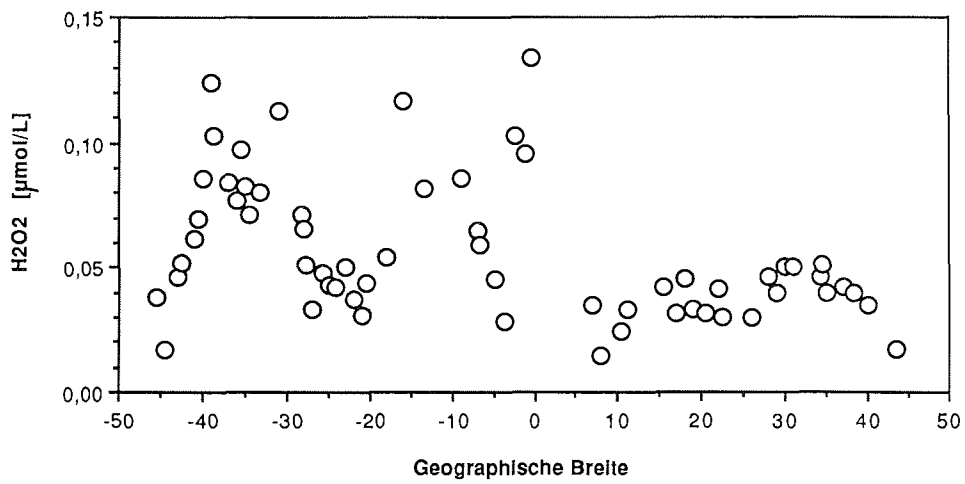

Fig. 8.4.4 Tiefenprofil der H_2O_2 Konzentration o: gemessen bei 13°24´S,30°40´W
Δ gemessen bei 9°8´S, 29°11´W; □: gemessen bei 11°9´N, 27°50´W.

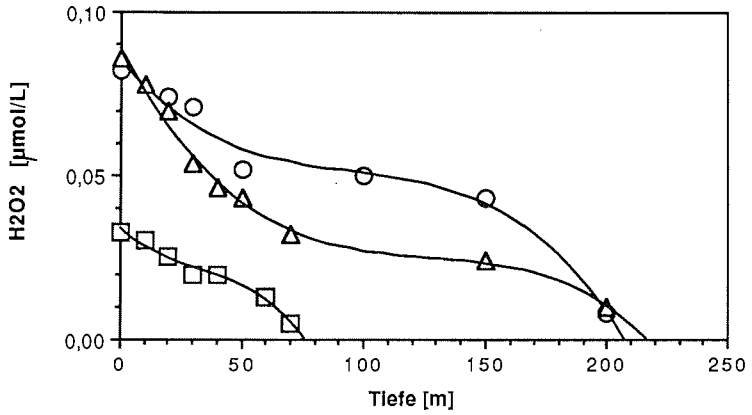

Die Rußbelastung der Atmosphäre ist im wesentlichen anthropogen bedingt (Verbrennung fossiler Brennstoffe), während der natürliche Eintrag durch Biomasseverbrennung (Waldbrände u. ä.) eine um Größenordnungen geringere Quellstärke aufweist. Die mit einem Aethalometer kontinuierlich durchgeführten Rußmessungen bestätigen, daß der Rußgehalt der relativ unbelasteten Südhemisphäre nahe der Nachweisgrenze des Gerätes bei ca. 5-10 ng/m³ liegt. Bei westlichen Winden stieg die Rußkonzentration parallel zur Ozonkonzentration periodenweise drastisch an. Erste Trajektorienanalysen zeigen, daß zu diesen Zeitpunkten Luftmassen aus verschiedenen Indutriezentren Südamerikas (Bahia Blanca, Buenos Aires und Montevideo) den Meßort erreichten. In der nördlichen marinen Troposphäre war der Gehalt an Ruß deutlich höher und lag zunächst bei 20-40 ng/m³, später in höheren Breiten bis zu 100 ng/m³, was auf die Verbrennung fossiler Brennstoffe in der stark industrialisierten Nordhemisphäre zurückzuführen ist. Bei ungünstigen Windverhältnissen wurden die Messungen jedoch episodenhaft ganz erheblich durch die Dieselabgase der FS Polarstern gestört und zwischen 2°N und 22°N dominierte der Eintrag von Saharastaub, transportiert durch den starken NO-Passat.

5. Latitudinal and temporal differences of CO_2 fluxes in the Atlantic Ocean

D.C.E. Bakker, A.A.J. Majoor (NIOZ)

Only 60% of the total industrial emission of CO_2 corresponds to the increase of atmospheric CO_2-content. Where the other 40% remains is unknown: it is absorbed by vegetation and, in particular, the oceans. Although 40% of the total industrial CO_2 emission is a considerable amount (about 70 to 100 gigatons carbon per year), it is only a minor fraction of total annual CO_2-exchange between oceans and atmosphere. This makes it difficult to measure the net uptake of CO_2 by the oceans. The aims of this project are to examine the CO_2 exchange between the atmosphere and the oceans and to determine which chemical, physical and biological factors

make a certain region a net CO_2 sink or well. The semi-annual cruises of FS Polarstern across the Atlantic are of great value, as CO_2 data of the South-Atlantic are rare, and they make a seasonal comparison of CO_2 exchange over a broad latitudinal range possible. Special attention is focused at 40° South, as there are some indications that a major CO_2 sink may occur at this latitude.

The CO_2-system consists of six variables (pH, Alkalinity, pCO_2, Total CO_2, $[HCO_3^-]$, and $[CO_3^{--}]$) and is described by four equations. Thus, knowledge of two variables enables to calculate the other parameters. Three parameters allow validation of the data by checking the accuracy of the techniques by calculating the internal consistency: e.g. using TCO_2 and alkalinity we can calculate the partial pressure of CO_2 (pCO_2), which one can compare with the value obtained by gaschromatography.

To realise this, pCO_2 in the atmosphere and the surface ocean are recorded online by a gaschromatograph. The temperature of the uppermost microns of the water column (skin temperature) is measured online by passive infrared detection. Alkalinity and total inorganic carbon (TCO_2) are determined eight times per 24 hours. To get a reliable view of the vertical distribution of CO_2, water samples at 200, 150, 100, 80, 60, 40, 20 and 10 meters depth are taken by CTD once a day. From preliminary data, which still have to be further corrected, some trends are visible: between 40° and 32°S undersaturation of pCO_2 in the surface waters occurs compared to the atmosphere, while at 30°S till 5°N a large supersaturation can be seen. A variable undersaturation is located at 5° till 40°N. TCO_2 data reveal an oceanward decrease of TCO_2 at the Patagonian shelf, resulting in very low TCO_2 values in the ocean waters of the southern hemisphere. TCO_2 increases at the northern hemisphere with latitude. CTD data show that TCO_2 is possitively correlated with depth, due to mineralisation of organic matter. Alkalinity data will be further processed to validate the data and to find the causes of the composition of the CO_2 system.

6. Ersteinsatz eines Schiffs-LIDAR-Systems

K. Ohm, A. Gorges (AWI), O. Nürnberg, P.Wagner, R. Willkomm (UOL)

Auf diesem Fahrtabschnitt wurde zur Hauptsache ein neuentwickeltes LIDAR-Gerät über dem Schieber, der den Bodendurchbruch verschließt, eingebaut und erstmals getestet. Daneben wurden Wasserproben auf die für die Interpretation der LIDAR-Signale wesentlichen Eigenschaften hin vermessen. Schließlich wurde eine neue Attenuationssonde mit veränderlicher Streckenlänge und spektraler Auflösung des Attenuationskoeffizienten im Einsatz erprobt, deren Daten ebenso zur Interpretation der LIDAR-Signale dienen sollten. Entsprechend diesen Aufgaben wird hier ein technischer Bericht gegeben und es werden keine meeresoptischen Eigenschaften dargestellt, zumal die endgültige Auswertung der Fluoreszenzmatrix erst in Oldenburg geschieht.

Der Transport der bis 250 kg schweren Teile in den Raum F 621 ging mit Hubwagen und Kettenzügen überraschend leicht vonstatten. Das Lasernetzgerät mußte wegen seiner Maße allerdings zerlegt und an seinem Aufstellungsort neu montiert werden. Der Geräteträger paßte nicht auf Anhieb auf den vorgesehenen Flansch. Wegen der komplizierten Geometrie des engen Raumes waren Kleinigkeiten übersehen worden. Aber mit Bordmitteln konnte alles nachgebessert werden, so daß am 4. Tag der mechanische Aufbau fertig war.

Der Schieber wurde mittels Hydraulik ohne Probleme geöffnet, das vorgesehene Ölvolumenmeßgerät zur Stellungsanzeige konnte allerdings nicht verwendet werden, weil es den Druck minderte und noch mit erhöhtem Druck gearbeitet werden muß. Die Präzision der optischen Justage schien über die Demontage in Oldenburg, Transport und Montage hinweg erhalten, jedenfalls soweit man dieses an der Signalform beurteilen kann. Die mechanische Reproduzierbarkeit muß später im Labor nachgewiesen werden.

Die Einzelkomponenten des Systems wurden schrittweise in Betrieb genommen, dabei konnte besonders im Empfänger nachgebessert werden. Am 8. Reisetag wurde der erste Laserblitz durch das Bodenfenster gesendet, ab dem 16. Tag wurde dann nachts ein automatischer Meßbetrieb aufgenommen, während tagsüber Systemparameter optimiert wurden.

Die Signale der Ramanstreuung mit einer Wellenlänge von 355 nm und das Streulicht im Grünen (532 nm) waren bis aus einer Tiefe von 40 m unter dem Quarzfenster gut zu empfangen (Fig. 8.6.1). Der Ramaneffekt ist hier nicht so gut zu beobachten, weil bei dieser Wellenlänge der Attenuationskoeffizient größer und der Wirkungsquerschnitt kleiner ist. Zum Nachweis von Chlorophyll muß die Empfindlichkeit des Empfängers noch gesteigert werden. Gelbstoffsignale konnten nicht beobachtet werden, weil in dem befahrenen Seegebiet die Konzentrationen zu gering waren. Zur Zeit werden Gelbstoff- und Ramansignal spektral auch noch nicht genügend getrennt, es müssen also schärfere Filter eingebaut werden, oder es muß ein besonderer Auswerte-Algorithmus angewendet werden. Diese erste Beurteilung geschah anhand der Rohdaten, die Auswertealgorithmen werden erst noch entwickelt und an dem hier erfaßten Datenmaterial erprobt.

Am 27. Tag wurden die Messungen beendet und innerhalb von 2 Tagen die Geräte abgebaut und verstaut. Die wichtigste Erfahrung über die Handhabung des Systems ist, daß der schwere Geräteträger beim Einfahren in Eisgebiete herausgenommen werden muß. Er kann wegen der Enge des Raumes nicht unten abgelegt werden, sondern muß durch den engen Schacht ins F-Deck geschafft werden. Dieses ist ein schwieriges Manöver, das ruhige See und speziell geschultes Personal verlangt. Für einen Routinebetrieb müßten das Teleskop verkleinert und der Geräteträger leichter werden, der Raum unten müßte vergrößert und mit vorbereiteten Ablagen und Hilfshebezeugen ausgestattet werden.

Zur Bestimmung der optischen Meerwassereigenschaften wurde kontinuierlich aus der Oberfläche Probenwasser gepumpt und in 170 Proben im Laborfluorometer Perkin Elmer LS50 vermessen. Dabei wurden verschiedene Anregungswellenlängen ausgewählt, die charakteristisch für die im Wasser enthaltenen Substanzen, wie Chlorophyll, Gelbstoff und aromatische Aminosäuren sind. Nach der Auswertung in Oldenburg wird man die zu diesen Messungen gehörige Fluoreszenzmatrix längs des Kurses durch den Atlantik erhalten.

Fig. 8.6.1 Sequenz von 19 Profilen der Ramanstreuung bei einer Anregungswellenlänge von 355 nm. Die Profile wurden im Atlantik bei 36°40'N 19°23'W (15.2.93) mit einem Abstand von etwa 1.5 km aufgezeichnet. Durch einen Anstieg der Algenkonzentration nimmt die Eindringtiefe des LIDAR-Signals stark ab.

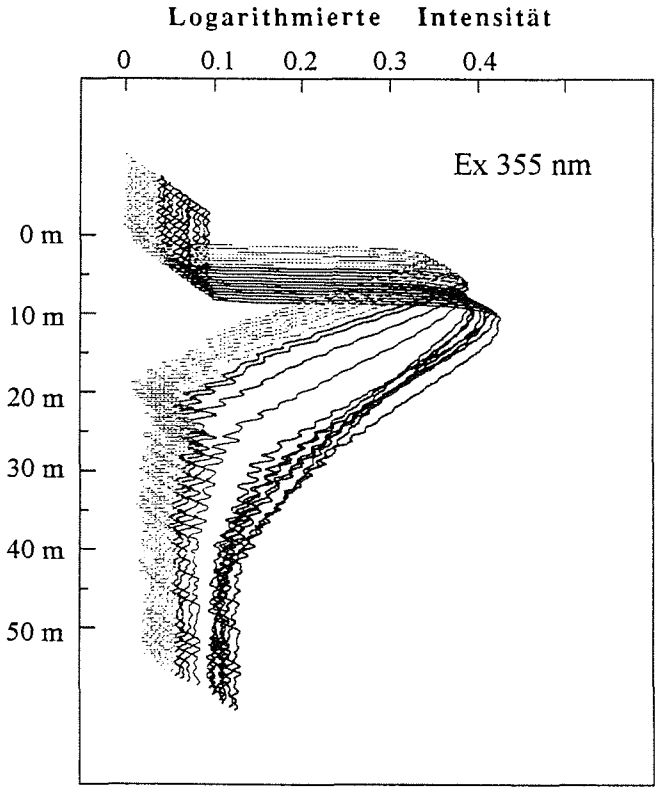

Die Wasserproben aus den CTD-Stationen wurden sowohl fluorometrisch als auch spektral auf ihren Attenuationskoeffizienten hin vermessen. Dazu diente ein La-bor-Attenuationsgerät mit einer Küvettenlänge von 1 m. Diese Meßwerte sollten auch zur Überprüfung der neuen In-situ-Sonde dienen. Aufgrund eines Transportschadens konnte die Attenuationssonde erst nach umfangreichen Reparaturarbeiten eingesetzt werden, und das auch nur auf wenigen Stationen bis zu einer maximalen Wassertiefe von 40 m. Es wurden Spektren der Trübung mit einer Tiefenauflösung von ca. 0,5 m im Spektralbereich von 360 bis 730 nm gewonnen. Diese Daten dienen ebenfalls zur Kalibrierung der LIDAR-Daten.

7. Optische Eigenschaften des Meerwassers und Anreicherungseffekte in Frontalzonen

G. Krause, K. Ohm (AWI)

Wie auf vergangenen Expeditionen wurden neben Temperatur und Salzgehalt die Mie-Rückstreuung und die Fluoreszenz von Chlorophyll und Gelbstoff mit einem Sensorpaket (s. Tab. 8.7.1) im hydrographischen Schacht in ca. 10 m Wassertiefe kontinuierlich erfaßt.

Tab. 8.7.1 Physikalische Kenngrößen der Mie-Rückstreuung und der Fluoreszenz von Chlorophyll und Gelbstoffen

	Anregung	Detektion	Bereiche
Chlorophyll	bis 520 nm breitbandig mit Blitzlampe 30 Hz	681 nm 20 nm Bandbreite	0 - 5 mg/m^3 0 - 50 mg/m^3
Rückstreuung	wie Chlorophyll	breitbandig	0 - 1.25%
Gelbstoff	450 ± 25 nm mit Blitzlampe 30 Hz	530 -590 nm	1: 1 1: 100

Diese Messungen tragen zu folgenden Themen bei:

- Statistische Erfassung der Akkumulationseffekte in den Konvergenzbereichen von Frontalzonen als Teilprogramm der Feldmessungen des SFB 261 zu den Partikelflußstudiem im Südatlantik

- Verbesserung der Kenntnisse über die optischen Eigenschaften des Meerwassers im Hinblick auf den Einsatz des LIDAR-Systems und der Satellitenfernerkundung

- Untersuchung der Möglichkeiten, Gelbstoff als Indikator für Wassermassen zu verwenden

Die Fig. 8.7.2 und 8.7.3 vermitteln eine Grobübersicht über das zwischen 53°S und 43°N registrierte Datenmaterial. Man erkennt aus der Asymmetrie der Temperaturregistrierung den erheblichen Unterschied zwischen der Sommer- und der Winter-Halbkugel. Im Süden befindet sich eine breite Vermischungszone zwischen dem Falkland- und dem Brasilstrom. Die höchsten Chlorophyllgehalte wurden auf dem Patagonischen Schelf gemessen während zwischen 29°S und 3°S die "Wüstenregionen" des Südatlantiks angetroffen wurden. Die Vergrößerung in Fig. 8.7.4 zeigt jedoch, daß Chlorophyllgehalt, Trübung und Gelbstoff-Fluoreszenz auch in diesen Gebieten noch ausgeprägte Strukturen aufweisen.

Bemerkenswert ist noch die Tatsache, daß bei etwa 42°S Wasser aus dem Rio de la Plata in 800 km Entfernung von seiner Mündung durch erhöhten Gelbstoffgehalt, niedrigeren Salzgehalt und erhöhte Chlorophyllwerte nachgewiesen werden konnte (Fig. 8.7.4 und 8.7.5)

Fig. 8.7.2 Oberflächenregistrierung von a) Themperatur, b) Salzgehalt und c) Chlorophyll zwischen 52°S und 42°N im Atlantik

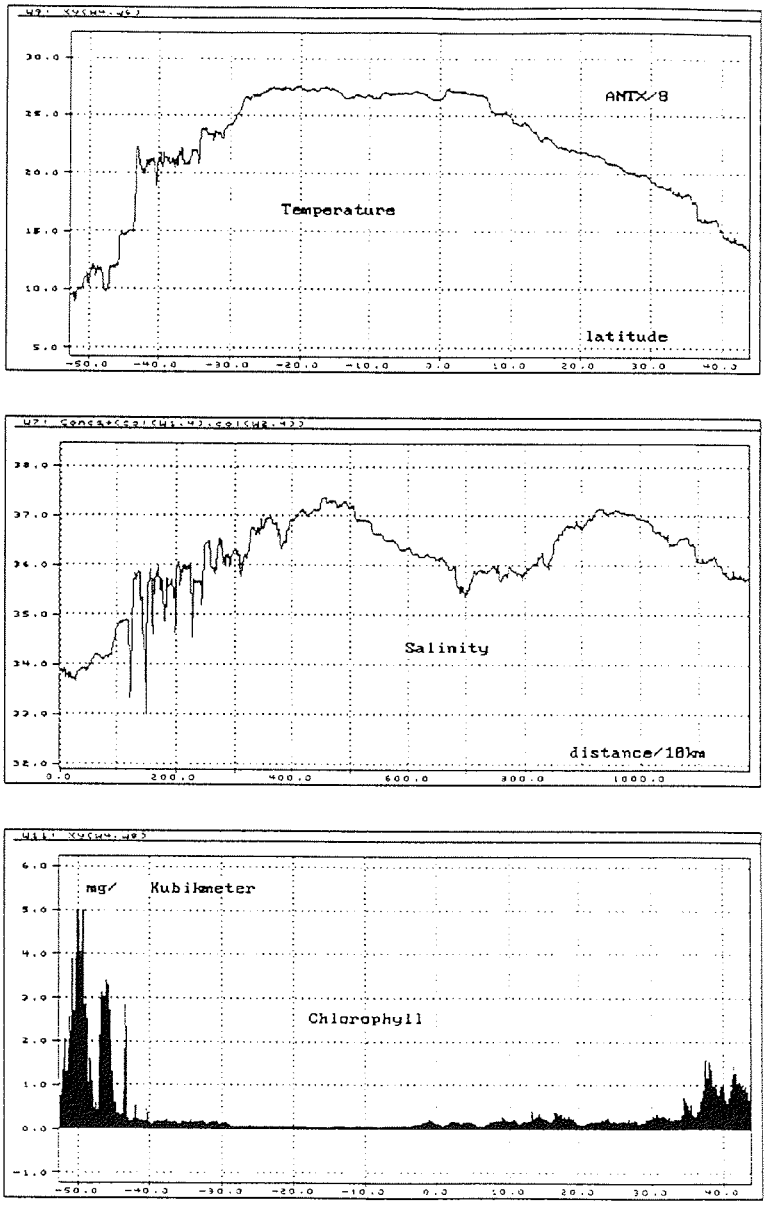

Fig. 8.7.3 Oberflächenregistrierung von a) Chlorophyll, b) Mie-Rückstreuung und c) Gelbstoff zwischen 52°S und 42°N im Atlantik

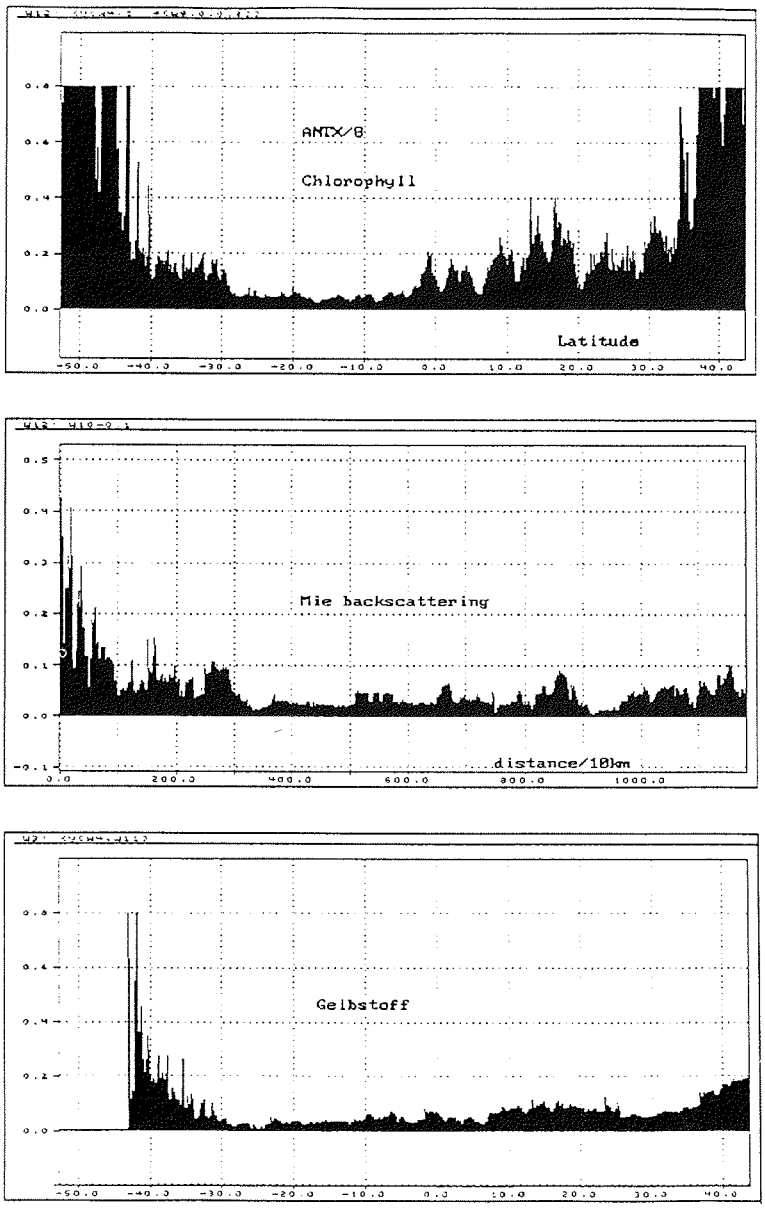

Fig. 8.7.4 Oberflächenregistrierung von a) Gelbstoff zwischen 52°S und 42°N. b) Vergrößerung des einsamen Gelbstoffpeaks und c) des Salzgehalts aus dem Rio de la Plata.

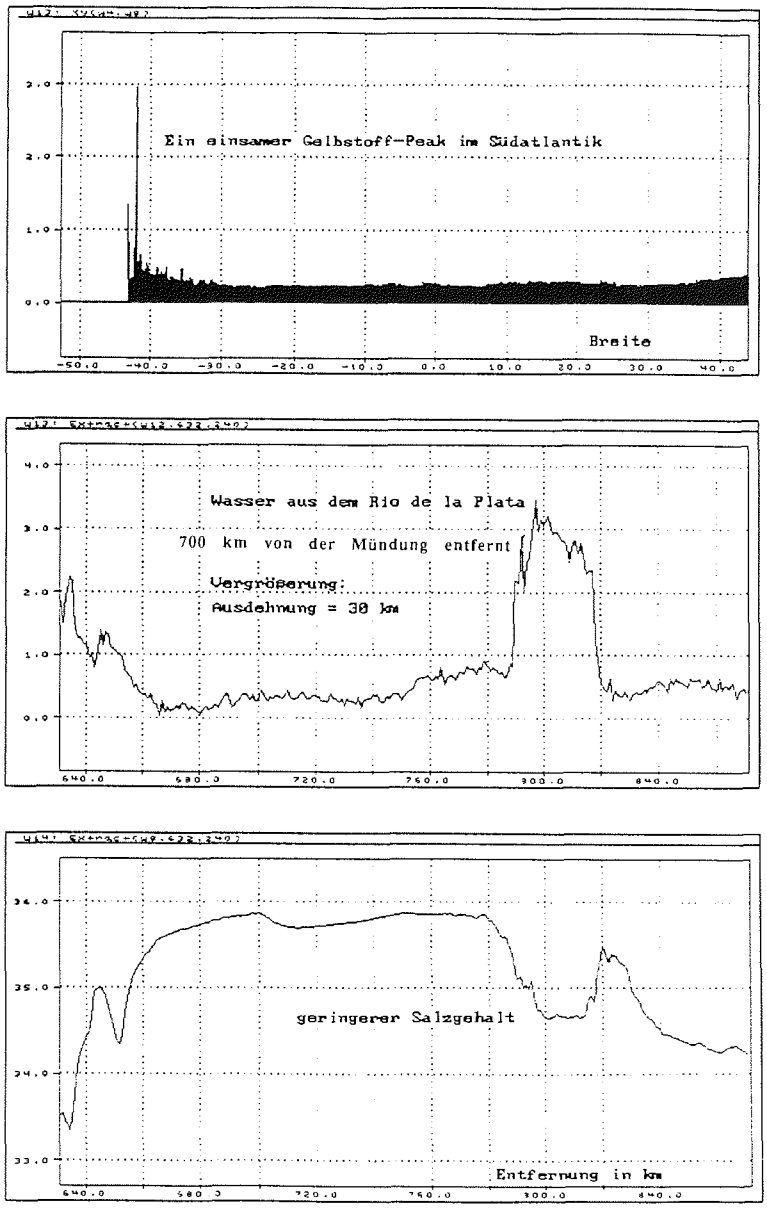

Fig. 8.7.5 Oberflächenregistrierung aus dem Rio de la Plata Einzugsgebiet von a) Chlorophyll und b) Temperatur.

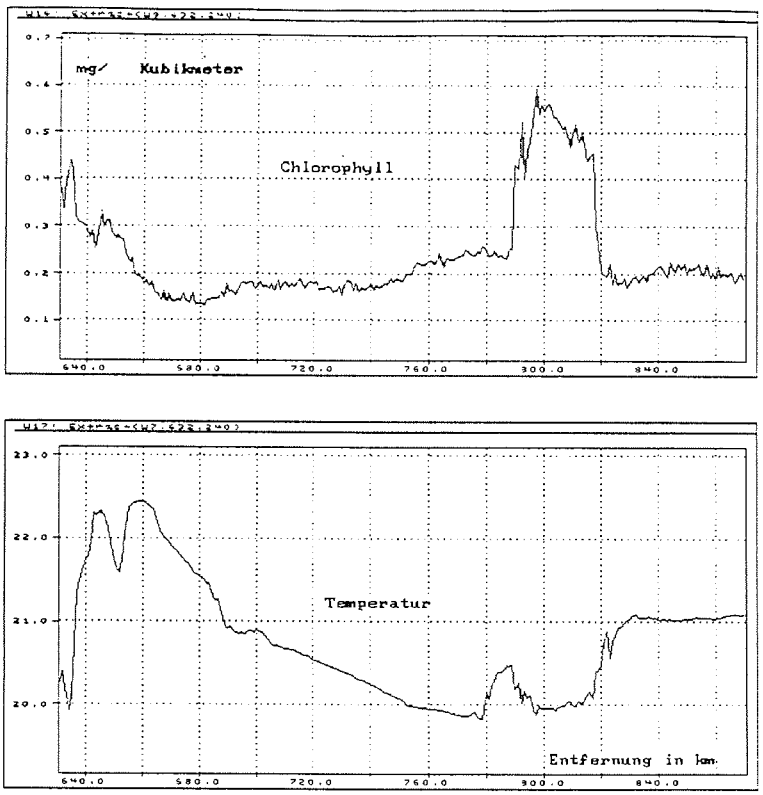

8. XBT-Schnitt und Radiosonden

Haika Fischer (AWI)

Im Rahmen des Klima- und Ozonforschungsprogramms des AWI wurden vom Patagonischen Schelf bis in den Golf von Biscaya Temperaturprofile mit XBTs aufgenommen. Die Messungen begannen am 26.01.93 bei 49°18'S, 60°28'W und erfolgten bei jedem ganzen und zusätzlich im Bereich der Subtropenfronten und des Äquators auf jedem halben Breitengrad. Bis zum 18.02.93 bei 47°45'N, 07°50'W wurden 157 Profile der Wassertemperatur bis zu einer Tiefe von 750 m aufgezeichnet. Daraus ergibt sich für die Fahrtroute der in Fig. 8.8.1 dargestellte Isothermenschnitt. Ferner fand auf jedem vollen Breitengrad ein Radiosondenaufstieg statt. Die bereits unter Kapitel 4 beschriebenen Ozonmessungen tragen ebenfalls zu dem o. g. Projekt bei.

Fig. 8.8.1 XBT Schnitt ANT X/8

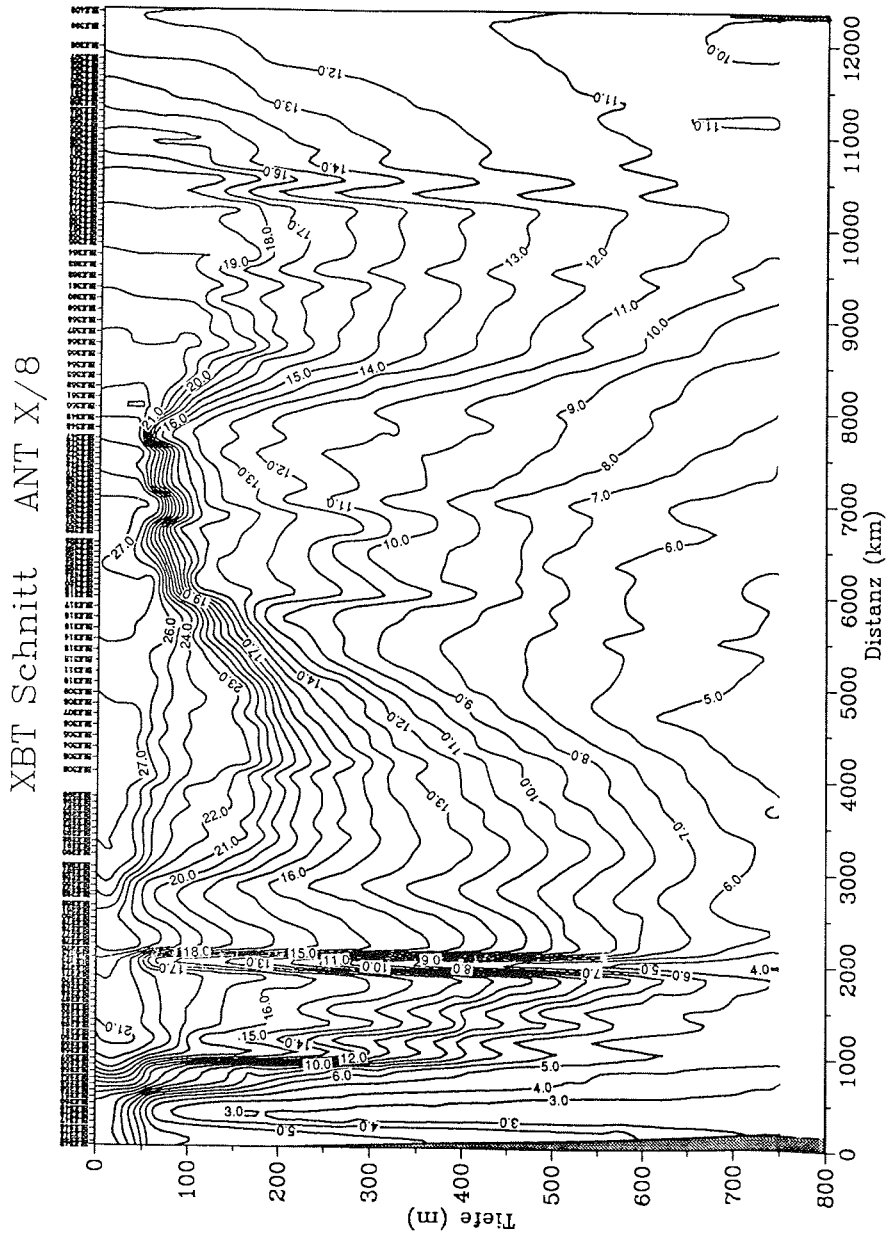

APPENDIX

1. Stationslisten/Station Lists

1.1 ANT X/6

856	2.10.92	56° 46.1 S	50° 00.1 W	4179	Teststation CTD	13:35	
857	2.10.92	56° 51.8 S	49° 35.4 W	3681	CTD 1; SD; APSN; MN 64, 200; GWS; MUC	16:00	1000
858	3.10.92	57° 00.1 S	45° 13.8 W	3648	CTD 1; MN 64, 200; APSN; SD; KVD; CTD 2	11:06	1500, 200
859	4.10.92	56° 59.9 S	38° 51.3 W	3250	CTD 1; MN 64, 200; APSN; CTD 2; ALW; RN; SD; LM; KVD	11:05	300, 1000
860	5.10.92	56° 59.4 S	30° 26.5 W	3374	CTD 1; SD; APSN; ALW; MN 64, 200; RN; CTD 2; GWS; CTD 3; KVD; MUC	18:06	300, 3465, 300
861	6.10.92	56° 58.3 S	29° 12.8 W	3405	CTD 1; LM; APSN; EISKORB; CTD 2; SD	10:04	300, 100
862	7.10.92	56° 59.6 S	23° 18.5 W	4872	CTD 1; MN 65, 200; APSN; SD; ALW; RN; LM; KVD; CTD 2; GWS+ISP	10:04	300, 4960
863	8.10.92	56° 51.0 S	21° 20.5 W	4658	CTD 1; APSN; SD; MN 64, 200; RN; LM	9:12	300
864	9.10.92	56° 09.1 S	15° 25.5 W	4675	CTD 1; SD; MN 64, 200; APSN; RN; KVD; LM; ALW	9:03	400
865	9.10.92	56° 09.1 S	15° 25.5 W	4887	CTD 1; APSN; GWS + ISP; KVD	21:32	4940
865a	10.10.92	56° 03.0 S	09° 32.6 W	4479	CTD TEST	17:14	1000
866	11.10.92	57° 44.7 S	06° 28.6 W	3880	GRUPPE AUF EIS; CTD 1; APSN; KVD; MN 64, 200; CTD 2; CTD 3; CTD 4; GWS + ISP; MUC; CTD 5	17:52	1500, 200,20, 3660, 200
867	12.10.92	57° 18.3 S	06° 12.5 W	3851	CTD 1; APSN; LM; SD; MN 64, 200;	15:27	300
868	12.10.92	56° 59.6 S	06° 00.4 W	3256	CTD 1; APSN; MN 64, 200; CTD 2; GWS	20:53	1500, 200
869	13.10.92	56° 30.8 S	05° 59.3 W	3539	CTD 1; APSN; MN 64, 200; CTD 2	5:37	1500, 600
870	13.10.92	55° 59.9 S	05° 59.8 W	3680	CTD 1; SD; APSN; KVD; LM; SB; CTD 2; MN 64, 200; CTD 3, CTD 4	13:13	1500, 1500, 200, 200
871	14.10.92	55° 28.4 S	05° 57.6 W	3289	CTD 1; APSN; MN 64, 200;	0:16	1500
872	14.10.92	55° 00.1 S	06° 02.8 W	3194	CTD 1; APSN; KVD; SD; MN 64, 200; CTD 2; LM; GWS; CTD 3; MUC	6:36	1500, 250, 200
873	14.10.92	54° 29.7 S	06° 00.3 W	3073	CTD 1; APSN; MN 64, 200; CTD 2; RMT	18:32	1500, 600
874	15.10.92	53° 59.9 S	05° 59.8 W	2319	CTD 1; APSN; KVD; MN 64, 200; CTD 2; CTD 3	2:14	1500, 200, 200
875	15.10.92	53° 30.0 S	06° 00.0 W	2736	CTD 1; APSN; MN 64, 200; SD; LM; RMT	10:10	1500
876	15.10.92	53° 00.1 S	05° 59.9 W	2688	CTD 1; APSN; KVD; MN; CTD 2; GWS; MUC	18:07	1500, 200
877	17.10.92	49° 00.3 S	06° 00.1 W	3718	ALW; APSN; CTD 1; SD; MN 64,200; CTD 2; LM; KVD; CTD 3; GWS; RMT	15:56	1000, 1500, 200
878	18.10.92	48° 30.3 S	06° 00.2 W	4161	CTD 1; APSN; MN 64, 200; CTD 2	4:35	1500, 600
879	18.10.92	48° 00.1 S	06° 00.1 W	4040	ALW; APSN; MN 64, 200; CTD 1; SD; LM; CTD 2; KVD; CTD 3; GWS; CTD 4, MUC; RMT	12:05	3916, 200, 1500, ?
880	19.10.92	48° 49.4 S	05° 59.5 W	3878	CTD 1	6:07	300

881	19.10.92	49° 30.2 S	05° 59.5 W	3260	CTD 1; APSN; MN 64, 200; LM	11:35	1500
882	19.10.92	49° 59.5 S	05° 59.8 W	2424	CTD 1; MN 64, 200; CTD 2	18:48	1500, 200
883	20.10.92	50° 29.8 S	05° 59.8 W	2247	CTD 1	2:50	1500
884	21.10.92	54° 16.9 S	06° 17.3 W	2928	MS - TEST	16:02	
885	22.10.92	55° 53.7 S	06° 59.9 W	4236	CTD 1	5:07	200
886	22.10.92	56° 04.3 S	06° 50.6 W	4156	DRIFTER; APSN; CTD 1, MUC; CTD 2; MN 64, 200; SD; LM; BO; GWS; CTD 3; CTD 4; KVD; CTD5; CTD 6; GWS; CTD 6; CTD 7; CTD 8; CTD 9; CTD 10	7:15	1500,1000, 1000, 150, 1500, 100, 600, 80, 200, 200
887	24.10.92	55° 59.3 S	06° 03.7 W	3738	CTD 1; KVD; CTD 2; SD; MN 200;LM; CTD 3; EISKORB	10:40	200, 1500, 200
888	24.10.92	55° 45.0 S	06° 00.1 W	3058	CTD 1	19:28	1500
889	24.10.92	55° 30.0 S	05° 59.8 W	3191	CTD 1; RMT	22:49	1500
890	25.10.92	55° 15.1 S	06° 00.0 W	3214	CTD 1	3:25	1500
891	25.10.92	55° 00.5 S	06° 00.3 W	3117	BL; CTD 1; MN 64, 200; CTD 2; APSN; BO; CTD 3; LM; SD; ALW; KVD; GWS; CTD 4; MUC	6:39	200, 1500, 600, 200
892	26.10.92	54° 30.3 S	05° 59.7 W	3022	CTD 1	0:46	1500
893	26.10.92	54° 00.0 S	06° 00.7 W	2380	CTD 1; MN 64, 200; CTD2; NIS; LM; KVD; APSN; ALW; BO; SD; CTD 3	5:05	1500, 200, 200
894	26.10.92	53° 30.1 S	06° 00.1 W	2698	CTD 1	14:20	1500
895	26.10.92	53° 00.0 S	05° 59.7 W	2630	ALW; CTD 1; APSN; MN 64, 200; CTD 2; KVD; CTD 3; GWS; CTD 4	18:12	1500, 200, 200, 600
896	27.10.92	52° 30.2 S	06° 00.1 W	2810	CTD 1	4:09	1500
897	27.10.92	52° 00.2 S	06° 00.0 W	2200	CTD1; MN64, 200; APSN; LM; CTD 2; SD; NIS; KVD; ALW; BO; CTD3	8:05	1500, 200, 200
898	27.10.92	51° 30.2 S	06° 00.3 W	2024	CTD 1	16:47	1500
899	27.10.92	50° 59.9 S	06° 00.0 W	2060	CTD 1; APSN; MN 64, 200; CTD 2; KVD; CTD3; GWS; BO; CTD4; MUC	20:51	1500, 200, 200, 600
900	28.10.92	50° 30.1 S	05° 59.8 W	2121	CTD 1; APSN	7:44	1500
901	28.10.92	50° 00.1 S	05° 59.6 W	2380	CTD 1; APSN; SD; BO; MN 64, 200; CTD 2; LM; CTD 3; NIS; KVD; ALW; CTD 4; CTD 5	12:15	1500, 1500, 200, 200, 200
902	28.10.92	49° 30.0 S	06° 00.1 W	3221	CTD 1	23:53	1500
903	29.10.92	49° 00.0 S	06° 00.1 W	3715	CTD 1; MN 64, 200; LM; CTD 2; APSN; KVD; ALW; CTD 3; BO; GWS; CTD 4; MUC; SD; RMT	4:04	1500, 200, 200,600
904	29.10.92	48° 30.5 S	06° 00.1 W	4018	CTD 1	18:24	1500
905	29.10.92	48° 00.0 S	06° 00.0 W	3944	CTD 1; APSN; MN 64, 200; CTD 2; NIS; KVD; BO; CTD 3	22:38	1500, 200, 200
906	30.10.92	47° 29.9 S	05° 59.9 W	3581	CTD 1	6:46	1500
907	30.10.92	46° 59.8 S	06° 00.0 W	3542	CTD1; GWS; APSN; CTD 2; SD; MN 64, 200; LM; NIS; CTD3; KVD;ALW; BO; CTD4; BL-TEST; RMT; CTD5	11:06	1000, 1500, 200, 200, 600
908	30.10.92	46° 52.3 S	05° 43.0 W	3756	CTD 1; GWS+ISP; CTD 2; KVD; MUC	22:49	3726, 2000
909	2.11.92	55° 00.1 S	06° 00.6 W	3169	RMT; MN 64, 200; APSN; BL-TEST; LM; BO; SD; KVD; CTD 1; ALW; NIS; CTD2	12:31	1500, 200
910	2.11.92	55° 29.9 S	05° 59.8 W	3164	CTD 1	22:27	1500
911	3.11.92	55° 51.0 S	05° 59.6 W	4059	CTD 1; GWS+ISP; CTD 2; MUC	1:43	4047, 2200
912	3.11.92	56° 01.1 S	06° 00.8 W	3547	CTD 1; APSN; MN 64, 200; SD; LM; NIS; CTD 2; ALW; BO	15:24	1500, 200
913	3.11.92	56° 30.1 S	06° 00.2 W	3374	CTD 1	22:38	1500
914	4.11.92	57° 00.2 S	05° 59.6 W	3294	CTD 1	3:25	1500

915	4.11.92	57° 29.4 S	06° 00.4 W	2478	CTD1; MN 64, 200; APSN; LM; CTD 2; SD; BO; KVD; CTD3; SB; ALW	7:37	1500, 200, 200
916	4.11.92	57° 59.8 S	05° 59.7 W	4190	CTD 1; APSN; MN 64, 200; NIS; CTD2; KVD; BO; CTD 3	19:09	1500, 200, 200
917	5.11.92	58° 29.2 S	05° 59.9 W	5039	CTD 1; CTD 2; APSN; GWS+ISP; CTD 3; MUC	4:34	1500, 5057, 2700
918	6.11.92	59° 00.2 S	06° 00.2 W	5147	CTD 1; MN 64, 200; APSN; NIS; CTD2; KVD; BO; CTD 3	2:06	1500, 200, 100
919	6.11.92	59° 29.4 S	05° 59.8 W	4944	CTD 1; SD; APSN; MN 64, 200; LM; CTD 2; GRUPPE AUF EIS;KVD; BO; CTD 3; CTD 4; ALW	11:28	1500, 200, 200, 600
920	7.11.92	57° 15.1 S	05° 58.6 W	3066	CTD 1; KVD	23:20	1000
921	8.11.92	57° 30.0 S	06° 01.5 W	2433	CTD 1; KVD	3:04	1000
922	8.11.92	57° 45.2 S	06° 00.7 W	3568	CTD 1; KVD	6:17	1000
923	8.11.92	58° 00.0 S	06° 00.2 W	4361	CTD 1; KVD	10:02	1000
924	8.11.92	58° 00.0 S	06° 30.6 W	4019	CTD 1; KVD	15:00	1000
925	8.11.92	57° 45.6 S	06° 30.1 W	3895	CTD 1; KVD	18:23	1000
926	8.11.92	57° 29.8 S	06° 30.7 W	1769	CTD 1; KVD	21:47	1000
927	9.11.92	57° 15.1 S	06° 29.8 W	4415	CTD 1; KVD	1:15	1000
928	9.11.92	57° 00.0 S	06° 30.3 W	2626	CTD 1; KVD	5:06	1000
929	10.11.92	59° 00.1 S	06° 16.3 W	4873	CTD 1	6:08	500
930	10.11.92	59° 30.1 S	06° 00.2 W	4966	CTD 1; APSN; LM; BO; KVD; SD; RMT; NIS; CTD 2; MN 64, 200; CTD3; ALW; EISPROBE SB	10:36	1500, 200, 200
931	10.11.92	58° 59.8 S	05° 59.5 W	5152	CTD 1; APSN; MN 64, 200; CTD 2; GWS;	23:55	1500, 200
932	11.11.92	58° 29.8 S	05° 59.5 W	5004	CTD 1	8:17	1500
933	11.11.92	58° 13.2 S	05° 59.1 W	3561	CTD 1; MN 64, 200; APSN; SB	11:41	1500
934	11.11.92	57° 59.7 S	06° 00.5 W	4335	CTD 1; APSN; SD; MN 64, 200; LM; CTD 2; BO; KVD; CTD 3; CTD 4	18:54	1500, 200, 200, 250
935	12.11.92	57° 58.8 S	05° 53.4 W	4419	CTD 1; CTD 2	1:47	300, 300
936	12.11.92	57° 59.1 S	06° 00.7 W	4146	CTD 1	3:47	250
937	12.11.92	57° 51.9 S	05° 59.9 W	4148	CTD 1	5:15	250
938	12.11.92	57° 44.7 S	06° 00.5 W	3465	CTD 1; MN 64, 200; APSN	6:33	1500
939	12.11.92	57° 29.7 S	06° 00.0 W	2441	CTD 1; MN 64, 200; APSN; BO; CTD2; SD; RMT	11:36	1500, 600
940	12.11.92	57° 14.9 S	06° 00.1 W	2891	CTD 1; LM	18:33	1500
941	12.11.92	57° 03.3 S	06° 00.5 W	3660	SCHNORCHEL; ALW; MUC; BL; CTD 1; MN 64, 200; APSN; CTD 2; BO; GWS; KVD; CTD 3	22:00	1500, 200, 1000
942	13.11.92	56° 30.1 S	06° 00.0 W	3419	CTD 1	13:09	1500
943	13.11.92	56° 00.5 S	06° 00.1 W	3631	ALW; CTD 1; APSN; LM; MN 64, 200; SD; CTD 2; KVD; CTD 3	17:00	1500, 200, 200
944	14.11.92	55° 30.0 S	05° 59.9 W	3186	CTD 1; CTD 2	2:15	1500, 600
945	14.11.92	55° 00.2 S	06° 00.8 W	3175	ALW; APSN; CTD 1; MN 64, 200; SD; LM; MS; CTD 2; CTD 3; GWS; KVD; CTD 4; RMT	7:20	1500, 200, 600, 200
946	14.11.92	54° 30.0 S	05° 59.9 W	3053	CTD 1	23:09	1500
947	15.11.92	53° 59.8 S	06° 00.2 W	2341	ALW; MUC; BL; CTD 1; MN 64, 200; LM; CTD 2; KVD; APSN; CTD 3; SD	3:03	1500, 200, 2600
948	16.11.92	52° 59.9 S	05° 59.5 W	2608	CTD 1	6:00	1500
949	16.11.92	52° 59.9 S	05° 59.5 W	2608	ALW; CTD 1; BL; CTD 2; APSN; KVD; NIS; MN 64, 200; LM; CTD 3; SD; GWS; KVD; CTD 4	6:00	500, 1500, 200, 600
950	16.11.92	52° 29.7 S	06° 00.2 W	2651	CTD 1	18:41	1500

951	16.11.92	52° 00.0 S	06° 00.0 W	2154	CTD 1; CTD 2; CTD 3	23:30	1500, 200, 2117
952	17.11.92	51° 29.9 S	06° 00.5 W	2068	CTD 1	8:32	1500
953	17.11.92	50° 59.7 S	06° 00.6 W	2085	CTD 1; APSN; MN 64, 200; SD; LM; CTD 2; GWS; KVD; CTD 3; ALW	13:12	1500, 200, 600
954	17.11.92	50° 30.0 S	06° 00.0 W	2218	CTD 1	22:50	1500
955	18.11.92	50° 15.0 S	06° 00.1 W	2347	CTD 1	1:40	1500
956	18.11.92	49° 59.0 S	06° 00.2 W	2347	ALW; ISP; MUC; BL; CTD 1; APSN; MN 64, 200; LM; SD; CTD 2; BO; KVD; CTD 3	4:18	1500, 200, 2500
957	18.11.92	49° 44.9 S	05° 59.7 W	3611	CTD 1	20:00	1500
958	18.11.92	49° 30.0 S	06° 00.0 W	3248	CTD 1	22:50	1500
959	19.11.92	49° 15.0 S	05° 59.8 W	3086	CTD 1	1:50	1500
960	19.11.92	49° 00.0 S	05° 59.9 W	3808	ALW; CTD 1; MN 64, 200; LM; SD; CTD2; APSN; BL; GWS; KVD; CTD3	5:10	1500, 200, 600
961	19.11.92	48° 44.8 S	05° 59.1 W	3973	CTD 1	14:08	1500
962	19.11.92	48° 30.2 S	05° 59.8 W	4127	CTD 1	17:30	1500
963	19.11.92	48° 15.1 S	06° 00.0 W	3677	CTD 1	21:07	1500
964	20.11.92	48° 00.1 S	06° 00.1 W	3696	ALW; CTD 1; KVD; MN 64, 200; APSN; CTD 2; BO; CTD 3	0:41	1500, 290, 600
965	20.11.92	47° 44.8 S	05° 59.9 W	3819	CTD 1	8:28	1500
966	20.11.92	47° 30.0 S	06° 01.0 W	3607	CTD 1	11:30	1500
967	20.11.92	47° 46.1 S	06° 11.4 W	3798	SB (Eisbergaktion)	14:48	
968	20.11.92	47° 14.9 S	06° 00.0 W	3666	CTD 1	23:18	1500
969	21.11.92	46° 59.5 S	06° 00.1 W	3546	ALW; BL; CTD 1; APSN; KVD; MN 64, 200; CTD 2; BO; GWS; CTD 3; SD; LM; RMT	1:57	1500, 200, 600
970	21.11.92	48° 00.1 S	05° 59.9 W	3701	CTD 1; MN 64	17:26	1500
971	21.11.92	48° 15.2 S	06° 00.3 W	3701	CTD 1; MN 64	20:50	1500
972	22.11.92	48° 30.1 S	06° 00.2 W	4091	ISP; APSN; DRIFTER; MUC; BL; CTD1; MN 64, 200; CTD 2; CTD 3; GWS; KVD; ALW; CTD 4; CTD 5	0:13	1500, 200, 3164, 600, 3786
973	23.11.92	49° 00.2 S	06° 00.0 W	3761	CTD 1	5:19	1500
974	23.11.92	49° 14.9 S	05° 59.7 W	3097	CTD 1; MN 64, 200	8:12	1500
975	23.11.92	49°30.0 S	06° 00.0 W	3246	CTD 1	12:30	1500
976	23.11.92	49°45.0 S	06° 00.0 W	3562	CTD 1	15:22	1500
977	23.11.92	50°00.2 S	06° 00.0 W	2451	ALW; CTD 1; APSN	18:13	1500
978	23.11.92	49°45.0 S	06° 00.0 W	3584	ALW; CTD 1; APSN; NIS; CTD 2; MN64, 200; KVD; CTD 3	21:45	200, 200, 300
979	25.11.92	45°29.7 S	01° 08.2 E	4186	CTD 1	9:03	4174

Gear used:

ALW Ausleger Winsh
APSN Apstein net
BL Bottom lander
BO Bongo net
CTD Conductivity, temperature, pressure probe
DRIFT Drifting Sediment trap, multisampler
EISKORB
GWS Gerad large volume water bottles
ISP In situ pumps
KVD Kevlar winsh with KVD bottles
LM Light meter
MN Multinet
MUC Multicorer
MS Multisampler
NIS Niskin bottle
RMT Retangular midwater trawl
RN Ringnet
SD Secchi disk
SB Rubber boat

1.2 ANT X/7

Station No.	Date	Time (UTC)	Latitude (S)	Longitude	Depth (m)	Operation
23/001	07.12.92	10.19	50°06.1'	05°55.6'E	3774	R-PF5
		15.56	50°07.5'	05°51.4'E	3791	
23/002		16.24	50°06.7'	05°54.1'E	3778	D-PF6
		18.05	50°05.0'	05°51.2'E	3788	
23/003		18.18	50°04.8'	05°51.1'E	3752	CTD
		21.00	50°04.4'	05°52.1'E	3751	
23/004	09.12.92	06.30	54°21.1'	03°24.3'W	2860	R-BO_2
		10.00	54°20.3'	03°19.7'W	2734	
23/005		10.39	54°20.1'	03°18.3'W	2734	D-BO3
		11.44	54°20.1'	03°20.9'W	2756	
23/006		12.04	54°19.1'	03°22.4'W	2777	CTD,SD,APSN
		12.42	54°18.9'	03°22.3'W	2779	
23/007	10.12.92	15.52	57°37.4'	04°02.5'E	4412	R-AWI400-1
		18.25	57°36.8'	04°03.6'E	4470	
23/008		18.33	57°36.8'	04°03.6'E	4470	CTD
		21.08	57°35.7'	04°04.5'E	4363	
23/009	14.12.92	03.27	64°01.8'	08°57.5'W	5175	R-Buoy 9364,
		04.30	64°01.9'	08°57.2'W	5168	IC
23/010		10.34	64°59.9'	08°48.1'W	5087	MN, SD, APSN, MN,
		13.50	64°58.5'	08°41.6'W	5094	BS,CTD
23/011	17.12.92	20.18	70°29.6'	08°14.5'W	250	CTD, SD,APSN,BO
		21.30	70°29.3'	08°14.2'W	263	
23/012	18.12.92	11.14	71°03.3'	11°44.8'W	385	R-AWI 214/3,LM,
		14.24	71°03.5'	11°45.1'W	373	D-AWI 214/4,CTD
23/ 013		15.32	71°06.9'	11°24.8'W	367	CTD,SD,APSN,MN,
		19.37	71°05.5'	11°29.5'W	305	CTD,BO,BS
23/014a		20.47	70°59.7'	11°47.1'W	923	KN 4
		21.36	70°59.7'	11°48.6'W	990	
23/014b		21.47	70°59.8'	11°48.9'W	1012	CTD, APSN,SD
		22.27	70°59.5'	11°48.9'W	1037	
23/015		23.35	70°54.6'	11°57,6'W	1587	CTD, SD,APSN,MN,
	19.12.92	16.04	70°54.2'	11°56.3'W	1559	BO,Dred.-AWI 212/2
23/016		17.08	70°59,4'	11°46.1'W	864	Dred.-KN 4
		20.42	70°59.3'	11°45.7'W	867	
23/017		23.35	70°42.0'	12°33.2'W	2244	CTD,SD,APSN,CTD
	20.12.92	02.39	70°41.7'	12°31.3'W	2234	
23/018		06.13	70°54.6'	11°57.2'W	1584	D-AWI 212/3
		07.33	70°54.6'	11°57.9'W	1590	
23/019		11.53	70°29.5'	13°08.4'W	2423	LM,Dred.-AWI211/2, CTD,SD,APSN,
		22.49	70°30.2'	13°13.6'W	2407	BS,MN, BO
23/020	21.12.92	00.10	70°23.1'	13°33.3'W	2968	CTD
		02.02	70°23.1'	13°33.0'W	2969	
23/021		02.30	70°20.6'	13°36.9'W	3797	CTD,SD,APSN,MN,
		09.50	70°19.4'	13°40.6'W	4298	BS,BO,R-AWI 225
23/022		10.46	70°23.2'	13°32.2'W	2970	R-AWI226, LM, CTD,
		12.58	70°23.0'	13°33.6'W	2969	SD,APSN
23/023		18.08	70°05.6'	14°20.2'W	4596	CTD, SD,APSN
		18.30	70°11.4'	14°10.7'W	4615	
23/024	22.12.92	00.03	69°52.7'	15°02.7'W	4742	CTD, SD
		03.07	69°52.7'	15°02.7'W	4742	
23/025	22.12.92	06.08	69°39.5'	15°39.7'W	4755	MN,BO,CTD,LM,CTD, SD,APSN,BS,R-AWI 210/2, IC,BS
	23.12.92	03.06	69°38.5'	15°43.6'W	4751	D-AWI 210/3

Station No.	Date	Time (UTC)	Latitude (S)	Longitude	Depth (m)	Operation
23/026		06.48	69°22.8'	16°27.8'W	4732	CTD
		09.30	69°21.9'	16°25.3'W	4732	
23/027		12.27	69°06.2'	17°14.5'W	4760	LM, CTD, SD
		14.17	69°05.8'	17°13.5'W	4760	
23/028		19.40	68°49.8'	17°54.3'W	4789	R-AWI 224, IC,CTD,
						SD,APSN,MN, BO,
	24.12.92	6.56	68°47.6'	17°54.6'W	4788	CTD,BS
23/029		9.20	68°33.4'	18°36.0'W	4772	CTD
		11.54	68°33.2'	18°35.7'W	4771	
23/030	26.12.92	6.05	68°19.1'	19°17.3'W	4850	CTD
		9.10	68°15.1'	19°17.2'W	4853	
23/031		12.22	68°02.1'	19°57.8'W	4892	LM, CTD, SD,APSN,
						BS, BO,IC,MN,CTD,
	27.12.92	17.45	67°59.6'	19°58.3'W	4896	Dred.- AWI 223
23/032		21.13	67°47.8'	20°56.9'W	4923	CTD
	28.12.92	00.04	67°47.3'	20°56.7'W	4922	
23/033		5.18	67°37.2'	21°56.7'W	4899	CTD, SD, APSN,BS,
		12.18	67°37.8'	21°58.0'W	4898	MN,BO,LM, CTD,IC
23/034		14.51	67°25.9'	22°52.6'W	4896	CTD
		17.30	67°26.2'	22°53.7'W	4896	
23/035		20.56	67°14.7'	23°53.4'W	4863	CTD
		23.47	67°13.9'	23°54.5'W	4863	
23/036	29.12.92	03.00	67°03.6'	24°51.8'W	4849	R-AWI 222, CTD,SD,
						APSN,BS, MN, CTD,
		12.27	67°02.5'	24°52.4'W	4850	BO,CTD, LM
23/037		15.46	66°50.6'	25°59.6'W	4840	CTD, IC
		19.08	66°49.7'	25°57.9'W	4841	
23/038		22.39	66°37.3'	27°07.3'W	4861	CTD,SD,APSN,MN,
						BO, CTD,Dred.-AWI
	31.12.92	03.30	66°37.4'	27°07.2'W	4861	209/2,D-AWI 209/3
23/039		6.38	66°30.5'	28°11.4'W	4837	CTD, LM
		9.36	66°30.6'	28°11.1'W	4837	
23/040	01.01.93	11.57	66°23.5'	29°15.0'W	4815	LM, CTD
		14.51	66°23.5'	29°16.0'W	4814	
23/041		18.03	66°16.7'	30°18.1W	4804	R-AWI 221,CTD,SD,
	02.01.93	02.43	66°16.7'	30°21.0'W	4804	APSN,BS,MN,BO,CTD
23/042		05.35	66°10.8'	31°18.6'W	4800	CTD, IC
		08.55	66°09.7'	31°20.6'W	4801	
23/043		11.40	66°04.3'	32°20.2'W	4787	LM, CTD
		14.40	66°04.3'	32°22.0'W	4788	
23/044		17.37	65°58.3'	33°20.3'W	4787	R-AWI 220,CTD, SD,
	03.01.93	02.14	65°57.6'	33°27.1'W	4786	APSN, BO,CTD,MN
23/045		04.59	65°51.7'	34°23.9'W	4785	CTD
		07.55	65°51.4'	34°23.6'W	4784	
23/046		11.07	65°45.1'	35°26.3'W	4770	CTD,LM
		14.18	65°44.7'	35°29.2'W	4767	
23/047		17.12	65°38.2'	36°30.3'W	4766	R-AWI208/2,D-AWI
						208/3, CTD,SD,APSN,
	04.01.93	09.21	65°37.7'	36°29.3'W	4765	MN,CTD,BO,CTD
23/048		12.42	65°39.9'	37°42.7'W	4751	R-AWI 219, LM
		18.17	65°39.9'	37°43.1'W	4754	CTD
23/049		19.51	65°29.9'	37°30.1'W	4727	CTD, SD
		20.34	65°29.9'	37°30.1'W	4727	
23/050	05.01.93	02.19	65°21.8'	38°31.7'W	4589	CTD
		04.58	65°22.3'	38°31.3'W	4746	
23/051		08.11	65°13.0'	39°31.0'W	4758	CTD,SD,APSN, MN,
		16.25	65°13.7'	39°32.5'W	4756	CTD,BO,LM,CTD, IC

Station No.	Date	Time (UTC)	Latitude (S)	Longitude	Depth (m)	Operation
23/052		18.37	65°07.2'	40°43.2'W	4758	ID, CTD
		22.22	65°05.4'	40°30.4'W	4756	
23/053	06.01.93	02.19	64°56.7'	41°30.5'W	4736	CTD
		05.00	64°57.3'	41°31.1'W	4737	
23/054		10.30	64°49.0'	42°29.6'W	4705	R-AWI 218, LM, SD, CTD,APSN,MN,
		21.39	64°48.9'	42°29.1'W	4702	BO,CTD,ID
23/055	07.01.93	02.03	64°42.8'	43°19.9'W	4656	CTD
		04.49	64°42.6'	43°22.5'W	4651	
23/056		08.10	64°36.9'	44°10.8'W	4608	CTD
		10.53	64°37.3'	44°08.6'W	4616	
23/057		12.16	64°35.1'	44°26.5'W	4569	CTD,SD,APSN, MN,
		19.28	64°34.1'	44°25.5'W	4576	IC,LM,BO,CTD
23/058		22.08	64°29.0'	45°11.8'W	4493	CTD
	08.01.93	00.38	64°28.9'	45°10.4'W	4509	
23/059		03.02	64°24.2'	45°55.0'W	4452	CTD,SD,APSN,MN, BO,CTD,R-AWI 217,
		14.46	64°25.0'	45°49.8'W	4441	D-AWI 217/2, LM
23/060		17.23	64°18.2'	46°40.9'W	4380	CTD, BO
		20.50	64°17.6'	46°42.1'W	4378	
23/061		23.17	64°11.3'	47°30.8'W	4199	CTD
	09.01.93	01.41	64°11.3'	47°31.2'W	4197	
23/062		04.12	64°04.2'	48°19.2'W	3957	CTD, BO, SD,CTD,
		10.13	64°03.0'	48°17.5'W	3984	APSN,MN,CTD
23/063		12.50	63°56.8'	49°08.3'W	3534	CTD, LM,R-AWI 216,
		15.23	63°57.1'	49°10.1'W	3525	SD,CTD
23/064		19.54	63°51.1'	50°02.1'W	2905	CTD
		21.42	63°50.9'	50°01.6'W	2912	
23/065	10.01.93	00.10	63°45.4'	50°51.2'W	2528	CTD,SD,R-AWI 207/2
		11.28	63°44.3'	50°54.3'W	2507	D-AWI 207/3
23/066		13.12	63°35.5'	50°33.1'W	2656	Dred.
		19.30	63°36.2'	50°30.6'W	2671	
23/067		21.25	63°29.6'	51°04.5'W	2289	Dred.
	11.01.93	02.21	63°29.4'	51°04.3'W	2270	
23/068		04.06	63°37.3'	51°30.3'W	2058	CTD,SD,APSN,MN,
		09.41	63°37.4'	51°31.4'W	2050	BO,CTD
23/069		11.46	63°29.4'	52°05.8'W	967	R-AWI 206/2,D-AWI
		14.49	63°29.8'	52°07.7'W	941	206/3,LM, CTD,SD
23/070		16.55	63°24.8'	52°32.6'W	521	CTD
		17.58	63°24.9'	52°31.9'W	523	
23/071		19.31	63°19.9'	52°59.2'W	451	Dred.AWI 215, D-AWI 215/2,CTD, MN, BO,
	12.01.93	02.32	63°18.9'	53°03.7'W	451	CTD,APSN
23/072		04.52	63°13.2'	53°42.4'W	292	CTD
		05.26	63°13.1'	53°43.0'W	292	
23/073	14.01.93	09.30	68°59.9'	60°42.9'W	294	MN,CTD,SD,APSN,
		13.10	68°58.6'	60°38.5'W	295	BO,CTD,AGT
23/074		15.09	69°00.0'	60°00.1'W	287	LM,CTD,AGT
		17.12	69°00.5'	59°57.6'W	295	
23/075		20.05	68°59.9'	59°00.0'W	360	CTD
		20.44	69°00.0'	59°00.3'W	361	
23/076		23.55	69°00.0'	57°59.8'W	426	AGT,BS,CTD,SD,
	15.01.93	03.09	69°00.0'	57°59.2'W	426	APSN,MN,BO
23/077	15.01.93	08.53	69°00.0'	56°29.8'W	395	CTD
		09.24	69°00.0'	56°29.8'W	397	
23/078		11.08	68°55.5'	56°16.6'W	770	CTD,SD
		11.34	68°55.5'	56°16.6'W	770	

Station No.	Date	Time (UTC)	Latitude (S)	Longitude	Depth (m)	Operation
23/079		12.45	68°51.0'	56°03.6'W	1035	CTD
		13.57	68°50.2'	56°03.7'W	1033	
23/080		16.40	68°38.8'	55°27.6'W	1434	CTD,SD,APSN,MN,
		20.17	68°38.8'	55°29.4'W	1417	BO,CTD
23/081		23.13	68°29.6'	54°42.6'W	2006	CTD
	16.01.93	00.48	68°29.8'	54°43.0'W	2009	
23/082		03.52	68°16.6'	54°00.2'W	2467	CTD,SD
		04.39	68°16.5'	53°59.9'W	2426	
23/083		08.18	68°04.0'	53°16.2'W	2835	CTD,SD
		09.11	68°03.7'	53°15.8'W	2840	
23/084		13.35	67°51.1'	52°34.8'W	3104	CTD,SD,APSN,MN,
		18.09	67°50.9'	52°35.1'W	3047	BO,CTD
23/085		21.14	67°32.6'	51°34.2'W	3416	CTD,SD
		22.21	67°32.6'	51°35.2'W	3413	
23/086	17.01.93	03.24	67°11.1'	50°22.6'W	3637	CTD,SD
		05.29	67°11.1'	50°22.4'W	3638	
23/087		09.36	66°48.8'	49°13.1'W	3721	CTD,SD
		10.51	66°48.9'	49°12.9'W	3722	
23/088		15.32	66°24.6'	47°53.9'W	3934	CTD
		17.40	66°24.8'	47°54.9'W	3932	
23/089		22.42	65°52.6'	48°05.3'W	4037	CTD
	18.01.93	01.01	65°52.7'	48°04.4'W	4035	
23/090		04.58	65°20.0'	48°49.0'W	3882	CTD
		07.10	65°20.0'	48°50.3'W	3876	
23/091		11.26	64°47.6'	47°35.3'W	4187	CTD
		13.49	64°47.6'	47°35.7'W	4187	
23/092		16.02	64°40.0'	48°28.9'W	4011	CTD
		16.56	64°39.9'	48°29.0'W	4011	

AGT = Agassiz trawl
APSN = Apsteinnet
BO = Bongonet
BS = Baumann water sampler
CTD = CTD with Rosette water sampler
D- = Deployment of mooring
Dred. = Dredging of mooring
IC = Ice collection
ID = Ice drilling
LM = Light detector
MN = Multinet
R- = Recovery of mooring or buoy
SD = Secchi disc

1.2 ANT X/8

Auf folgenden Stationen wurden CTD-Messungen durchgeführt:

Station	Date	Time	Latitude	Longitude
194	05.02.93	08:24	09°15'S	029°14'W
204	06.02.93	14:30	03°58'S	027°25'W
212	07.02.93	05:57	01°16'S	026°30'W
229	08.02.93	14:27	06°13'N	026°54'W
243	09.02.93	12.23	11°09'N	027°51'W
243A	09.02.93	12:41	11°09'N	027°51'W
247	10.02.93	08:27	14°46'N	028°33'W
257	11.02.93	08:24	19°07'N	028°20'W
267	12.02.93	15:56	24°51'N	025°40'W
271	13.02.93	08:26	27°53'N	024°14'W
283	14.02.93	08:25	31°49'N	022°17'W
295	15.02.93	08:25	35°56'N	019°50'W
308	16.02.93	12:24	40°29'N	016°35'W
315	17.02.93	08:26	43°37'N	014°11'W

2. Fahrtteilnehmer / Participants

2.1 ANT X/6

Antia, Avan	SFB
Bakker, Dorothe	NIOZ
Bakker, Karel	NIOZ
Bathmann, Ulrich	AWI
Becquevort, Sylvie	ULB
Bjørnsen, Peter K.	MBL
Bolt, Bärbel	FBB
Crawford, Richard	AWI
David, Pascal	IEM
De Hénau, Thierry	ULB
de Baar, Hein J.W.	NIOZ
de Koster, Ronald	NIOZ
Dehair, Frank	VUA
deJong, Jeroen	NIOZ
Detmer, A. C.	IFM
deWall, I.	IFM
Dubischar, Corinna	AWI
Friedrichs, Jana	AWI
Fritsche, Peter	IFM
Giesenhagen, Hanna	IFM
Gonzalez, Santiago	NIOZ
Hill, Heinz	DWD
Hinz, Friedel	AWI
Hölzen, Heike	AWI
Holby, Ola	AWI
Jochem, Frank	IFM
Kähler, Paul	SFB
Klaas, Christine	AWI
Köhler, Herbert	DWD
Kuipers, Bouwe	NIOZ
Lochte, Karin	AWI
Löscher, Bettina	NIOZ
Manuels, M.	NIOZ
Mathot, Sylvie	ULB
Meyerdierks, Doris	FBB
Nielsen, Alexandra C.	MBL
Ober, Sven	NIOZ
Peeken, Ilka	SFB
Poncin, Jacques	IEM
Queguiner, Bernard	IEM
Reitmeier, Sven	SFB
Rommets, Joop	NIOZ
Ruttgers v.d.Loeff, Michiel	AWI
Scharek , Renate	AWI
Smetacek, Victor	AWI
Stoll, Michel	NIOZ
Tessier, Laetitia	IEM
van Franeker, Jan Andries	IBN
vanLeeuwe, Maria A.	NIOZ
Veth, Cornelis	NIOZ
Wunsch, Marita	SFB

2.2 ANT X/7

Ahlers, Petra	AWI
Balen van, Antonius	NIOZ
Baumann, Marcus	AWI
Boehme, Tobias	AWI/FPB
Brandini, Frederico	CBM
Büchner, Jürgen	HSW
Corleis v. d. Voet, Janja	AWI
Döhler, Günter	BIF
Fahl, Kirstin	AWI
Fahrbach, Eberhard	AWI
Fischer, Haika	AWI/FPB
Goeyens, Leo	AWI/VUB
Gorny, Matthias	AWI
Günther, Sven	AWI
Hamann, Rudolph	AWI/FPB
Hanke, Georg	AWI
Hillebrandt, Marc-Oliver	HSW
Hoppema, Mario	AWI/NIOZ
Jesse, Sandra	AWI
Klatt, Olaf	AWI/FPB
Kolb, Leif	AWI/FPB
Kurbjeweit, Frank	AWI
Latten, Andrees	AWI/FPB
Lundström,Volker	HSW
Nachtigäller, Jutta	DÜI
Richter, Klaus-Uwe	AWI
Riegger, Lieselotte	AWI
Rohardt, Gerd	AWI
Röttgers, Rüdiger	AWI
Schreiber, Detlef	HSW
Schröder, Sabine	AWI
Schütt, Ekkehard	AWI
Schweimler, Imgrun	AWI/FPB
Seifert, Wolfgang	DWD
Seiß, Guntram	AWI/FPB
Skoog, Annelie	AMK
Sonnabend, Hartmut	DWD
Strass, Volker	AWI
Tibcken, Michael	AWI
Vosjan, Jan H.	NIOZ
Wedborg, Margareta	AMK
Witte, Hannelore	AWI
Zwein, Frank	AWI/FPB

To Neumayer-Station

Ahammer, Heinz	PM
Behnsen; Uwe	AWi
Behrens, Detlev	KRA
Damm, Michael	AWI
Eckstaller, Alfons	AWI
El Naggar, Saad El D.	AWI
Etspüler, Wolfgang	AWI
Gruhne, Mario	AWI
Heinrich, Andreas	TRE
Hofmann, Jörg	AWI
Koenig, Roland	TRE
Mertens, Rolf	KRA

Muhle, Heiko	AWI
Nixdorf, Uwe	AWI
Nolting, Michael	AWI
Reder, Giselher	CN
Reiter, Alois	AWI
Rosenberger, Andreas	AWI
Schneider, Hans	AWI
Strecke, Volker	AWI
Terzenbach, Uwe	AWI
Trendelkamp, Joseph	TRE
Tüg, Helmut	AWI
Wicht, Manfred	AWI
Wissing, Manfred	TRE
Witt, Ralf	AWI
Wunder, Hans	CN
Zimmermann, Frerich	CN

2.3 ANT X/8

Bakker, Dorothee, C.E.	NIOZ
Ballschmiter, Karlheinz	UNU
Bluszcz, Thaddäus	AWI
Fischer, Haika	AWI
Führer, Ursula	UNU
Gorges, Anita	AWI
Günther, Sven	AWI
Krause, Gunther	AWI
Lilischkis, Rainer	AWI
Luxenhofer, Oliver	UNU
Majoor, Bram	NIOZ
Meier, Brigitta	AWI
Nürnberg, Olaf	UOL
Ohm, Klaus	AWI
Pagel, Peter	UNU
Reuter, Ulrich	UNU
Sonnabend, Hartmut	DWDS
Wagner, Peter	UOL
Weiland, Hans	DWDS
Weller, Rolf	AWI
Wessel, Silke	AWIP
Wiedmann, Thomas	UNU
Willkomm, Rainer	UOL

3. Beteiligte Institute/Participating institutes

Germany

AWI	Alfred-Wegener-Institute für Polar- und Meeresforschung Columbusstraße 275 68 Bremerhaven Außenstelle Potsdam Telegraphenberg A43 144 73 Potsdam
BIF	Johann Wolfgang Goethe-Universität Botanisches Institut Siesmayerstr. 70 W-6000 Frankfurt am Main 11
DÜI	Deutsches Übersee-Institut Neuer Jungfernstieg 21 W-2000 Hamburg 36
DWD	Deutscher Wetterdienst, Seewetteramt Bernhard-Nocht-Str. 76 2000 Hamburg 4
FBB	Universität Bremen Meeresbotanik, FB2 Postfach 33 04 40 2800 Bremen 33
FGB	Universität Bremen Fachbereich Geowissenschaften FB5 Postfach 33 04 40 2800 Bremen 33
HSW	Helicopter Service, Wasserthal GmbH Kätnerweg 43 2000 Hamburg 65
IFM	Institut für Meereskunde Abt. Planktologie Düsternbrooker Weg 20 2300 Kiel 1
SFB	Universität Kiel SFB 313 Olshausenstr. 40-60 2300 Kiel 1

UOL Universität Oldenburg
Fachbereich Physik 8
Carl-von-Ossietzky-Str. 9-11
2900 Oldenburg

UNU Universität Ulm
Abt. Analyt. Chemie & Umweltchemie
Albert-Einstein-Allee 11
7900 Ulm

Belgium

VUB Vrije Universiteit Brussel-Anch
Pleinlaan 2
B-1050 Brussel, BELGIUM

ULB Groupe de Microbiologie des Milieux Aquatiques
Université Libre de Bruxelles ULB
Campus de la Plaine, CP 221
B-1050 Brussels, BELGIUM

Brasil

CBM Centro de Biologia Marinha/UFPr
Av. Beira Mar s/n, Pontal do Sul
Paranaguá 83200, PR, Brasil

Denmark

MBL Københavns Universitet Marine Biological Laboratory
Strandpromenaden 5
DK-3000 Helsingør, Denmark

Estonia

IEMR Institute of Ecology and Marine Research
Paldiski Road 1
200031 Tallinn, Estonia

France

IEM Université de Bretagne Occidentale
Institut d'Etudes Marines
Laboratoire de Chimie des Ecosystemes Marins
6 Avenue V. Le Gorgeu
F-29287 Brest Cédex, France

Netherlands

NIOZ Nederlands Instituut voor Onderzoek der Zee NIOZ
Postbox 59
NL-1790 AB Den Burg, The Netherlands

IBN Institute for Forestry & Nature Research (IBN-DLO)
Postbox 167
NL-1790 AD Den Burg, The Netherlands

Sweden

AMK University of Göteborg and
Chalmers University of Technology
Analytical and Marine Chemistry
S-412 96 Göteborg, Sweden

United States of America

OSU Oregon State University
College of Oceanography
Oceanography Admin. Bld. 104
Corvallis, Oregon 97331-5503, U.S.A.

To Neumayer Station

CN Fa. Christiani & Nielsen
Basedowstr.
W-2000 Hamburg 26

KRA Fa. J.H. Kramer
Labradorstr.
W-2850 Bremerhaven

TRE Fa. Trendelkamp Stahl-
und Maschinenbau
Westring 18
W-4418 Nordwalde

PM POLARMAR GmbH
Bürger
W-2850 Bremerhaven

4. Schiffsbesatzung/Ship's Crew;

Dienstgrad	ANT X/6	ANT X/7	ANT X/8
Kapitän	L. Suhrmeyer	H. Jonas	H. Jonas
1. Offizier	I. Varding	K.D. Gerber	K.D. Gerber
Naut. Offizier	M. Bürger	U. Grundmann	U. Grundmann
Naut. Offizier	M. Müller	M. Rodewald	M. Rodewald
zusl.Offizier	---	S. Schwarze	---
Arzt	R. Petersen	J. Riedel	J. Riedel
Ltd. Ingenieur	D. Knoop	K. Müller	K. Müller
1. Ingenieur	W. Delff	G. Erreth	G. Erreth
2. Ingenieur	W. Simon	R. Fengler	R. Fengler
2. Ingenieur	H. Folta	O. Ziemann	O. Ziemann
Elektriker	R. Erdmann	G. Schuster	G. Schuster
Elektroniker	K. Hoops	H. Elvers	H. Elvers
Elektroniker	U. Lembke	H. Muhle	Hel. Muhle
Elektroniker	A. Piskorzynski	A.Greitemann-Hackl	A.Greitemann-Hackl.
Elektroniker	M. Fröb	J. Roschinsky	J. Roschinsky
Funkoffizier	E. Müller	H. Geiger	H. Geiger
Funkoffizier	J. Butz	K.H. Wanger	K.H. Wanger
Koch	W. Köwing	E. Kubicka	E. Kubicka
Kochsmaat	F. Roggartz	H. Wübber	H. Wübber
Kochsmaat	M. Kästner	H. Hüneke	H. Hüneke
1. Steward	D. Peschke	H. Vollmeyer	H. Vollmeyer
Stewardess/Nurse	U.Teichmann	S. Hoffmann	S. Hoffmann
Stewardess	A. Hopp	M. Hoppe	M. Hoppe
Stewardess	V. Kuhlmann	J. Hasler	J. Hasler
Stewardess	A. Neves	K. Mund	K. Mund
2. Steward	Ch. L. Yu	Ch. L. Yu	Ch. L. Yu
2. Steward	Ch. Yang	J. M. Tu	J. M. Tu
Wäscher	J. M. Tu	Ch. Ch. Chang	Ch. Ch. Chang
Bootsmann	W. Hopp	H.D. Junge	H.D. Junge
Zimmermann	P. Kassubeck	K. Marowsky	K. Marowsky
Matrose	L.Gil Iglesias	M. Winkler	M. Winkler
Matrose	H. Blödorn	F.Garcia Martinez	F. G. Martinez
Matrose	M. Meis Torres	S.Pousada Martinez	S. P. Martinez
Matrose	K. Bindernagel	J.Soage Curra	J.S. Curra
Matrose	B.Pereira Portela	J.Novo Loveira	J.N. Loveira
Matrose	A. Prol Otero	B. Iglesias Bermudez	B. I. Bermudez
Matrose	R.Ponte Dourado	A.Suarez Paisal	---
Matrose	H. Thiele	M. Schmidt	---
Lagerhalter	B. Barth	K. Müller	K. Müller
Masch-Wart	T. Rothe	G. Dufner	G. Dufner
Masch-Wart	G. Fritz	M. Lesch	M. Lesch
Masch-Wart	F. Buchas	U. Husung	U. Husung
Masch-Wart	S. Reimann	E. Carstens	E. Carstens
Masch-Wart	G. Jordan	E. Heurich	E. Heurich